

THE STATE OF WYOMING

GEOLOGIST'S OFFICE

BULLETIN NUMBER X 19

The Mineral Hot Springs
of Wyoming



FALLS OF BIG HORN HOT SPRINGS, THERMOPOLIS, WYOMING

ALBERT B. BARTLETT
STATE GEOLOGIST OF WYOMING

CHEYENNE, WYOMING

MAY 6, 1926

LIBRARY
OF THE
UNIVERSITY OF WYOMING
LARAMIE

AREA
WY
HotSpgs

UNIVERSITY OF WYOMING
RESEARCH INSTITUTE
EARTH SCIENCES

GLASS & 351579

Form #181/SM/2-79

Future Loans.

U

55787

W9942-b

no. 19

Cop. 3 MINERAL HOT SPRINGS
OF WYOMING

Wyoming has been endowed by Nature in countless ways. In some locations from its secret hiding places in the earth, petroleum gushes forth in the oil fields, placing this State high in the petroleum industry; in other places, underneath its surface abound rich minerals, non-metallic minerals and precious metals, and here and there within its borders, sometimes in the midst of a great barren waste, there is a mineral spring bubbling forth hope and promise to those who seek rest and drink of its health-giving waters. In the past, these springs have not been advertised to any extent, with the exception of one or two of the larger ones. It is the purpose of this Bulletin to give publicity to these springs. Warm mineral springs usually contain medicinal properties and many of these springs are situated where climatic conditions would attract on account of the winter mildness and summer coolness.

No attempt was made to study the geology of the various mineral springs for this Bulletin, but it has been noted that most of the springs have one point in common, the fact that the springs come to the surface through outcrops of the Chugwater formation of Triassic Age and are associated with anticlines or monoclines, faulted in some cases, this being true of the majority of the most important springs of the State. In the vicinity of the Big Horn Hot Springs at Thermopolis, four wells have been drilled and have been successful in developing important flows of hot water of practically the same temperature and mineralization as the waters of the Big Horn Hot Springs. These wells were drilled through the lower part of the Chugwater formation and into the Embar. Considerable pyrite was encountered in the bottoms of two of the wells. One of these wells flows at the rate of 121,508 gallons per day and another 2,223,330 gallons per day. The drilling of these wells has not apparently reduced the flow of the springs and it is believed that a tremendous underground reserve of hot mineralized water occurs in this immediate vicinity, and the same may be true of the regions surrounding other mineral springs where wells have not been drilled, in a number of places in Wyoming.

No theory has yet been advanced which accounts for the heat or the mineral constituents in the water of these wells and springs. Taking the present available information into consideration, it is believed that the temperature of the waters is derived from heat generated by chemical reaction among the elements



View from Mount Hill showing Terraces of Big Horn Hot Springs in foreground, buildings on State Reserve in middle ground, and Town of Thermopoles in back ground across the river.

present in the Chugwater and Embar formations. These formations contain gypsum, limestone, iron both in the form of pyrite and as an oxide, also, magnesium, sodium and potassium. A detailed study of the chemistry and geology of these hot mineral springs, undoubtedly, would throw more light on the origin of these hot mineral waters and will be taken up by the State Geologist in a later Bulletin.

BIG HORN MINERAL HOT SPRINGS

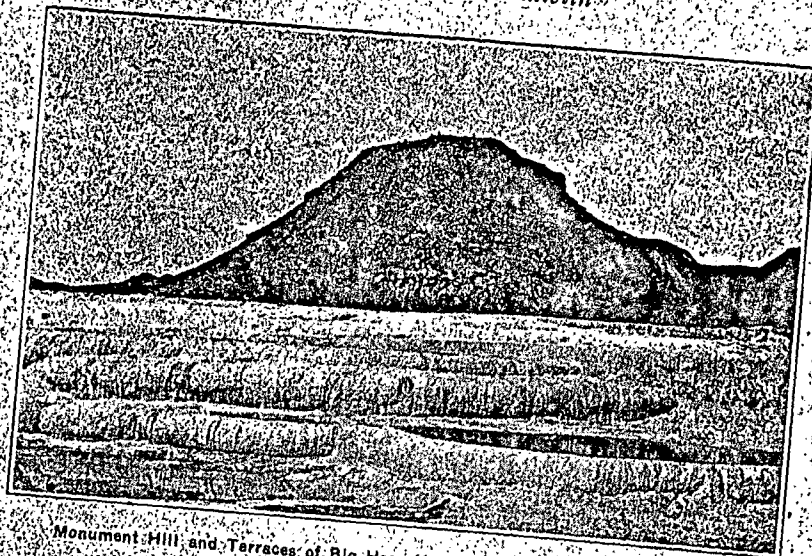
By an Act of Congress, approved June 7, 1897, these springs were made the property of the State of Wyoming. There was a treaty in connection with this Act providing that the Big Horn Mineral Hot Springs should be free to the public always. "Washakie", Chief of the Shoshone Indians, deserves credit for this wonderful gift to humanity which has brought relief from disease and suffering to many men.

The Wyoming Legislature, in 1899, enacted a law providing for bath houses to be constructed, open and free to the use of the public. Since that time the State Legislatures have appropriated about a half million dollars for parking streets, lighting system, water systems, bridges and buildings. A bath house at a cost of \$50,000 was built and state-appointed attendants are constantly in charge.

These baths are located at the city of Thermopoles, Wyoming, which is about five miles north of the Wind River Canyon, one of the most interesting natural formations of the world. Thermopoles is about ninety miles southeast from Yellowstone National Park and on the main line of the Burlington Route. It is on the Yellowstone, Buffalo, Park-to-Park and Atlantic Yellowstone Pacific Highways.

There are several good hotels there, open all year and having all modern conveniences. There are also a number of up-to-date apartments and boarding houses offering accommodations at reasonable rates. In addition to the hotels and rooming houses, there is a tourist camp ground, where a charge of fifty cents per day is made for the conveniences, and also a free camp ground for those who desire to use it.

Here one may spend an ideal vacation in this atmosphere of pure mountain air. There are ample opportunities for out-door amusements, golf, tennis, horseback riding, mountain climbing, and motoring down the scenic roadway of the Wind River Canyon, which was opened in July, 1924. In this canyon are three tunnels which were cut through solid rock at a cost of about a million dollars to the state and federal governments. One writer has said that "this is one of the most wonderfully picturesque spots, possibly, in the world, where the Big Horn river gathers the voices



Monument Hill and Terraces of Big Horn Hot Springs, Thermopolls, Wyoming.

of the streams of the hills into a grand chorus and roars a wonderful concert, telling in a language all its own of the joys of life in the vicinity of the Big Horn Springs.

Among the other scenic attractions in this vicinity are Monument Hill, Devil's Punch Bowl, Old Roundtop, Hot Water Lakes, Hot Water Geyser, Hot Water Falls, stock and dude ranches, game preserve and zoo of Rocky Mountain wild animals.

The Big Horn, Black Sulphur, White Sulphur, and Ponce de Leon are the four largest springs, and besides these, there are hundreds of smaller Mineral Hot Springs bubbling up in the Big Horn River, and at different places on the State Reserve.

Analysis by Prof. M. P. Scheutzenburger of the College of France of the waters of the springs follows:

	Grams per Liter	Grains per Gal.
Silica	0855	4.986
Iron and Alumina	0039	227
Potassium Chloride	1756	10.240
Sodium Chloride	4492	26.195
Sodium Sulphate	2591	15.110
Magnesium Sulphate	3334	19.443
Calcium Sulphate	2256	13.156
Calcium Carbonate	6937	40.454
Total Solids	2.2260	129.811

Temperature 134 Degrees Fahr.
Flow 4,100,235 Gals. Every 24 Hours

Mineral Hot Springs of Wyoming

Foregoing analysis re-calculated to comply with Federal Government formula.

Parts per Million Hypothetical Combinations—	Big Horn Hot Springs
Potassium Chloride (KCl)	175.60
Sodium Chloride (NaCl)	449.20
Sodium Sulphate (NaSO ₄)	259.10
Magnesium Sulphate (MgSO ₄ ·O)	333.40
Calcium Sulphate (CaSO ₄)	225.60
Calcium Carbonate (CaCO ₃)	693.70
Ferrous Oxide and Alumina (Fe ₂ O ₃ A 1/2 O ₂)	3.90
Silica (Si O ₂)	85.50
Total Solids per Million	2,226.00
Temperature 57.4° C. (135° F.)	

SARATOGA HOT SPRINGS

Located at Saratoga, Wyoming, are both hot and cold mineral springs and the baths are very beneficial. Saratoga is a town of about one thousand inhabitants, beautifully located on the North Platte River. The Saratoga Valley has a mild and healthful climate and is surrounded by fishing streams and beautiful scenery, all of which add to the advantages of Saratoga as a pleasant summer and health resort.

The water from the various springs comes out of the ground at a heat averaging 120° F. The waters are Radio-active and contain all of the elements that have made other similar resorts famous the world over. The climate is ideal all the year around, being not too cold in winter and with cool, refreshing nights in summer. The altitude is 6,785 feet. The wooded islands scattered along the North Platte River at this point add to the beauty of the natural picture and the pure mountain water, the tonic air from the mountains and the freedom from alkali produce unusually good conditions for recuperation from overwork, nerve and brain lag, tubercular troubles, etc. Catarrh and hay fever are relieved and cured by the water and pure air.

An analysis of the Saratoga Water by C. F. Chandler, Ph. D., New York, follows:

	Grains per U. S. Gal.	Pints per 100,000
Sodium Chloride	52.0807	89.3322
Sodium Sulphate	10.2510	17.5832
Potassium Sulphate	10.4603	17.9422
Calcium Sulphate	21.0410	36.0909
Calcium Carbonate	4433	7604
Magnesium Carbonate	1.2782	2.1924
Silica	3.7195	6.3799
Iron and Aluminum (oxides)	1.108	1.900
Total	99.3848	170.4712

Sanitary analysis shows the water to be absolutely free from contamination.

The medicinal waters bring thousands of visitors to this remote place each year for the purpose of resting, recovering lost health or for the enjoyment of the fishing and hunting in the valley or hills. Notable personages from all over the west become enamored of the beautiful surroundings and come, year after year. Physicians whose names are known throughout the west visit the springs and advise many patients to try the waters for stubborn and chronic diseases. Helpless rheumatics have been cured in from two to six weeks. Victims of the liquor and tobacco habits have been entirely cured. Sufferers from stomach and intestinal diseases have been sent away happy at the first freedom from pain, completely cured.

The Medicinal Well at Saratoga deserves mention. From this well comes a wonderful "Radio-active" Mineral Water, which is bottled and sold throughout the country, some carbonated and some "still" or just as it comes from the well.

The continued use of the water stimulates the action of, and restores to a normal condition, all the organs engaged in the process of digestion, assimilation, secretion, and excretion. It is a laxative when drunk in the morning before breakfast, used during the day and afternoon, it acts as an alterative and diuretic and cures all acid and gaseous conditions of the stomach. In June, 1911, its wonderful remedial properties were discovered, and since that time this mineral water has rapidly increased in favor. At a first glance, one asks what accounts for Nature storing up this wonderful medicinal water in such an apparently remote, out-of-the-way place as Saratoga, Wyoming. However, when one investigates, it is found that Nature has selected the ideal, on account of the fact that the mountains and brooks around Saratoga, Wyoming, abound in mineral and medicinal properties.

ALCOVA HOT SPRINGS

The Alcova Hot Springs are located in Natrona County, about thirty-five miles southwest of Casper. The water from these springs is noted for medicinal properties, and the place will become famous as a health resort. The country abounds in picturesque scenery, is rich in minerals, and rock formations, and is favored with a delightful climate. The land in the valleys is fertile and suited to agriculture. The Fremont Canyon where the springs gush out from the base of a rock 700 feet high, into the North Platte River, is the nucleus of a town. Two and one-half miles up the river is another canyon, more wonderful, being six miles long, and in some places 1,500 feet high. Gypsum, marble, graphite, saponite, agates, coal, oil and paint rock, lime stone, clay, quartz-bearing gold and silver are found in this vicinity. Extensive improvements are being made in hotels and bath houses this season. No



North Platte River near Alcova Hot Springs.

country can be found more interesting to prospectors and those seeking pleasure. One can find accommodations at the Fremont House on the bank of the river, with delightful boating and fishing. The Red Reef Chute will be an addition this summer.

The following is an analysis of the water of the Alcova Hot Springs:

Analysis of Water	Grams per Liter	Grains per Gallon
Silica SiO ₂	0397	2.315
Iron and Alumina, Fe ₂ O ₃ , Al ₂ O ₃	0022	128
Lithia, Li ₂ O	Trace	Trace
Potash, K ₂ O	0159	927
Soda, Na ₂ O	2837	16,544
Lime, CaO	2279	13,291
Magnesia, MgO	0990	5,773
Hydrochloric Acid, Cl	2970	17,320
Sulphuric Acid, SO ₄	3848	22,441
Carbonic Acid, CO ₂ (calc)	1002	5,843
(Less O equiv. of Cl)	0670	3,908
Total Solids	13,834	80,674
Temperature, 139° Fahr		

FORT WASHAKIE SPRINGS

The Fort Washakie Springs are located at the Shoshone Agency, Fremont County, Wyoming.

Following is the analyses of Spring No. 30:

Radicals

Nitrate (NO ₃)	10	Sod. Nitrate (NaNO ₃)	14	Ammonia, Manganese
Chloride (Cl)	43	Sod. Chloride (NaCl)	46	metals of hydrogen
Sulphate (SO ₄)	363	Sod. Sulphate (Na ₂ SO ₄)	65	sulphide group, car-
Bicarbonate (HCO ₃)	281	Sod. Bicarbonate (NaHCO ₃)		bonate, phosphate, bro-
Potassium (K)	17	Mag. Chloride (MgCl ₂)		mise, and iodid;
Sodium (Na)	43	Mag. Sulphate (MgSO ₄)	178	none
Magnesium (Mg)	36	Mag. Bicarbonate (Mg(HCO ₃) ₂)		Strontium, arsenic,
Calcium (Ca)	166	Calcium Chloride (CaCl ₂)	251	nitrate, boric acid;
Iron Oxide	8	Calcium Sulphate (CaSO ₄)	251	traces
Aluminum (Al)		Calcium Bicarbonate	278	
Silica (SiO ₂)	46	See note		
		Ferrous Oxide (Fe ₂ O ₃)	8	Hydrogen sulphid
		Silica (SiO ₂)		0.9 m. p. l.
		Potassium Chloride (KCl)	32	Lithium 0.2 m. p. l.
				Very slight sediment
				consisted of silica;
				the amount has been
				included in the analysis
Total	1005.8	Total	1005.8	

*Note:—(Ca(HCO₃)₂)

CONCLUSION

This water is rather highly mineralized and contains hydrogen sulphide. It is classed as a sulphurated, alkaline, sulphate water. The constituents which give to its chief characteristics are hydrogen sulphide, calcium bicarbonate (dissolved limestone), calcium sulphate (gypsum) and magnesium sulphate (Epsom salts.)

CAPTAIN BONNEVILLE, by Washington Irving, Chapter XXV, page 260, contains the following interesting reference to Fort Washakie Springs:

"Having forded Wind River a little above its mouth, Captain Bonneville and his three companions proceeded across a gravelly plain, until they fell upon the Popo-Agie, up the left bank of which they held their course, nearly in a southerly direction. * * * and then turned in for the night and slept soundly like weary and well-fed hunters.

"At daylight they were in the saddle again, and skirted along the river, passing through fresh grassy meadows, and a succession of beautiful groves of willows and cottonwood. Towards evening Captain Bonneville observed a smoke at a distance rising from among hills directly in the route he was pursuing. Apprehensive of some hostile band, he concealed the horses in a thicket, and accompanied by one of his men, crawled cautiously up a height, from which he could overlook the scene of danger. Here, with a spy-glass, he reconnoitered the surrounding country, but not a lodge nor fire, not a man, horse, nor dog, was to be discovered; in short, the smoke which had caused such alarm proved to be the

vapor, from several warm, or, rather, hot springs of considerable magnitude, pouring forth streams in every direction over a bottom of white clay. One of the springs was about twenty-five yards in diameter, and so deep that the water was of a bright green color."

These springs are about eighteen miles distant from the Chicago & Northwestern Railroad, and although the place is open for the reception of the public, there is no resort operated here. The waters from the springs are found to be beneficial for rheumatism and skin diseases.

THE DEMARIS SPRINGS

About four miles from Cody, Wyoming, which is on the Burlington Route, the DeMaris Needle Springs are found. These are located adjacent to the Shoshone River. The upper springs has a temperature of 100° F. and the lower one has a temperature of 76° F. Around the lower spring a plunge has been built. A resort has been operated there for thirty-two years. The waters are highly mineralized. An analysis follows:

	Grains per Gallon	Hot Spring	Cold Spring
Aluminum and Iron Oxides	2.2	5.0	
Calcium Oxide	15.5	17.8	
Magnesium Oxide	34.6	16.6	
Sodium Oxide	25.8	26.0	
Silicic Dioxide	2.2	1.1	
Carbon Dioxide	36.6	28.6	
Sulphur Trioxide	31.2	1.9	
Sulphur as Sulphide	6.1	12.0	
Chlorine as Chloride	1.7	1.0	
Lithium and Strontium		Traces	
Temperature	100 Fahr.	75 Fahr.	

CAPTAIN BONNEVILLE, by Washington Irving, Chapter XXIII, page 251, contains the following reference to these springs of the region along the Shoshoni or Stinkingwater River: "Here the earth is hot and cracked; in many places emitting smoke and sulphurous vapors, as if covering concealed fires. A volcanic tract of similar character is found on Stinking River, one of the tributaries of the Bighorn, which takes its unhappy name from the odor derived from sulphurous springs and streams. This last mentioned place was first discovered by Colter, a hunter belonging to Lewis and Clarke's exploring party, who came upon it in the course of his lonely wanderings and gave such an account of the gloomy terrors, its hidden fires, smoking pits, noxious streams, and the all-pervading smell of brimstone that it received, and has ever since retained among trappers the name of 'Colter's Hell!'"



DeMaries Hot Springs near Cody, Wyoming

YELLOWSTONE NATIONAL PARK SPRINGS

The Mammoth Hot Springs are located near the Gardiner, Montana, or northern entrance to the Park at an altitude of 6,284 feet. Located there are the Administrative Offices of the Park, the Superintendent's Office, United States Commissioner's Office, Mammoth Hotel, postoffice, curio store, etc. Mammoth Camp is straight ahead and not far distant a herd of buffalo is run.

The large and wonderful hot springs and terraces are the chief attractions at Mammoth. These terraces and springs are numerous. The deep coloring at Mammoth Hot Springs is due to minerals in the water, and to a low form of vegetable life which will grow in the water up to a temperature of 180° F., however, at Jupiter Spring and many places elsewhere in the Park the deep blue coloring of the water is not a reflection of the sky nor is it due to vegetable matter, but is natural and incomparably beautiful. Some of the most important springs besides Mammoth Hot Springs are the Jupiter, Canary, Glen, Orange, Dedolph and Diana.

An analyses of the Mammoth Hot Springs follows:

Constituents	Grams per Kilo of Water	Percent of Total Material in Solution	Grains per U. S. Gallon
KCl	0.0046	1.67	0.2685
K ₂ SO ₄	0.0015	0.54	0.0875
Na ₂ SO ₄	0.0448	16.25	2.6151
MgSO ₄	0.0076	2.76	0.4436
MgCO ₃	0.0258	9.36	1.5060
CaCO ₃	0.0790	28.65	4.6114
Al ₂ O ₃	0.0021	0.76	0.1225
SiO ₂	0.0355	12.88	2.0722
CO ₂	0.0748	27.13	4.3662
	0.2757	100.00	16.0930

A hot spring deposits clear water into Bath Spring and the luke-warm water there is excellent for bathing.

There are many enjoyable side trips from Mammoth Springs, consisting of beautiful walks and drives. Mountain climbers find it a place of delight, for there are many mountains to climb, the principal ones being Electric Peak (11,555 feet), Bunsen Peak (8,600 feet), Mount Everts (7,900 feet), and Sepulcher Mountain (9,500 feet).

The general panorama at Mammoth Hot Springs is one of the most striking in the Park. The steaming tinted terraces and Fort Yellowstone near by; the long, palisaded escarpment of Mount Everts to the east; the dominating presence of Bunsen Peak to the south with Gardiner Canyon and the distant eleva-

tions of the Mount Washburn group, the rugged slopes of Terrace Mountain to the west, and the distant peaks of the Snowy Range to the north—all together form a surrounding landscape of wonderful beauty and contrast.

OTHER WYOMING SPRINGS

In addition to the Hot Springs on which detailed information has been given, there are a number of other springs in various parts of the State which have not been investigated, mainly by reason of their being too remote from transportation.

A number of these springs undoubtedly have great possibilities and will bear further investigation. A few of them may be listed as follows:

Hot Springs near Hailey, Wyoming, a few miles off the road between Lander and Rawlins. From what information we could gather, this spring is a Sulphur Spring, having a composition similar to the Fort Washakie Hot Springs and a temperature of 100° to 120°. The flow is probably in the neighborhood of 100 to 200 gallons per minute. At the present time, it is not used for any purpose besides irrigation.

Hot Springs near Fremont Butte in Sublette County, in T. 32 N., R. 107 W. Information concerning these springs is very meagre. Small bath houses have been erected, and the springs are used for bathing purposes by the residents of that locality.

Hot Springs on the Snake River: This spring is situated on the east side of the Snake River in a meadow of about fifty acres extent, about twenty miles south of Jackson and about four miles below the junction of the Hoback River and Snake River, from which point it is necessary to travel by horseback to reach the spring. It is a sulphur spring, coming through the red beds of the Chugwater formation. It has a temperature of from 100° to 120° F. A small log cabin has been erected over the spring for a bath house. The flow of the spring has not been measured, but has been estimated to be 100 gallons per minute or more. It is used by residents of that locality and is said to be good for rheumatism. Water is used to a limited extent for irrigation and is valuable for that purpose, as crops can be grown earlier in the spring and later in the fall than on lands where cold water is used.

This would make a wonderful location for a dude ranch, as it is situated in a very mountainous region on Snake River Canyon where big game of all kinds is numerous and where trout fishing is unsurpassed. It will not be but a few years until a State or Forest Service Highway is built through the Snake River Canyon, and this location would then be upon this highway. Pure cold water for domestic purposes could be piped down from a

spring on the side of the mountain a short distance from the hot springs.

There are a number of mineral springs in Uinta County, though none of them are hot springs. The largest of these springs is located near the Union Pacific Railroad, near the Leroy station. It was formerly customary for the Union Pacific trains to stop at this point in order that the passengers could drink waters of this spring, which are said to be highly beneficial.

Along the Spring Valley, near the highway and also above the town of Spring Valley, are several mineral springs. Waters of these springs were formerly bottled and sold in large quantities by a Spring Valley druggist, now deceased. Analyses of these springs have not yet been secured.

Nine miles due south of Douglas, not far from the point where Wagonhound Creek empties into the North Platte River, is a warm spring, whose temperature, composition, and rate of discharge has not been determined. This spring has been used to a small extent for bathing purposes and for irrigation.

Analysis of Magnetic Anomalies Over Yellowstone National Park: Mapping of Curie Point Isothermal Surface for Geothermal Reconnaissance

B. K. BHATTACHARYYA¹ AND LEI-KUANG LEU²

Department of Materials Science and Engineering, University of California, Berkeley, California 94720

The bottom of the magnetized crust determined from the spectral analysis of residual magnetic anomalies is generally interpreted as the level of the Curie point isotherm. This paper studies the spatial variation of the Curie point isotherm level in Yellowstone National Park with the help of aeromagnetic data. A very shallow isothermal surface at a depth of only 5–6 km below sea level is associated with the central part of the Yellowstone caldera. It seems to extend along a narrow corridor toward the southwestern and eastern edges of the map. Except in a few localized spots, the isotherm deepens considerably in the areas outside the caldera. Because the caldera encloses most of the areas of hydrothermal alteration, fumaroles, and boiling springs in the park, this study indicates a strong correlation between the spatial variation of the Curie isotherm level and the concentration of subsurface geothermal energy.

AREA
WY
Park
Yellowstr
Isotherm

INTRODUCTION

Crustal rocks lose their magnetization at the Curie point temperature. At this temperature, ferrimagnetic rocks become paramagnetic, and their ability to generate detectable magnetic anomalies disappears. Thus the deepest level in the crust containing materials which create discernible signatures in a magnetic anomaly map is generally interpreted as the depth to the Curie point isotherm.

One of the important parameters that determines the relative depth of the isotherm with respect to sea level is the heat content in a particular region. The heat content is generally proportional to the local temperature gradient, thermal capacity, and generation of heat. A region with significant geothermal energy near the surface of the earth is characterized by an anomalously high temperature gradient and heat flow. It is therefore to be expected that regardless of the composition of the rocks, the region will be associated with a conspicuously shallow Curie point isotherm relative to the adjoining regions. For example, according to Blackwell [1971] the Curie isotherm lies at an average depth of approximately 10 km in the Basin and Range province, whereas it rises to 10–15 km below sea level in Yellowstone National Park [Smith et al., 1974]. The park is well known for its surface manifestations of geothermal energy.

The expected correlation between the spatial variation of the Curie isotherm level and the concentration of subsurface geothermal energy can be tested by means of an analysis of the magnetic anomalies over a specified region. The anomalies are analyzed for estimating the depths to the bottoms of magnetized bodies in the crust. These depths, when contoured over the entire area, should provide a picture of the spatial variation of the Curie isotherm level. This picture, in turn, should correlate to a significantly high degree with various known indices of geothermal activity in the area under consideration. We chose Yellowstone National Park for such a study not only because of its obvious geothermal manifestations but also because of the possible presence of molten magma at shallow depths, as was strongly indicated by various types of data [Eaton et al., 1975].

The practical importance of a study on the above correlation

lies in the possibility of establishing a useful reconnaissance method, based on aeromagnetic data, for rapid, regional geothermal exploration. It is obvious that the principal objective of this study is to delineate the Curie point isotherm surface over the entire area and thus to trace the changes in the isotherm level as one moves from the central area of geothermal manifestation, the Yellowstone caldera, to adjoining areas. These changes are expected to reflect the relative variation in geothermal activity in the area. For such a study the average isotherm depth for the whole area [Shuey et al., 1973; Smith et al., 1974] is not of great importance.

DATA

The Branch of Theoretical and Applied Geophysics of the U.S. Geological Survey conducted an aeromagnetic survey over the Yellowstone National Park area [U.S. Geological Survey, 1973]. The applied geophysics group of the University of Utah, Salt Lake City, Utah, digitized the data and removed the main geomagnetic field. The data were digitized with a spacing of 2.08 km. The digital data available to us cover an area, 131 km by 131 km, extending from 44°1'N to 45°7'N latitude and from 109°40'30"W to 111°15'W longitude. The area includes all of Yellowstone National Park. The flight elevation was 3.96 km with respect to sea level over the area from 44°1'N to 44°45'N latitude and 109°40'30"W to 110°15'W longitude. For the rest of the area the elevation was 3.66 km.

TREATMENT OF THE DATA

Residual. The observed magnetic field at a point is the vectorial combination of fields produced by various sources. The most predominant of these fields is the normal geomagnetic field entirely uncorrelated to crustal geology. This field, as was mentioned before, has been removed from the observations. The remaining field contains not only the effect of bodies of finite dimensions in the crust but also the effect of large-scale geologic features extending considerably beyond the borders of the limited area of investigation. The latter effect is called 'regional' and appears in the form of a smooth surface in the data. In order to remove this effect a quadratic surface is fitted to the data by the method of least squares. The mathematical expression for the surface is given by

$$T = -69.373 + 5.737y + 1.764x + 0.208y^2 + 0.172xy - 0.017x^2 \quad (1)$$

¹Present address: U.S. Geological Survey, Federal Center, Denver, Colorado

²Present address: Mobil Oil Corporation, Dallas, Texas 75221.

where x and y , expressed in terms of the unit distance of 2.08 km, point to the north and the east, respectively, and the origin of coordinates is taken at the center of the area. For a higher-order polynomial the coefficients of the third-degree terms are found to be relatively very small, and so they have not been considered.

This simple analysis shows that the available data contain north-south and east-west field gradients of 0.85 γ /km and 2.76 γ /km, respectively. These gradients are significant in magnitude and are not likely to be produced by bodies limited in horizontal extent in the crust of the earth. They are, however, related to the northeast-trending magnetic lineament or belt which extends from north central Nevada into Canada through Yellowstone National Park [Eaton *et al.*, 1975, Figure 7]. Since for the present study the effects of these lineaments are not desirable, the values obtained from (1) are subtracted from the available data. The remaining or residual values are assumed to be generated by magnetized bodies localized in the crust. The residual field map is shown in Figure 1.

Filtering. The residual map contains a large number of small-wavelength, high-intensity anomalies created by magnetized sources at the surface or at shallow depths. These anomalies distort and sometimes completely mask the effects of deep-seated bodies. The study of these deeper seated effects, which mainly generate large-wavelength anomalies, is greatly facilitated by a significant reduction of the small-wavelength components in the data. This reduction requires the use of a low-pass filter which transmits without distortion wavelengths larger than a critical or cutoff wavelength and attenuates all other wavelengths.

Let us now briefly consider the use of such a low-pass filter in relation to the objective of the study reported in this paper. The basic goal of the study is to calculate and map the depths

to the bottoms of the magnetized masses in the crust of earth. The potential field effects of these bottoms are contained in the large wavelengths of the spectrum of the total anomalies. So low-pass filtering does not alter these effects in any appreciable way, while it removes the short-wavelength features from the total field map.

For the filtering operation, three different zero phase dimensional low-pass filters are designed with cutoff frequencies at (1) 0.08 cycles/km, (2) 0.10 cycles/km, and (3) 0.2 cycles/km, respectively. Thus the smallest wavelength transmitted by these filters is around 10 km. The radial responses of these filters, as shown in Figure 2, remain flat in the low frequency region up to the cutoff frequency and then decrease very sharply.

The three filters were used individually to operate upon the residual field data. A study of the resulting filtered maps indicates that the filter with cutoff frequency at 0.10 cycles/km removes the small-wavelength anomalies with the least visible sign of distortion. The corresponding map is shown in Figure 3.

ANALYSIS OF THE FILTERED DATA

For determining the bottom depths of deep-seated magnetized bodies the filtered data have been analyzed in two ways. First, the whole area is divided into separate blocks, and the mean bottom depths of bodies causing magnetic anomalies are estimated for each block. Second, individual anomalies are carefully selected and analyzed to determine the vertical extent of causative bodies. The method remains essentially the same for analysis of the data corresponding to either a block or an anomaly. The two sets of results are then integrated to produce a map showing depths to the base of the magnetized section, Curie point isotherm, with respect to sea level. In the following

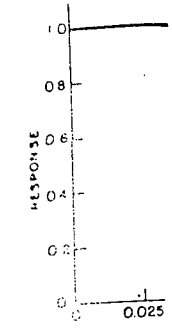


Fig. 2. Radial response of three low-pass filters with cutoff frequencies used to filter the Yellow

stone magnetic anomalies we show in Figure 3. As noted before, the filtered data contain a block of () km \times 31 km. The remaining blocks of the map are covered by blocks of varying size. The data in each block are used to determine the magnetic field anomalies. The anomalies are then compared with the anomalies of the reference field and the anomalies of the filtered data. The anomalies of the filtered data are then compared with the anomalies of the reference field and the anomalies of the filtered data. The anomalies of the filtered data are then compared with the anomalies of the reference field and the anomalies of the filtered data.

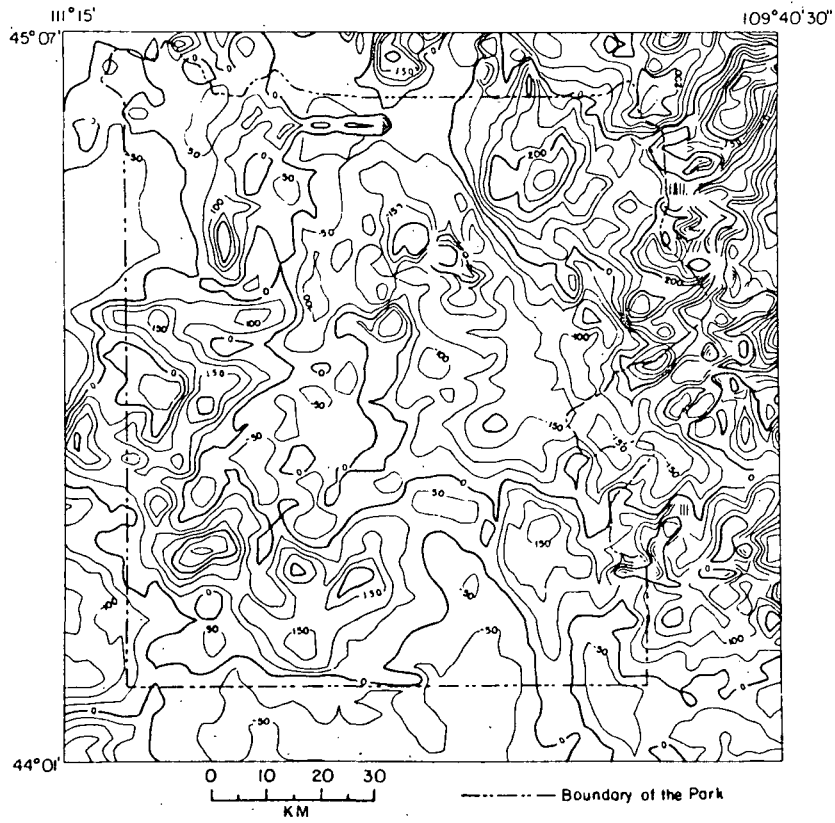


Fig. 1. Residual total field aeromagnetic map over the Yellowstone National Park. Both the international geomagnetic reference field and a least squares quadratic surface fitted to the data have been removed.

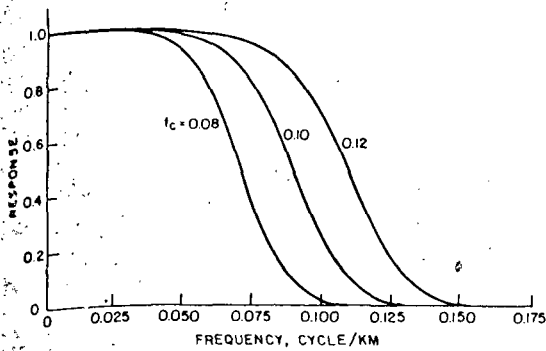


Fig. 2. Radial frequency-domain response of three zero phase, low-pass filters with different cutoff frequencies designed for and applied to the Yellowstone residual magnetic map.

In the following paragraphs we shall first consider the analysis of the data in a block.

As noted before, the residual data cover an area, 131 km by 131 km, and contain (64 × 64) data points. Let us then consider a block of (16 × 16) data points with an areal coverage of 31 km by 31 km. If the total area is now divided into overlapping blocks of this size with one half of the area of one block shared by the succeeding block, the total number of blocks available for analysis becomes 49.

The data in each block are analyzed in the frequency domain. Let us now consider one block alone. Since discontinuities in data values at the edges of the area give rise to the Gibbs phenomenon and aliasing, it is assumed that the residual field vanishes at a point which is located at a distance of 1 unit of data spacing from the boundary of the block. Inclusion of these points results in (18 × 18) nonequispaced data points in the block. Bicubic splines [Bhattacharyya, 1969] are

then fitted to the data in such a way that the residual field and the continuity of the first and second derivatives are maintained at each of the data points. These splines are used to generate (64 × 64) data points over the extended area of the block.

The two-dimensional spectrum $F_0(u, v)$ of the new set of data in the block is obtained with the help of the fast Fourier transform algorithm. $F_0(u, v)$ is therefore the discrete Fourier transform of the magnetic data. The angular frequencies u and v correspond to the x and y axes, respectively. Now, by using a method outlined in a paper by Bhattacharyya and Leu [1975], the spectra $F^x(u, v)$ and $F^y(u, v)$ of the first-order x and y moments, respectively, of the residual field are computed.

In the block under consideration there may be a few bodies producing anomalies. The mean location $(\bar{x}, \bar{y}, \bar{h})$ of the centroid of these bodies is determined with the help of the following equations in the low-frequency region:

$$\bar{x} - \frac{i u \bar{h}}{s} = \frac{F^x(u, v)}{F_0(u, v)} - i \frac{u}{s^2} \tag{2}$$

$$\bar{y} - \frac{i v \bar{h}}{s} = \frac{F^y(u, v)}{F_0(u, v)} - i \frac{v}{s^2}$$

where $s^2 = u^2 + v^2$.

The above equations are valid at high geomagnetic latitudes. The frequency range in both u and v selected for this computation runs from the fundamental frequency to its fifth harmonic. For several frequencies in this region, \bar{x} , \bar{y} , and \bar{h} are calculated, and the average of their values provides a good estimate of the location of the centroid. With careful choice of frequencies the accuracy of this estimate can be kept fairly high. However, it should be noted that the effect of shallow sources, unless removed completely from the data, will produce error in the estimate.

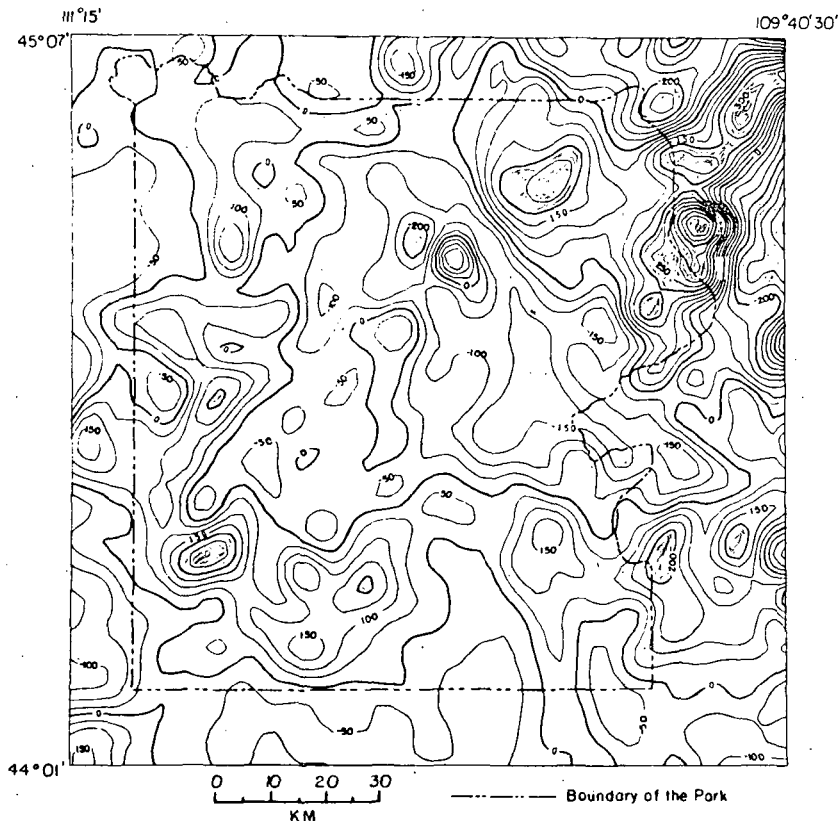


Fig. 3. Filtered map of the residual total field, after application of the 0.10-cycles/km low-pass filter.

OF MAGNETIC BODY

Next, the radial spectrum $F_0(s)$ is generated by evaluating, with the help of $F_0(u, v)$, the amplitude spectrum along the line at 45° with the frequency axes. The spectra $F^x(s)$ and $F^y(s)$ of the first-order x and y moments of the residual field are then computed. A combination of $F_0(s)$, $F^x(s)$, and $F^y(s)$ is used to determine the mean depth to the tops of magnetized bodies for the block. Again, for the sake of accuracy the range of frequency should not exceed the tenth harmonic of the fundamental frequency.

With the average location of the centroid and the mean depth to the tops of magnetized bodies known, it is simple and straightforward to calculate the mean depth to the bottoms of these bodies. The calculated depth is interpreted as the depth to the Curie point isotherm for the block.

The spectral analysis briefly discussed in the preceding paragraphs is applied not only to the data of each of the 49 blocks but also to individual anomalies found suitable for study throughout the area. The total number of anomalies studied in this way was 35.

RESULTS OF ANALYSIS

Figure 4 presents the calculated depths, rounded off to the nearest whole kilometer, to what we believe to be the Curie point isotherm with respect to sea level. The circle and triangle symbols indicate the locations of the centers of anomalies and blocks, respectively. The central part of the caldera is marked by a very shallow Curie isotherm at a depth of only 5–6 km. The closed 6-km-depth contour that is centered within the ring fracture zone of the caldera coincides very closely with the zone of observed attenuation for compressional seismic waves from local earthquakes, as shown by *Eaton et al.* [1975, Figure 5]. The isotherm outside the central part, but within the caldera rim, lies generally at a depth of 6–8 km. Around the southeastern and southern sections, just outside the rim, there are a few places with significantly shallow depths (4–6 km) of the isotherm, possibly indicative of the presence of local hot

spots. Small scattered areas of surface hydrothermal alteration are seen to occur in association with them [*Eaton et al.*, 1975, Figure 3], but the relationship is not as marked as in the interior of the caldera. Further to the southeast, the isotherm seems to be deepening. In the northwestern section outside the rim, the depths of the isotherm are, in general, greater than 10 km. It is perhaps of significance that the general trend of the isotherm contours is northeast-southwest, parallel to and coextensive with the axis of the Snake River Plain with which the park has shared a common volcanic history. We are presently engaged in an examination of magnetic data for the Snake River Plain and upon its completion will have a clearer understanding of the regional depth to the base of the magnetized section outside the park.

The average elevation of the ground surface in Yellowstone National Park is about 2.5 km above sea level. Taking this elevation into account and assuming a Curie point temperature of 560°C , the temperature gradient seems to fall between $66^\circ\text{C}/\text{km}$ and $72^\circ\text{C}/\text{km}$ in the central part of the caldera. The remaining parts of the caldera have a gradient somewhere between $53^\circ\text{C}/\text{km}$ and $66^\circ\text{C}/\text{km}$. These figures are anomalously high for heat flow in continental areas. The continuation well to the east of the caldera, into an area underlain by Tertiary volcanic rocks, is puzzling and merits further investigation.

This study finds a strong correlation between geothermal hot regions and the thickness of the magnetized crust. A picture of the isotherm level as shown in Figure 4 suggests the presence of an extremely high degree of geothermal activity. This study therefore leads to the conclusion that appropriate analysis of aeromagnetic data can play an important role in regional reconnaissance for potential geothermal energy resources.

Acknowledgments. This work has been supported by the U.S. Geological Survey grant 14-08-0001-G-101. The authors are grateful to Gordon P. Eaton of the U.S. Geological Survey in Denver for his

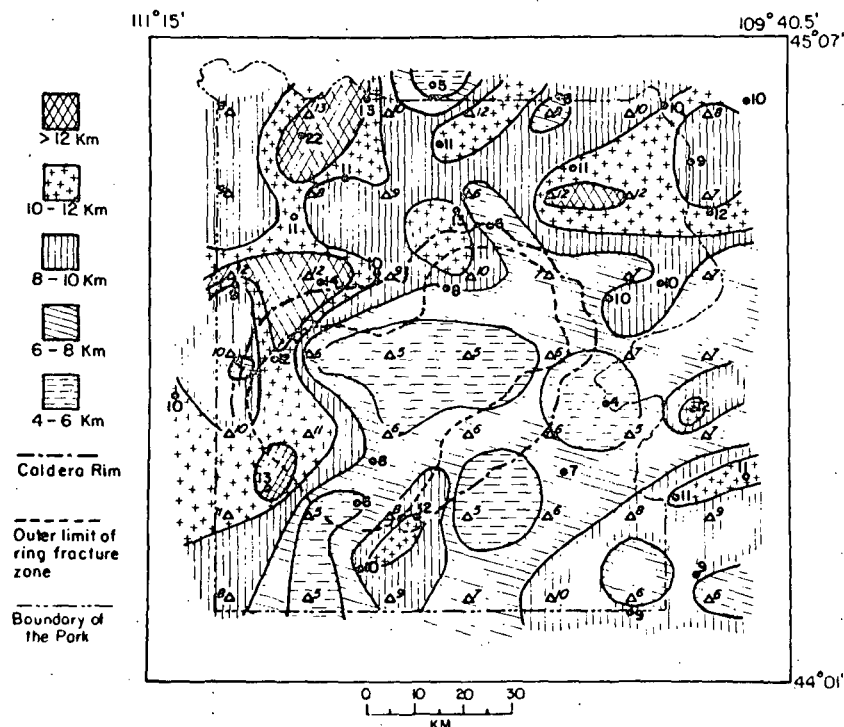


Fig. 4. Contoured map of the depths to the Curie point isotherm. Circles and triangles represent the locations of the centers of individual anomalies and grid blocks, respectively.

critical and thoughtful suggestions for improvement.

Bhattacharyya, B. K. treatment of potential magnetic anomalies. *Journal of Geophysical Research*, 1975, vol. 80, p. 10,000. *The Structure and Petrology of the Snake River Plain*, D. C. Eaton, Ed., R. L. Ch

critical and thoughtful review of the paper and for his many excellent suggestions for improving its presentation.

REFERENCES

- Bhattacharyya, B. K., Bicubic spline interpolation as a method for treatment of potential field data, *Geophysics*, **34**, 402, 1969.
- Bhattacharyya, B. K., and L. Leu, Spectral analysis of gravity and magnetic anomalies due to two-dimensional structure, *Geophysics*, **40**, in press, 1975.
- Blackwell, D. D., The thermal structure of the continental crust, in *The Structure and Physical Properties of the Earth's Crust*, *Geophys. Monogr. Ser.*, vol. 14, edited by J. G. Heacock, pp. 169-184, AGU, Washington, D. C., 1971.
- Eaton, G. P., R. L. Christiansen, H. M. Iyer, A. M. Pitt, D. R. Mabey, H. R. Blank, Jr., I. Zietz, and M. E. Gettings, Magma beneath Yellowstone National Park, *Science*, **188**, 787, 1975.
- Shuey, R. T., D. K. Schellinger, E. H. Johnson, and L. B. Alley, Aeromagnetism and the transition between the Colorado plateau and Basin range provinces, *Geology*, **1**, 107, 1973.
- Smith, R. B., R. T. Shuey, R. O. Friedline, R. M. Otis, and L. B. Alley, Yellowstone hot spot: New magnetic and seismic evidence, *Geology*, **2**, 451, 1974.
- U. S. Geological Survey, Aeromagnetic map of Yellowstone National Park and vicinity, Wyoming-Montana-Idaho, open file map, Denver, Colo., 1973.

(Received April 25, 1975;
revised July 2, 1975;
accepted July 31, 1975.)

AREA
WY
HotSpgs
Thermop
Springs

THE JOURNAL OF GEOLOGY

A Semi-Quarterly Magazine of Geology and
Related Sciences

VOLUME 14

1906

UNIVERSITY OF UTAH
RESEARCH INSTITUTE
EARTH SCIENCE LAB.

Reprinted with the permission of the original publishers

JOHNSON REPRINT CORPORATION
NEW YORK, NEW YORK

THE HOT SPRINGS AT THERMOPOLIS, WYOMING

N. H. DARTON

At the southern end of the Bighorn Basin there is a great spring which presents some notable geologic features and an interesting question as to the source of the hot water. The spring at the town of Thermopolis, a village and health resort which owes its existence largely to the reputed therapeutic value of the water. The locality is on the bank of Bighorn River, a few miles north of a high range which may be regarded as the southwestern continuation of the Bighorn Mountains. There are several springs, one of them has by far the greatest volume. They issue from the red beds, here brought to the surface by a prominent local anticline. The present springs and their predecessors—for the region has been one of thermal activity for many centuries—have been extensive terraces of travertine or hot spring deposits similar to some of those in the Yellowstone National Park.

The geologic structure at Thermopolis is relatively simple. Owing to the extensive exposures of the formations, it is perfectly plain. The cross-section (Fig. 1) shows the relations from the crest of the Bighorn uplift in the mountain summit 10 miles or more to a point a few miles north of the springs.

South of the springs there is the long monocline consisting of the north slope of the anticline of Bighorn Mountains, and in the vicinity of Thermopolis this monocline is crenulated by a small anticline. The axis of this flexure crosses Bighorn River, a short distance north of Thermopolis, and along it there are exposed the Chugwater red beds, while on either side is a succession consisting of Sundance (Jurassic), Morrison, Cloverly ("Dakota"), and Benton formations. The dips on the south limb of the anticline are 50° to 65°, while those on the north side are gentle. The Cloverly sandstone on either side gives rise to a prominent "hogback" ridge

¹ Published with permission of the Director of the U. S. Geological Survey.

shown in the distance in the upper view in Fig. 2, facing a region of red bed hills about a mile wide and with outer slopes descending to valleys of Benton basal shales. Thermopolis is on the eastern limb of the anticline, the village extending across the outcrop zones of the Sundance, Morrison, and Cloverly formations, locally covered by an alluvial plain which extends back a few hundred rods from the river. There is no evidence of igneous rocks in the region.

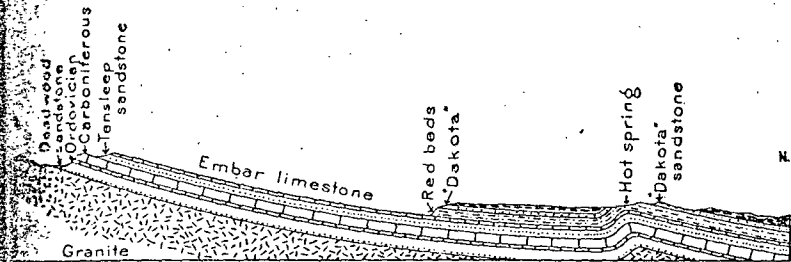


FIG. 1.—Section through the hot springs at Thermopolis, Wyo. Looking west. Length of section about fourteen miles.

The springs rise from the middle beds of the Chugwater formation, apparently through a number of deep cracks. The largest one issues from the foot of a high bank of 80 feet of red sandstones, as shown in Figs. 2 and 2a, with a volume stated to be over a thousand gallons a second. The water is clear and hot, having a temperature of 135°. It flows over a wide terrace built of hot-spring deposits, over the edge of which it falls into the river. A part, however, is diverted into conduits of various kinds which lead to various bathhouses, and to the reservoirs in which a portion of the water is cooled so that it may be used for diluting the hot water to the required temperature for bathing. The spring flows with great force, and evidently comes from considerable depth under high pressure. Numerous algæ of various colors grow in the hot cooling water, as in the Yellowstone Park and other places. Besides the main spring, there are on the east side of the river a hot pool which does not overflow and, some distance farther north, a hot sulphur spring which gushes out of the travertine bank 200 feet above the river. On the west side are several small springs, one of which is utilized for a bathhouse and swimming-

pool. An analysis of the water from the great spring, by Professor E. E. Slosson is as follows:

ANALYSIS OF WATER FROM HOT SPRINGS AT THERMOPOLIS, WYO.

	Grains per Gallon
SiO ₂	4.986
Fe ₂ O ₃ and Al ₂ O ₃	0.227
K Cl	10.249
Na ₂ SO ₄	15.110
Mg ₂ SO ₄	19.443
Ca SO ₄	13.156
Ca CO ₃	40.454
Na Cl	26.193
Total	129.820

Hot Spring deposits.—The hot-spring deposits in the vicinity of Thermopolis indicate a long period of accumulation, for they occur on several distinct terraces, some of which date back probably to Tertiary time. The most recent deposits are being laid down on a broad terrace about 30 feet above the river, which is being built up very gradually. No precise estimate has been made of the rate of increase, but objects placed in the water are rapidly coated with the deposit, and a thickness of an eighth of an inch is accumulated in a short time. There are wide areas of the deposit on both sides of the river below the present springs, which were formed at a distant date, while, on the buttes which rise above this terrace there are caps of hot-spring deposits at various elevations. Some of the relations of these are shown in Figs. 3 and 4. The highest deposit caps a prominent butte near the cemetery, at an altitude of about 700 feet above the river. A larger terrace remnant remains on a butte which rises immediately west of the river to a height of about 350 feet above the water. It is probable that these terraces represent three distinct stages of deposition, and, although possibly hot-spring action has been continuous since the formation of the first or highest terrace, most of the deposits at intermediate levels have been removed. As travertine is often deposited on slopes, it is possible that the hot-spring waters issuing at the level of the higher buttes flowed to somewhat lower levels, with a continu-

deposit from one to the other. It is evident, however, from the relations that there has been extensive erosion since the earliest period marked by the higher terraces on which the travertine caps are now found. The high butte near the cemetery—the one shown to the left in Figs. 3 and 4—is probably the remnant of a much

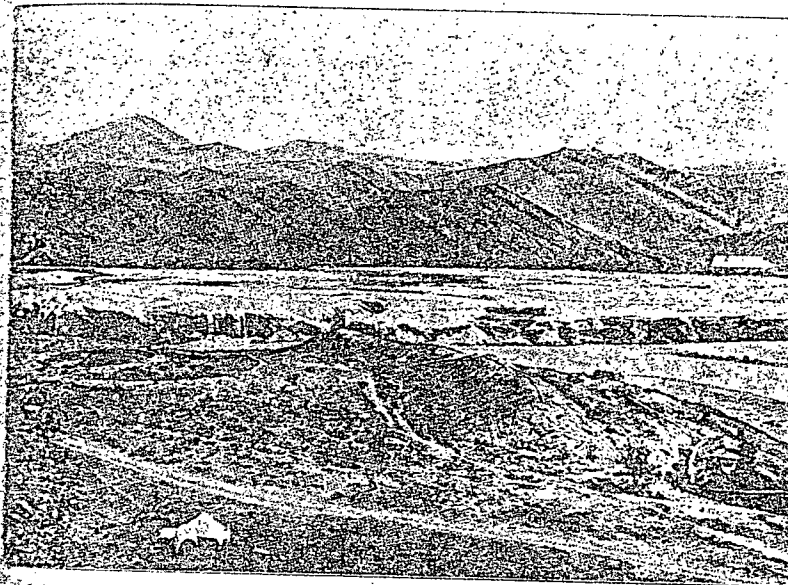


FIG. 2.—Travertine terrace of the Great Hot Spring on the east bank of Bighorn River near Thermopolis, Wyo. The spring is under the S. In the foreground are distinct hot-spring craters and a low ridge with long fissure in its summit. Shows upturned red beds and overlying formations.

more extended sheet of the travertine which was largely removed prior to or during the development of the lower terraces.

It is evident, from the disposition of the material, that the springs have shifted their position, but in general the outflow has been in the immediate vicinity of the crest of the anticline. The hot-spring deposits show remnants of numerous hot-spring craters and cracks, some of the most marked of which are on the terraces near the river. On the west bank, a short distance north of the bathhouse, there is an empty crater 30 feet in diameter, shown in Fig. 2, indicating the former existence of a large hot pool, and there is another similar

crater of still larger size, a short distance northeast of the sulphur spring on the east bank. One of the same character, but much less distinct, is found on the high terrace west of the cemetery, 500 feet above the river. It is probable, from the present appearance

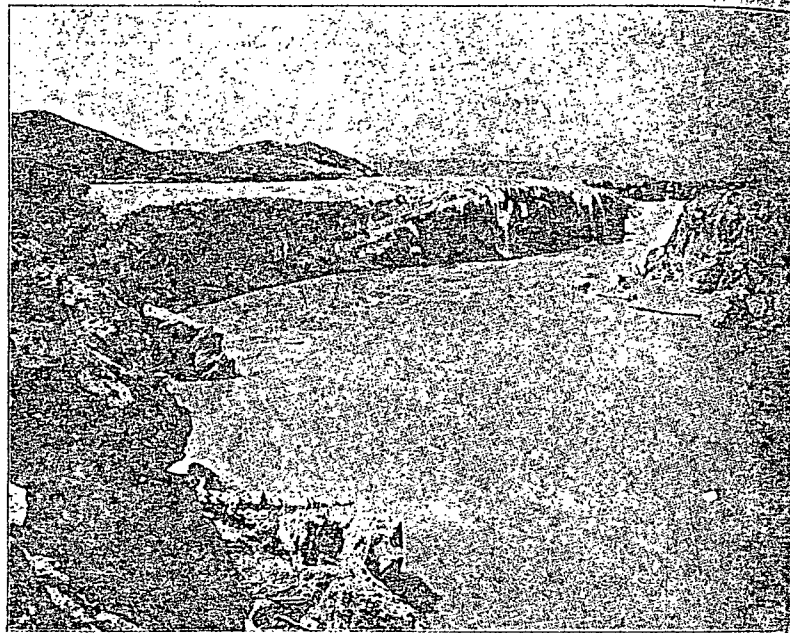


FIG. 2a.—Terrace of hot-spring deposit on the bank of Bighorn River. Looking south to Thermopolis, with Owl Creek Mountains in the distance. Shows overflow of hot spring.

of the deposits, that formerly the hot-spring activity was much greater than at present. Whether or not there were geysers is difficult to state, but some of the features of the deposits strongly suggest

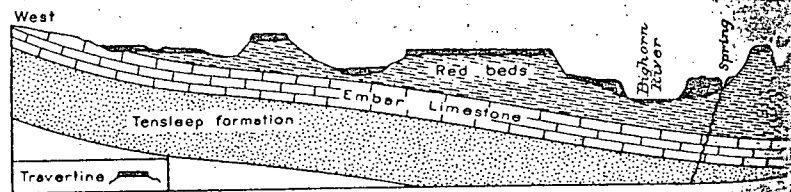


FIG. 3.—Cross-section of travertine terraces a short distance north of Thermopolis, Wyo. Looking north. Length of section about one mile.

that if the water was not thrown out by geyser action, it at least flowed in large volume.

Source of the water.—The source of the water in the Thermopolis springs is difficult to ascertain, but undoubtedly the flow is not derived from the adjacent Red beds, nor from the underlying Embar limestone. Probably the strata are somewhat fractured in the

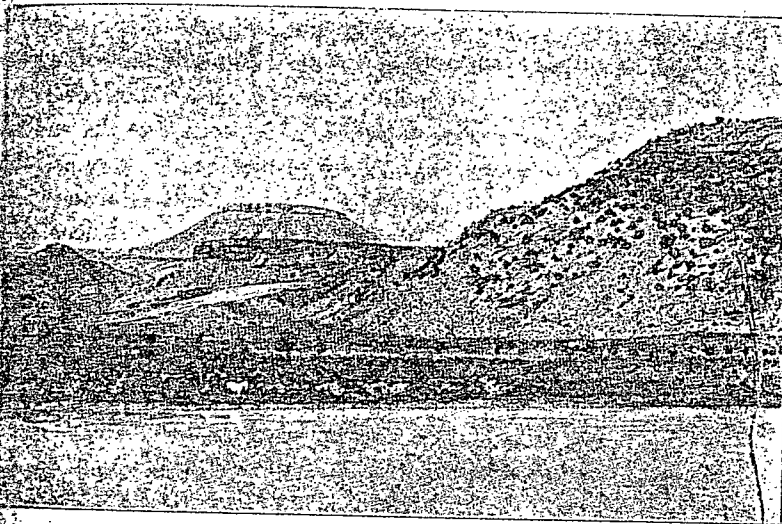


FIG. 4.—Hot Spring deposits on old terraces at various heights in western part of Thermopolis, Wyoming. Looking south across Bighorn River.

rest of the arch and permit the escape of the water from deep-seated sources. One of the most likely of these might be thought to be the porous Tensleep sandstone which outcrops high on the mountain slopes southward. It undoubtedly carries a water supply which passes beneath the syncline south of Thermopolis, and retains sufficient head to rise to and above the surface in any part to the northward. If the water is from no greater depth than this horizon, there is difficulty in accounting for the high temperature, for the top of the sandstone does not lie at a greater depth than 500 feet at the spring and 2,000 feet in the bottom of the syncline a short distance south. Assuming that the mean annual temperature at Thermopolis is 50°, and that the temperature of water increases one degree for every 50 feet underground below

the first 50 feet—where the mean annual temperature is the underground temperature—a depth of 4,300 feet would be required for the spring water to become heated to 135° under ordinary conditions. As the granite probably lies only 2,500 feet below the spring or 4,000 feet below the surface in the syncline south, this rate of increase would indicate a source at least as low as the base of the Deadwood formation. If the water is derived from the base sandstone of that formation, it passes underground in the outcrop area in the high mountain slopes to the southeast, and becomes heated in the bottom of the syncline a short distance south of Thermopolis. In order to preserve this heat in its course to the outlet, there must exist cavernous channels affording rapid flow, as heat would be lost in slow percolation through the interstices of the rock. It is possible also that the source of the water is much less deep, and the heat may be due to deep-seated igneous rocks in this vicinity which have not yet cooled. As the nearest outcrops of igneous rocks are in the Shoshone Mountains 40 miles west, it appears improbable that there are any intrusions under the Thermopolis region.

THE SEDIMENTARY ROCKS OF SOUTH MOUNTAIN, PENNSYLVANIA¹

GEORGE W. STOSE

The area described in this paper is the western portion of South Mountain, Pa., and the adjacent part of the Cumberland Valley near the Maryland state line to the vicinity of Shippensburg. It is about 15 miles in length. The accompanying topographic map of this area (Fig. 1) is taken from the Chambersburg part of the United States Geological Survey and the South Mountain atlas of the Pennsylvania Geological Survey. South Mountain is the local name for the Blue Ridge which parallels the Great Valley of the Appalachian Province on the east, and Cumberland Valley, a section of the Great Valley.

TOPOGRAPHY

The Cumberland Valley is a broad, rolling lowland extending from the Potomac River to the Susquehanna River. Its general elevation is from 400 to 800 feet, and scattered, low eminences rise to 1,100 feet. These hills are usually of the rounded form characteristic of limestone country, but in part they are shale tablelands with steep escarpments. The valley has a width of approximately 15 miles in the vicinity of Harrisburg, but expands to 20 miles in the area under discussion. The southern half of the valley is drained by Conococheague Creek and its tributaries into the Potomac, the northern half by Yellow Breeches Creek into the Susquehanna. South Mountain is a more or less irregular aggregate of ridges with a general northeast-southwest trend. Although cut across by numerous gaps, and deflected in places by sharp bends, the ridges maintain a marked continuity. The mountain front rises abruptly from the plain to elevations of 1,700 or 1,900 feet. The higher ridges are generally higher, reaching 2,100 feet in places, and as they decline again eastward into lower hills.

¹Published by permission of the Director of the U. S. Geological Survey.

AREA
BY
HotSpgs
Sulfur

DEPARTMENT OF THE INTERIOR
UNITED STATES GEOLOGICAL SURVEY
GEORGE OTIS SMITH, DIRECTOR

BULLETIN 380

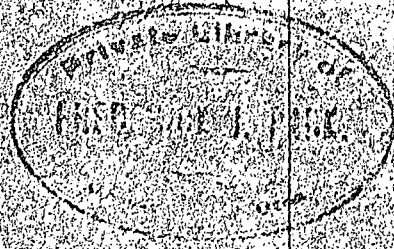
CONTRIBUTIONS
TO
ECONOMIC GEOLOGY

UNIV. OF UTAH

ENGINEERING LIBRARY

PART I—METALS AND NONMETALS, EXCEPT FUELS

C. W. HAYES AND WALDEMAR LINDGREN
GEOLOGISTS IN CHARGE



WASHINGTON

GOVERNMENT PRINTING OFFICE

1909

UNIVERSITY OF UTAH
RESEARCH INSTITUTE
EARTH SCIENCE LAB.

UNIVERSITY OF
RESEARCH INSTITUTE
EARTH SCIENCE LAB.

Woodruff

TRAVERTINE AND SULPHUR.

NATURE AND OCCURRENCE.

tains northeastward to the valley of Owl Creek. The rocks in this small anticline have been sharply folded and probably sufficiently fractured along the crest to form passages, through which the heated water escapes to the surface.

HOT SPRINGS.

At the present time one mammoth hot spring and several small ones are discharging their water into Bighorn River near Thermopolis, at a rate estimated to be 3,000 to 4,000 gallons a minute. The water issues from the large spring at a temperature of 135° F. The odor of hydrogen sulphide is strong about the spring and the quantity of carbon dioxide escaping indicates that the water is saturated with that gas also. An analysis has shown potassium, sodium, magnesium, calcium, and iron salts in large quantities. These salts are deposited when the water spreads out and cools, and in this way the terraces are built up.

Though the springs are now building their terraces rapidly, there is evidence that they have had a long period of activity and that they have been distributed over several square miles, as extinct cones and terraces along the river show a wider distribution at about the present level. The earlier positions of the springs are indicated by the terraces at various levels along the side and crest of the anticline. One bed of travertine caps a mesa 3 miles northwest of Thermopolis and 700 feet higher than the mammoth spring. This does not indicate, however, that the travertine is 700 feet thick at any one point, but that there has been continuous deposition while the streams of the region have lowered their channels that amount. Although the travertine is not thick its distribution is rather widespread, as is shown by remnants of terraces over an area of several square miles. It is most extensive adjacent to Bighorn River, but occurs at short intervals on the crest and slopes of the anticline between the river and Owl Creek. The remnants of the travertine are too few and scattered to determine with precision the previous extent of these beds or their greatest thickness. The first springs seem to have been situated at the crest of the anticline, about 3 miles northwest of Thermopolis; since they began to issue there has been a gradual progression toward the present site on Bighorn River, the springs probably following the stream in its meandering and downward cutting. To the west, however, there seem to have been two periods of activity, one along the crest of the anticline and another, of later date, during which the travertine and sulphur were deposited along the base of the uplift.

The travertine is composed in part of carbonate of lime and in part of sulphate of lime in small crystals of the mineral selenite, which seems to be an alteration product due to the action of the sulphur waters. It occurs in small irregular plates formed by the evaporation of the water on plane surfaces or in fibers when deposited about the threads of algæ, which are abundant in the thermal waters. The travertine generally contains some native sulphur in isolated crystals or small nodules, but the quantity of the mineral is too small to be extracted with profit. The minable sulphur deposits occur in the altered Embarras limestone which lies immediately below the travertine and through which the sulphur-bearing waters passed in their course to the surface. The sulphur seems to be present in very irregular deposits or pockets about the sites of extinct springs, where the sulphur-bearing water came into contact with the limestone. Few if any of these deposits exceed 100 feet in horizontal diameter; their depth is uncertain, but probably the beds do not connect with large deep-seated masses. One drill hole is reported to have passed through 30 feet of barren rock before entering the ore, and then to have continued for 15 feet in the mineral without reaching its base. There is no uniformity in the shape, size, or arrangement of these ore-bearing pockets. In general they occur in groups where the sulphur-bearing waters found passage to the surface through a number of vents. The number and arrangement of these pockets in the groups depend, therefore, on varying subterranean conditions which can not be determined from a surface investigation. The cross section (fig. 2S) shows the relation of the travertine and sulphur to the structure of the region.

Native sulphur in this district occurs in two forms—in small yellow crystals filling veins or cavities in the rocks, and in a massive form where the original structure of the limestone is retained, but where the calcium carbonate is replaced by the sulphur. The sulphur is found in crevices, channels, or cavities such as water courses make where they traverse limestone beds. The cavities seem to be portions of subterranean channels through which the hot sulphur-bearing waters flowed and on the walls of which the sulphur was gradually deposited until the chambers were completely filled or, in some places, only partly filled before the passage was stopped at some point and the water diverted to other channels. As previously stated, no regular arrangement of the cavities can be discovered, though they seem to occur in groups at places where the water found free passage. In the areas between the groups of cavities only a small amount of

After the sulphur is cooled and pulverized to an impalpable powder it is then packed in sacks and taken to various points in Wyoming.

of 20 tons a day, but has according to a statement of December 15, 1908, the amount of sulphur and was then round sulphur is reported

SURVEY PUBLICATIONS ON SULPHUR AND PYRITE.

The list below includes the important publications of the United States Geological Survey on sulphur and pyrite.

These publications, except those to which a price is affixed, may be obtained free by applying to the Director, U. S. Geological Survey, Washington, D. C. The priced publications may be purchased from the Superintendent of Documents, Government Printing Office, Washington, D. C.

- ADAMS, G. I. The Rabbit Hole sulphur mines, near Humboldt House, Nev. In Bulletin No. 225, pp. 497-500. 1904. 35c.
- DAVIS, H. J. Pyrites. In Mineral Resources U. S. for 1885, pp. 501-517. 1886. 40c.
- ECKEL, E. C. Gold and pyrite deposits of the Dahlonega district, Georgia. In Bulletin No. 213, pp. 57-63. 1903. 25c.
- Pyrite deposits of the eastern Adirondacks, N. Y. In Bulletin No. 260, pp. 587-588. 1905. 40c.
- LEE, W. T. The Cove Creek sulphur beds, Utah. In Bulletin No. 315, pp. 485-489. 1907.
- MARTIN, W. Pyrite. In Mineral Resources U. S. for 1883-84, pp. 877-905. 1886. 60c.
- PHALEN, W. C. Sulphur and pyrite. In Mineral Resources U. S. for 1907, pt. 2, pp. 673-683. 1908.
- RANSOME, F. L. Geology and ore deposits of Goldfield, Nev. Professional Paper No. 66. (In press.)
- RICHARDSON, G. B. Native sulphur in El Paso County, Tex. In Bulletin No. 260, pp. 589-592. 1905. 40c.
- ROTHWELL, R. P. Pyrites. In Mineral Resources U. S. for 1886, pp. 650-675. 1887. 50c.
- SPURR, J. E. Alum deposit near Silver Peak, Esmeralda County, Nev. In Bulletin No. 225, pp. 501-502. 1904. 35c.
- WOODRUFF, E. G. Sulphur deposits at Cody, Wyo. In Bulletin No. 340, pp. 451-456. 1908.

UNITED STATES
DEPARTMENT OF THE INTERIOR
J. A. KRUG, SECRETARY

BUREAU OF MINES
R. R. SAYERS, DIRECTOR

REPORT OF INVESTIGATIONS

EXPLORATION OF THE BRUTCH SULFUR DEPOSITS
HOT SPRINGS COUNTY, WYO.

UNIVERSITY OF UTAH
RESEARCH INSTITUTE
EARTH SCIENCE LAB.



BY

FOREST H. MAJORS

REPORT OF INVESTIGATIONS

UNITED STATES DEPARTMENT OF THE INTERIOR - BUREAU OF MINES

EXPLORATION OF THE BRUTCH SULFUR DEPOSITS
HOT SPRINGS COUNTY, WYO.^{1/}

By Forest H. Majors^{2/}

INTRODUCTION

The Brutch sulfur deposits were explored by the Bureau of Mines during the spring and summer of 1944. Old workings were rehabilitated and sampled, test pits and shafts were sunk, and trenches were cut through the surface alluvium.

ACKNOWLEDGMENTS

In its program of exploration of mineral deposits, the Bureau of Mines has as its primary objective the more effective utilization of our mineral resources to the end that they make the greatest possible contribution to national security and economy. It is the policy of the Bureau to publish the facts developed by each exploratory project as soon as practicable after its conclusion. The Mining Branch, Lowell B. Moon, chief, conducts preliminary examinations, performs the actual exploratory work, and prepares the final report. The Metallurgical Branch, R. G. Knickerbocker, chief, analyzes samples and performs beneficiation tests. Both these branches are under the supervision of Dr. R. S. Dean, assistant director.

Special acknowledgment is due S. R. Zimmerley, regional engineer, and Paul T. Allsman, principal engineer, Bureau of Mines, Salt Lake City, for their supervisory aid, and to the metallurgical staff, Salt Lake City, for beneficiation of samples.

LOCATION AND ACCESSIBILITY

The Brutch property is 3-1/2 miles northwest of Thermopolis, Hot Springs County, Wyo. (figs. 1 and 2). It may be reached from Thermopolis over State highway 120, which continues northwest through Cody, Wyo. U. S. highway 20 also passes through Thermopolis.

The Chicago, Burlington & Quincy Railroad passes through Thermopolis, and connects with the Chicago & Northwestern line at Shoshoni, Wyo.

^{1/} The Bureau of Mines will welcome reprinting of this paper provided the following footnote acknowledgment is used: "Reprinted from Bureau of Mines Report of Investigations 3964."

^{2/} Mining engineer, Salt Lake City Division, Mining Branch, Bureau of Mines.

PHYSICAL FEATURES AND CLIMATE

The topography of the area is characteristic of central Wyoming - moderate relief and treeless, rolling hills. Altitudes range from 4,600 feet in Owl Creek Valley to over 5,000 feet at the crest of the asymmetrical anticline which contains the sulfur deposits. Owl Creek, which flows along the northeast side of the anticline and empties into the Big Horn River at Thermopolis, is a perennial stream fluctuating in volume with the seasons.

The climate in the Thermopolis area is typical of central Wyoming. Summers usually are hot and dry, with considerable wind. Winters are severe with high winds and many ground blizzards.

HISTORY AND PRODUCTION

Mining claims were located as early as 1908 in the Owl Creek side of the anticline, and a plant for the extraction of sulfur was constructed. A thermal process was employed, but, as shown by tailing piles, which assay as much as 10 percent sulfur, poor recovery was made. The process consisted essentially of enclosing cars of hand-mined and sorted raw ore in a cylindrical steel retort and injecting steam to melt the sulfur. As late as 1922, 1923, a similar plant was operated on the opposite limb of the anticline. As shown by tailings and pit workings in this area, the operation did not continue long and was terminated by an underground fire in 1923. The mill workings are reported to have been hand-sorted to a 30-percent sulfur content. The portals of the main workings were closed, and superficial investigation indicates that the workings are caved. Toxic gases emanate from the portals as hydrogen sulfide, carbon dioxide, and sulfur dioxide.

Production records are not obtainable. However, judging by the size of the tailing dumps and the mine dumps, production was not large.

PROPERTY AND OWNERSHIP

The Brutch sulfur property comprises 550 acres: SE1/4 sec. 20; NE1/2 sec. 28; NW1/4 NE1/4 SW1/4, S1/2 NE1/4 SW1/4, SE1/4 SW1/4, and W1/2 SW1/4 sec. 21; and the SE1/4 NW1/4, S1/2 NE1/4, and NE1/4 SE1/4 sec. 28, T. 43 N., R. 95 W., sixth principal meridian. Eighty acres are held by deed and the remainder by placer location. Lin I. Noble, Thermopolis, Wyo., is attorney in fact for the owners.

DESCRIPTION OF THE DEPOSITS

The sulfur deposits of the Brutch occur along both limbs of a north-west-trending asymmetrical anticline for approximately half a mile on the northeast limb and 1-1/2 miles on the southwest limb (figs. 2 and 4).

Sulfur pods and lenses ranging from a few inches to more than 100 feet in horizontal diameter, enclosed in travertine, mantel rock, or limestone, represent the better-grade deposits in the area. Other types of deposits are

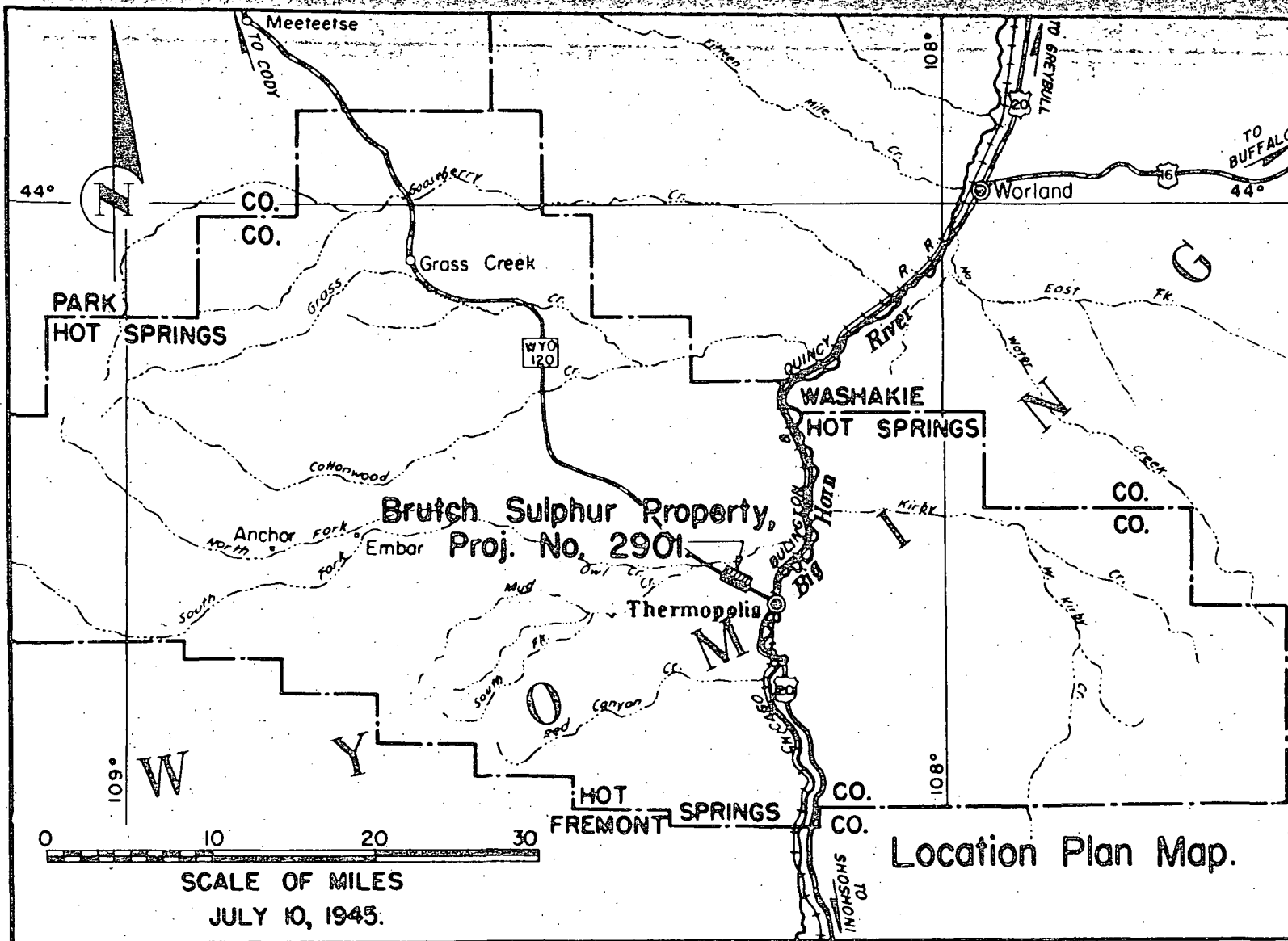


Figure 1. - Location Map, Brutch Sulphur, Thermopolis, Hot Springs Co., Wyoming.

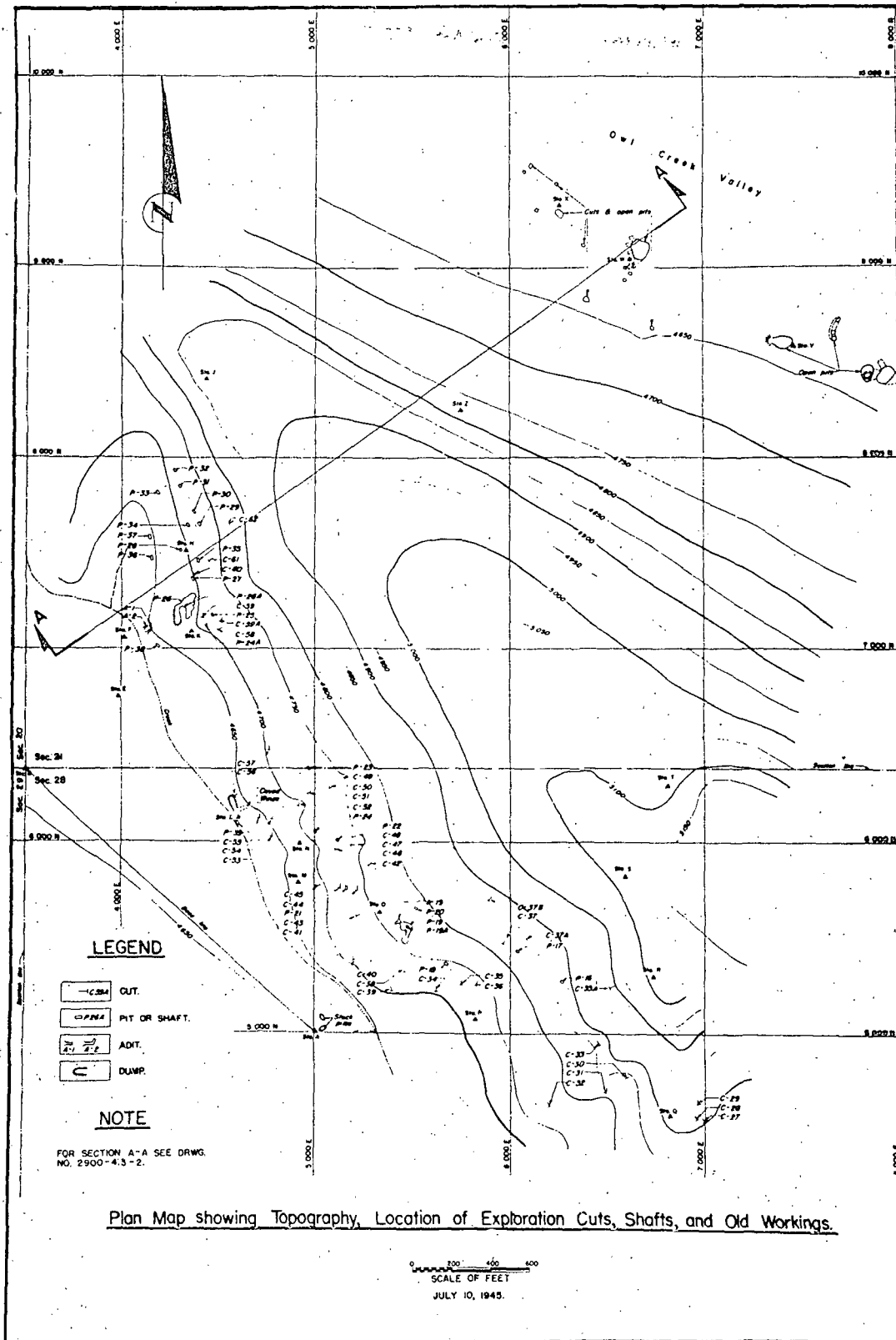


Figure 2. - Plan of Brutch Sulphur Property, near Thermopolis, Hot Springs Co., Wyoming.

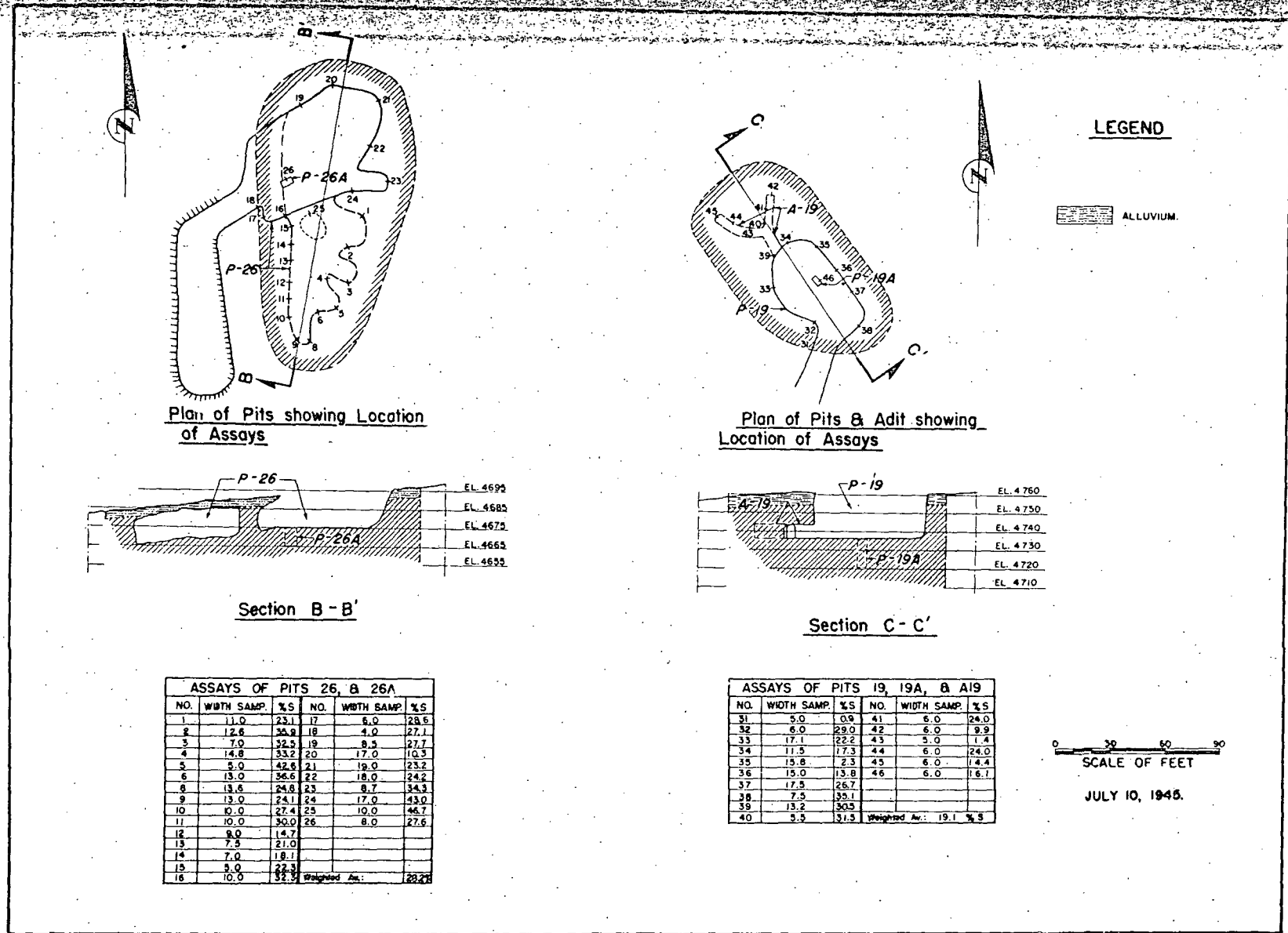


Figure 3. - Plans, Sections, Assays, & Inferred Ore, Brutch Sulphur Property, near Thermopolis, Hot Springs Co., Wyoming.

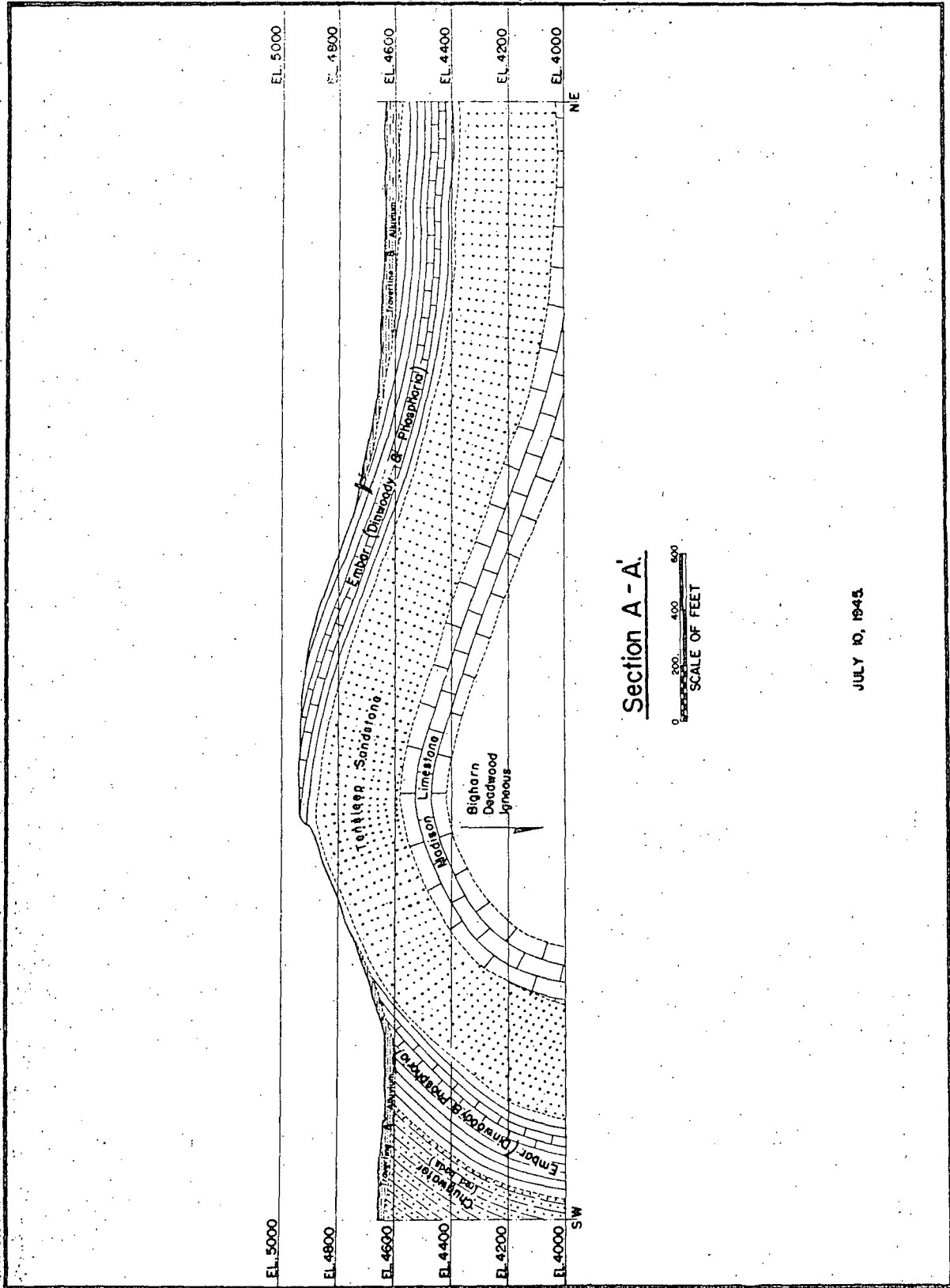


Figure 4. - Section A-A, Brutch Sulphur Property, near Thermopolis, Hot Springs Co., Wyoming.

incrustations along solution channels and dissemination of sulfur in limestone. Gypsum is associated with the deposits, probably as an alteration product.

Excavations in the sulfur areas have exposed sulfur to a depth of slightly more than 100 feet. These openings further demonstrate the erratic occurrence of the deposits, in which sulfur is abundantly exposed in one place and is entirely absent.

Abundant evidence of extinct hot springs in the area and the occurrence of hot water in one working indicate that hot water may have been an agent in the formation of the deposits.

THE ORE

Two forms of elemental sulfur are found on the property - the yellow crystalline variety and a massive brown to almost black sulfur that apparently is a replacement of limestone. Sulfur is associated with soluble salts of sodium, calcium, magnesium, and aluminum. Gypsum is also a common constituent in the travertine incrustations of the hot springs. Gangue rock consists of altered shale and limestone.

A chemical analysis of a sample from pit 19 follows:

Total S	Elemental S	Insol.	SiO ₂	Fe	CaO	H ₂ O so	H ₂ O sol.
						Al ₂ O ₃	Al ₂ O ₃
32.0	27.8	47.2	41.6	0.75	6.3	4.9	1.0

Sampling and Analyses

Samples were cut in all accessible old and new workings giving evidence of sulfur. 219 samples were cut and assayed. Weighted analyses of groups of samples were made for convenience in listing the samples. These combinations are shown later in this paper. The resultant weighted sulfur averages and sample widths are shown in the following table. Sample locations are shown on figure 5.

Sample	Width sampled, ft.	Percent sulfur	Sample	Width sampled, ft.	Percent sulfur
1.....	10.0	0.7	12.....	7.5	35.1
2.....	9.2	32.2	13.....	13.2	30.5
3.....	4.0	8.0	14.....	5.5	31.5
4.....	Unsampled		15.....	6.0	24.0
5.....	5.0	.9	16.....	6.0	9.9
6.....	6.0	29.0	17.....	5.0	1.4
7.....	17.1	22.2	18.....	6.0	24.0
8.....	11.5	17.3	19.....	6.0	14.4
9.....	15.8	2.3	20.....	6.0	16.1
10.....	15.0	13.8	21.....	5.0	.6
11.....	17.5	26.7	22.....	Unsampled	

Sample	Width sampled, ft.	Percent sulfur	Sample	Width sampled, ft.	Percent sulfur
23.....	Unsampled		71.....	Unsampled	
24.....	10.0	.5	72.....	Unsampled	
25.....	16.0	3.7	73.....	3.0	12.9
26.....	12.9	3.9	74.....	5.0	14.6
27.....	20.0	4.8	75.....	5.5	16.4
28.....	11.0	23.1	76.....	5.5	30.0
29.....	12.6	35.9	77.....	4.0	1.2
30.....	7.0	32.5	78.....	5.5	8.2
31.....	14.8	33.2	79.....	5.5	5.0
32.....	5.0	42.6	80.....	3.0	.4
33.....	13.0	36.6	81.....	5.0	1.8
34.....	13.6	24.8	82.....	5.0	7.3
35.....	13.0	24.1	83.....	4.0	17.6
36.....	10.0	27.4	84.....	2.7	22.8
37.....	10.0	30.0	85.....	3.5	.2
38.....	9.0	14.7	86.....	4.0	.9
39.....	7.5	21.0	87.....	4.0	.4
40.....	7.0	18.1	88.....	10.0	1.0
41.....	5.0	22.3	89.....	5.0	.8
42.....	10.0	32.3	90.....	Unsampled	
43.....	6.0	28.6	91.....	3.7	.9
44.....	4.0	27.1	92.....	Unsampled	
45.....	8.5	27.7	93.....	Unsampled	
46.....	17.0	10.3	94.....	Unsampled	
47.....	19.0	23.2	95.....	4.5	0.9
48.....	18.0	24.2	96.....	3.0	25.3
49.....	8.7	34.3	97.....	4.0	16.5
50.....	17.0	43.0	98.....	5.0	2.4
51.....	10.0	46.7	99.....	Unsampled	
52.....	8.0	27.6	100.....	Unsampled	
53.....	14.3	5.2	101.....	Unsampled	
54.....	5.0	21.6	102.....	Unsampled	
55.....	5.0	4.2	103.....	Unsampled	
56.....	5.0	36.4	104.....	Unsampled	
57.....	5.0	13.6	105.....	Unsampled	
58.....	15.0	2.6	106.....	Unsampled	
59.....	16.2	33.5	107.....	Unsampled	
60.....	1.2	4.6	108.....	Unsampled	
61.....	10.8	11.9	109.....	5.0	.1
62.....	4.0	3.4	110.....	Unsampled	
63.....	12.0	3.4	111.....	5.0	.6
64.....	5.0	2.7	112.....	2.0	.7
65.....	8.9	5.1	113.....	Unsampled	
66.....	16.2	3.2	114.....	5.0	.6
67.....	1.3	11.9	115.....	Unsampled	
68.....	11.8	2.1	116.....	Unsampled	
69.....	9.2	2.7	117.....	Unsampled	
70.....	2.8	.6	118.....	5.0	.6

Sample	Width sampled, ft.	Percent sulfur	Sample	Width sampled, ft.	Percent sulfur
119.....	5.0	.8	123.....	9.5	3.0
120.....	Unsampled		124.....	6.3	12.7
121.....	8.0	1.3	125.....	16.8	1.4
122.....	9.5	1.5	126.....	5.0	.9

MINE WORKINGS

The workings on the property consist of numerous open cuts, pits, shafts, and room-and-pillar stopes on both limbs of the anticline. Sulfur has been mined from pits slightly over 100 feet deep on the Owl Creek side of the anticline. These pits are now inaccessible.

WORK BY THE BUREAU OF MINES

The Bureau of Mines exploratory work on the Brutch sulfur property consisted of rehabilitation and sampling of old workings, sinking test pits or shafts, and trenching through surface alluvium. Accessible workings on both sides of the anticline were mapped, but sampling and exploratory work were confined to the southwest limb of the anticline. All new and old workings showing sulfur were sampled. A total of 523 vertical feet of test pits or shafts was sunk. These shafts range in depth from 5 to 33 feet. A total of 442 linear feet of trenching was completed, and 219 samples were cut and assayed. A total of 32 existing excavations was cleaned and sampled where there was evidence of sulfur.

All workings on both limbs of the anticline were surveyed by transit and mapped. Because of limited funds, exploration by the Bureau of Mines was confined to the more promising areas on the southwest limb of the anticline on property controlled by Lin I. Noble.

METALLURGICAL TESTS

A sample of sulfur ore from the Brutch property was submitted to the metallurgical laboratories for test. The sample assayed 27.8 percent elemental sulfur. By employing stage grinding and flotation, 50.5 percent of the sulfur was recovered from the ore at a grade of 88.0 percent sulfur. A total of 76.2 percent of the sulfur was recovered at a grade of 70.6 percent. The addition of scavenger concentrate floated from the rougher tailings increased the recovery to 83.4 percent at a grade of 66.7 percent sulfur. A grade of 56.3 percent sulfur was made with a recovery of 88.0 percent.

Standard fire-refining processes may be used to improve the grade of the flotation concentrate.

Following is a detailed account of the metallurgical tests:

Assay lab. No.	Location	Chan- nel No.	Width of sample, feet	Sul- fur, per- cent	Total width of channel, feet	Sulfur, percent wt. av.	Assay map No.	Remarks
1351	P-26	1	2.0	18.7				Pit 26 is a combination room and pillar stope and open pit. See fig. 5 for location of samples.
1352	P-26	1	4.0	34.6				
1353	P-26	1	5.0	15.7	11.0	23.1	28	
1354	P-26	2	5.0	36.3				
1355	P-26	2	4.0	39.9				
1356	P-26	2	3.6	30.9	12.6	35.9	29	
1357	P-26	3	3.0	32.7				
1358	P-26	3	4.0	32.3	7.0	32.5	30	
1359	P-26	4	1.5	16.2				
1360	P-26	4	3.3	24.6				
1361	P-26	4	5.0	40.4				
1362	P-26	4	5.0	36.9	14.8	33.2	31	
1363	P-26	5	5.0	42.6	5.0	42.6	32	
1364	P-26	6	4.0	27.5				
1365	P-26	6	4.0	28.8				
1366	P-26	6	5.0	50.0	13.0	36.6	33	
1367	P-26	8	4.0	24.9				
1368	P-26	8	3.6	24.6				
1369	P-26	8	3.0	17.5				
Re- sample								
4712								
1370	P-26	8	3.0	32.1	13.6	24.8	34	
1371	P-26	9	4.0	10.7				
1372	P-26	9	4.0	33.0				
1373	P-26	9	5.0	27.7	13.0	24.1	35	
1374	P-26	10	5.0	33.1				
1375	P-26	10	5.0	21.8	10.0	27.4	36	
1376	P-26	11	5.0	25.2				
1377	P-26	11	5.0	34.9	10.0	30.0	37	
1378	P-26	12	4.0	10.6				
1379	P-26	12	2.0	27.1				
1380	P-26	12	3.0	12.0	9.0	14.7	38	
1381	P-26	13	1.5	38.8				
1382	P-26	13	3.0	16.9				
1383	P-26	13	3.0	16.1	7.5	21.0	39	
1384	P-26	14	3.0	14.6				
1385	P-26	14	4.0	20.8	7.0	18.1	40	
1386	P-26	15	5.0	22.3	5.0	22.3	41	
1387	P-26	16	5.0	24.4				
1388	P-26	16	5.0	40.2	10.0	32.3	42	
1389	P-26	17	4.0	27.3				
1390	P-26	17	2.0	31.2	6.0	28.6	43	
1391	P-26	18	4.0	27.1	4.0	27.1	44	
1392	P-26	19	3.0	40.8				
1393	P-26	19	3.0	16.0				

1189

Assay lab. No.	Location	Chan- nel No.	Width of sample, feet	Sul- fur, per- cent	Total width of channel, feet	Sulfur, percent wt. av.	Assay map No.	Remarks	Assay lab. No.
1394	P-26	19	2.5	26.1	8.5	27.7	45		1485
1395	P-26	20	4.5	6.8					1486
1396	P-26	20	4.5	2.6					1487
1397	P-26	20	3.5	18.3					
1398	P-26	20	5.0	15.5	17.0	10.3	46		4731
1399	P-26	21	4.0	37.1					
1400	P-26	21	5.0	34.5					4732
1401	P-26	21	5.0	15.3					
1402	P-26	21	5.0	8.7	19.0	23.2	47		1324
1403	P-26	22	2.0	34.5					1325
1404	P-26	22	5.0	29.3					1326
1405	P-26	22	3.0	28.3					
1406	P-26	22	4.0	22.6					
1407	P-26	22	4.0	11.1	18.0	24.2	48		
1408	P-26	23	5.0	27.7					
1409	P-26	23	3.7	43.2	8.7	34.3	49		
1410	P-26	24	5.0	49.0					1488
1411	P-26	24	3.0	49.8					
1412	P-26	24	4.0	41.8					
1413	P-26	24	5.0	34.0	17.0	43.0	50		1489
1414	P-26	25	5.0	50.8					1490
1415	P-26	25	5.0	42.7	10.0	46.7	51		1491
1467	P-19	1	5.0	.9	5.0	.9	5	Pit 19 is an open pit with adit, shown in figs. 3 and 5.	1492
Re-sampled 4719									1493
1468	P-19	2	3.0	33.9					1494
1469	P-19	2	3.0	24.1	6.0	29.0	6		1495
1470	P-19	3	3.6	0.4					1496
1471	P-19	3	6.0	26.5					1497
1472	P-19	3	3.5	35.3					1498
1473	P-19	3	4.0	23.9	17.1	22.2	7		1499
1474	P-19	4	5.5	4.4					1329
1475	P-19	4	6.0	29.2	11.5	17.3	8		
1476	P-19	5	4.8	2.8					
1477	P-19	5	5.0	3.3					
1478	P-19	5	6.0	1.2	15.8	2.3	9		
1479	P-19	6	5.0	4.7					
1480	P-19	6	5.0	4.6					
1481	P-19	6	5.0	32.1	15.0	13.8	10		
1482	P-19	7	5.0	4.8					
1483	P-19	7	5.0	32.7					
1484	P-19	7	4.0	37.2					4723

Assay lab. No.	Loca- tion	Chan- nel No.	Width of sample, feet	Sul- fur, per- cent	Total with of channel, feet	Sulfur, percent wt. av.	Assay map No.	Remarks
1485	P-19	7	3.5	37.5	17.5	26.7	11	
1486	P-19	8	4.0	27.9				
1487	P-19	8	3.5	43.4	7.5	35.1	12	
4731	P-16	1	5.0	.5				Shaft 3 by 14 by 17 feet; 7 feet of alluvium.
4732	P-16	1	5.0	.9	10.0	.7	1	Sampled top to bottom.
1324	P-17	1	5.0	24.3				
1325	P-17	1	4.2	41.7	9.2	32.2	2	
1326	P-17	2	4.0	8.0	4.0	8.0	3	
	P-18						4	Shaft 3 by 7.5 by 8 feet. Barren shale, unsampled.
1488	P-19A	1	5.0	31.3				Shaft 4 by 6 by 15.3 feet in floor of pit 19.
1489	P-19A	1	5.0	32.2				Shown on fig. 3.
1490	P-19A	1	3.2	26.5	13.2	30.5	13	
1491	A-19	1	5.5	31.5	5.5	31.5	14	Adit driven from pit 19. Shown on fig. 3.
1492	A-19	2	6.0	24.0	6.0	24.0	15	
1493	A-19	3	6.0	9.9	6.0	9.9	16	
1494	A-19	4	5.0	1.4	5.0	1.4	17	
1495	A-19	5	6.0	24.0	6.0	24.0	18	
1496	A-19	6	6.0	14.4	6.0	14.4	19	
1497	A-19	7	6.0	16.1	6.0	16.1	20	
1498	A-19			38.3				Grab sample from stock- pile pit 19.
1499	A-19			35.2				Grab sample from stock- pile pit 19.
1329	P-20	1	5.0	0.6	5.0	0.6	21	Shaft 5 by 6 by 13 feet Sample from bottom 5 feet of shaft.
	P-21						22	Shaft 4.5 by 4 by 8.6 feet. Unsampled.
	P-22						23	Shaft 4 by 5.5 by 5 feet. Unsampled.
4723	P-23	1	5.0	5.8				Shaft 6 by 6 by 27 feet. 17 feet of alluvium. Sampled from bottom 10 feet.

Assay lab. No.	Loca- tion	Chan- nel No.	Width of sample, feet	Sul- fur, per- cent	Total width of channel, feet	Sulfur, percent wt. av.	Assay No.	Remarks	Assay Lab. No.
4724	P-23	1	5.0	2	10.0	0.5	24		1334
1447	P-24	1	5.0	6.5				Shaft 8 by 11 by 25.4	1340
1448	P-24	1	4.4	3.7				feet. 5 feet of allu-	1346
1449	P-24	1	3.5	2.3				vium. Samples pointed	
1450	P-24	1	3.1	.9	16.0	3.7	25	to 21 feet in shaft.	1335
1451	P-24A	1	5.0	4.1				Shaft 6 by 7 by 14 feet	
1452	P-24A	1	3.4	5.9				1 foot of alluvium.	
1453	P-24A	1	4.5	2.1	12.9	3.9	26	Sampled top to bottom	1335
								of shaft.	1336
1443	P-25	1	5.0	2.7				Shaft 7.5 by 10 by 21	
1444	P-25	1	5.0	2.6				feet. 1.5 feet of allu-	
1445	P-25	1	5.0	6.8				vium. Sampled top to	
1446	P-25	1	5.0	7.1	20.0	4.8	27	bottom of shaft.	1348
4713	P-26A	1	2.8	3.1				4 by 6 by 10.5 feet.	1350
4714	P-26A	1	5.2	40.8	8.0	27.6	52	Shaft in floor of pit	1302
								26, shown in fig. 3.	1303
								Sampled top to bottom	
								of shaft. 2.5 feet dia-	1341
								bris in bottom of pit	1342
								26.	1343
1416	P-27	1	5.0	1.9				Shaft 6 by 8 by 24.3	
1417	P-27	1	5.0	9.3				feet. Sectional sam-	
1418	P-27	1	4.3	4.4	14.3	5.2	53	ples from top to bott-	1344
1419	P-27	2	5.0	21.6	5.0	21.6	54	of shaft.	1345
1420	P-27	3	5.0	4.2	5.0	4.2	55		
1422	P-28	1	5.0	36.4	5.0	36.4	56	Shaft 5 by 8 by 28 feet	
1423	P-28	2	5.0	13.6	5.0	13.6	57	Sectional samples top	1318
1424	P-28	3	5.0	6.1				to bottom, 3 feet allu-	
4715	P-28	3	5.0	.5				vium was not sampled	
4716	P-28	3	5.0	1.3	15.0	2.6	58		
1426	P-29	1	2.0	22.8				Shaft 8 by 10 by 22 feet	
1427	P-29	1	5.2	46.4				Sectional samples top	
1428	P-29	1	4.0	22.2				to bottom of shaft.	1463
1429	P-29	1	4.1	37.6					1464
1337	P-29	1	.9	14.8	16.2	33.5	59		1465
1430	P-30	1	1.2	4.6	1.2	4.6	60	Shaft 8 by 8 by 17.5	
1431	P-30	2	2.9	19.3				feet. 1.5 feet of allu-	1466
1432	P-30	2	6.0	9.6				vium. Sectional samples	
1433	P-30	2	2.0	8.7	10.8	11.9	61	from top to bottom of	
1339	P-30	3	4.0	3.4	4.0	3.4	62	shaft.	1454

Assay lab. No.	Loca- tion	Chan- nel No.	Width of sample, feet	Sul- fur, per- cent	Total width of channel, feet	Sulfur, percent wt. av.	Assay map No.	Remarks
1334	P-31	1	2.0	2.3				Shaft 4 by 6 by 12 feet.
1340	P-31	1	5.0	3.2				Sectional samples top to
1346	P-31	1	5.0	4.1	12.0	3.4	63	bottom of shaft.
1355	P-32	1	5.0	2.7	5.0	2.7	64	Shaft 6 by 6 by 6 feet. Old work. 1 foot of all- uvium.
1335	P-33	1	2.7	6.1				Shaft 4 by 6 by 25.5
1336	P-33	1	6.1	4.7	8.8	5.1	65	feet. Soil and boulders 15 feet. Sampled top to bottom.
1348	P-34	1	2.2	2.9				Shaft 4 by 6 by 34.3
1349	P-34	1	5.0	1.2				feet. 15 feet of soil
1350	P-34	1	3.5	4.5				and boulders. Sampled
1702	P-34	1	5.5	4.4	16.2	3.2	66	top to bottom.
1703	P-34	2	1.3	11.9	1.3	11.9	67	
1341	P-35	1	5.0	2.7				Shaft 4 by 6 by 31 feet.
1342	P-35	1	5.0	2.0				16 feet of surface soil
1343	P-35	1	1.8	.5	7.8	2.1	68	and boulders. Sectional samples from 16 to 27.8 feet.
1344	P-36	1	5.0	2.5				Shaft 4 by 6 by 28 feet.
1345	P-36	1	4.2	2.9	9.2	2.7	69	Samples from points 17 feet to bottom of shaft. 17 feet of alluvium.
1718	P-37	1	2.8	.6	2.8	.6	70	Shaft 4 by 6 by 11 feet. 8 feet of alluvium. Sampled at bottom of shaft.
	P-37						71	Unsampled.
	P-37						72	Unsampled.
1463	A-1	1	3.0	12.9	3.0	12.9	73	Above portal of adit.
1464	A-1	1	5.0	14.6	5.0	14.6	74	3 feet from portal west side.
1465	A-1	1	5.5	16.4	5.5	16.4	75	9 feet from portal west side.
1466	A-1	1	5.5	30.0	5.5	30.0	76	Face of adit. 16 feet from portal
1454	A-2	1	4.0	1.2	4.0	1.2	77	Above portal on surface.
1455	A-2	2	5.5	8.2	5.5	8.2	78	10 feet from portal west side.

Assay lab. No.	Loca- tion	Chan- nel No.	Width of sample, feet	Sul- fur, per- cent	Total width of channel, feet	Sulfur, percent wt. av.	Assay map No.	Remarks
1456	A-2	3	5.5	5.0	5.5	5.0	79	20 feet from portal west side.
1457	A-2	4	3.0	.4	3.0	.4	80	29 feet from portal east face.
1459	A-2	5	5.0	1.8	5.0	1.8	81	39 feet from portal, top of drift.
1460	A-2	6	5.0	7.3	5.0	7.3	82	49 feet from portal, top of drift.
1461	A-2	7	4.0	17.6	4.0	17.6	83	59 feet from portal west side of drift.
1462	A-2	8	2.7	22.8	2.7	22.6	84	Face of drift.
4738	C-27	1	3.5	.2	3.5	.2	85	Cut 4 by 8.5 by 6 feet. 2.5 feet of alluvium. Sample from face.
4737	C-28	1	4.0	.9	4.0	.9	86	Cut 4 by 10 by 5 feet. 10 feet of alluvium. Sample from face.
4736	C-29	1	4.0	.4	4.0	.4	87	Cut 4 by 20 by 5 feet. 1.0 feet of alluvium. Sample from face.
4739	C-39	1	5.0	1.2				Cut 4 by 14.5 by 16 feet. 6.0 feet of soil and boulders.
4740	C-30	1	5.0	.9	10.0	1.0	88	
4741	C-31	1	5.0	.8	5.0	.8	89	Cut 6 by 31 by 10 feet. 5 feet of soil and boulders.
	C-32						90	Trench 7 by 16 by 12 feet. Barren shale. Unsampled.
4733	C-33	1	3.7	0.9	3.7	0.9	91	Cut 4.5 by 35 by 16 feet. 9.3 feet of lime- stone boulders and shale.
	C-34						92	Trench 4 by 16 by 12 feet. Barren shale. Unsampled.

Assay lab. No.	Loca- tion	Chan- nel No.	Width of sample, feet	Sul- fur, per- cent	Total width of channel, feet	Sulfur, percent wt. av.	Assay map No.	Remarks
	C-35						93	Pit 3 by 7 by 5 feet. Barren shale. Unsam- pled.
	C-35A						94	Cut 4 by 10 by 8 feet. Barren shale. Unsam- pled.
734	C-36	1	4.5	.9	4.5	.9	95	Cut 6 by 10 by 7 feet. 25 feet of alluvium. Bottom 4.5 feet of cut sampled.
1327	C-37	1	3.0	25.3	3.0	25.3	96	Cut 6 by 11 by 8 feet. Bottom 7 feet of cut sampled.
1328	C-37	2	4.0	16.5	4.0	16.5	97	
1330	C-37A	1	5.0	2.4	5.0	2.4	98	Cut 4 by 10 by 7 feet. 2 feet alluvium. Sample from face of cut.
	C-37B						99	Cut 3 by 7 by 10.8 feet. Soil and boulders. Unsampled.
	C-38						100	Cut 4 by 11 by 10 feet. Barren alluvium. Unsampled.
	C-39						101	Trench 4 by 14 by 7 feet. Barren alluvium and boulder.
	C-40						102	Cut 4.5 by 18 by 12 feet. Barren alluvium and boulder. Unsam- pled.
	C-41						103	Cut 4.5 by 19 by 9 feet. Barren alluvium and boulders. Unsam- pled.
	C-42						104	Cut 5 by 11 by 5.5 feet. Barren shale. Unsam- pled.
	C-43						105	Cut 5 by 6.5 by 5 feet. Barren shale. Unsam- pled.
	C-44						106	Cut 5.5 by 7.5 by 4 feet. Barren shale. Unsam- pled.

R.I. 3964

Assay lab. No.	Loca- tion	Chan- nel No.	Width of sample, feet	Sul- fur, per- cent	Total width of channel, feet	Sulfur, percent wt. av.	Assay map No.	Remarks	Assay lab. No.
	C-45						107	Cut 6 by 12 by 13 feet. Barren shale. Unsampled.	4722
	C-46						108	Cut 4 by 7.5 by 4.5 feet. Barren shale. Unsampled.	
4730	C-47	1	5.0	0.1	5.0	0.1	109	Cut 5.5 by 11 by 7.5 feet. 2.5 feet alluvium. Bottom 5.0 feet of 11- stone, sampled.	1439
	C-48						110	Cut 4 by 10 by 7.5 feet. Barren shale. Unsampled.	1440
4729	C-49	1	5.0	.6	5.0	.6	111	Trench 3 by 7 by 25 feet. 2 feet of alluvium. Bot- tom 5 feet of trench sampled.	1441
4727	C-50	1	2.0	.7	2.0	.7	112	Cut 4 by 15 by 15 feet. Soil and shale. Sample from bottom 7 feet.	1442 4706
	C-51						113	Cut 5 by 10 by 5.5 feet. Gypsum and altered shale. Unsampled.	4707 4708 4709
4726	C-52	1	5.0	0.6	5.0	0.6	114	5 feet cut at bottom of shale scarp.	1437 1438 4704 4705
	C-53						115	Cut 4 by 14 by 12 feet. Altered, barren shale. Unsampled.	
	C-54						116	Cut 5 by 14 by 9 feet. Altered, barren shale. Unsampled.	1347
	C-55						117	Cut 6 by 15 by 12 feet. Barren shale. Unsampled.	
4725	C-56	1	5.0	.6	5.0	.6	118	Cut 4.5 by 8 by 10 feet. 5 feet of alluvium. 3 feet of shale. Sampled from face of cut.	

Assay lab. No.	Loca- tion	Chan- nel No.	Width of sample, feet	Sul- fur, per- cent	Total width of channel, feet	Sulfur, percent wt. av.	Assay map No.	Remarks
4722	C-57	1	5.0	.8	5.0	.8	119	Cut 4 by 13 by 11 feet. 6 feet alluvium. Bottom 5 feet of shale sampled.
	C-58	1		-			120	Cut 4 by 10 by 8 feet. Barren alluvium and boulders. Unsampled.
1439	C-59	1	3.0	.9				Cut 4 by 24.5 by 11 feet. 4 feet of alluvium. Samples from face of cut.
1440	C-59	1	5.0	1.6	8.0	1.3	121	Old work.
1441	C-59A	1	5.0	1.1				Cut 4 by 8.2 by 21.7 feet. 4 feet of alluvium. Samples from face of cut to 8 feet from floor.
1442	C-59A	1	4.5	2.0	9.5	1.5	122	
4706	C-60	1	5.0	2.1				Shaft 4 by 6 by 11 feet
4707	C-60	1	4.5	4.1	9.5	3.0	123	sunk from 9-foot cut. 2 foot bed of magnesium
4708	C-60	2	4.6	13.2				and alluminum.
4709	C-60	2	1.7	11.2	6.3	12.7	124	
1437	C-61	1	4.0	.9				Shaft 4 by 6 by 11.4
1438	C-61	1	4.0	1.1				feet sunk from 10 foot
4704	C-61	1	6.5	1.4				cut. 2 feet of alluvium.
4705	C-61	1	2.3	2.5	16.8	1.4	125	Samples taken from 2 feet from top of cut to 1.6 feet from bottom of shaft. 1.6 feet of barren shale in bottom.
1347	C-62	1	5.0	.9	5.0	0.9	126	Cut 4 by 12 by 6 feet. 1 foot of alluvium.

JOHN C. REED, JR.
R. E. ZARTMAN

} U.S. Geological Survey, Federal Center, Denver, Colorado 80225

Geochronology of Precambrian Rocks of the Teton Range, Wyoming

Note: This paper is dedicated to Aaron and Elizabeth Waters on the occasion of Dr. Waters' retirement.

ABSTRACT

The oldest rocks in the Teton Range are complexly deformed interlayered biotite gneiss, plagioclase gneiss, amphibole gneiss, and amphibolite. Also, within these rocks, there are concordant bodies of strongly lineated quartz monzonite gneiss, here named the Webb Canyon Gneiss, which may be of volcanic origin. Coarse metagabbro, here named the Rendezvous Metagabbro, is intrusive into the layered gneiss sequence and was metamorphosed and deformed along with the enclosing rocks.

These older rocks are cut by discordant plutons and swarms of undeformed dikes of quartz monzonite and associated pegmatite. The quartz monzonite, which makes up much of the central part of the Teton Range, is here named the Mount Owen Quartz Monzonite.

The youngest Precambrian rocks are undeformed dikes of slightly metamorphosed tholeiitic diabase.

A Rb-Sr whole-rock isochron on the Webb Canyon Gneiss and the Rendezvous Metagabbro indicates that these rocks were metamorphosed $2,875 \pm 150$ m.y. ago. The initial Sr. ratio of 0.700 suggests that the original rocks are probably not significantly older than the metamorphism. The Mount Owen Quartz Monzonite has a whole-rock isochron age of $2,495 \pm 75$ m.y. and an unusually high initial ratio of 0.732. Plagioclase-microcline isochrons from two samples of the quartz monzonite indicate partial re-equilibration of the Rb-Sr system during a thermal event 1,800 m.y. ago.

The age of the diabase dikes has not been definitely determined, but biotite in the wall rocks of one major dike has a K-Ar age of 1,450 m.y. This suggests that the dike was emplaced

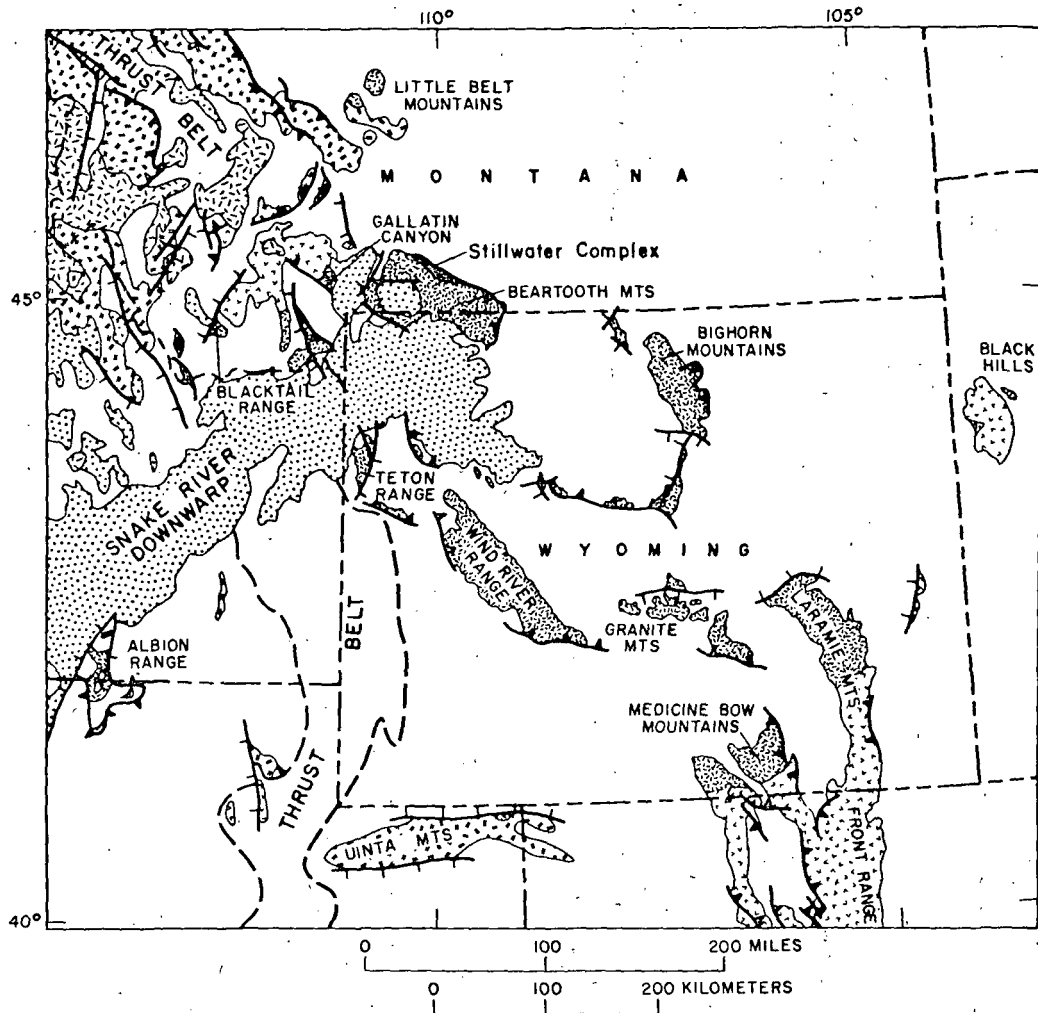
during or prior to a thermal event 1,300 to 1,500 m.y. ago that was responsible for resetting many of the previously reported K-Ar mineral ages throughout the range.

The geochronologic record in the Teton Range is very similar to that elsewhere in the Wyoming Precambrian province. Major metamorphic events with ages between 2,700 and 2,900 m.y. have been identified in the Bighorn, Beartooth, Little Belt, and Granite Mountains. Post-tectonic granitic rocks with ages of 2,500 to 2,700 m.y. have been found in the Wind River Range and the Granite Mountains. Later thermal events have affected Rb-Sr systematics of rocks in the Beartooth Mountains, Wind River Range, and Granite Mountains, as well as in the Teton Range at about the same time as major episodes of regional metamorphism in terranes flanking the Wyoming province in southwestern Montana and in the Front Range in Colorado.

INTRODUCTION

The Teton Range (Fig. 1) in northwestern Wyoming affords some of the northwesternmost exposures of ancient continental crust in the central Rocky Mountains. The Precambrian rocks of the Tetons are part of a terrane exposed in most of the uplifts in Wyoming and north-central Montana that has yielded metamorphic and plutonic ages greater than 2.5 b.y., similar to those in the Superior province of the Canadian Shield. This terrane has been referred to as the Wyoming province (Engel, 1963; Condie, 1969).

The Teton Range is a fragment of a large northwest-trending Laramide uplift that was sundered in late Pliocene or Pleistocene time by a zone of major north-south normal faults along which the eastern edge of the Teton block was uplifted and the floor of Jackson Hole was dropped. The total displacement on the fault zone is estimated to be as much as



EXPLANATION


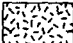
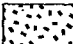
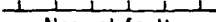


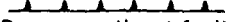
- | | |
|--|--|
| <p> Quaternary and Tertiary volcanic rocks</p> <p> Mesozoic granitic rocks</p> <p> Precambrian sedimentary rocks less than 1,500 m.y. old</p> <p> Normal fault</p> | <p> Precambrian metamorphic and plutonic rocks from which no ages greater than 1,800 m.y. have been reported</p> <p> Precambrian metamorphic and plutonic rocks from which ages greater than 2,400 m.y. have been reported (Wyoming province)</p> <p> Reverse or thrust fault
<i>Teeth on upper plate</i></p> |
|--|--|

Figure 1. Index map of Wyoming and parts of adjacent states showing outcrop areas of Precambrian rocks and extent of the Wyoming province. Modified from King (1969).

30,000 ft (Love and Reed, 1968). Although the area of exposed Precambrian rocks in the Teton Range is only about 170 sq mi (Fig. 2), the precipitous eastern face of the range provides a nearly continuous vertical cross section with a maximum relief of nearly 7,000 ft (Fig. 3). Problems of exposure in a geologic sense are less critical than those of exposure in a mountaineering sense.

Since 1962, mile-to-the-inch scale geologic mapping of the Precambrian rocks of the Tetons has been completed as part of a U.S. Geological Survey project to produce a geologic map of Grand Teton National Park and vicinity, and several nontechnical accounts of the geology of the Teton Range have been published (Reed, 1963; Love and Reed, 1968; U.S. Geol. Survey, 1971). In the present paper, we report the results of an investigation of the geochronology of the Precambrian rocks of the Tetons that was carried on in conjunction with the mapping program.

GEOLOGY OF THE PRECAMBRIAN ROCKS

Metamorphic Rocks

Layered Gneiss and Migmatite. The oldest rocks in the Teton Range are complexly deformed layered biotite and amphibole gneisses, amphibolites, and migmatites that are believed to be of Precambrian W age in the interim classification recently adopted by the U.S. Geological Survey (James, 1972). The sequence commonly contains lenses and layers of light-gray to white quartz-plagioclase gneiss, and in several places pods of layered magnetite iron-formation a few feet thick and a few tens of feet long have been found. No identifiable quartzite has been found in the gneiss sequence. The occurrences of quartzite reported by Horberg and Fryxell (1942) have all proved to be either light-colored plagioclase gneiss, sheared quartz veins, or downfaulted slices of Flathead Quartzite.

The most common mineral assemblages in the gneisses are

quartz + oligoclase or andesine + biotite ±
garnet ± potassium feldspar

in the biotite gneisses and

quartz + andesine or labradorite +
hornblende ± biotite ± garnet

in the amphibole gneisses and amphibolites.

Thin layers of amphibole schist interleaved with the gneisses locally contain actinolite, anthophyllite, and cummingtonite in association with quartz, andesine or labradorite, biotite, and garnet. In a few places in the northern part of the range, the gneisses contain cordierite and gedrite. Primary muscovite is rare or absent and no aluminosilicate minerals have been found. The rock reported as sillimanite schist by Reed (1963) on the basis of study of the hand specimens has proved by thin section study to be anthophyllite schist.

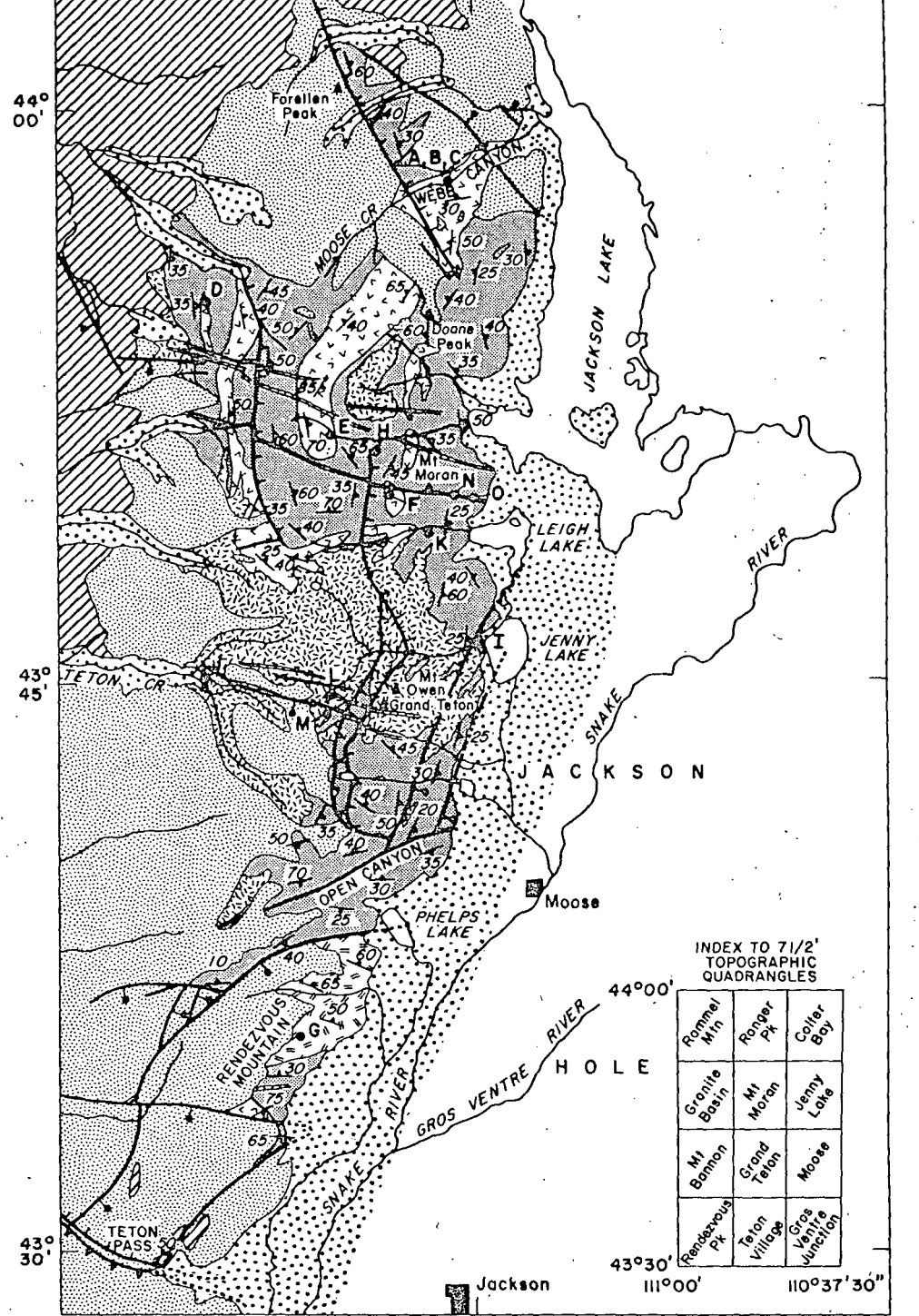
In broad areas adjacent to the larger masses of Mount Owen Quartz Monzonite (Fig. 2), the biotite gneisses are lighter colored, less conspicuously layered, and contain abundant potassium feldspar in porphyroblasts, in quartzofeldspathic folia, and in small grains intergrown with quartz and plagioclase throughout the rock. These migmatitic effects are apparently related to the emplacement of the quartz monzonite and are superimposed on the older metamorphic assemblages.

Most of the gneisses display some degree of alteration or retrogression, including chloritization of ferromagnesian minerals, sericitization of feldspars, and partial decalcification of plagioclase. Some rocks are barely altered, whereas others are almost completely altered.

The conspicuous layering in much of the gneiss sequence (Fig. 4) suggests that most of the gneisses are supracrustal. Some, such as the iron formation and the local layers of marble, are clearly metasedimentary, but the vast bulk of the sequence could be derived from volcanic or volcanoclastic rocks. The mineral assemblages suggest that the rocks were metamorphosed in the amphibolite facies, and the occurrence of cordierite may indicate metamorphism of the low-pressure or low-pressure-intermediate type described by Miyashiro (1961). The scarcity of primary muscovite and the absence of aluminosilicate minerals is probably due to the absence of rocks of pelitic composition.

Webb Canyon Gneiss. The name "Webb Canyon Gneiss" is here proposed for a medium- to coarse-grained strongly foliated nonlayered biotite-and-hornblende-bearing gneiss of quartz monzonitic composition that forms several large concordant bodies in the northern part of the Teton Range. Rb-Sr data discussed below show that the rock is of Precambrian W age (James, 1972). The map pattern suggests that the largest body of Webb Canyon Gneiss

111°00' 110°45' 110°30'



INDEX TO 7 1/2' TOPOGRAPHIC QUADRANGLES

Rommel Mtn	Ranger Pk	Collier Bay
Granite Basin	Mt Moran	Jenny Lake
Mt Bonnon	Grand Teton	Moose
Rendezvous Pk	Teton Village	Gros Ventre Junction

0 5 10 MILES
0 5 10 KILOMETERS

Jackson

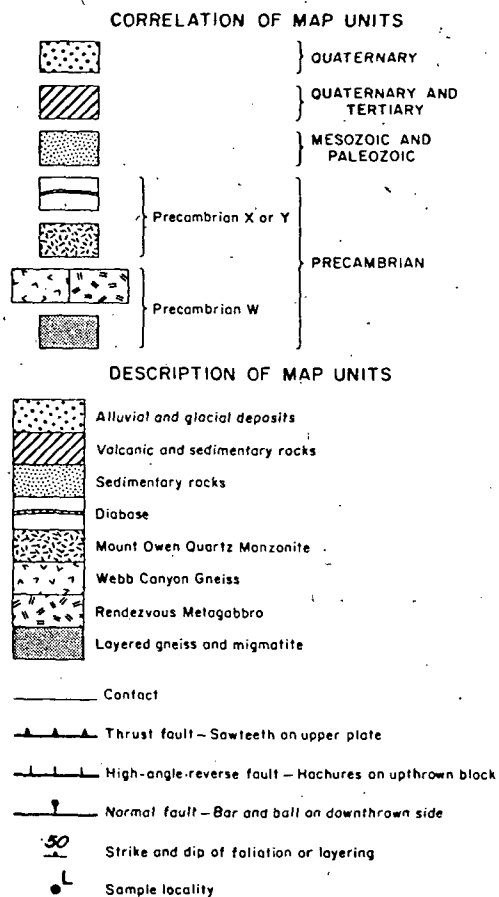


Figure 2. Generalized geologic map of the Precambrian rocks of the Teton Range showing sample localities.

is exposed in the core of an isoclinal fold and that the smaller discontinuous bodies lie at a different stratigraphic horizon. However, the structure is so complex that other interpretations are possible. The type locality is designated as the lower parts of the cliffs on the northwest side of Moose Creek in the lower part of Webb Canyon 1.9 mi S. 78° E. of Owl Peak in the Ranger Peak 7½' quadrangle, Wyoming (Fig. 2, sample loc. A, V, and C).

The type locality is near the northeast end of the largest exposed body of Webb Canyon Gneiss in the Teton Range. The contact of the body with layered biotite and amphibole gneisses to the northwest lies about midway up the cliffs. The contact strikes approximately east-west and dips 20° to 40° north, parallel to foliation in the Webb Canyon Gneiss and layering in the layered gneisses.

The Webb Canyon commonly contains layers of amphibolite a few inches to several hundred feet thick. Several thick amphibolite layers are conspicuous in the gneiss at the type locality. Contacts of these amphibolite layers are knife-sharp.

Contacts of the Webb Canyon Gneiss with the enclosing rocks are commonly marked by a layer of similar amphibolite. Where amphibolite is absent, contacts with the layered biotite gneisses are gradational over a few tens of hundreds of feet, and the Webb Canyon Gneiss becomes finer grained and rudely layered near the contact.

The origin of the Webb Canyon Gneiss is uncertain. No primary textures or structures are preserved. Chemically the rock closely resembles an alkalic granite or rhyolite; its texture and grain size suggest that it may be a plutonic rock, but the lack of intrusive relations and the continuity and extent of the concordant amphibolite layers within it seem to preclude an intrusive origin. It therefore seems most likely that the gneiss is derived from felsic volcanic rocks, either flows or tuffs interlayered with flows or sills of basalt that were metamorphosed to produce the amphibolite layers.

Rendezvous Metagabbro. We suggest the name "Rendezvous Metagabbro" in this report for the coarse-grained mafic rock that is exposed between Open Canyon and Rock Springs Canyon in the southern part of the Teton Range. The unit is believed to be of Precambrian W age on the basis of Rb-Sr data discussed below (James, 1972).

The type locality is designated as the freshly blasted outcrops between elevations 8,400 and 9,000 ft in the small valley on the east slopes of Rendezvous Mountain, just north of the aerial tramway at the Jackson Hole ski area (Fig. 2, sample loc. G). The type locality is about 1.6 mi N. 65° W. of the lower terminus of the tramway in Teton Village, Teton Village 7½' quadrangle, Wyoming. The rock is non-layered and very weakly foliated. Typically it has a blotchy appearance due to irregular clots of dark-green hornblende 1 inch to several inches across set in a matrix of light-gray plagioclase. Similar rock that occurs in pods in the layered gneisses north of Phelps Lake was aptly described by Bradley (1956) as "leopard diorite." The rock typically consists of about 60 to 70 percent finely twinned plagioclase (about An₇₅) and 25 and 35 percent hornblende. A few plagioclase grains are faintly

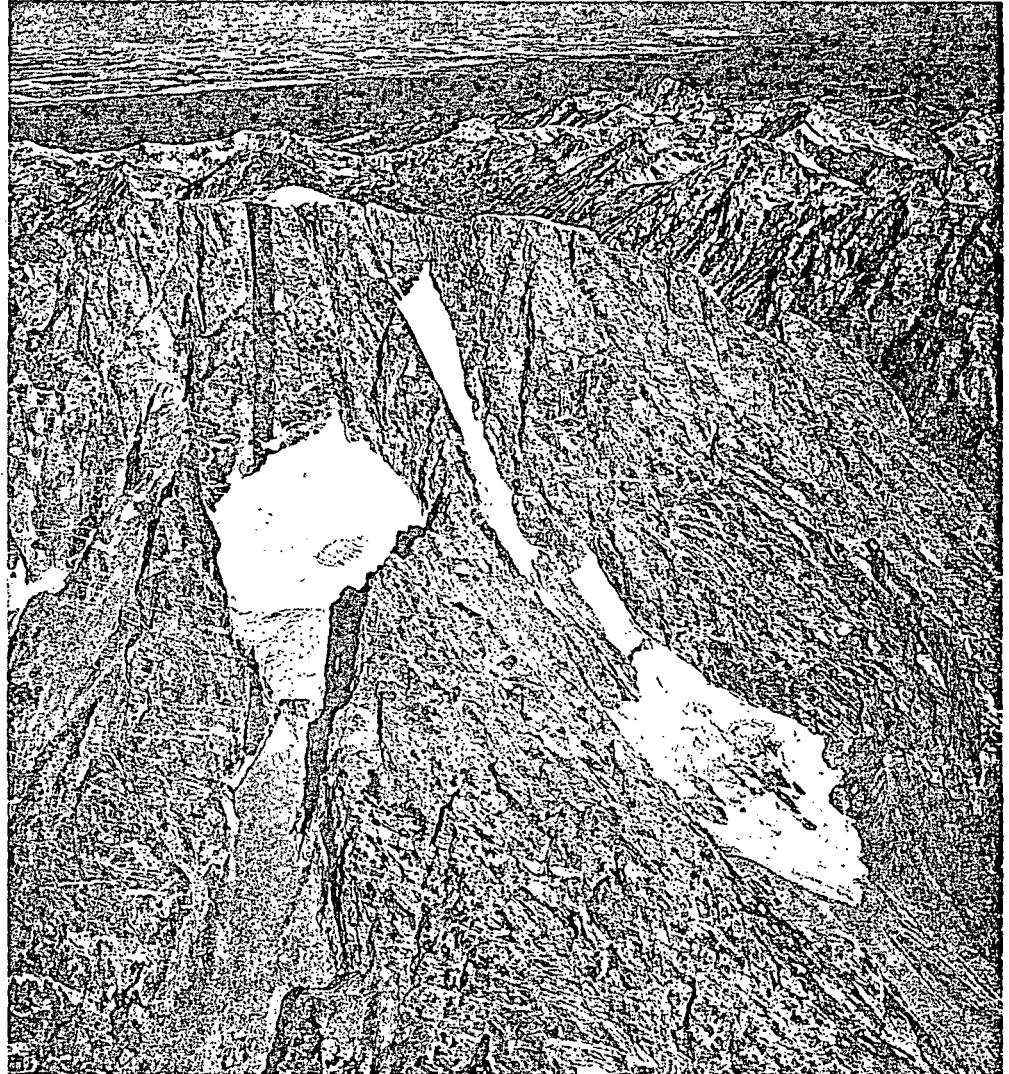


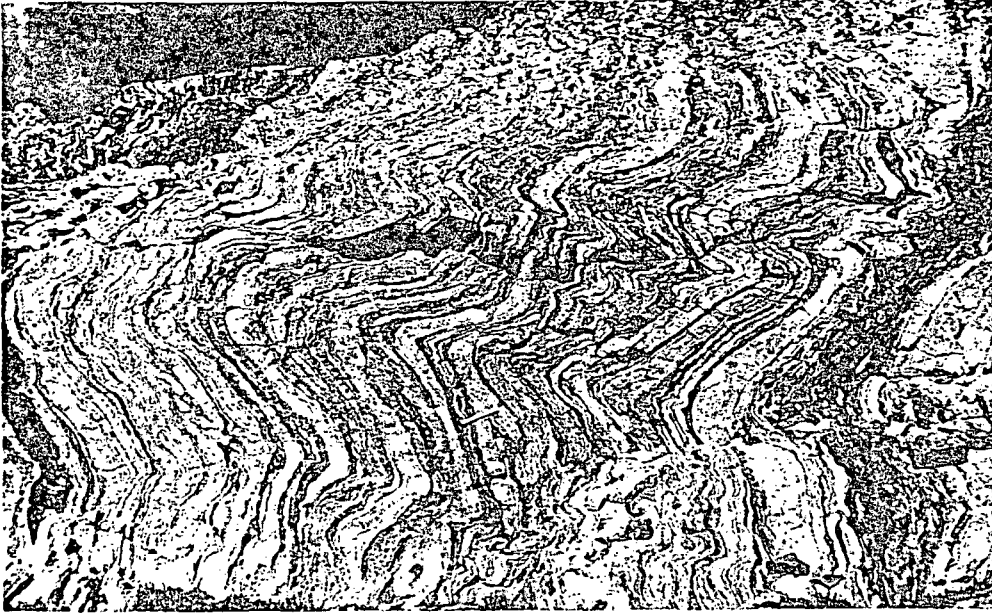
Figure 3. Oblique aerial photograph of the east face of Mount Moran. Direction of view is northwest. Vertical relief from bottom to summit, as pictured, is about 3,400 ft. Country rock is predominantly migmatitic biotite gneiss. Light-colored dikes, most of which dip gently to the north (right), are Mount Owen Quartz Monzonite and related pegmatite. Prominent

dark band is a diabase dike 100 to 150 ft thick. Light-gray cap on summit is Flathead Quartzite of Cambrian age that rests unconformably on the dike. Sample locality N is about midway up the lowest outcrop of the dike visible in the photograph. Photograph by Austin Post.

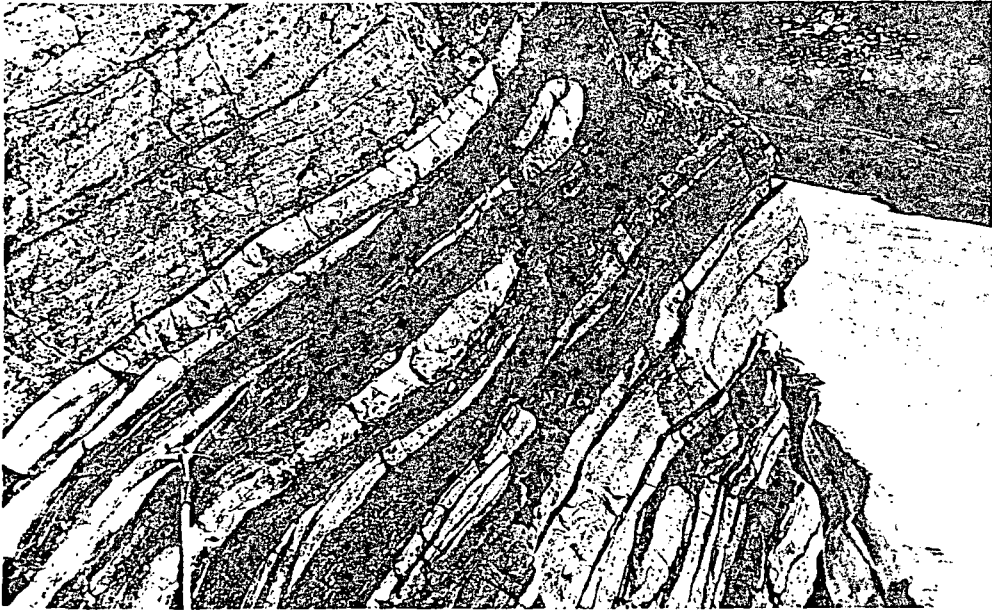
zoned. Commonly the plagioclase is partly sericitized and decalcified. The hornblende, which probably replaces original pyroxene, is partly jacketed with actinolite and locally is partly altered to chlorite and epidote. A few small grains of quartz occur as poikilitic inclusions in hornblende and between the larger plagioclase grains, and scattered small flakes

of reddish-brown biotite are intergrown with the hornblende.

The northern contact of the metagabbro is marked by a fault. On the west, the rock passes beneath Paleozoic sedimentary rocks; on the east, it passes beneath surficial deposits (Fig. 2). The contact between the metagabbro and migmatitic biotite gneiss to the south is sharp



A



B

Figure 4. Photographs of layered gneiss. A. Thinly layered biotite gneiss, amphibole gneiss, and amphibolite west of Static Peak, about 2 mi northwest of Phelps Lake (Fig. 2). B. Interlayered plagioclase gneiss (white), biotite gneiss (medium gray), amphibole gneiss and amphibolite (dark gray) displaying rootless isoclinal folds and sheared-out layers. About 1.5 mi northwest of Doane Peak (Fig. 2).

and concordant. The metagabbro near the contact is finer grained and lighter colored. The gneiss near the contact is highly contorted and contains pods of metagabbro a few inches to a few feet across. The intrusive nature of the metagabbro is confirmed by the widespread occurrence of similar lenses and pods, presumably boudinaged sills or dikes, in the enclosing layered gneisses, and by the occurrence of angular inclusions of biotite gneiss in the main body of metagabbro.

Deformation of the Metamorphic Rocks. The layered gneisses display at least two generations of folds (Reed, 1963). The earliest folds are rootless isoclinal folds with axial planes and limbs parallel to layering. The largest isoclinal folds observed have limbs a few tens of feet long, but much larger ones may be present. Some layers are contorted by isoclinal folds, whereas other layers above and below are not contorted (Fig. 4B). This suggests that many of the layers are limbs of sheared-out isoclinal folds and that, although the layers probably reflect original compositional differences, their original sequence has been completely obliterated by shearing parallel to layering.

Superimposed on the early isoclinal folds are more open folds with diverse axial orientations. The folds may belong to several generations, but analyses of the structures have not yet been completed and therefore a sequence has not been worked out.

Foliation in the gneisses is parallel to the layering, and mineral lineations are generally parallel to axes of the younger folds. This suggests that amphibolite-grade metamorphism was synchronous with the younger folds. Parallelism between foliation and lineation in the Webb Canyon Gneiss and similar structures in the enclosing rocks indicates that the Webb Canyon was deformed at the same time as the enclosing rocks.

The Rendezvous Metagabbro does not display any conspicuous lineation, but the rude foliation is parallel to that in the nearby migmatitic gneisses. The occurrence of boudins and deformed layers of metagabbro in the surrounding layered gneisses suggests that the original gabbro was emplaced prior to or during deformation and metamorphism of the gneisses.

Younger Intrusive Rocks

Mount Owen Quartz Monzonite. Much of the central part of the Teton Range is underlain by an irregular pluton of light-colored

quartz monzonite and associated pegmatite for which we here propose the name "Mount Owen Quartz Monzonite." Isotopic data discussed below indicate that the rock could be Precambrian X or Precambrian W (James, 1972). The rock is named from its exposures on the slopes of Mount Owen, but the type locality is designated as the more easily accessible exposures along the trail in the South Fork of Cascade Canyon at elevation 8,880 ft, 1.9 mi due west of the summit of Mount Owen, Grand Teton 7½' quadrangle, Wyoming (Fig. 2, sample locality L).

Typically the Mount Owen Quartz Monzonite is a medium- to fine-grained light-colored rock consisting of 30 to 40 percent quartz, 20 to 30 percent potassium feldspar, 25 to 35 percent plagioclase, 5 percent or less biotite, and a trace of muscovite. The potassium feldspar is microcline and micropertthite; the plagioclase is generally finely twinned unzoned sodic oligoclase.

The rock is generally nonfoliated but locally displays a faint foliation marked by biotitic streaks that is believed to be a flow structure. Except near fault zones the quartz monzonite is unshaped, but in many specimens the biotite is partly altered to chlorite or fringed with secondary muscovite and the feldspars are slightly clouded and contain small granules of clinozoisite.

Dikes, pods, and irregular bodies of pegmatite ranging in thickness from a few inches to several tens of feet are common throughout much of the main mass of the Mount Owen Quartz Monzonite. Locally they comprise a quarter or more of the rock mass. The pegmatites contain irregular masses of gray quartz, subhedral crystals of milky white oligoclase, and blue-gray microcline as much as 2 ft long, muscovite in plumose aggregates or tabular books as much as 3 in. across, and long flat blades 1 to 2 in. across and as much as 1 ft long. Generally an individual pegmatite body contains muscovite or biotite, but not both. A few pegmatites contain garnet crystals as much as 6 inches in diameter (Love and Reed, 1968, Fig. 25).

The contacts of the Mount Owen Quartz Monzonite are highly irregular and difficult to depict on a geologic map. Blocky inclusions of wall rocks a few feet to several feet across are common throughout the pluton (Fig. 5A). As the margins are approached, these inclusions become more and more abundant until one

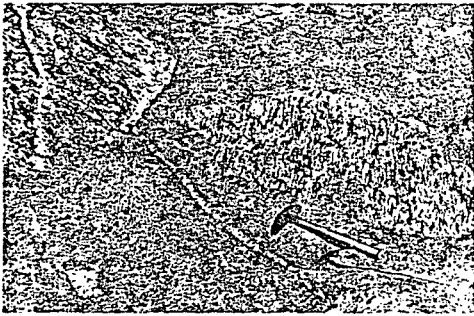


Figure 5A. Angular inclusions of strongly foliated Webb Canyon Gneiss in Mount Owen Quartz Monzonite. Note rotation of the foliation in the blocks. Light-colored slightly sheared quartz-feldspar dike in inclusion at upper left is truncated by contact; small biotite pegmatite dike (left of hammer) cuts across both the inclusions and the quartz monzonite, although it is inconspicuous in the inclusions because of similarity in grain size. About 3 mi northwest of sample locality M (Fig. 2).



Figure 5B. Network of dikes of Mount Owen Quartz Monzonite and related pegmatite cutting migmatitic biotite gneiss on the north face of the West Horn of Mount Moran. Note rude layering in gneiss dipping about 60° E. (left). Face is about 700 ft high.

passes imperceptibly from quartz monzonite and pegmatite containing abundant inclusions of wall rocks into wall rocks containing myriad cross-cutting dikes of quartz monzonite and pegmatite. Many of the dikes in the wall rocks

are composed partly of pegmatite and partly of fine-grained quartz monzonite. The finer grained rock may occupy either the center or the margins of an individual dike. Dikes of quartz monzonite cut dikes of pegmatite and vice versa, indicating a complex, overlapping order of emplacement.

The wall rocks for as much as 5 mi from the contacts of the main pluton are cut by smaller plutons and laced with swarms of quartz monzonite and pegmatite dikes, many of which are emplaced along low-dipping joint sets (Figs. 3 and 5B). The dikes become less and less abundant farther from the main pluton, and only a few dikes are found cutting the gneisses in the northern and southern ends of the range.

Undeformed dikes of quartz monzonite and pegmatite cut cleanly through complexly folded layered gneisses, and angular rotated blocks of wall rock are widespread as inclusions in the main pluton, showing clearly that the Mount Owen Quartz Monzonite was emplaced after the folding and metamorphism of the enclosing rocks.

Contacts of individual dikes with the wall rocks and of individual inclusions with the quartz monzonite are generally very sharp. There is no evidence of local contact metamorphic effects on the wall rocks and only local evidence of digestion of inclusions. Apparently the Mount Owen Quartz Monzonite was emplaced in rather brittle country rocks by some combination of dilation of fractures and magmatic stoping, without appreciable deformation of the wall rocks.

Diabase. The youngest Precambrian rock in the Teton Range is tholeiitic diabase which forms a series of west-northwest-trending dikes that cut all the other Precambrian rocks but which are unconformably overlain by the basal beds of the Flathead Quartzite of Middle Cambrian age. The largest dike is prominently exposed on the east face of Mount Moran (Fig. 3). It is about 150 ft thick and has been traced along strike for almost 10 mi, completely across the Teton Range. The vertical extent of the exposures on Mount Moran is more than 5,000 ft. The prominent dikes exposed on the Grand Teton and on Middle Teton are 40 to 60 ft thick; other dikes range in thickness from a few inches to several tens of feet. Isotopic data discussed below suggest that the dikes are of Precambrian X or Precambrian Y age (James, 1972).

The diabase consists essentially of subcalcic

augite, sodic labradorite (An₅₀₋₅₅), pigeonite, and opaque ores, and contains a few small grains of brown hornblende and biotite. Most of the dikes have chilled margins a few inches thick that consist of a very fine-grained, dark felted groundmass containing subhedral phenocrysts of pyroxene and euhedral laths of plagioclase; some of these display a flow orientation parallel to the walls (Fig. 6).

Whereas the dikes are undeformed (except for shearing along faults), most of the diabase exhibits some evidence of incipient alteration or metamorphism. Plagioclase is partly altered to sericite and pyroxene is locally converted to chlorite, epidote, and bluish-green amphibole. In some specimens, the pyroxene is almost completely converted to amphibole, but the plagioclase is little altered.

ISOTOPIC STUDIES

Analytical Methods

Rb and Sr analyses were carried out using procedures similar to those described by Peterman and others (1967, 1968). Preliminary x-ray fluorescence analyses for Rb and Sr were made using the technique described by Doering (1968). Measurements of isotopic ratios were made on a 6-in., 60°, single-focusing mass spectrometer using triple filament surface ionization. Precision of results is believed to be about the same as that quoted by Peterman and others (1968): for individual Rb determinations, ± 1.5 percent at the 95-percent confidence level; for individual Sr determinations, ± 2.2 percent at the 95-percent confidence level; for Rb/Sr ratios by isotope dilution, ± 2.7 percent; for Sr⁸⁷/Sr⁸⁶ ratios calculated from measurements on spiked samples, about ± 3 percent; and for Sr⁸⁷/Sr⁸⁶ ratios measured on unspiked samples, ± 0.15 percent. All Sr⁸⁷/Sr⁸⁶ ratios were normalized to a value of Sr⁸⁶/Sr⁸⁸ = 0.1194. In all Rb-Sr calculations, the following constants were used:

$$\text{Rb}^{87}\lambda_{\beta} = 1.39 \times 10^{-11}/\text{yr}, \text{ corresponding to} \\ \text{half life of Rb}^{87} = 50 \times 10^9 \text{ yrs. Rb}^{87} = \\ 0.283 \text{ g/g Rb.}$$

Rb-Sr ages quoted from the literature have been recalculated using the 50×10^9 yr half-life if the original authors used a different value.

Ar extractions were made using the fusion technique described by Dalrymple and Lanphere (1969). Potassium contents of biotites were determined by flame photometry; all



Figure 6. Sawed slab showing chilled margin of diabase dike. Average grain size of diabase in center of dike is about the same as that of the larger phenocrysts of plagioclase and pyroxene in the chilled margin. Paper match shows scale. South wall of 20-ft-thick dike in Garnet Canyon about 2 mi southeast of summit of Grand Teton (Fig. 2).

other potassium contents were determined by isotope dilution.

The following constants were used in the K-Ar calculations:

$$\text{K}^{40}\lambda_{\epsilon} = 0.584 \times 10^{-10}/\text{yr} \\ \lambda_{\beta} = 4.72 \times 10^{-11}/\text{yr} \\ \text{K}^{40} = 1.19 \times 10^{-4} \text{ moles/mole K.}$$

All sample localities are indicated on Figure 2. Detailed locations and petrographic descriptions are available.¹

Age of the Webb Canyon Gneiss and Rendezvous Metagabbro

The results of Rb and Sr analyses of five whole-rock samples of Webb Canyon Gneiss, one sample of plagioclase gneiss in the layered gneiss sequence adjacent to the Webb Canyon Gneiss, and three samples of Rendezvous Metagabbro are given in Table I. Taken alone, the five analyses of the Webb Canyon Gneiss define a whole-rock isochron with an age of $2,790 \pm 400$ m.y. and an initial Sr⁸⁷/Sr⁸⁶ ratio of 0.703 ± 0.017 (model 4 of McIntyre and others, 1966). No meaningful independent isochron could be calculated for the three Rendezvous Metagabbro samples because of their low Rb/Sr ratios.

Although the age relation between the Webb Canyon Gneiss and the Rendezvous Metagabbro is uncertain, field relations show that both they and the enclosing gneisses have

¹ This material (NAPS no. 01969) may be obtained by writing to Microfiche Publications, Div. of Microfiche Systems Corp., 305 East 46th St., New York, New York 10017, enclosing \$5 for photocopies, or \$1.50 for microfiche. Make checks payable to Microfiche Publications.

TABLE 1. WHOLE-ROCK RUBIDIUM AND STRONTIUM ANALYSES

Sample locality*	Field no.	Rb (ppm)	Sr (ppm)	Rb ⁸⁷ /Sr ⁸⁶ **	(Sr ⁸⁷ /Sr ⁸⁶) [†]	Age (m.y.)	
Plagioclase gneiss adjacent to Webb Canyon Gneiss							
A	986A	13.7	282.7	0.140	0.7062*	} 2875 ± 150	
Webb Canyon Gneiss							
B	984A	35.7	76.9	1.35	0.7756 [§]		
C	985A	41.6	60.9	1.98	0.7770 [§]		
D	1181A	67.1	78.5	2.50	0.8079 [§]		
E	416	63.0	52.2	3.56	0.8464 [§]		
F	437	78.3	128.5	5.03	0.8991 [§]		
Rendezvous Metagabbro							
G	1294A	11.5	144.7	0.232	0.7082 [§]		
G	1294B	23.0	151.8	0.438	0.7192 [§]		
G	1294G	39.0	167.5	0.675	0.7265 [§]		
Mount Owen Quartz Monzonite							
H	421	104.9	68.1	4.54	0.8915 [§]	} 2495 ± 75	
I	R-1	173.2	65.3	7.91	1.016		
J	TC-1	210.2	58.8	10.75	1.110		
K	542	161.6	38.9	12.60	1.181		
L	847	172.6	29.1	17.83	1.346		
M	962	215.0	33.0	20.12	1.456		

*Sample localities are shown on Figure 2.

†Normalized to Sr⁸⁶/Sr⁸⁸ = 0.1194.

§Indicates determinations made on unspiked sample; all other determinations made on spiked samples.

undergone the same episodes of high-grade regional metamorphism and deformation. We have therefore also calculated a single composite isochron (Fig. 7) for all of the Webb Canyon Gneiss and Rendezvous Metagabbro analyses, plus the analysis of the plagioclase gneiss in the layered gneiss sequence. This yields an age of 2,875 ± 150 m.y. with an initial Sr⁸⁷/Sr⁸⁶ ratio of 0.700 ± 0.002 (model 4 solution of McIntyre and others, 1966). The slope of this isochron and therefore the age is dependent largely on the analyses of the Webb Canyon Gneiss; the initial Sr⁸⁷/Sr⁸⁶ ratio is controlled principally by the metagabbro and plagioclase gneiss analyses.

Because all the rocks included have undergone extensive recrystallization during high-grade regional metamorphism, we interpret the isochron age to be the approximate date of the metamorphism. K-Ar ages of 2,780 and 2,800 m.y. on hornblende from amphibolite interlayered with biotite gneisses on Mount Moran (Table 4) are in accord with this interpretation. The isochrons constructed for both the Webb Canyon Gneiss alone and for the composite samples show scatter in the data which exceeds the experimental error. The basic assumptions of the Rb-Sr dating method are that all the samples started with the same Sr⁸⁷/Sr⁸⁶ ratio and subsequently retained all

of their Rb and Sr. The departure of the data points from a straight line by more than the experimental error shows that one or the other of these assumptions is not strictly correct. However, the reasonable initial ratio and the agreement with other geochronologic results in nearby areas suggest that the isochron age is probably meaningful to within the stated uncertainty.

The initial Sr⁸⁷/Sr⁸⁶ ratio (the y-intercept of the isochron line) is an indication of the source and history of the strontium in the rocks. The Sr⁸⁷/Sr⁸⁶ ratio in the mantle 2.9 b.y. ago is inferred to have been between 0.700 and 0.701 (Hedge and Walthall, 1963; Hedge, 1966). Because the initial Sr⁸⁷/Sr⁸⁶ ratio in the Webb Canyon Gneiss and Rendezvous Metagabbro is in the same range as mantle strontium 2.9 b.y. ago, we conclude that unless substantial increases in Rb/Sr ratios occurred during metamorphism, the original rocks were removed from the mantle only shortly before the episode of high-grade regional metamorphism dated by the isochron.

Age and Strontium Composition of the Mount Owen Quartz Monzonite

Six whole-rock samples of the Mount Owen Quartz Monzonite (Table 1), define an isochron (Fig. 8) with an age of 2,495 ± 75 m.y. and

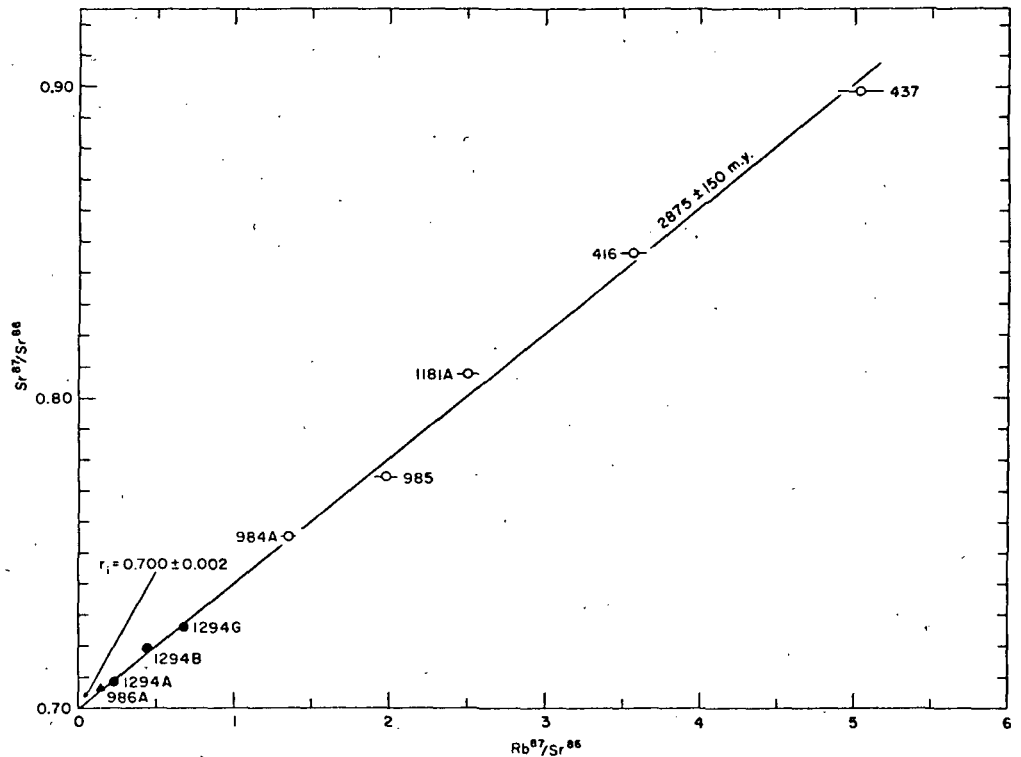


Figure 7. Rb-Sr isochron diagram for whole-rock samples of Webb Canyon Gneiss (open circles), Rendezvous Metagabbro (solid circles), and plagioclase

gneiss (triangle). Horizontal lines through circles indicate analytical uncertainty in Rb^{87}/Sr^{86} .

an initial Sr^{87}/Sr^{86} ratio of 0.732 ± 0.009 (model 1 of McIntyre and others, 1966). The age is consistent with preliminary Pb^{207}/Pb^{206} isotopic ages on four separates of zircon from the sample from locality J which range from 2,420 to 2,510 m.y. However, the zircons contain appreciable amounts of common lead and are highly discordant, making a unique interpretation of their isotopic ages difficult.

The initial Sr^{87}/Sr^{86} ratio is extremely high for a Precambrian rock. There is a possibility that this is a result of postcrystallization disturbance of the isotopic system. So-called "rotated isochrons" characterized by a reduced age and an anomalously high apparent initial ratio arising during postcrystallization metamorphism have been documented by Zartman and Stern (1967) and Zartman and Marvin (1971). However, both the very close fit of the points to the isochron (Fig. 8) and the apparent agreement between the isochron age and the Pb^{207}/Pb^{206} ages on zircon are difficult to explain on the basis of isochron

rotation. The anomalously high initial Sr^{87}/Sr^{86} ratio is probably real, and we interpret the isochron age as being close to the age of emplacement of the quartz monzonite.

If the high initial Sr^{87}/Sr^{86} ratio is an isotopic characteristic of the magma, the magma could not have been derived directly from the mantle, which 2.5 b.y. ago should still have had a Sr^{87}/Sr^{86} ratio of between 0.700 and 0.701 (Hedge and Walthall, 1963; Hedge, 1966).

Evidently the anomalous strontium was derived from crustal rocks, either at the present level of exposure or at deeper levels. We have determined Rb and Sr concentrations and Rb-Sr ratios on a number of samples of the wall rocks of the Mount Owen and have calculated their Sr^{87}/Sr^{86} ratios and radiogenic Sr^{87} contents 2.5 b.y. ago on the assumption that they would plot on the same isochron as the Webb Canyon Gneiss and Rendezvous Metagabbro. The results are summarized in Table 2 and Figure 9. Of the 33 samples analyzed, only one would have had a Sr^{87}/Sr^{86} ratio higher

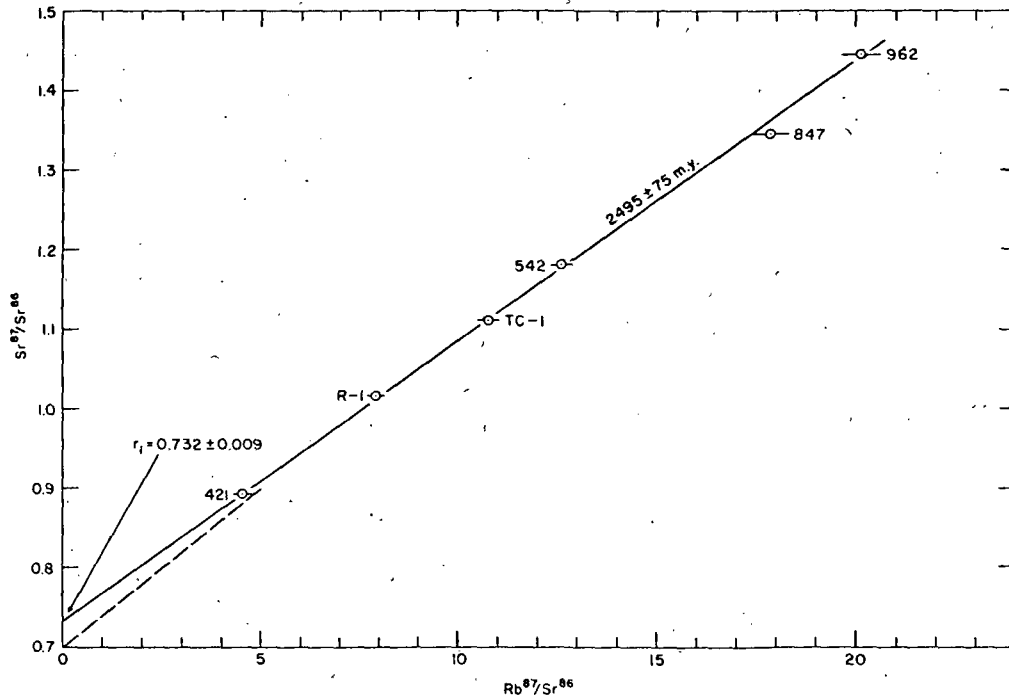


Figure 8. Rb-Sr isochron diagram for whole-rock samples of Mount Owen Quartz Monzonite. Horizontal lines through circles indicate analytical uncertainty in Rb⁸⁷/Sr⁸⁶. Dashed line is Webb Canyon Gneiss-Rendezvous Metagabbro whole-rock isochron from Figure 7.

than that of the Mount Owen Quartz Monzonite. This strongly suggests that the anomalous strontium in the Mount Owen was not derived from the wall rocks by any process such as large-scale digestion of inclusions or replacement of wall rocks. This result is in accord with the field evidence and with the bulk chemistry of the rocks.

The high Sr⁸⁷/Sr⁸⁶ ratio in the Mount Owen would appear to be the result of either (1)

incorporation of strontium representative of crustal rocks with Sr⁸⁷/Sr⁸⁶ ratios much higher than those of the present wall rocks, or (2) selective incorporation of radiogenic Sr⁸⁷ through some process involving isotopic fractionation, perhaps partial anatexis or hydrothermal flushing of radiogenic strontium, or (3) some combination of (1) and (2).

If a process of preferential extraction of radiogenic strontium from rocks like the

TABLE 2. AVERAGE Rb AND Sr CONTENTS AND Rb-Sr RATIOS FOR VARIOUS ROCK TYPES AND ESTIMATED Sr⁸⁷/Sr⁸⁶ RATIOS AND RADIOGENIC Sr⁸⁷ CONTENTS 2.5 B.Y. AGO

Rock type	Number of samples	Rb (ppm)		Sr (ppm)		Rb/Sr		Estimated Sr ⁸⁷ /Sr ⁸⁶ 2.5 B.Y. ago	Estimated radiogenic Sr ⁸⁷ 2.5 B.Y. ago (ppm)
		Average	Range	Average	Range	Average	Range		
Biotite Gneiss	14	68	16 to 149	220	56 to 917	0.309	0.047 to 2.68	0.7049	0.107
Amphibolite	3	12	5 to 17	98	86 to 119	0.122	0.063 to 0.192	0.7019	0.018
Rendezvous Metagabbro	7	23	8 to 43	185	167 to 207	0.124	0.040 to 0.217	0.7019	0.035
Webb Canyon Gneiss	9	69	35 to 105	87	57 to 109	0.793	0.445 to 1.74	0.7127	0.109
Mount Owen Quartz Monzonite	12	201	116 to 368	44	18 to 74	4.57	1.57 to 12.51	0.732	--

Rb and Sr contents and Rb/Sr ratios determined by x-ray fluorescence methods similar to those described by Doering (1968) using samples analyzed by isotope dilution methods (Table 1) as standards. Analyst, W. P. Doering.

present wall rocks were operative; the volume of rock involved can be estimated. Assuming the magma originally contained 44 ppm strontium (Table 2) with a Sr^{87}/Sr^{86} ratio of about 0.703 (typical of 2.5-b.y.-old granitic rocks), the equivalent of 0.13 ppm of pure Sr^{87} must be added to raise the ratio to 0.732. This would require *complete* extraction of radiogenic Sr^{87} from a volume of rock with radiogenic Sr^{87} contents like the biotite gneisses or Webb Canyon Gneiss slightly greater than the volume of the Mount Owen Quartz Monzonite or *partial* extraction from correspondingly greater volumes.

Later Events

The only Precambrian events in the geologic record subsequent to the emplacement of the Mount Owen Quartz Monzonite are (1) intrusion of the diabase dikes, (2) widespread incipient low-grade metamorphism of the dikes and the older rocks, and (3) local shearing and alteration along fault zones.

In an attempt to evaluate the effect of later events on the mineral ages, we have studied the Rb-Sr systematics in the major mineral phases in two typical samples of the Mount Owen Quartz Monzonite and have made a detailed K-Ar study of the large diabase dike exposed on the east face of Mount Moran (Fig. 3). Analytical data on the major minerals from whole-rock samples of Mount Owen Quartz Monzonite from localities J and M are given in Table 3 and plotted in Figure 10. Whole-rock analyses of the same samples are given in Table 1. If no redistribution of Rb or Sr had taken place since crystallization of the quartz monzonite, all of the data points for the individual minerals would plot on the whole-rock isochron. The fact that most of the minerals do not fit the whole-rock isochron shows that significant redistribution of these elements has occurred. However, the excellent fit of the whole-rock analyses to the isochron in Figure 8 shows that the redistribution did not affect volumes of rock as large as the whole-rock samples (1 to 5 kg).

The plagioclase and microcline data from each of the rocks define mineral isochrons (Fig. 11) whose slopes correspond within analytical uncertainty to an age of about 1,800 m.y. Each line passes through the corresponding whole-rock point, but, as has been pointed out by Naylor and others (1970), this is required by material balance since most of the

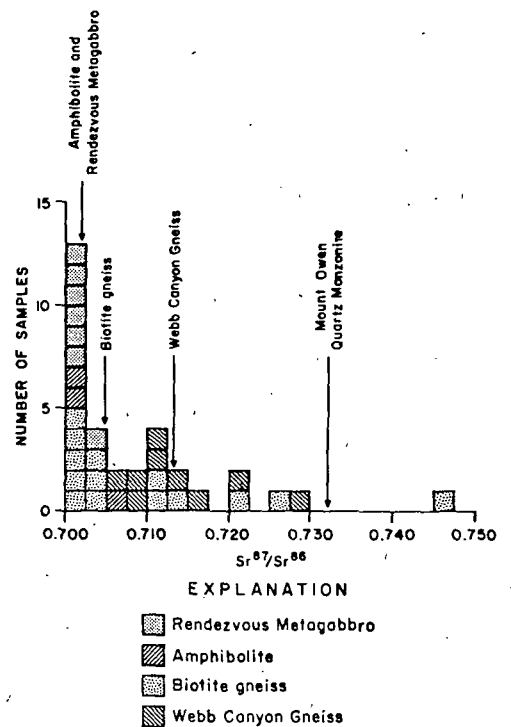


Figure 9. Estimated Sr^{87}/Sr^{86} ratios of various wall rocks at the time of emplacement of the Mount Owen Quartz Monzonite. Data from Table 2. Average values for various rock types are indicated by vertical arrows.

Rb and Sr in the rocks are contained in the feldspars. The muscovite from locality M lies nearly on the whole-rock isochron, indicating that the mineral did not participate in any later re-equilibration, but the muscovite for locality J lies close to the feldspar isochron, showing that it did participate. Both biotite points fall well below the mineral isochrons. The apparent ages of the biotites are 1,440 and 1,550 m.y.

Table 4 summarizes K-Ar ages in and adjacent to the diabase dike on Mount Moran (Fig. 3). All the samples from locality N were collected along a single horizontal traverse northward from the center of the dike at an elevation of about 9,700 ft where the dike is 110 ft thick. The sample from locality O came from near the center of the dike at elevation 8,100 ft. Hornblende from locality B came from a segregation pegmatite in the Webb Canyon Gneiss that is unrelated to the Moran dike but is included for comparison.

Hornblende from the wall rocks has ages

TABLE 3. RUBIDIUM AND STRONTIUM DATA AND APPARENT AGES OF MINERALS FROM MOUNT OWEN QUARTZ MONZONITE

Sample locality*	Mineral	Rb (ppm)	Sr (ppm)	Rb ⁸⁷ /Sr ⁸⁶	(Sr ⁸⁷ /Sr ⁸⁶) _n [†]
M	Plagioclase	40.0	56.5	2.10	0.9808 [‡]
M	Microcline	539.3	47.2	33.06	1.761
M	Muscovite	643.5	40.8	54.62	2.720
M	Biotite	636.9	60.3	33.44	1.662
J	Plagioclase	20.5	50.1	1.24	0.8754
J	Microcline	409.0	75.2	16.62	1.278
J	Muscovite	551.2	17.5	118.9	3.852
J	Biotite	1,189.2	39.1	108.0	3.032

*Sample localities are shown on Figure 2.
 †Normalized to Sr⁸⁶/Sr⁸⁸ = 0.1194.
 ‡Indicates determination made on unspiked sample; all other determinations made on spiked samples.

ranging from 2,800 m.y. to 2,600 m.y. The older age corresponds very closely to the time of regional metamorphism inferred from the Webb Canyon Gneiss-Rendezvous Metagabbro whole-rock isochron. The lower age is found within 2 ft of the dike contact and may be due to partial Ar loss from heating of the wall rocks during intrusion of the dike. The difference, however, is only slightly greater than analytical uncertainty, and hornblende from the Webb Canyon Gneiss well removed from any known diabase dike is even younger.

The three ages for biotite from the wall rocks (1320, 1350, and 1450 m.y.) are analytically indistinguishable, and all lie in the same range as biotite from elsewhere in the Teton Range. No further decrease in the apparent age of the wall-rock biotite was found even within 5 ft (0.045 dike widths) of the contact. Rock from the chilled margin of the dike has an apparent age of 775 m.y., whereas plagioclase from near the center of the dike has apparent ages of 583 and 396 m.y.

The results are ambiguous as to the time of

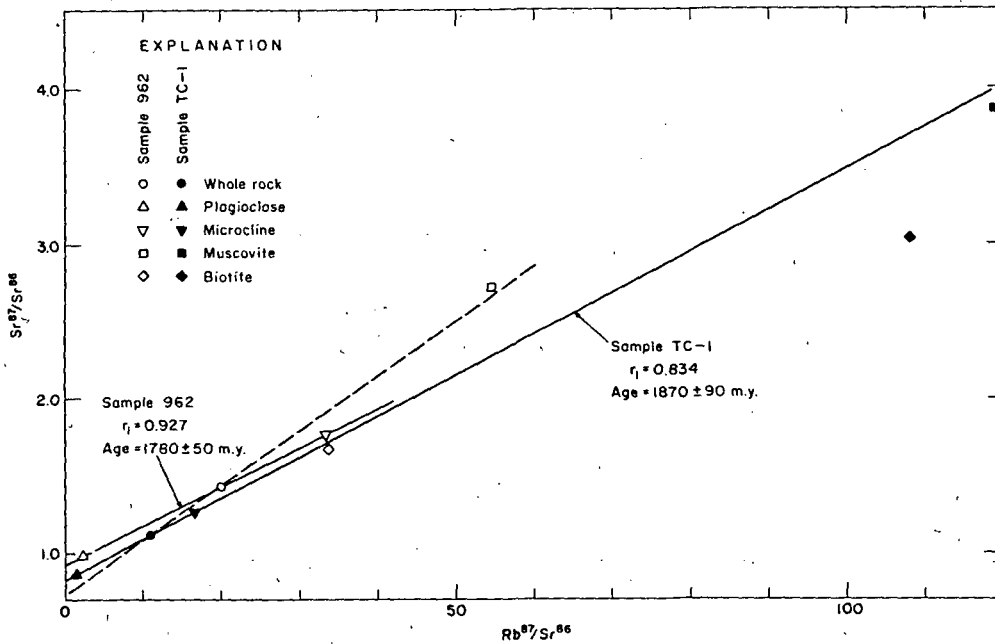


Figure 10. Rb-Sr isochron diagram for minerals from Mount Owen Quartz Monzonite samples from localities J and M. Dashed line is whole-rock isochron from

Figure 8. Solid lines are plagioclase-microcline isochrons for each sample.

TABLE 4. POTASSIUM-ARGON AGES FROM THE TETON RANGE, CHIEFLY FROM THE DIABASE DIKE ON MOUNT MORAN AND ITS WALL ROCKS

Material	K ₂ O* (percent)	Ar ⁴⁰ radiogenic† (moles x 10 ⁻⁹ /gm)	Ar ⁴⁰ radiogenic (percent)	Age ±2σ (m.y.)
Pegmatite in Webb Canyon Gneiss, sample locality B [‡]				
Hornblende	1.711*	13.90	99	2580 ± 25
Wall rocks of diabase dike, Mount Moran, sample locality N [‡]				
Hornblende 0.7 ft from dike	0.620*	5.308	98	2,650 ± 25
Hornblende 2.0 ft from dike	0.523*	4.311	99	2,600 ± 80
Hornblende 10 ft from dike	0.519*	4.535	99	2,800 ± 90
Hornblende 20 ft from dike	0.638*	6.010	99	2,780 ± 80
Biotite 5 ft from dike	0.96	3.094	75	1,450 ± 90
Biotite 40 ft from dike	6.20	17.58	99	1,320 ± 50
Biotite 100 ft from dike	7.65	22.20	88	1,350 ± 50
Diabase from dike on Mount Moran, sample locality N [‡]				
Whole rock from chill zone	0.809*	1.142	90	775 ± 50
Plagioclase near center of dike	1.209*	0.7862	88	396 ± 6
Diabase from dike on Mount Moran, sample locality O [‡]				
Plagioclase near center of dike	1.331*	1.343	96	583 ± 8

*Indicates determination by isotope dilution, W. H. Henderson, analyst; all other determinations by flame photometer, Violet Merritt, analyst.

†H. H. Wehnert and R. F. Harvin, analysts.

‡Sample localities are shown on Figure 2.

emplacement of the dike. The plagioclase ages are in conflict with the field relations, for the same dike is overlain unconformably by the Cambrian Flathead Quartzite (Fig. 3). The 775-m.y. age on the chilled margin is geologically permissible and agrees approximately with whole-rock K-Ar ages on the chilled margin of a similar dike in the Beartooth Mountains reported by Hanson and Gast (1967) and Condie and others (1969). Condie, however, found a wide range of whole-rock K-Ar ages of the chilled margins of diabase dikes elsewhere in the Wyoming province.

If the 775-m.y. whole-rock age is accepted as the age of the dike, there is no explanation for the consistency of the biotite K-Ar ages in the wall rocks. According to the model of Hanson and Gast (1967, Fig. 8) a dike 110 ft thick and having an initial temperature of 1,100°C will heat the wall rock 5 ft away to a maximum temperature of nearly 700°C and will keep it above 300°C—the estimated minimum temperature required for complete loss of Ar from biotite—for more than 100 yrs. This should be reflected by a significant decrease in the apparent age of the biotite near the contact. We suggest that the dike was emplaced during or before the time recorded by the biotite K-Ar ages. According to this interpretation,

the *minimum age* of the dike is 1,450 ± 90 m.y., the oldest apparent age of biotite in the wall rocks, and the *maximum age* is 2495 ± 75 m.y., the age of the Mount Owen Quartz Monzonite.

K-Ar and Rb-Sr mineral ages from the Teton Range available in the literature (Giletti and Gast, 1961; Menzie, 1966; Giletti, 1968) are summarized in Figure 11. Except for two Rb-Sr ages on muscovite from pegmatites, none of the mineral ages approaches those that are inferred from the whole-rock Rb-Sr isochrons. Muscovite ages scatter all the way from 2,500 to 1,390 m.y. without any significant maxima in distribution.

K-Ar and Rb-Sr biotite ages tend to cluster in the range 1,100 to 1,500 m.y. A single Rb-Sr age for microcline from a pegmatite is close to the age indicated by our plagioclase-microcline isochrons.

While data from the Teton Range do not conclusively demonstrate an 1,800 m.y. thermal event, events at about that time have been identified elsewhere in the Wyoming province and in adjacent regions. Such an event may be responsible for re-equilibration of the Rb-Sr systems indicated by our plagioclase-microcline isochrons for the Mount Owen Quartz Monzonite. Most of the Rb-Sr and K-Ar ages on

biotite and some of the K-Ar ages on muscovite are appreciably younger than the 1,800 m.y. These lower ages indicate either a prolonged interval of high temperature following an 1,800 m.y. event or a distinctly younger and less intense thermal event.

The conspicuous chilled margins displayed by the diabase dikes suggest that the dikes were emplaced in relatively cool wall rocks and thus are compatible with the interpretation of a later episode of reheating. If so, the local low-grade metamorphism of the dike rocks and chloritization and sericitization of some of the minerals in the older rocks may also date from this time. We suggest that a distinct thermal event occurred between 1,330 and 1,500 m.y. ago and that the younger biotite and muscovite ages (Fig. 11) reflect slow uplift and cooling following the thermal maximum. Local shearing and alteration along Precambrian fault zones were concurrent with or postdated this event.

REGIONAL INTERPRETATION

Figure 12 is a summary of the Precambrian geochronology of the Teton Range and of selected other areas in and adjacent to the Wyoming province. Catanzaro (1967) summarized much of the earlier data and, although considerable new data are now available, many of the conclusions he presented are not substantially changed.

Ages greater than 3,000 m.y. have been re-

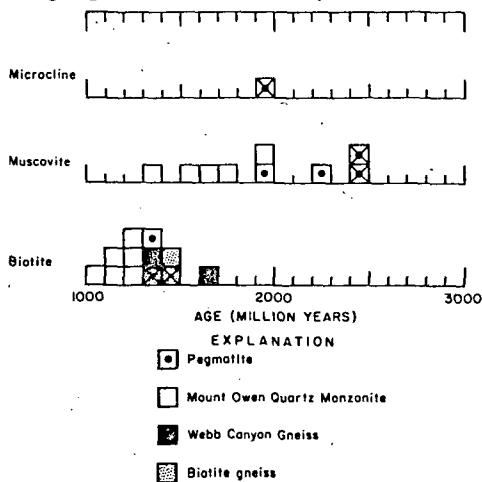


Figure 11. Histogram of K-Ar and Rb-Sr mineral ages from the Teton Range reported by Giletti and Gast (1961) and Menzie (1966). Boxes with X's are Rb-Sr ages; all others are K-Ar ages.

ported in several areas in the Wyoming province. Giletti (1966, 1968) found a single Rb-Sr age of 3,260 m.y. for granitic gneiss from the Blacktail Range, Montana, and K-Ar ages of 3,220 and 3,270 m.y. on biotite from granitic gneiss in the Gallatin Canyon, Montana. Heimlich and Banks (1968) have reported K-Ar ages of 3,100 and 3,180 m.y. on biotite from one body of quartz diorite and 3,060 m.y. on biotite from a schist skialith in another body of quartz diorite in the Bighorn Mountains. In view of the uncertainties inherent in single Rb-Sr and K-Ar age determinations in complex metamorphic terranes, the significance of these scattered ages will be in doubt until they are confirmed by further geochronologic studies.

The only other ages older than 3,000 m.y. are discordant isotopic ages on apparently detrital zircon from metasedimentary schists, hornfels (Nunes and Tilton, 1971) and granitic paragneiss (Catanzaro and Kulp, 1964; Catanzaro, 1968) in the Beartooth Mountains. These ages suggest a source terrane for at least some of the metasedimentary rocks of the Wyoming province that is older than 3,140 m.y. (assuming an episodic lead loss model) or 3,300 m.y. (assuming a continuous diffusion model).

Ages in the range 2,500 to 2,900 m.y. are found throughout the Wyoming province and have generally been interpreted as indicating an episode of intense regional metamorphism, migmatization, and emplacement of plutonic rocks.

The northernmost exposures of rocks from which ages in this range have been reported are in the Little Belt Mountains, Montana, where Catanzaro and Kulp (1964) and Catanzaro (1968) have found that zircons from migmatitic gneisses have discordant ages that can be interpreted by a continuous diffusion model as 2,700 m.y. and which they suggest may date an episode of intrusion and migmatization.

Metamorphic rocks in the Beartooth Mountains, Montana, have yielded a Rb-Sr whole-rock isochron age of 2,730 ± 150 m.y. (Powell and others, 1969), whereas zircon from the Stillwater Complex has nearly concordant Pb²⁰⁷/Pb²⁰⁶ ages of 2,750 m.y. (Nunes and Tilton, 1971). Brookins (1968) has obtained a whole-rock Rb-Sr age of 2,660 m.y. for the late synkinematic or postkinematic Crevice Mountain Granite in the southern Beartooth Mountains in Wyoming.

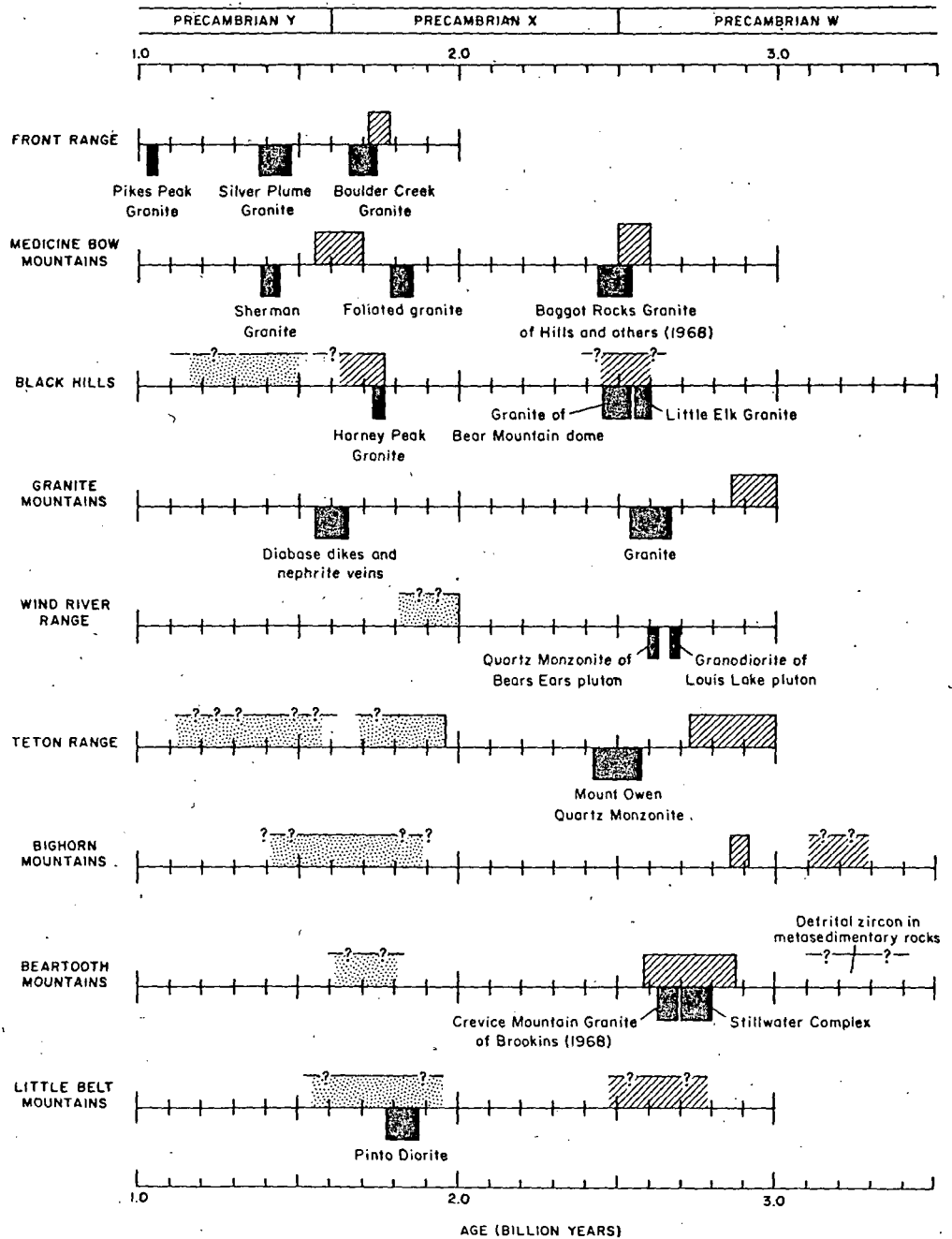


Figure 12. Summary of Precambrian geochronology of selected areas in and adjacent to the Wyoming province. Sources of data are cited in text. Solid boxes below time lines indicate intrusive events. Lined boxes above time lines indicate principal metamorphic episodes; stippled boxes indicate re-equilibration of isotopic systems without significant metamorphism. Lengths of boxes indicate analytic or geologic uncertainties.

Basement rocks exposed in the cores of the gneiss domes in the Albion Range, Idaho, have a whole-rock isochron age of $2,610 \pm 300$ m.y. (Armstrong and Hills, 1967; Armstrong, 1968). These rocks have undergone amphibolite facies regional metamorphism during the Mesozoic, and therefore their Precambrian history is difficult to decipher, but they represent the westernmost known occurrence of rocks of the Wyoming province.

Heimlich and Banks (1968) obtained concordant Pb-U ages of 2,930 m.y. on monazite from a quartz monzonite gneiss in the northern Bighorn Mountains which they believe is of metasomatic origin. Zircons from the same rock have Pb^{207}/Pb^{206} ages of 2,820 to 2,830 m.y. Heimlich and Banks suggest that the zircons may be detrital and that they have been reset during a metamorphic event that led to formation of the gneiss. The same authors found a maximum K-Ar age of 2,780 m.y. on biotite from nonmigmatitic metasedimentary gneiss in the southern part of the Bighorn Mountains.

Rb-Sr whole-rock isochron ages of $2,825 \pm 80$ m.y. on paragneisses and orthogneisses in the Granite Mountains have been reported by Peterman and others (1971) and interpreted as dating major regional metamorphism. Granite from small postkinematic plutons has a Rb-Sr whole-rock isochron age of $2,610 \pm 70$ m.y. In the nearby Wind River Range, Naylor and others (1970) have found ages on zircons that suggest primary ages of $2,607 \pm 15$ m.y. and $2,687 \pm 15$ m.y. for the apparently postkinematic Bears Ears and Louis Lake plutons.

Hills and others (1968) have found a whole-rock isochron age of $2,550 \pm 50$ m.y. for gneisses from the northern part of the Medicine Bow Mountains. They interpreted this as dating a metamorphic event, but concluded on the basis of the initial Sr ratio that the rocks are not more than 200 m.y. older than the metamorphism. Zircon concordia and whole-rock Rb-Sr isochron ages indicate that their late synkinematic and postkinematic Baggot Rocks Granite was emplaced 2,400 to 2,480 m.y. ago.

Rocks comparable in age to those of the Wyoming province, have also been identified in the Black Hills, South Dakota. Zartman and Stern (1967) reported a Pb-U concordia age of 2,560 m.y. for the Little Elk Granite in the northeastern Black Hills, and Ratté and Zartman (1970) found a whole-rock Rb-Sr age of about 2,500 m.y. for granite in the Bear Moun-

tain dome in the west-central part of the Black Hills. These granitic rocks, which appear in the cores of gneiss domes, seem to be part of a metamorphic terrane that is older than the bulk of the surrounding Precambrian rocks and that forms a link between the Wyoming province and the Superior province of the Canadian shield (Zartman and others, 1964).

Thus the inferred episode of migmatization and metamorphism in the Bighorn Mountains, the major metamorphism and emplacement of the Stillwater complex in the Beartooth Mountains, a possible episode of intrusion and migmatization in the Little Belt Mountains, and the major regional metamorphism in the Granite Mountains are synchronous or nearly so with the principal regional metamorphic episode in the Teton Range. Except for the 3,000-m.y.-old detrital zircon identified in the Beartooth Mountains, there is no direct evidence of the original age of the rocks affected by these metamorphic episodes. The inference from the initial Sr composition that many of the rocks in the Teton Range are not much older than the metamorphic event may also apply to some or all of the rocks elsewhere in the Wyoming province. Late synkinematic and postkinematic granitic rocks with ages 100 to 300 m.y. younger than the principal metamorphic events have been identified in the Beartooth Mountains, Granite Mountains, and Wind River Range, as well as in the Teton Range.

The principal metamorphic event and the late synkinematic to postkinematic granite in the northern Medicine Bow Mountains all seem to be somewhat younger than those recorded farther north and west. Metamorphic events associated with emplacement of the older granitic rocks in the Black Hills and the poorly dated Precambrian metamorphism in the Albion Range may be comparable in age to the metamorphism in the Medicine Bow Mountains. Although the evidence is far from conclusive, ages of rocks in the Wyoming province may decrease toward the western, southern, and eastern margins.

The effects of younger thermal events like those recorded by mineral ages in the Teton Range are widespread elsewhere in the Wyoming province. Brookins (1968) found an 1,850-m.y. potassium-feldspar whole-rock isochron for the Crevice Mountain Granite in the Beartooth Mountains and K-Ar ages of 1,180 m.y. for potassium feldspar, 1,650 m.y. for biotite, and 1,820 m.y. for muscovite. He interpreted

these ages as indicating a metamorphic episode 1,600 to 1,800 m.y. ago which may have produced the slightly granulated texture in the granite. Nunes and Tilton (1971) found evidence of disturbance of the Pb-U system in apatite from the Stillwater Complex about 1,600 m.y. ago.

In the Wind River Range, Naylor and others (1970) found evidence of disturbance of the Rb-Sr systems in the 2,600- to 2,700-m.y.-old granitic rocks less than 2,000 m.y. ago. They noted no obvious petrographic evidence of this disturbance, but mineral isochrons were appreciably affected, and one biotite-whole rock isochron is as young as 1,680 m.y. In the Granite Mountains, K-Ar and Rb-Sr mineral ages indicate that diabase dikes similar to those in the Teton Range and associated nephrite veins were emplaced about 1,600 m.y. ago (Peterman and others, 1971).

No large intrusive bodies that might be related to the 1,600 to 1,800 m.y. events have been identified in the central part of the Wyoming province, but intrusions in this age range have been found in several areas near the margins of the province, and they are widespread in the flanking terranes. They include the 1,820-m.y.-old Pinto Diorite in the Little Belt Mountains (Woodward, 1970); the 1,740-m.y.-old Harney Peak Granite in the Black Hills, South Dakota (Riley, 1970), the 1,820-m.y.-old granitic rocks in the southern Medicine Bow Mountains (Hills and others, 1968) and the 1,700-m.y.-old Boulder Creek Granite and related rocks in the Front Range, Colorado (Peterman and others, 1968). In most of these areas, the granitic rocks seem to be nearly synchronous with episodes of medium- and high-grade regional metamorphism.

The hypothesized 1,300 to 1,500 m.y. thermal event in the Tetons has not been generally recognized elsewhere in the Wyoming province, although mineral ages within this range do occur in the Black Hills (Aldrich and others, 1958; Zartman and others, 1964). To the south of the Wyoming province, this interval includes emplacement of the Sherman Granite in the Medicine Bow Mountains (Hills and others, 1968) and the Silver Plume Granite in the Colorado Front Range (Peterman and others, 1968).

ACKNOWLEDGMENTS

We are indebted to T. B. Ransom, J. V. Dieterich, D. B. Steller, A. C. Chidester, D.

A. Coates, and R. W. Blair for assistance in the field. The co-operation and interest of the personnel of Grand Teton National Park were essential. We especially acknowledge the help of Howard C. Chapman, Willard C. Dille, Charles H. McCurdy, R. Alan Mebane, and the late Fred C. Fagergren. J. David Love, with his deep interest in all phases of Teton geology, was a constant source of advice and encouragement.

The senior author is deeply grateful to the personnel of the U.S. Geological Survey geochronology laboratories in Denver for their patient instruction, generous forbearance, and unselfish sharing of space and equipment while he was a guest in their facilities. Individuals who performed or assisted with specific analytical procedures are W. T. Henderson, R. F. Marvin, H. H. Mehnert, R. A. Hildreth, W. P. Doering, C. E. Hedge, and Z. E. Peterman. C. E. Hedge and Z. E. Peterman deserve particular thanks for their continued interest in the project and their advice in interpreting some of the analytical results.

REFERENCES CITED

- Aldrich, L. T., Wetherill, G. W., Davis, G. L., and Tilton, G. R., 1958, Radioactive ages of micas from granitic rocks by Rb-Sr and K-A methods: *Am. Geophys. Union Trans.*, v. 39, no. 6, p. 1124-1134.
- Armstrong, R. L., 1968, Mantled gneiss domes in the Albion Range, southern Idaho: *Geol. Soc. America Bull.*, v. 79, no. 10, p. 1295-1314.
- Armstrong, R. L., and Hills, F. A., 1967, Rubidium-strontium and potassium-argon geochronologic studies of mantled gneiss domes, Albion Range, southern Idaho, U.S.A.: *Earth and Planetary Sci. Letters*, v. 3, no. 2, p. 114-124.
- Bradley, C. C., 1956, The pre-Cambrian complex of Grand Teton National Park, Wyoming, *in* Wyoming Geol. Assoc. Guidebook, 11th Ann. Field Conf.: p. 34-50.
- Brookins, D. G., 1968, Rb-Sr and K-Ar age determinations from the Precambrian rocks of the Jardine-Crevise Mountain area, southwestern Montana: *Earth Sci. Bull.*, v. 1, no. 2, p. 5-9.
- Catanzaro, E. J., 1967, Correlation of some Precambrian rocks and metamorphic events in parts of Wyoming and Montana: *Mtn. Geologist*, v. 4, no. 1, p. 9-21.
- 1968, The interpretation of zircon ages, *in* Hamilton, E. I., and Farquhar, R. M., eds., *Radiometric dating for geologists*: New York, Interscience, p. 225-258.
- Catanzaro, E. J., and Kulp, J. L., 1964, Discordant zircons from the Little Belt (Montana), Bear-

- tooth (Montana), and Santa Catalina (Arizona) Mountains: *Geochim. et Cosmochim. Acta*, v. 28, no. 4, p. 87-124.
- Condie, K. C., 1969, Geologic evolution of the Precambrian rocks in northern Utah and adjacent areas: *Utah Geol. and Mineralog. Survey Bull.* 82, p. 71-95.
- Condie, K. C., Leech, A. P., and Baadsgaard, H., 1969, Potassium-argon ages of Precambrian mafic dikes in Wyoming: *Geol. Soc. America Bull.*, v. 80, p. 899-906.
- Dalrymple, G. B., and Lanphere, M. A., 1969, Potassium-argon dating: San Francisco, W. H. Freeman and Co., 258 p.
- Doering, W. P., 1968, A rapid method for measuring the Rb/Sr ratio in silicate rocks, in *Geological Survey research 1968: U.S. Geol. Survey Prof. Paper 600-C*, p. C164-C168.
- Engel, A.E.J., 1963, Geologic evolution of North America: *Science*, v. 140, no. 3563, p. 143-152.
- Giletti, B. J., 1966, Isotopic ages from southwestern Montana: *Jour. Geophys. Research*, v. 71, no. 16, p. 4029-4036.
- 1968, Isotopic geochronology of Montana and Wyoming, in Hamilton, E. I., and Farquhar, R. M., eds., *Radiometric dating for geologists*: New York, Interscience, p. 111-146.
- Giletti, B. J., and Gast, P. W., 1961, Absolute age of Pre-Cambrian rocks in Montana and Wyoming, in *Geochronology of rock systems*: New York Acad. Sci. Annals, v. 91, p. 454-458.
- Hanson, G. N., and Gast, P. W., 1967, Kinetic studies in contact metamorphic zones: *Geochim. et Cosmochim. Acta*, v. 31, no. 7, p. 1119-1153.
- Hedge, C. E., 1966, Variations in radiogenic strontium found in volcanic rocks: *Jour. Geophys. Research*, v. 71, no. 24, p. 6119-6129.
- Hedge, C. E., and Walthall, F. G., 1963, Radiogenic strontium-87 as an index of geologic processes: *Science*, v. 140, no. 3572, p. 1214-1217.
- Heimlich, R. A., and Banks, P. O., 1968, Radiometric age determinations, Bighorn Mountains, Wyoming: *Am. Jour. Sci.*, v. 266, no. 3, p. 180-192.
- Hills, F. A., Gast, P. W., Houston, R. S., and Swainbank, I. G., 1968, Precambrian geochronology of the Medicine Bow Mountains, southeastern Wyoming: *Geol. Soc. America Bull.*, v. 79, no. 12, p. 1757-1784.
- Horberg, C. L., and Fryxell, F. M., 1942, Precambrian metasediments in Grand Teton National Park: *Am. Jour. Sci.*, v. 240, no. 6, p. 385-393.
- James, H. L., 1972, Subdivisions of the Precambrian: An interim scheme to be used by the U.S. Geological Survey: *Am. Assoc. Petroleum Geologists Bull.*, v. 50, no. 6, p. 1026-1030.
- King, P. B., compiler, 1969, Tectonic map of North America: U.S. Geol. Survey, scale, 1:5,000,000.
- Love, J. D., and Reed, J. C., Jr., 1968, Creation of the Teton landscape—The geologic story of Grand Teton National Park: Moose, Wyoming, Grand Teton Nat. History Assoc., 120 p.
- McIntyre, G. A., Brooks, C., Compston, W., and Turek, A., 1966, The statistical assessment of Rb-Sr isochrons: *Jour. Geophys. Research*, v. 71, no. 22, p. 5459-5468.
- Menzie, J. C., 1966, Potassium-argon ages of the Teton Range, Wyoming [M.A.T. thesis]: Providence, Rhode Island, Brown Univ.
- Miyashiro, Akiho, 1961, Evolution of metamorphic belts: *Jour. Petrology*, v. 2, p. 277-311.
- Naylor, R. S., Steiger, R. H., and Wasserburg, G. J., 1970, U-Th-Pb and Rb-Sr systematics in 2700×10^6 year old plutons from the southern Wind River Range, Wyoming: *Geochim. et Cosmochim. Acta*, v. 3, p. 1133-1159.
- Nunes, P. D., and Tilton, G. R., 1971, Uranium-lead ages of minerals from the Stillwater igneous complex and associated rocks, Montana: *Geol. Soc. America Bull.*, v. 82, p. 2231-2250.
- Peterman, Z. E., Doe, B. R., and Bartel, Ardith, 1967, Data on the rock GSP-1 (granodiorite) and the isotope-dilution method of analysis for Rb and Sr, in *Geological Survey research 1967: U.S. Geol. Survey Prof. Paper 575-B*, p. B181-B186.
- Peterman, Z. E., Hedge, C. E., and Braddock, W. A., 1968, Age of Precambrian events in the northeastern Front Range, Colorado: *Jour. Geophys. Research*, v. 73, no. 6, p. 2277-2296.
- Peterman, Z. E., Hildreth, R. A., and NKomo, Ignatius, 1971, Precambrian geology and geochronology of the Granite Mountains, central Wyoming: *Geol. Soc. America, Abs. for 1971*, v. 3, no. 6, p. 403-404.
- Powell, J. L., Skinner, W. R., and Walker, D., 1969, Whole-rock Rb-Sr age of metasedimentary rocks below the Stillwater complex, Montana: *Geol. Soc. America Bull.*, v. 80, p. 1605-1612.
- Ratté, J. C., and Zartman, R. E., 1970, Bear Mountain gneiss dome, Black Hills, South Dakota—Age and structure: *Geol. Soc. America, Abs. for 1970*, v. 2, no. 5, p. 345.
- Reed, J. C., Jr., 1963, Structure of Precambrian crystalline rocks in the northern part of Grand Teton National Park, Wyoming, in *Short papers in geology and hydrology: U.S. Geol. Survey Prof. Paper 475-C*, p. C1-C6.
- Riley, G. H., 1970, Isotopic discrepancies in zoned pegmatites, Black Hills, South Dakota: *Geochim. et Cosmochim. Acta*, v. 34, p. 713-725.
- U.S. Geological Survey, 1971, Grand Teton National Park topographic map, scale, 1:62,500.
- Woodward, L. A., 1970, Time of emplacement of Pinto Diorite, Little Belt Mountains, Mon-

- tana: *Earth Sci. Bull.*, v. 3, p. 15-26.
- Zartman, R. E., and Marvin, R. F., 1971, Radiometric age (Late Ordovician) of the Quincy, Cape Ann, and Peabody Granites from eastern Massachusetts: *Geol. Soc. America Bull.*, v. 82, p. 937-958.
- Zartman, R. E., and Stern, T. W., 1967, Isotopic age and geologic relationships of the Little Elk Granite, northern Black Hills, South Dakota, in *Geological Survey research 1967*: U.S. Geol. Survey Prof. Paper 575-D, p. D157-D163.

Zartman, R. E., Norton, J. J., and Stern, T. W., 1964, Ancient granite gneiss in the Black Hills, South Dakota: *Science*, v. 145, no. 3631, p. 479-481.

MANUSCRIPT RECEIVED BY THE SOCIETY MAY 15, 1972

REVISED MANUSCRIPT RECEIVED AUGUST 25, 1972
PUBLICATION AUTHORIZED BY THE DIRECTOR, U.S. GEOLOGICAL SURVEY

Seismic Geyser and Its Bearing on the Origin and Evolution of Geysers and Hot Springs of Yellowstone National Park

GEORGE D. MARLER *Thornton, Idaho 83453*
DONALD E. WHITE *U.S. Geological Survey, Menlo Park, California 94025*

UNIVERSITY OF UTAH
RESEARCH INSTITUTE
EARTH SCIENCE LAB.

ABSTRACT

The major Hebgen Lake earthquake on August 17, 1959, profoundly affected the hot springs and geysers of Yellowstone National Park. The epicenter of this earthquake was about 48 km northwest of Upper Geyser Basin, and its magnitude was 7.1 on the Richter scale. No earthquake of closely comparable intensity had previously jarred the geyser basins in historic time. By the day after the earthquake, at least 289 springs in the geyser basins of the Firehole River had erupted as geysers; of these, 160 were springs with no previous record of eruption.

New hot ground soon developed in some places or became apparent by the following spring as new fractures in hot spring sinter or as linear zones of dead or dying trees. Some new fractures developed locally into fumaroles, and a few of these evolved into hot springs or geysers.

One fracture was inspected frequently as it evolved into a fumarole and, in about 2½ yr, into a small geyser. During the next few years, it became a very vigorous geyser, now named "Seismic," that erupted to heights of 12 to 15 m and explosively excavated a jagged-walled vent more than 12 m in maximum diameter and more than 6 m deep. Major eruptions ceased in 1971 when a small satellite crater formed and then assumed dominance.

The formation and evolution of Seismic Geyser provide the keys for understanding the origin of the craters and vents of other geysers and probably also the large smooth-walled nongeysering pools and springs of the morning glory type that provide no direct evidence of their origin.

Earthquakes, largely localized just outside the Yellowstone caldera, result in violent shaking of the large high-temperature convection systems of the geyser basins. New fractures form in the self-sealed shallow parts of these systems where high-temperature water is confined at pressures much above hydrostatic. As old fractures and permeable channels become sealed by precipitation of hydrothermal minerals, new channels are provided by the periodic seismic activity.

Our explanations for the origin of geyser and hot spring vents apply specifically to the geyser basins of Yellowstone Park, where near-surface fluid pressure gradients are commonly 10 to 50 percent above the hydrostatic gradient, and temperature gradients and thermal energy available for explosive eruption are correspondingly high. The same general explanations seem likely to account for the origin of geyser tubes and hot spring vents in other less favored areas where pressures and maximum temperatures are limited by hydrostatic pressures, probably with little or no overpressure being involved. *Key words: geohydrology, geysers, hot springs, thermal waters, geothermal energy, volcanology, fumaroles, earthquakes, hydrothermal eruptions.*

INTRODUCTION

The most significant event that has affected the geyser basins of Yellowstone National Park since its discovery was the Hebgen

Lake earthquake, which occurred at 11:37 P.M. on August 17, 1959, with a Richter magnitude of 7.1. Its epicenter was just west of the park, about 48 km northwest of the Upper Geyser Basin. No earthquake of closely comparable intensity had previously jarred the geyser basins in historic times. A greater number of hydrothermal changes occurred in response to this crustal disturbance than during the previous 90 yr of the park's history (Marler, 1964, 1973).

During the first few days after the earthquake, a reconnaissance was made of most of the thermal features in the Firehole geyser basins. Early results of the survey revealed that at least 289 springs had erupted as geysers. Of these, 160 were springs with no previous record of eruption. Some previously obscure springs had erupted very powerfully, and large pieces of sinter were strewn about their craters.

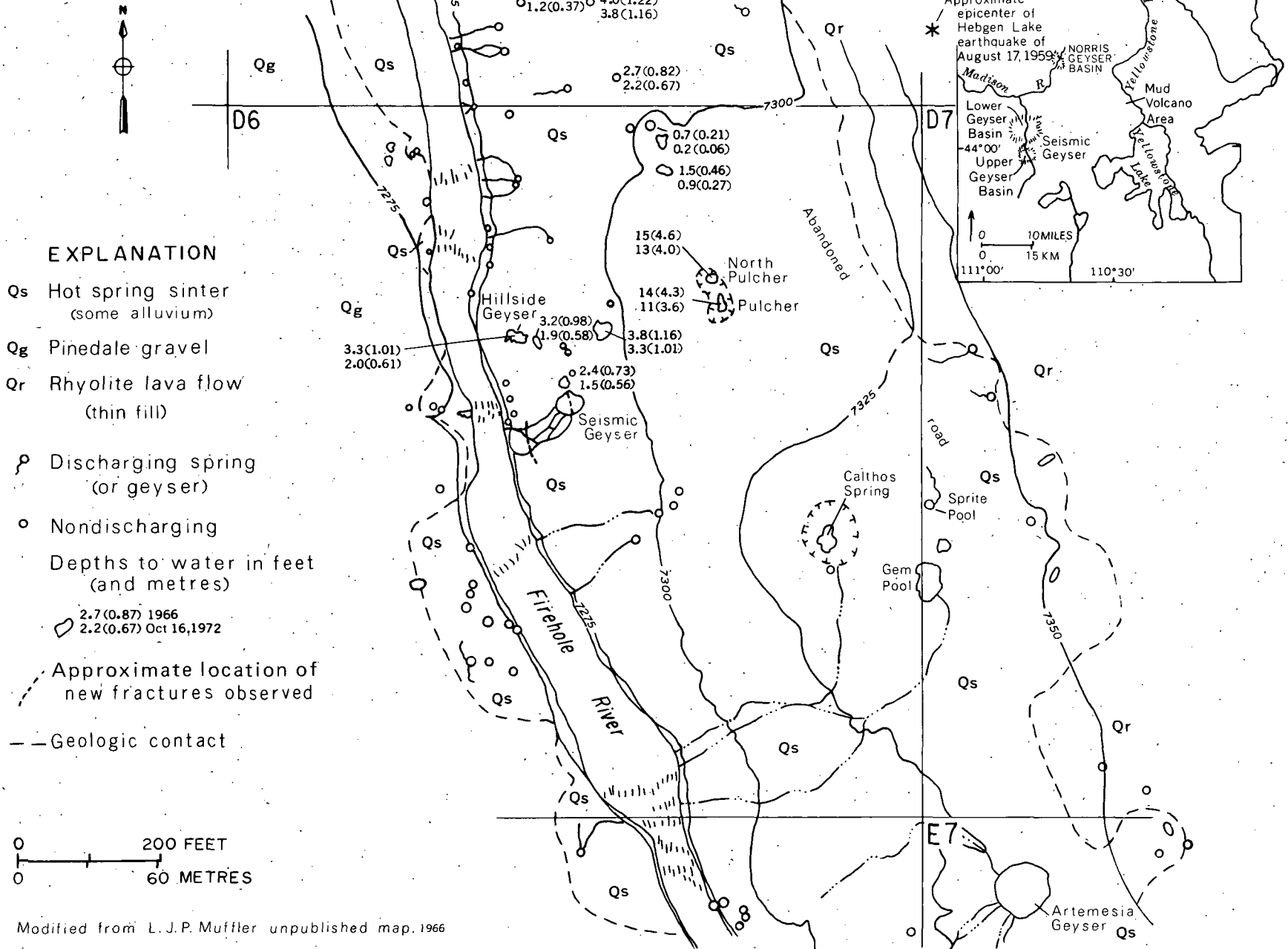
The beautifully colored and limpid water of hundreds of springs had become light gray to muddy. An early count revealed that 590 springs had become turbid. During the first few days after the earthquake, most springs began to clear, but several years passed before clearing was generally complete.

During the night of the earthquake, all major geysers erupted that had been recently active, and some that had been dormant for many years were rejuvenated. Several important geysers began to erupt on shorter intervals, and most of these have persisted in having shorter intervals between eruptions. A few geysers soon became dormant, and some of these are still dormant at the present time (1974). After varying periods of quiescence of months to years duration, others that temporarily became dormant were rejuvenated. In 1960, temperature data of all important springs along the Firehole River showed an average increase of about 3°C above their pre-earthquake temperatures. By 1964, the average temperature had declined slightly below the 1960 level.

One of the important changes in the Firehole geyser basins that resulted from the earthquake was the development of new hot ground. In a few places these hot spots were evident as new fractures that developed in the hot-spring sinter which generally mantles the active areas. Most of the less conspicuous hot spots did not become evident until the spring of 1960 when they were revealed as linear distributions of dead or dying lodgepole pines, generally trending northwest toward Hebgen Lake. Twenty-seven such sites were counted, most of which were in the Upper and Lower Geyser Basins. Some fumaroles related to these new fractures later became the sites of hot springs and geysers. The evolution of one of these fractures into a fumarole and then into a large geyser (Seismic) has far-reaching significance in understanding the formation of other geysers, geyser tubes, and hot-spring vents, and is the main subject of this paper.

Among the thousands of thermal springs in Yellowstone Park, Seismic Geyser is one of the few that is totally recent in origin. It is not a quiescent or dormant spring that was reactivated but rather is one that had its genesis as a direct result of the earthquake on August 17, 1959. The following is a résumé of its development and evolution during its first fifteen years of existence.

Figure 1. Geologic map of the area near Seismic Geyser, Upper Basin, Yellowstone National Park (map and 1966 data by L.J.P. Muffler, U.S. Geol. Survey).



Modified from L. J. P. Muffler unpublished map, 1966

EVOLUTION OF SEISMIC GEYSER

Within several days after the earthquake, two new fractures were observed in an embankment of old sinter that borders the east bank of the Firehole River in Upper Geysir Basin about 550 m south of the Biscuit Basin parking area. The fractures were nearly parallel to the river; their original locations, as nearly as can now be determined, are shown in Figure 1. The breaks had a north-northwest alignment, nearly on the southeastern extension of the Hebgen Lake fault, probably reflecting the regional stress pattern. The break nearest the river was the most conspicuous, being about 20 m long. The eastern fracture was about 15 m east of the edge of the steep declivity to the river and was about 10 m long. Steam was issuing near the central part of each break. The width of the upper (eastern) break near its prominent steam vent was about 1 cm. Recorded temperatures of both the upper and lower fumaroles were about 95°C (but the thermometer had not been standardized). The fact that steam was escaping under pressure indicates a temperature above the boiling temperature at this elevation, about 92.9°C. The upper break traversed an area of densely growing lodgepole pines that were about 50 yr old. One of the first wagon roads into the Upper Basin crossed directly over the site of the upper break.

During the remainder of 1959, the discharge of steam under slight pressure continued unabated from both fumaroles. When this site was first visited by Marler in the early spring of 1960, not only was a heavy discharge of steam still evident (Fig. 2), but also the pines over an area of at least 150 m² were either dead or dying. In addition to the heat that was visibly discharging from the fumaroles, these dying trees were evidence that new hot ground had developed, with near-surface temperatures too high to be tolerated by the vegetative cover.

By the fall of 1960, the evolution of steam from both fumaroles had increased in intensity. The shorter break farthest from the river showed the most pronounced change, and at the point of steam egress, its width was then about 2½ cm. By October, its temperature had risen to 96.1°C, and the ground near this fumarole had subsided somewhat, suggesting some change in underground conditions. The possibilities seemed excellent for a new spring or geyser to develop.

During 1961 and 1962, frequent inspections of these steam vents indicated that the vigor of steam discharged from both fumaroles was persisting in a manner comparable to that of 1960. During both years, it seemed likely that water would start to discharge from the upper fumarole.

When the site of the fumaroles was first visited in the early spring of 1963, a major change had taken place. Sometime during the previous winter, explosive activity had occurred at the site of the upper fumarole. Where steam previously had been hissing through a narrow rift, there was now a large crater. Numerous large blocks of sinter from 0.3 to 1 m in diameter were strewn about randomly, bearing evidence that the crater had formed explosively (Fig. 3). The trees that had formerly been over the site of the crater were now scattered and prostrate, especially south and west of the vent. The crater was 1.5 to 2 m deep and was elongated perpendicular to the river, measuring about 2.7 to 4.9 m. Surprisingly, the long axis was perpendicular to the original break, apparently because of the angle at which the explosion(s) occurred, from west to east.

During all of 1963, water jets about 1 m high played into the crater every few seconds; the jets shot at an angle of about 45° from the west end of the crater. The water drained from the bottom of the crater immediately after each jetting. Thus, the former fumarole had evolved into a small geyser.

Further change in the evolution of the new geyser was noted during 1964. The action became more forceful than it was in 1963, but the eruptions were less frequent. Some of the jets angled eastward almost the length of the crater, which was then about 4 m long.

Also, water began to remain in the bottom of the crater between eruptions. By the end of summer, the water generally stood between 0.9 and 1.2 m below the rim. The fumarole on the western fracture along the steep embankment below the new geyser had waned in forcefulness and eventually ceased to discharge steam as increased energy was manifested in the new geyser.

The winter of 1964–1965 resulted in new marked changes in the geyser. Sometime prior to April 1965, a new explosion or a series of explosions occurred near the west end of the crater. Sudden release of energy had not only greatly enlarged the earlier orifice but had also torn out obstructions. The water, now discharged in much greater volume, erupted vertically instead of at an angle.

Yellowstone evidently now had a new geyser of no mean proportions. Because of the nature of its origin, Marler (1973, p. 53) suggested that it be named "Seismic." During 1965, little change occurred in the nature of its activity. Massive bursts of water rocketed from the crater every 1 to 3 min. Most of the bursts were from about 2 to 6 m high, but occasionally, water jetted to a height of nearly 15 m.

The eruptions increased in vigor in the late winter or spring of 1966 (Figs. 4 and 5). By this time, the diameter of vigorously washed ground around the geyser was about 21 m, having recently increased to the east by about 3 m. The change was caused by nearly vertical fall of erupted water on ground not previously affected directly. Broken sinter fragments protected by the tree stump shown in Figure 5 and by larger fragments were temporarily preserved, but all fragments lying on firm sinter closer to the vent had been swept away. By the fall of 1966 when the area was mapped in detail (by L.J.P. Muffler of the U.S. Geol. Survey; Fig. 1), Seismic's crater was about 9 by 12 m.

During the years of 1967 through 1969, the pattern of Seismic's eruptive activity underwent progressive changes. The length of the quiet phase between eruptions slowly increased to about 40 to 50 min. Each eruption was complex, with a duration of about 15 to 20 min, during which 30 or more separate bursts occurred, similar to the burst shown in Figure 6. The first burst of each sequence explosively broke the surface of the pool, as indicated in Figure 4. The crater was still slowly being enlarged on its margins.

On several occasions during 1970, Marler spent 2 hr or more at a time at Seismic to determine the nature of its eruptive pattern, which seemed to have changed somewhat from that of the three previous seasons. Each complex eruption consisted of at least three separate periods of activity, of which the second was always the longest, on one occasion lasting for 19 min. The duration of a complex eruption was variable, with extremes from about 19 to 31

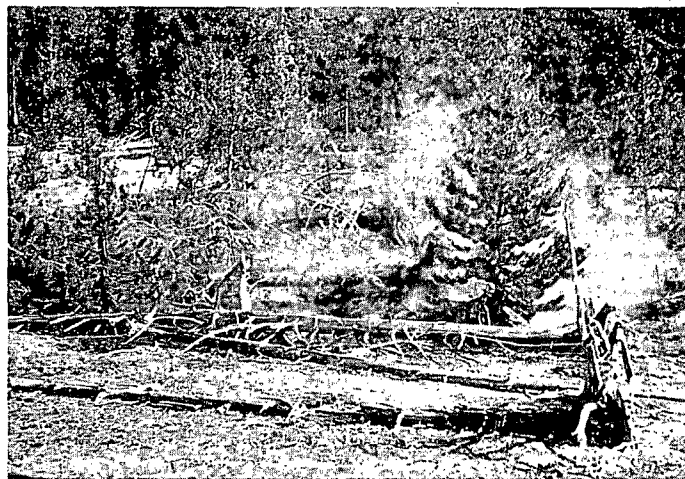


Figure 2. Earliest photograph of the fumarole area that later developed into Seismic Geyser (spring, 1960).

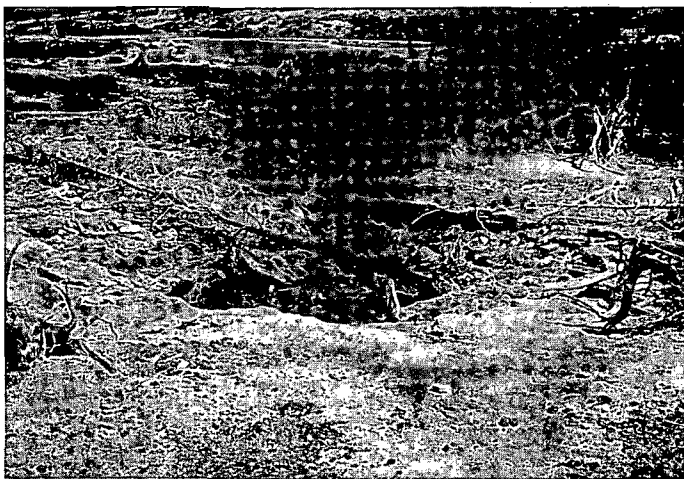


Figure 3. Seismic Geyser after initial eruptions in spring of 1963. Note large blocks of sinter near the vent, with fine debris absent in splashed area.

min. An unailing sign of the termination of each complex eruption was a drop in water level of about 0.35 m in the crater. For comparison, during the quiet periods within a complex eruption, the water stood about 10 cm below the rim. The quiet and eruptive phases were about equal in duration, with each ranging from about 20 to 30 min. The heights of the 1970 eruptions were similar to those observed during the 1967–1969 period. The maximum height was about 12 m or slightly less than the estimated maximum bursts of the 1965–1966 period; many of the highest bursts came near the termination of an eruption.

Sometime between late February and late April of 1971, a vent (now called "Satellite") developed on the east shoulder of the crater. Satellite's vent, like Seismic's, resulted from one or more explosions. Sinter fragments were strewn about the small new crater, which was about 1.8 by 2.4 m when first observed. During the season, some further enlargement occurred. There was a break of about 0.6 m in the side next to Seismic, which resulted in the water of both springs being continuous at the surface.

When first observed in 1971, the water was boiling vigorously in Satellite's crater, welling up from 0.6 to 1 m. Steady boiling was generally characteristic of its pattern throughout the remainder of the season; but periodically, Satellite erupted, with massive bursts to a height of about 3 to 3.7 m and occasionally to 6 m. Its eruptions were synchronized with those of Seismic, with both vents erupting simultaneously. The new geyser's activity decreased the vigor of Seismic's eruptions. However, at times, Seismic erupted to heights as much as 7½ to 9 m.

By the spring of 1972, further changes were evident. During the previous winter of 1971–1972, Satellite's vent had enlarged to about 3.7 by 3.7 m, compared with the 1.8 by 2.4 m vent of 1971, and had become heart shaped. No further change took place in Seismic's crater during the 1971–1972 winter, probably because it had ceased eruptive activity; its crater was then 12.5 m north-northwest by 13.4 m east-northeast, excluding Satellite's vent as a protuberance on the southeast side. Geyser activity was confined wholly to Satellite's vent, while Seismic had become an intermittently overflowing spring.

Intervals between eruptions of the new vent during 1972 ranged from 15 to 37 min; each eruption lasted 21 to 31 min and consisted of either two or three separate periods of spouting. Each eruption was initiated by a rise in water level of about 20 cm in both craters. During each period of activity, Seismic discharge without boiling at an estimated rate of about 1,000 lpm (liters per minute). At times, Seismic overflowed for a few minutes with no consequent eruption of Satellite. Boiling in Satellite was continuous from eruption to

eruption, with surges of 0.6 to 1 m between eruptions. As each eruption progressed, massive surges rose from 2 to 3 m high (Fig. 7), with an occasional burst to 6 m. Some eruptions were more powerful than others. From 30 to 45 m east and southeast of Seismic, new hot ground had developed, killing additional lodgepole pines.

In June 1974, all eruptive activity was confined to Satellite, most commonly surging to heights of about 1 m but with some spurts to 3 m or a little higher. During an eruption, discharge at rates estimated to range from 750 to 4,000 lpm flowed over the sill from Satellite into Seismic's crater, but the net discharge from both vents (almost entirely from Seismic) was only 200 to 400 lpm. These relationships indicate that previously erupted water, probably near 90°C, was flowing beneath the surface in convective circulation from Seismic to Satellite and mixing with a small part of new hot upflowing water.

The duration of observed eruptions of Satellite ranged from 31 to 47 min, and the eruption intervals ranged from 49 to 66 min (data from Roderick Hutchinson, Natl. Park Service). At times, between eruptions, both pools were quiet (Fig. 8), in striking contrast to earlier almost constant activity. Layers of nearly horizontal sinter were clearly visible in both vents to depths of about 1½ m; massive jagged-edged rocks without conspicuous bedding were visible at greater depths. Within the sinter, individual beds had been disrupted, with the radius of disruption increasing upward to form a jagged-walled, funnel-shaped vent.

Seismic's vent was probed extensively in 1974, but the maximum accessible depth was 6.6 m, where temperatures ranged from 89.6° to 95.6°C. Temperatures at the bottom were, in general, slightly below those at –3.7 m, where the observed range was 88.9° to 99.0°C. Satellite's vent was probed to a maximum depth of –3.7 m, where the temperature range was from 94.3° to 97.8°C (temperature data from M. Nathenson, U.S. Geol. Survey).

INTERCONNECTED THERMAL SPRINGS

Seismic and its satellite vent are evidently connected subterraneously with many other nearby springs as well as the 1959 fumarole on the river embankment. Hillside Geyser (Fig. 1; Marler, 1973, p. 49) had been very active from 1948 to 1961, with some eruptions as high as 9 m. Eruptions then decreased in intensity and ceased in 1964 as Seismic became more vigorous. As the 1965 season progressed, Hillside's water level slowly declined and was 1.0 m below discharge level when observed in 1966 by L.J.P. Muffler (Fig. 1). Its minimum observed level was –1.2 m in 1970 and, with declining activity in Seismic and creation of its satellite vent, Hillside's water level then rose to –0.6 m in October of 1972. Observed temperatures in Hillside's vent were 95°C in 1963 and 75°C in 1970. After the beginning of Seismic's major geyser activity, the water levels in Pulcher and North Pulcher (Fig. 1) dropped quite rapidly at first and were 4.3 to 4.6 m below discharge level in 1966. By 1972, their levels had risen slightly.

Seismic's indicated underground connection with Hillside Geyser is not at all surprising, because the initial break in the sinter extended in the general direction of Hillside (Fig. 1). The fact that Seismic evidently has underground connections with other hot springs, several of which were geysers, does not augur well for future consistency of performance. Geysers in other groups known to be connected subterraneously commonly become dormant when the thermal energy shifts to one of the related springs (Marler, 1951, 1973).

HISTORIC FORMATION OR ENLARGEMENT OF OTHER VENTS

Other less dramatic events recorded by Marler (1973) were either directly or indirectly related to the Hebgen Lake earthquake,

and evolutionary changes were not as diverse or were not documented at as many stages as for Seismic Geyser.

On the south side of White Creek about 170 m directly south of Great Fountain Geyser in Lower Basin, one or more violent eruptions scattered great quantities of sinter around two existing craters, probably at the time of or very soon after the 1959 earthquake. At some time early in 1960, a new crater formed in Lower Basin on the eastern shoulder of Honeycomb Geyser in the Kaleidoscope Group. When first observed, the vent was about 1 by 2.4 m, but it was enlarged to 1.8 by 3.7 m by 1972, and large blocks were strewn around the crater. As closely as could be determined by Marler, this vent immediately became an active geyser that erupted to heights of 1.5 to 2.4 m; by 1972, the eruptions rose to heights of 4½ to 7½ m.

In 1963, about 18 m northwest of Kaleidoscope Geyser, a violent eruption that may have been a single event scattered scores of blocks of sinter about a newly created crater about 3 m in diameter. The explosion was directed to the southwest, with a debris ring still recognizable in 1966 and mapped by White (unpub. data) as much as 24 m southwest of the vent. In 1972, water nearly filled the new crater but did not discharge. Also in 1963, two small geysers in Biscuit Basin evolved from earthquake-created fumaroles, with explosions forming the present craters.

At the southern base of a sinter mound on which the cone of Sponge Geyser is located (Geyser Hill Group of Upper Basin), a violent eruption in 1969 scattered fragmental sinter about a newly created crater. Since the initial explosion, occasional geyser eruptions from 3 to 4½ m high have further enlarged the crater. In this same group of springs, two new fumaroles developed soon after the earthquake, and these were enlarged by explosions. One, named "Bench Geyser," is very active and erupts several times daily (1972) to a height of 1½ to 2 m.

Since the earthquake, other explosions have formed craters, mostly small and in the vicinity of active geysers. One occurred in 1969 on the east shoulder of Spasm Geyser in the Fountain Group, forming a crater about 1.2 by 1.5 m.

A large explosion that may have occurred in the early 1900s was responsible for a crater about 15 m in diameter called "Black Opal Spring" in Biscuit Basin. In 1931 when Marler first observed Black Opal, large blocks of cemented sandstone were strewn about the crater. During the winter of 1932–1933, Frank Childs, a Park Ranger, reported a powerful eruption from Black Opal that tore out new sandstone blocks. This eruption was evidently much smaller than the earlier one(s). The sandstone contains granules of rhyolite and obsidian and is similar to the cemented and partly altered drill core from shallow depths in a research drill hole of the U.S. Geological Survey (White and others, 1975; Y-8, 140 m east-southeast of Black Opal).

The explosion that created Black Opal's crater was of considerable magnitude. Since Marler's first observations in 1931 of the great array of sandstone blocks north of the crater, weathering has disintegrated most of the smaller blocks, but erupted debris was recognized in 1966 (D. E. White, unpub. map) as much as 240 m north, 180 m west, and 30 m south of Black Opal, thus indicating explosions directed to the north and west. Some of the blocks near the crater were as much as 0.6 m thick and 0.9 m in diameter.

Black Opal Pool is immediately east of Wall Pool, and the two pools are separated by a narrow septum of cemented gravel. Wall Pool is a spring about 9 to 18 m wide and 58 m long, elongated northwest. This vent probably also formed by explosions that may have occurred concurrently with those of Black Opal. The southern edge of Wall Pool's crater is vertical and consists of abruptly terminated horizontal laminated sinter. The evidence for historic explosions from both vents is indirect: Hague's detailed map of Upper Basin (Hague, 1904, sheet XXIV) does not show either of these two prominent pools in spite of the fact that the wagon road to the Biscuit Basin group was only 15 m to the south, and a discharge



Figure 4. Explosive burst just breaking surface pool of Seismic Geyser with water level below level of discharge (May 30, 1966).

stream from Sapphire Geyser was mapped across the middle of Wall's present location. Could Hague have missed these prominent features, was there a major cartographic error, or did the craters form within the next 30 yr but were not recorded? The almost total absence of reliable records from 1904 to 1931 (Marler, 1973) preclude resolution of these questions, but we favor the latter explanation.

Similar evidence suggests that the vent of West Flood Geyser in the Midway Geyser Basin formed by explosive activity sometime after 1904 and was enlarged before 1940 (Marler, 1973, p. 389). Hague's detailed map of Midway (1904, sheet XXIII) shows no vent in West Flood's present location. The crater is about 9 by 10½ m in diameter and was formed in cemented gravels overlain by sinter. Large blocks or slabs of cemented gravel in the crater indicate enlargement over the years due to undermining of the crater's walls by explosive eruptive activity.

SEISMIC ACTIVITY IN AND NEAR YELLOWSTONE PARK

Historic Record

Since the discovery of Yellowstone Park, earthquakes of sufficient intensity to be recognized have occurred rather frequently with occasional reports of rattling dishes, swinging lamps, and creaking buildings. The earliest report of an earthquake in the Yellowstone country was by the first scientific expedition to the area (Hayden, 1872, p. 82):

While we were encamped on the northwest side of (Yellowstone) lake, near Steamboat Point, on the night of the 20th of July (1871), we experienced several severe shocks of an earthquake, and these were felt by two other parties, fifteen or twenty-five miles distant, on different sides of the lake. We were informed by mountain men that these earthquake shocks are not uncommon, and at some seasons of the year severe, and this fact is given by the Indians as the reason why they seldom or never visit that portion of the country. I have no doubt that if this part of the country should ever be settled and careful observations made, it will be found that earthquake shocks are of very common occurrence.

One of the parties to which Hayden refers as being camped 24 to 40 km distant (Barlow, 1872, p. 38–39) reported: "We experienced last night the singular sensation of an earthquake. There were two shocks, the first one being quite severe accompanied by a rumbling and rushing sound."

After the 1959 earthquake, the National Park Service, in cooperation with the U.S. Geological Survey, installed three seismo-



Figure 5. Border of splashed area very recently enlarged to 7.6 m east of vent. Loose debris under tree stump and large sinter fragments protected from nearly vertical fall of water (May 30, 1966).

graphs in the park. One was also set up at Hebgen Lake. According to Keefer (1972, p. 87) seismographs record an average of about five shocks daily in and around the park; on rare occasions, they may record 100 or more in a single day. Most events are so slight that they cannot be felt by man; but occasionally strong earthquakes occur, such as that of August 17, 1959.

Seismic records indicate that on an average of about once in ten years, a strong earthquake occurs in the states adjoining Yellowstone, particularly in Montana. The last strong earthquake prior to August 17, 1959, was on November 23, 1947. Although neither the 1947 earthquake nor any earlier historical one was sufficiently intense to produce major hydrothermal changes, some of the evident changes in hot-spring functioning that have occurred over the centuries are probably associated with strong seismic activity. The Hebgen Lake earthquake, far from being the only incident to markedly affect the geyser basins, was no doubt preceded by many earthquakes of equal or greater intensity during the past millenia.

Microearthquake monitoring of the park in recent years by the U.S. Geological Survey and by the University of Utah has revealed a pattern of frequent small events that tend to be localized immediately outside of the Yellowstone caldera but rarely occur inside the caldera (A. M. Pitt, D. P. Hill, H. M. Iyer, R. B. Smith, 1973, 1974, personal commun.). The active belt extends eastward from Hebgen Lake to Norris Basin and thence eastward adjacent to the caldera rim as mapped by Christiansen and Blank (1975; Keefer, 1972, Fig. 35). Thus, of the major geyser basins, only Norris is near the most active seismic belt; Shoshone, the major Firehole geyser basins, and West Thumb are all within the relatively inactive caldera.

Prehistoric Geologic Record

Recent geologic mapping in Yellowstone Park (U.S. Geol. Survey, 1972b; Christiansen and Blank, 1975) indicated extensive faulting associated with the eruption of ash-flow tuffs and collapse of the double-centered Yellowstone caldera about 600,000 yr ago. The caldera ring faults approximately underlie the Firehole geyser basins and seem likely to provide the deep controls over circulation of thermal fluids. Extensive faulting was also associated with the resurgent Mallard Lake and Sour Creek domes near the two centers of the double caldera about 150,000 yr ago. Nearly all recognizable fault scarps inside the caldera are localized within or between these two resurgent domes (R. L. Christiansen, 1974, oral commun.). A very few faults near the margins of Yellowstone Lake cut

glacial and alluvial deposits that are less than 150,000 yr old, but other young fault scarps are scarce throughout most of the caldera and, specifically, in or near the major Firehole geyser basins. The steep margins of the geyser basins are the fronts of very viscous thick rhyolite lava flows that range from about 90 to 160 thousand years old and are not fault scarps. Thus, the present-day relatively low level of seismicity within the caldera also seems to have characterized this area for the past 150,000 yr.

However, this evidence indicates only that fault displacements and hypocenters of earthquakes seldom occur within the caldera. The geyser basins have without doubt been subjected frequently to seismic shaking from activity outside the caldera, just as in the 1959 Hebgen Lake earthquake. Many springs and geysers in the geyser basins are aligned on the northeast-, northwest-, and north-striking trends that agree with regional tectonic patterns. Local alignments, probably controlled by fractures, have been recognized for many years by Marler (1964, 1973), and many are shown on detailed maps of the geyser basins (L. J. P. Müffler, R. O. Fournier, A. H. Truesdell, and D. E. White, unpub. data). Some of these may be locally controlled, but most are consistent with regional stress patterns.

Specific fracture-controlled vents that can be cited as examples include Old Faithful Geyser, Fan and Spiteful Geysers, the Chain Lake group of vents southeast of Morning Glory Pool, and the Three Sisters in the Myriad Group, all of Upper Basin. Two lines of vents and visible fractures west and northwest of Clepsydra Geyser of the Fountain Group and four distinct lines of vents between Gentian Pool and Deep Blue Geyser of the Kaleidoscope Group of Lower Basin are also examples.

GENERAL CHARACTERISTICS OF HIGH-TEMPERATURE GEYSER-BEARING CONVECTION SYSTEMS

Many advances have been made in the past 25 yr in understanding the large high-temperature convection systems of the world that are associated with natural geysers. Much of this new understanding has resulted from deep drilling for geothermal energy, but a significant part is from general scientific study and research drilling.

Wells drilled in a few geothermal areas produce dry or superheated steam with little or no associated liquid water (Larderello, Italy; The Geysers, California, with no true geysers; and the Mud Volcano area of Yellowstone). Such areas have been called "vapor-dominated" (White and others, 1971).

With only a few exceptions such as the above, most geothermal areas are dominated by liquid water, including all drilled areas that have natural geysers. In such areas, temperatures generally increase rapidly with depth in drill holes and are close to the temperatures of boiling at existing water pressures. At some depth and temperature characteristic of each particular system (if drilled deep enough), temperatures level off and show little further increase within explored depths (the base temperature of Bodvarsson, 1964). White (1967) listed the maximum temperatures found in 19 drilled areas then thought to have natural geysers. All except five had temperatures above 180°C; of these five, three are now known to have intermittently erupting hot-water wells but no natural geysers. Deeper drilling in a fourth (Bradys, Nevada) yielded temperatures as high as 215°C (White, 1970).

Subsurface temperatures, either indicated by the silica geothermometer (Fournier and Rowe, 1966; Fournier and Truesdell, 1970) or measured in wells in areas of natural geysers (White, 1970, Table 4) have added Rotorua, New Zealand (~230°C), Uzon-Geyzerny, Kamchatka, USSR (~200°C) and El Tatio, Chile (>200°C) to White's earlier list of geyser areas with temperatures above 180°C. Siliceous sinter is also characteristic of geyser areas, and its presence indicates subsurface temperatures in excess of 180°C, either now or in the past (White, 1970).

The highest temperatures tend to occur within the central core of

each system, surrounded by zones of lower temperature (Elder, 1965). The distribution patterns of temperature demand active convection with hot water rising in the core of each system because of thermal expansion, and with descending cold water in other parts of the total system. Few details are actually known about the descending cold parts of these systems, but light stable isotopes have proved an overwhelming dominance of water of surface origin in the thermal waters. In general, at least 95 percent of the water is of such origin, with no positively identified water of magmatic or other deep origin (Craig, 1963; White, 1970).

The geyser-bearing convection systems are large and deep — much deeper than had been assumed prior to geothermal exploration. Most known geyser areas have now been drilled to depths from 610 m to more than 2,400 m with no evidence that the base of meteoric convective circulation was attained in any of them (White, 1970).

These high-temperature convection systems tend to fill their outlet channels and pore spaces in adjacent rocks by depositing silica minerals, zeolites, calcite, and other minerals (White and others, 1975) as temperatures decrease upward and as mineral solubilities decrease (calcite because of increasing pH with loss of CO₂ as boiling occurs). The resultant decrease in permeability is called "self-sealing."

SUMMARY OF SUBSURFACE CHARACTERISTICS OF YELLOWSTONE'S GEYSER BASINS

The temperature and pressure gradients in the upper few hundred feet of Yellowstone's geyser basins provide the basis for understanding how and why new vents form; these data also help to explain why Yellowstone Park has the greatest display of geysers and other hydrothermal phenomena in the world.

Two research holes were drilled in Yellowstone Park by the Carnegie Institution of Washington in 1929 and 1930 (Fenner, 1936), and thirteen holes were drilled by the U.S. Geological Survey in 1967 and 1968 (White and others, 1975). Depths of the holes range from 65.5 m to 331.6 m, and maximum measured temperatures in the 13 holes (excluding one in the travertine terrace of Mammoth) range from 143° to 237.5°C. Nine of the thirteen holes attained 180°C or higher, and the four of lowest temperature were either shallow or were drilled on the margins of upflowing systems. Most holes were drilled in rocks of initial high permeability, but permeabilities have decreased greatly from deposition of hydrothermal minerals in fractures and pore spaces.

The depth to the water table ranged from 0.3 m to 8.8 m below ground, depending on local relationships of drill holes to nearby springs and topography. As drilling progressed, the standing level of water in each hole rose to the ground surface and then attained positive pressures (in capped holes) that ranged up to an equivalent level of 65.5 m above ground! The excess pressure gradients above simple hydrostatic exceeded 10 percent for all holes except one, and the gradient in one hole exceeded hydrostatic by 47 percent!

The very high near-surface fluid pressure gradients in rocks of initial high permeability imply that self-sealing has been extensive (but not complete). Water leaks through any available permeable channels, generally into near-surface rocks or sediments of somewhat higher permeability. In the geyser basins of Yellowstone Park, the greatest tendency for self-sealing occurs in the temperature range from about 125° to 180°C. Sinter, sands, and gravels near the basin floors where temperatures are below 100°C are generally porous and only partly cemented and hydrothermally altered. Thus, the high-pressure fluids probably flow upward in a few principal channels through the nearly self-sealed zone to the near-surface, where increasing permeability in channel walls then permits the escape of some water into adjacent ground with lower fluid pressures.

The relationships just described help to explain the otherwise

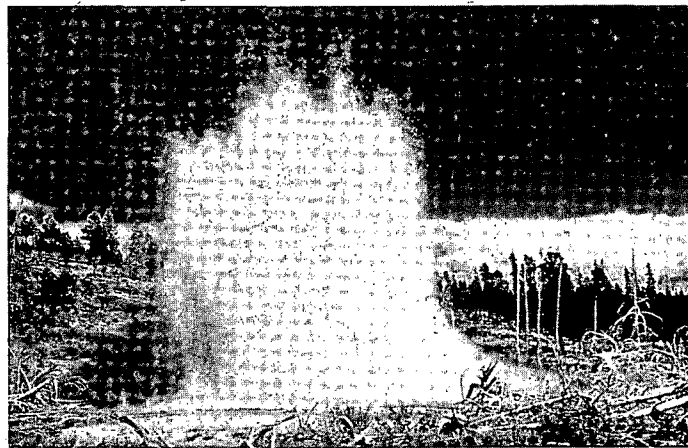


Figure 6. Bursting eruption of Seismic Geyser (August 1968).

puzzling occurrence of adjacent springs discharging at different altitudes; of discharging springs located adjacent to nondischarging vents of lower altitude; and the fact that the water table, as first identified in drill holes, is generally lower in altitude than nearby discharging springs.

The drill cores also show that much of the floor of Upper Basin is underlain by stream-deposited silt, sand, and gravel ranging in thickness from more than 61 m in the southern part of the basin to about 53 m in the northern part (Biscuit Basin). These sediments were deposited rapidly as kames adjacent to the margins of glaciers of Pinedale stage (U.S. Geol. Survey, 1972a). Bedrock is shallow, however, along much of the northeastern side of Upper Basin and crops out in places (Christiansen and Blank, 1975; L.J.P. Muffler and others, unpub. data). The depth of stream sediments under Seismic Geyser is not known but is probably less than the 52 to 55 m found in the two Biscuit Basin drill holes about 550 m to the north.

HYPOTHESIZED EVOLUTION OF HYDROTHERMAL ACTIVITY IN UPPER BASIN

No evidence has been found for pre-Pinedale hydrothermal activity in Upper Basin, although such activity seems likely in view of evidence for its existence in Lower Basin and Norris Basin (L.J.P. Muffler and others, unpub. data). Relatively well-sorted sands and gravels of early or middle Pinedale stages (U.S. Geol. Survey, 1972a) were deposited in Upper Basin by streams adjacent to melting ice. The core from four research drill holes in the basin shows no break in the hydrothermal record from the underlying lava flows up through the entire sequence of stream sediments. Hot-spring deposits generally overlie the sediments but are absent within or below the sediments; soil zones and organic matter also seem to be absent in the drill core. Thus, regardless of the possibility of early unrecognized hydrothermal activity in Upper Basin, the sedimentary fill within the basin seems to have evolved as if in response to a single period of thermal perturbation that is still continuing. The following model of evolution of activity is based on this assumption.

When thermal waters first flowed upward into the newly deposited permeable basin sediments, vigorous convection and mixing with cold ground waters from the surrounding area must have occurred. Fluid pressures in these sediments must have been hydrostatically controlled, and temperatures, because of mixing and convection, were probably much below the reference boiling-temperature curve except perhaps locally in upflow currents near the water table. With time, however, permeability decreased drastically as a result of deposition of hydrothermal minerals and conversion of abundant obsidian granules into zeolites, partly devit-

rifying in place but also dissolving and redepositing (with silica minerals) in pore spaces (Honda and Muffler, 1970; unpub. data on other drill holes). In some sediments, porosity did not decrease as much as permeability; in others, both porosity and permeability decreased greatly.

In consequence of these changes, the ease of upflow of thermal fluids decreased with time as impedances were imposed. Convective circulation within the sediment pile must have become more and more constricted, and fluid overpressures only then could start to develop. With time, thermal water started to discharge over various parts of the sediment-filled basin with decreasing regard for differences in surface altitude, in contrast to former outlets that presumably were localized at low altitudes adjacent to streams. Temperatures could then generally increase within the sediments, at first approximately up to the reference boiling-temperature curve (which assumes a water table at ground level) and then locally exceeding the curve as water overpressures started to develop. Direct inflow of cold water from the valley floor and surrounding terrain gradually decreased as fluid overpressures developed to exclude such water. Important consequences of these changes were that, with time, boiling temperatures at points of discharge became more characteristic, and the SiO_2 contents of discharged waters increased because of rapid cooling from higher temperatures and also because of decreased dilution by cold water. Broad shields of nearly horizontal sinter were deposited around centers of discharge. Geysers, or at least large geysers, were not yet characteristic because the underlying stream sediments were not yet thoroughly cemented and average permeabilities were still too high. The broad sinter shields were probably not strictly contemporaneous with each other but probably developed at different rates and at different times. It is significant that parts of Upper Basin, as in the western part of the area shown in Figure 1, are still floored by these stream sediments, considered to be of the same general age but not yet having undergone any of the described changes. The northern Biscuit Basin drill hole (Y-7) is in the less-cemented outer border of such an area; its vertical water-pressure gradient is only about 1 percent above hydrostatic, in contrast to a pressure gradient nearly 30 percent above hydrostatic in the second Biscuit Basin drill hole (Y-8) only 150 m to the south and 550 m north of Seismic Geyser (White and others, 1975).

The response to the formation of a new fracture in an overpressured environment is best illustrated by the data provided here for Seismic Geyser and other comparable features. In contrast, a new fracture in bedrock lavas overlain by permeable gravel outside of an overpressured area probably would not be recognized, and it

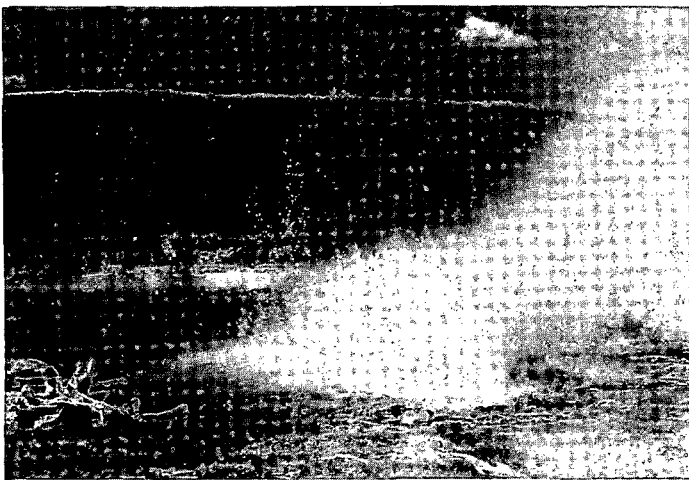


Figure 7. Satellite vent erupting, with Seismic Geyser's pool in background (August 1972).

could not evolve immediately into either a fumarole or a new geyser.

The evolution of activity in the parts of Upper Basin where bedrock either crops out or is at shallow depth, as from Old Faithful northwestward to Artemesia Geyser (300 m southeast of Seismic; Fig. 1) is less predictable. Similar stages of self-sealing, development of high near-surface overpressures, and exclusion of abundant cold meteoric water were probably necessary before sinter shields and then major geysers could form, but these stages in evolution may already have occurred in the bedrock lava flows before the stream sediments were deposited in Upper Basin. At least in favorable places the rate of evolution to major geysers was probably much faster than in areas underlain by deep permeable stream sediments. In fact, the localization of major geysers along the northeast side of Upper Basin may be related to shallower depths to competent bedrock.

EVOLUTION OF VENTS FORMED BY SEISMIC DISTURBANCE OF AN OVERPRESSURED HYDROTHERMAL SYSTEM

A high-temperature hydrothermal system characterized by near-surface pressure gradients 10 to 50 percent above the simple hydrostatic gradient has subsurface temperatures that may be much above the reference boiling-temperature curve (Honda and Muffler, 1970; White and others, 1975). The seismic response of such a system evidently differs greatly from place to place. Some responses are nearly instantaneous, but others evolve slowly over a period of years. Most previously existing spring vents, sufficiently disturbed in 1959 to permit increased discharge from the overpressured system, erupted immediately as geysers. A few vents, such as that of Clepsydra in the Fountain Group of Lower Basin, evidently tapped one or more deep aquifers that were sufficiently high in permeability to maintain continuous discharge, much like a continuously erupting geothermal well.

The new fractures formed by the 1959 earthquake provided new channels for escape of thermal fluids from the overpressured systems. Some new fractures were immediately conspicuous, such as the one that evolved into Seismic. Others did not become prominent until enough thermal fluid had escaped to produce near-surface ground temperatures that were too high for pine trees to tolerate. How are these delayed reactions best explained?

A new fracture first permits the upflow of some fluid and heat at a locus where near-surface temperatures were formerly controlled by conductive gradients, as in the shallow parts of most of the research drill holes in Yellowstone (White and others, 1975). As a consequence of the new upflow, temperatures rise, and if liquid accompanies steam, the added supply of water raises the local water table, eventually to the surface if surrounding ground is not very permeable. The vent then changes from a fumarole to a spring, a perpetual spouter, or a geyser.¹

The historic record of development of vents suggests that some may form as results of single explosions but that others evolve gradually from a continuing series of eruptions of increasing vigor. The single explosions (or a closely spaced flurry of explosions) are similar to (but much smaller in scale than) the major hydrothermal explosions that occurred in 1951 in northeastern California (White, 1955) and that formed Pocket Basin in Lower Basin

¹A perpetual spouter (also called a "steady geyser" in Yellowstone) forms where high-temperature water flows up a channel of restricted dimensions and where a local reservoir is absent; the rate of total mass discharge of water and steam (but with proportion of steam increasing upward) is nearly constant, equaling the rate of supply from depth. Wherever a vent is large enough and a local reservoir can form (by processes to be described), discharge tends to become intermittent with rates during eruption exceeding the rate of supply from depth. An interval of repose, with both fluids and heat being supplied from depth, are essential before the geyser can erupt again (White, 1967).

(Muffler and others, 1971). All of these explosions, as well as geyser eruptions, derive their energy from hot water at initial temperatures much above surface boiling, permissible where pressures are higher than atmospheric. Single explosions are especially likely to occur where near-surface fluid pressure gradients are much above hydrostatic and locally exceed the lithostatic gradient.

The explosions are not simple steam explosions resulting from rapid expansion of steam decompressing from an initial high pressure to a lower pressure. Instead, they are caused by the thermal energy contained in liquid water at temperatures above the new boiling temperature at the new decompression pressure; this extra thermal energy is utilized to convert part of the water to steam. White (1955, p. 1124) calculated that one volume of water decompressing from a temperature of 200°C and 225 psia (pounds per square inch, absolute or 15.82 kg/cm²), to 100°C (sea-level atmospheric pressure assumed) increases its initial volume by 278 times as 19.2 percent of the original water is converted into low-density steam.

If this expansion were contained in a vent of constant diameter, such as a well casing, a mass unit of liquid water flowing upward and flashing to a mixture of water and steam must increase in velocity by 278 times, assuming equilibrium at ground level and atmospheric pressure. Instead, in natural vents, the rising column approaching the free face (ground surface) tends to expand horizontally by enlarging its channel as well as to increase in velocity upward.

The water immediately involved in forming new geyser vents is likely to be supplied relatively near the surface where deep temperatures of 200°C or more have already decreased to the general range of 150° to 125°C. Corresponding volume increases of water when flashed from 150° or 125°C to mixtures of water and steam at atmospheric pressure (calculated to 100°C or sea-level boiling rather than 92.9°C for surface boiling in Upper Basin) are approximately 145 and 75 times the initial volumes, respectively. This large increase in volume of a given mass of fluids as the ground surface is approached, along with decreasing cementation of sinter and sediments upward, explains the general tendency for the upward flaring of vents.

Other relationships help to explain the enlargement of deep channels and the increasing volume of the immediate reservoir of an evolving geyser. When an eruption occurs and water is discharged faster than its rate of supply through narrow fractures from the overpressured environment at depth, the local reservoir becomes depleted, with consequent decreases in fluid pressures. Liquid in pores in adjacent sinter and cemented sediments is then exposed to lower fluid pressures and consequently lower temperatures of boiling than immediately prior to eruption. The pore water thus tends to flash into steam, with additional heat being supplied by the rocks. If permeabilities are low enough, the high fluid pressures within the pores cannot be relieved rapidly, and pressure gradients² may be sufficiently high to break and disrupt the rocks.

For the most part, channels are widened and cavities are created and enlarged in the less competent layers of rock where initial porosity or degree of fracturing is greatest. Especially subject to disruption are the less thoroughly cemented beds of sediments. As a consequence of such enlargements, the magnitude and vigor of eruption of a geyser can increase as its local reservoir increases with time.

Each explosion that ejects fragments tends to clear and enlarge

² Pressure gradients locally may greatly exceed the lithostatic gradient in channels that feed directly from a highly overpressured environment into the local reservoir of a geyser; the water in this local reservoir is in direct contact with the atmosphere, and pressures are therefore controlled by a hydrostatic gradient down to the feeding channels. In and near these channels where pressure gradients may be extremely high, the tendency for enlargement during and immediately after an eruption is great and can be resisted only by hard competent rocks that are not intimately fractured.

the channel near the surface as well as at depth, thus increasing the rate of discharge and also the average heat content of the escaping fluids as a smaller proportion is lost by conduction. Eventually, however, a vent attains some maximum surface diameter and deep-channel dimensions. This attainment of stability probably occurs when dimensions become so large and remaining constrictions are so limited that convection *within* the reservoir becomes completely dominant. The excess energy contained in the very hot recharging water from depth can then be lost by steady-state processes, including surface evaporation from hot pools, the rise of individual steam bubbles, near-surface boiling, and conductive loss of heat from the channels to cooler adjacent rocks. Dominance of these mechanisms is probably also fostered by deposition of silica and other minerals in the deep channels, now no longer subjected to the extreme pressure gradients resulting from eruption and reservoir depletion.

New fractures that develop in bedrock lava flows, competent sinter, and thoroughly cemented gravels with large heavy interlocking blocks may commonly evolve into cone geysers with near-surface vents and tubes of relatively small diameter. In contrast, where an evolving geyser of increasing vigor can fragment and eject near-surface incompetent rocks, an upward-flaring vent and a geyser with fountain-type activity are the normal consequences.

EXPLOSIVE ORIGIN FOR ALL GEYSER VENTS

The known craters that resulted from the disruption and ejection of near-surface sinter and cemented sediments suggest a similar explanation for all of Yellowstone's spring and geyser vents. Like Seismic's crater and other similar craters of recent origin, jagged ledges of sinter and sediments in the crater walls bear mute evidence that powerful eruptions were responsible for the origin of such vents. The vents of the following well-known springs are typical examples: in the Upper Basin, Oblong Geyser, Rainbow Pool, Emerald Pool, Green Spring, Artemesia Geyser, Cauliflower Geyser, and Sapphire Pool; in the Lower Basin; Celestine Pool, Silex Spring, Fountain Geyser, Gentian Pool, and Diamond Spring.

Our hypothesis of explosive origin of geyser vents is especially attractive for Yellowstone's geyser basins where fluid-pressure gradients are commonly 10 to nearly 50 percent above the hydrostatic gradient and very high temperatures are correspondingly closer to



Figure 8. View southeastward across vent of Seismic Geyser toward Satellite's vent during a quiet interval between eruptions. Individual beds of sinter are visible; each bed was originally continuous but was fragmented as the geyser increased in vigor. The vent flares upward, probably as a consequence of increasing volume of an erupting two-phase mixture as pressure decreases upward (June 16, 1974).

the surface. A similar explosive origin of vents is also indicated in other less favored geyser areas where pressure and temperature gradients are probably not so high.

If geyser craters are generally formed by hydrothermal explosions, why then are rock fragments not found around most of them? This question was considered by Allen and Day (1935, p. 135). Three examples of known explosions that ejected great quantities of disrupted rock illustrate how rapidly the surface evidence is obliterated.

The sundered rock is most commonly hot-spring sinter or partly cemented stream sediments that are porous and disintegrate rapidly when exposed to weathering and especially to frost action. Less commonly, the ejected fragments are either dense sinter or thoroughly cemented sediments that do not disintegrate easily. During the 1957 and 1958 seasons, unusually powerful eruptions of Link Geyser in the Chain Lake Group of Upper Basin tore a score or more of large blocks of sinter from its crater walls. Some of these blocks were fully 1 m in diameter and were deposited 4½ to 6 m away from the vent (Marler, 1973, p. 88-92). Ten years later, all of these blocks had disappeared and no direct evidence exists today.

Four days after the 1959 earthquake, Sapphire Pool of Biscuit Basin became one of the park's most powerful geysers (Marler, 1973, p. 26-34) with eruptions up to 45 m high and jetting to widths of as much as 75 m. With diminishing frequency, the mammoth eruptions continued through 1960 and 1961, and the geyser then declined in force and power. Due to the explosive nature of the major eruptions, the crater nearly doubled in surface diameter. Layers of sinter 0.2 to 1 m thick, including most of the ornate fringing "biscuits," were torn from the shallow borders of the original vent, thus increasing the upward-flaring of its margins, as discussed for Seismic's vent. The great deluge of water from each major eruption, estimated to weigh about 50 tons, washed the broken sinter fragments 18 to 30 m away from the crater and formed an encircling wall about 1 m high. Two large deltas of sinter fragments formed in the Firehole River to the south and east. The clastic rim was still sharp and easily recognized when mapped in detail by White in 1966 (unpub. data) but by 1974 was evident only when specifically sought.

Excelsior Geyser of Midway Basin was one of the most powerful geysers in the park and is now the most copiously flowing thermal spring (Marler, 1973, p. 367-368). Its huge crater is 45 to 75 m wide and 107 m long and elongated to the northeast; it clearly was formed by explosions. The crater walls rise almost vertically as much as 4 m above the water level of the spring. These walls, which encircle Excelsior on all sides except on the northeast near the Firehole River, consist of thinly laminated sinter that was probably deposited by Grand Prismatic Spring over a period of many centuries. These sinter deposits rise unchanged in character through the 4-m-thick section visible in Excelsior's southwest crater wall. Excelsior's crater abruptly terminates these beds and thus is of comparatively recent origin. Further, observational data indicate enlargement of the crater to its present dimensions in the early years after the park was established. Colonel F. P. Norris (1881, p. 60), then superintendent of Yellowstone Park, described an eruption of Excelsior in 1878:

Crossing the river above the geyser and hitching my horse, with bewildering astonishment I beheld the outlet at least tripled in size, and a furious torrent of hot water escaping from the pool, which was shrouded in steam, greatly hiding its spasmodic foamings. The pool was considerably enlarged, its immediate borders swept entirely clear of all movable rock, enough of which had been hurled or forced back to form a ridge from knee to breast high at a distance of from 20 to 50 feet from the ragged edge of the yawning chasm.

Excelsior was not known to erupt again until 1881 when much eruptive activity was observed. In reference to the power of the eruptions and the discharge of rocks, Norris (1881, p. 61) stated, "During much of the summer the eruptions were simply incredible, elevating to heights of 100 to 300 feet sufficient water to render the rapid Firehole River nearly 100 yards wide, a foaming torrent of steaming hot water, and hurling rocks from 1 to 100 pounds weight, like those of an exploded mine, over surrounding acres."

Today, 90 yr after the great discharge of sinter "knee to breast high," not a shred of direct evidence remains that solid matter ever was disgorged from Excelsior's crater.

SPECULATIONS ON THE ORIGIN OF HOT-SPRING VENTS NOT KNOWN TO HAVE ERUPTED AS GEYSERS

The geyser basins contain hundreds of vents that lack direct evidence of their origin. The smooth upward-flaring margins of Morning Glory's classic vent in Upper Basin are characteristic of many of these, ranging from a few feet in diameter up to the magnificent symmetrical funnel of Grand Prismatic Spring in Midway Basin, which is about 180 m in diameter. The internal structures of the vents are largely concealed by deposits of sinter, algae, and silica gel, at least partly in layers parallel to the borders of the funnels. Fracture-bounded blocks and irregular surfaces, such as are visible in the vents of Seismic (Fig. 8), Excelsior, West Flood, and Artemesia, are generally absent. Can small pools and vents evolve into large-diameter pools by some nonviolent process such as an upward-flaring deposition of scores or hundreds of feet of sinter? Or have these vents formed explosively by Seismic's general mechanism, followed by evolution from rough-walled geyser vents to quietly discharging smooth-walled pools and eventually to inactive vents as maximum dimensions are first attained and then as self-sealing of channels becomes significant. In our opinion, the evidence is indirectly but strongly in favor of the second mechanism.

The broad terraces of sinter in general extend only to depths on the order of 1½ to 5 m but most of the large morning glory vents extend down into underlying rocks. Six of Yellowstone's research drill holes were collared in hot-spring sinter, and these, with only one exception, penetrated only 1.5 to 3.5 m of sinter. The single exception, near Hot Lake in Lower Basin, penetrated alternating sinter and hot-spring travertine to 10.0 m, with travertine being dominant (but rare elsewhere in the geyser basins). The depth of vertical penetration of large funnels such as that of Grand Prismatic is not known; but the intense blue color of this pool suggests a depth of scores of feet. Smaller flaring funnels have been probed to depths as much as 11 m, and others no doubt penetrate deeply into cemented stream sediments and perhaps into underlying volcanic rocks. The nearly vertical throats of these funnels could not have been maintained in these stream sediments prior to their lithification.

A jagged-edged, explosively formed geyser vent probably evolves into a smooth-walled hot spring funnel as silica is deposited on the margins; the rate and temperature of discharge from the vent decrease with time as a consequence of self-sealing. The jagged near-surface borders, initially showing a clear sequence of sinter overlying cemented stream sediments or a lava flow, are eventually concealed by deposits of new sinter, algae, and silica gel.

Most hot spring vents, especially those that flare upward in geyser areas, probably involve the disruption and violent ejection of previously existing competent rocks. This mechanism of explosive ejection also helps to explain the nearly vertical tubes that characterize the throats of most geysers. Such openings must have formed mechanically and were not inherited from previously existing rocks.

CONCLUSIONS

The evidence suggests that the great majority and perhaps all vents in geyser areas were formed by mechanical enlargement of initial narrow channels. In the geyser basins of the Firehole River, the evidence is convincing that many hot springs started as fractures in older sinter. These rifts or breaks resulted largely and perhaps entirely from seismic shaking and fracturing of hydrothermal systems characterized by fluid pressures much above hydrostatic but below the lithostatic gradient. The epicenters of the earthquakes were largely outside the Yellowstone caldera, and appreciable fault displacements in the geyser basins were rarely if ever involved. In general, geyser craters evolved from fractures by repeated explosive decompression of hot water at local temperatures as high as 150°C and pressures at least as high as 4.85 kg/cm². Pressure gradients locally exceeded the lithostatic gradient, thus favoring the disruption, fragmentation, and ejection of rocks, thereby enlarging flow channels and increasing the volumes of individual local geyser reservoirs.

We suggest that cone-type geysers tend to form where near-surface rocks are competent and not easily fragmented and that fountain-type geysers with upward-flaring funnels tend to form where the near-surface rocks are easily broken and can be ejected.

Some effects of the 1959 earthquake include new breaks, many but not all of which show the same northwest-trending alignment as do many of the earlier breaks. These breaks provide evidence that earthquakes have played an important role in creating new channels for discharge of thermal fluids as old channels become clogged with hydrothermal minerals and cease discharging.

GENERAL CONSIDERATIONS
AND ACKNOWLEDGMENTS

Marler was a naturalist and geyser specialist for many years in Yellowstone with the National Park Service; he was privileged to observe the profound changes that have occurred, especially during and soon after the Hebgen Lake earthquake in 1959. White desires this opportunity to express his deep appreciation for many years of association and access to Marler's detailed knowledge and observations in the geyser basins. Both authors are especially indebted to L.J.P. Muffler, R. O. Fournier, A. H. Truesdell, and Manuel Nathenson for products of their geologic mapping, observations, and critical reviews that are incorporated in the present report.

REFERENCES CITED

- Allen, E. T., and Day, A. L., 1935, Hot springs of the Yellowstone National Park: Carnegie Inst. Washington Pub., p. 134-135.
- Barlow, J. W., 1872, Report of a reconnaissance of the Upper Yellowstone in 1871: Washington, D.C., U.S. Govt. Printing Office, p. 38-39.
- Bodvarsson, Gunnar, 1964, Physical characteristics of natural heat resources in Iceland: United Nations Conf. New Sources of Energy, Proc., Rome, 1961, v. 2, p. 82-98.
- Christiansen, R. L., and Blank, H. R., Jr., 1975, Quarternary volcanism of Yellowstone rhyolite plateau region of Wyoming, Idaho, and Montana: U.S. Geol. Survey Prof. Paper 729 (in press).
- Craig, Harmon, 1963, The isotopic geochemistry of water and carbon in geothermal areas, in Nuclear geology in geothermal areas; Spoleto: Consiglio Nazionale della Ricerche, Laboratorio de geologia nucleare, Pisa, p. 17-53.
- Elder, John W., 1965, Physical processes in geothermal areas, in Lee, W.H.K., ed., Terrestrial heat flow: Am. Geophys. Union Mon. 8, p. 211-239.
- Fenner, C. N., 1936, Borehole investigations in the Yellowstone Park: Jour. Geology, v. 44, p. 225-315.
- Fournier, R. O., and Rowe, J. J., 1966, Estimation of underground temperature from the silica content of water from hot springs and wet-steam wells: Am. Jour. Sci., v. 264, p. 685-697.
- Fournier, R. O., and Truesdell, A. H., 1970, Chemical indicators of subsurface temperature applied to hot spring waters in Yellowstone National Park, Wyoming, U.S.A.: Geothermics, Spec. Issue 2, v. 2, p. 1, p. 529-535.
- Hague, Arnold, 1904, Atlas to accompany Monograph XXXII on the geology of the Yellowstone National Park: U.S. Geol. Survey.
- Hayden, F. V., 1872, U.S. geological and geographical survey of the territories: Washington, D.C., U.S. Govt. Printing Office, p. 81-131.
- Honda, Sakuro, and Muffler, L.J.P., 1970, Hydrothermal alteration in core from research drillhole Y-1, Upper Geyser Basin, Yellowstone National Park, Wyoming: Am. Mineralogist, v. 55, p. 1714-1737.
- Keefer, W. R., 1972, The geologic story of Yellowstone National Park: U.S. Geol. Survey Bull. 1347, 92 p.
- Marler, G. D., 1951, Exchange of function as a cause of geyser irregularity: Am. Jour. Sci., v. 249, no. 5, p. 329-342.
- 1964, Effects of the Hebgen Lake earthquake on the hot springs of the Firehole Geyser Basins, Yellowstone National Park: U.S. Geol. Survey Prof. Paper 435-Q, p. 185-197.
- 1973, Inventory of thermal features of the Firehole River Geyser Basins and other selected areas of Yellowstone National Park: Natl. Tech. Inf. Service Rept., PB 221,289, 648 p.
- Muffler, L.J.P., White, D. E., and Truesdell, A. H., 1971, Hydrothermal explosion craters in Yellowstone National Park: Geol. Soc. America Bull., v. 82, p. 723-740.
- Norris, F. P., 1881, Fifth annual report of the Superintendent of Yellowstone National Park: Washington, D.C., U.S. Govt. Printing Office, p. 60-61.
- U.S. Geological Survey, 1972a, Surficial geological map of Yellowstone National Park: U.S. Geol. Survey Misc. Geol. Inv. Map I-710.
- 1972b, Geologic map of Yellowstone National Park: U.S. Geol. Survey Misc. Geol. Inv. Map I-711.
- White, D. E., 1955, Violent mud-volcano eruption of Lake City Hot Springs, northeastern California: Geol. Soc. America Bull., v. 66, p. 1109-1130.
- 1967, Some principles of geyser activity, mainly from Steamboat Springs, Nevada: Am. Jour. Sci., v. 265, p. 641-684.
- 1970, Geochemistry applied to the discovery, evaluation, and exploitation of geothermal energy resources: Geothermics, Spec. Issue 2, v. 1 (in press).
- White, D. E., Muffler, L.J.P., and Truesdell, A. H., 1971, Vapor-dominated hydrothermal systems compared with hot-water systems: Econ. Geology, v. 66, p. 75-97.
- White, D. E., Muffler, L.J.P., Fournier, R. O., and Truesdell, A. H., 1975, Physical results of research drilling in thermal areas of Yellowstone National Park, Wyoming: U.S. Geol. Survey Prof. Paper 892 (in press).

MANUSCRIPT RECEIVED BY THE SOCIETY DECEMBER 2, 1974

K-Ar Apparent Ages, Peninsular Ranges Batholith, Southern California and Baja California

DANIEL KRUMMENACHER }
R. GORDON GASTIL }
JONATHAN BUSHEE* }
JOAN DOUPONT* }

Department of Geology, San Diego State University, San Diego, California 92182

ABSTRACT

More than 200 K-Ar apparent ages have been determined from minerals from the Peninsular Ranges batholith of southern California and northern Baja California. In general, the apparent ages show a progressive decrease from about 120 m.y. in the southwestern (coastal) part of the batholith to less than 70 m.y. in the northeastern (desert) part. The gradients for biotite and hornblende ages can be represented by contours of equal ages. Both concordant and discordant hornblende-biotite pairs and minerals, from a variety of plutonic and metamorphic rock types, share in the apparent-age gradient. Ages for hornblende average 5 m.y. older than the ages for coexistent biotite. Isotopic U-Pb and Pb- α measurements on zircon indicate ages greater than those calculated from K-Ar ratios of hornblende or biotite. It is believed that in the Peninsular Ranges province, the U-Pb ages for zircon approximate the ages of emplacement, whereas concordant K-Ar ages may or may not approximate the ages of emplacement, depending on the depth of emplacement and the rate of uplift and denudation.

INTRODUCTION

The Peninsular Ranges province is bounded by the Pacific borderland on the west, the Gulf of California on the east, the Transverse Ranges of California on the north, and lat 28° N. in Baja California on the south. The K-Ar data presented in this paper were obtained (by us and by several students) from rocks in that part of the Peninsular Ranges which lies in Baja California north of lat 31° N. and in southern California to 50 km north of the international border. The work of Larsen and others (1958), Banks and Silver (1969), Silver and others (1969), Evernden and Kistler (1970), and Armstrong and Suppe (1973) is integrated with our work to demonstrate that the trends which we found to the south continue to the north (see Figs. 1 and 2).

The objective of this paper is not to determine the emplacement ages of the Peninsular Ranges batholith but to interpret the spatial pattern of K-Ar apparent ages. To make this interpretation, however, it is necessary to consider the evidence for the age of emplacement.

STRATIGRAPHIC LIMITS FOR THE AGE OF THE BATHOLITH

In the Santa Ana Mountains at the northern end of the province, granitic rocks intrude strata of Middle and Late Jurassic age (Imlay, 1963, 1964). In San Diego County, the granitic rocks intrude strata of Late Jurassic age (Fife and others, 1967). In northern Baja California, rocks of the batholith intrude strata of

Albian-Aptian age (Allison, 1955; Allen and others, 1960; Silver and others, 1963). These observations, however, only limit the maximum age of specific plutons. In western San Diego County, a variety of granitic clasts have been found in volcanoclastic strata that are believed to be Portlandian on the basis of paleontology. And, near Guadalupe Valley, northern Baja California, volcanoclastic strata rest on granitic rock (Ashley, 1972, unpub. data). We know, therefore, that some plutons are at least as young as Aptian (112 m.y. B.P.) and that others are at least as old as Portlandian (135 m.y. B.P.; time scale from Harland and others, 1964).

Granitic rocks are overlain by Turonian strata (~90 m.y. B.P.) in the Santa Ana Mountains (Popenoe and others, 1960). Unfossiliferous strata tentatively correlated with Popenoe's Turonian rocks are widespread in western San Diego County (Luzardi Formation of Nordstrom, 1970), and possible equivalents have been found in northern Baja California (Redonda Formation of Flynn, 1970).

Some of the undated Cretaceous strata in San Diego County and northern Baja California rest on amphibolite-grade metamorphic rocks; this indicates that considerable erosion of the batholith preceded their deposition. John Minch (1972, oral commun.) believed that some of the clast types in the upper portion of the Rosario Group (Campanian-Maestrichtian, ~70 m.y. B.P.) were derived from basement rocks in the desert ranges that border the Gulf of California. So, although the evidence is fragmentary, it suggests that the batholith was unroofed along the Pacific margin before 90 m.y. B.P. and was unroofed as far to the east as the desert ranges before 70 m.y. B.P.

U-Pb AND Rb-Sr AGES¹

The first extensive mineral dating of the Peninsular Ranges was done by the Pb- α method (Larsen and others, 1958). These authors dated 24 rocks from southern California and the northern part of Baja California. These determinations indicated ages of 92 to 136 m.y.; the median age was about 110 m.y. The ages reported from tonalite are generally older than those from more siliceous rocks, but the two groups overlap considerably. Because of the difficulty of obtaining appropriate minerals, no dates were reported for gabbro. Bushee and others (1963) reported 15 analyses that confirmed the results of Larsen and his colleagues. The Pb- α ages do not show a consistent pattern of age variation across the peninsula. Pb- α dates on zircons in plutonic rocks may be in error because of either loss of lead (which makes ages too young) or inherited zircon (which makes ages too old). In the volcanoclastic western part of the Peninsular Ranges, inheritable zircons are rare and the Pb- α dates can therefore be considered as minimum ages. Lepidolite from

¹ We are not suggesting that the credibility of nonisotopic ages compares with that of, for example, isotopic U-Pb work on zircons. The point we are trying to make is that all of these methods yielded a range of ages compatible with the stratigraphic limitations, whereas K-Ar does not.

* Present address: (Bushee) Department of Geology, Northern Kentucky State College, Covington, Kentucky 41011; (Doupons) Lawrence Livermore Laboratory, Livermore, California 94550.

RESISTIVITY, SELF-POTENTIAL, AND INDUCED-POLARIZATION SURVEYS OF A VAPOR-DOMINATED GEOTHERMAL SYSTEM†

A. A. R. ZOHDY*, L. A. ANDERSON*, AND L. J. P. MUFFLER‡

The Mud Volcano area in Yellowstone National Park provides an example of a vapor-dominated geothermal system. A test-well drilled to a depth of about 347 ft penetrated the vapor-dominated reservoir at a depth of less than 300 ft. Subsequently, 16 vertical electrical soundings (VES) of the Schlumberger type were made along a 3.7-mile traverse to evaluate the electrical resistivity distribution within this geothermal field. Interpretation of the VES curves by computer modeling indicates that the vapor-dominated layer has a resistivity of about 75–130 ohm-m and that its lateral extent is about 1 mile. It is characteristically overlain by a low-resistivity layer of about 2–6.5 ohm-m, and it is laterally confined by a layer of about 30 ohm-m. This 30-ohm-m layer, which probably represents hot water circulating in low-porosity rocks, also underlies most of the

survey area at an average depth of about 1000 ft.

Horizontal resistivity profiles, measured with two electrode spacings of an AMN array, qualitatively corroborate the sounding interpretation. The profiling data delineate the southeast boundary of the geothermal field as a distinct transition from low to high apparent resistivities. The northwest boundary is less distinctly defined because of the presence of thick lake deposits of low resistivities.

A broad positive self-potential anomaly is observed over the geothermal field, and it is interpretable in terms of the circulation of the thermal waters. Induced-polarization anomalies were obtained at the northwest boundary and near the southeast boundary of the vapor-dominated field. These anomalies probably are caused by relatively high concentrations of pyrite.

INTRODUCTION

Geophysical surveys of geothermal areas, particularly with electrical methods, have been made in several parts of the world. In Italy, Schlumberger electrical soundings were made in Larderello (Breusse and Mathiez, 1956) and in the two areas of Monte Labbro and San Filippo near Monte Amiata (Alfano, 1961). These surveys were made in order to map high-resistivity limestone bedrock under a low-resistivity and impermeable cover. Faults thus delineated in the limestone bedrock were interpreted to be zones where natural steam was most likely to be found. In New Zealand the boundaries of geothermal fields in the Taupo volcanic zone were outlined by the use of Wenner soundings, Wenner horizontal pro-

files, and bipole-dipole total field apparent resistivity mapping (Banwell and MacDonald, 1965; Hatherton et al, 1966; Risk et al, 1970). In Turkey (Duprat, 1970) and in Taiwan (Cheng, 1970), Schlumberger soundings were used to map geothermal areas. In the U.S., reconnaissance resistivity measurements were made in the Salton Trough, Imperial Valley, California, by Meidav (1970) and by McEuen (1970).

Geothermal systems, according to White et al (1971), are of two types: hot-water systems and (of less common occurrence) vapor-dominated systems. The Geysers, California, Larderello, Italy, and the Mud Volcano area, Yellowstone National Park, are examples of vapor-dominated systems. Geochemically, water samples from

† Publication authorized by the Director, U.S. Geological Survey. Presented at the Symposium on Electrical Properties of Rocks, Salt Lake City, Utah, March 16, 1972. Manuscript received by the Editor June 6, 1973; revised manuscript received July 24, 1973.

* U.S. Geological Survey, Denver, Colo. 80225.

‡ U.S. Geological Survey, Menlo Park, Calif. 94025.

© 1973 Society of Exploration Geophysicists. All rights reserved.

springs a:
dominate
concentra
trations o
the spring
bonate in
sulfate-ric
cally low
phuric ac
sodium b
have neu
water sy:
concentrat
subsurfac
duce hot

In May
Geologica
Yellowsto
pulled fro
lent erup
eruption t



FIG. 1. Ino

springs and drill holes in the vicinity of vapor-dominated systems are characterized by high concentrations of sulfate anions and low concentrations of chlorides (<20 ppm). Less commonly the spring waters may be rich in sodium bicarbonate instead of sulfate. The pH values of the sulfate-rich spring waters are also characteristically low (2 to 3) because of the formation of sulphuric acid from oxidation of rising H₂S gas. The sodium bicarbonate waters discharge feebly and have neutral pH values. In contrast, most hot-water systems are characterized by high concentrations of chlorides, and those systems with subsurface temperatures of 180°C or higher produce hot springs that deposit sinter.

In May 1968, hole Y-11 was drilled by the U.S. Geological Survey in the Mud Volcano area, Yellowstone National Park. After the core was pulled from depths of both 307 and 347 ft, a violent eruption of water occurred, followed by an eruption that consisted almost entirely of steam.

White et al (1971) estimated that in these eruptions steam was associated with less than 10 percent liquid water by weight. For a hot water system to yield a comparable ratio of vapor to liquid, the permeability of the rocks must be low; but in Y-11, high rock permeabilities were evidenced by the large losses in circulation at all depths below 122 ft. Therefore, it must be the deficiency in liquid water, rather than the low permeability of rocks, that caused the steam to dominate the eruptions. Furthermore, according to White et al (1971), all the geochemical manifestations of vapor-dominated systems are exhibited in the Mud Volcano area.

Subsequent to the drilling of Y-11, the USGS made VES (vertical electrical sounding), resistivity horizontal profiles, SP (self-potential), and IP (induced-polarization) measurements in the Mud Volcano area to evaluate the geoelectrical properties of a section containing a vapor-dominated geothermal system.

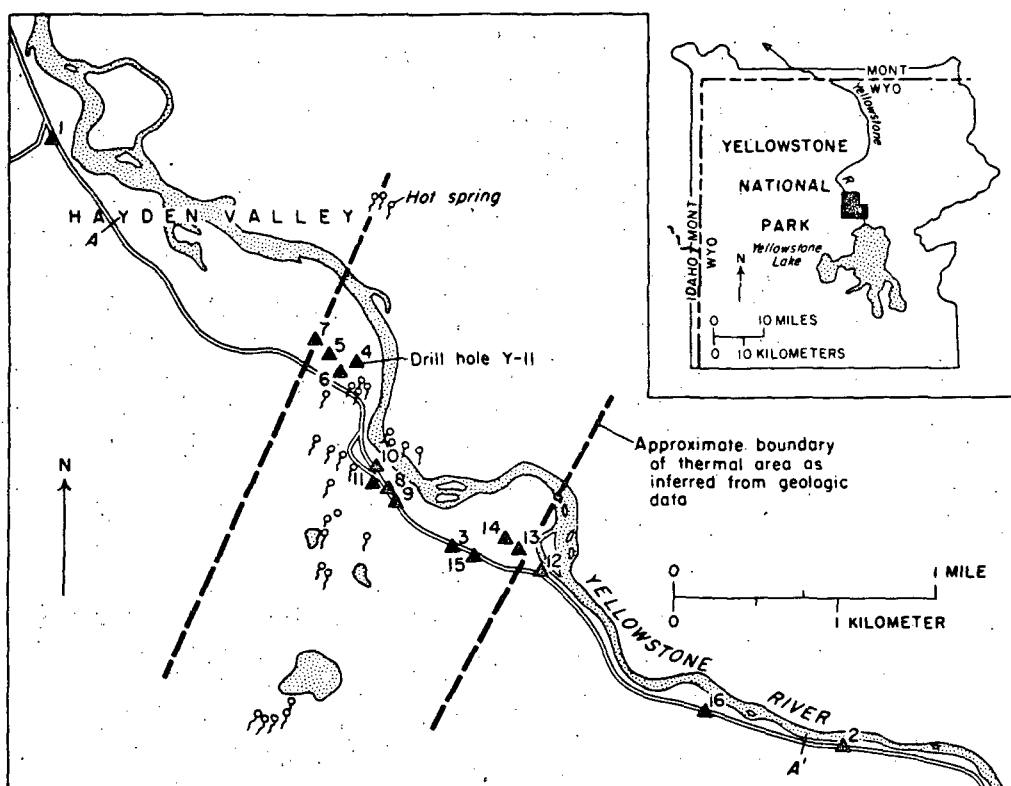


FIG. 1. Index map showing locations of VES stations (numbered triangles) and drill hole Y-11 in the Mud Volcano thermal area. Resistivity, SP, and IP profiles were measured along the road from A to A'.

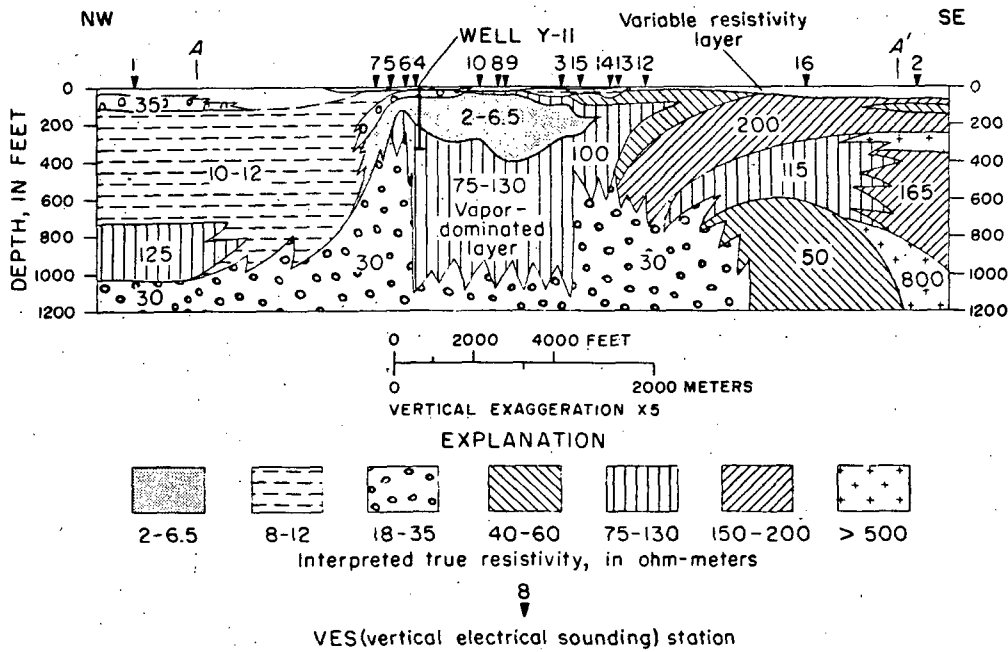


FIG. 2. Geoelectric section of the Mud Volcano area, Yellowstone National Park.

GENERAL SETTING

The Mud Volcano area (Figure 1) lies along the Yellowstone River approximately 5 miles north of Yellowstone Lake. Most of the area is covered by glacial silt, sand, and gravel which are underlain by rhyolitic ash-flow tuff; the area contains numerous mud pots and acid-sulfate springs. Some nearly neutral bicarbonate-sulfate springs occur along the river, but there are no chloride-rich springs in the area.

The location of the 16 VES stations, the test well Y-11, and the resistivity, SP, and IP profiles (which were made along the road from A to A') are shown in Figure 1. The approximate boundaries of the geothermal field, as inferred from geologic data are also shown.

THE GEOELECTRIC SECTION

Figure 2 shows the geoelectric section obtained from the interpretation of the VES curves. In the middle of the section, beneath VES 7 to VES 12, there are basically four electrical units. The first unit is composed of several near-surface layers, some of which are of small lateral extent (about 1,000 ft or less) and of variable resistivities. The second electrical unit is a fairly uniform single layer of remarkably low resistivity of about 2-6.5

ohm-m. It occurs at an average depth of about 50 ft and extends to an average depth of about 250 ft. This low-resistivity layer is interpreted as a layer where steam condenses into hot water, and where pyrite and clay minerals (kaolinite and montmorillonite) are present. The third electrical unit is a high-resistivity layer of about 75-130 ohm-m. Where this layer underlies the 2-6.5-ohm-m layer, it is interpreted as a zone where "dry steam," rather than liquid water, dominates the larger pores and open fractures in the rocks. The maximum depth to the bottom of this layer is unknown, but the minimum depth is about 1000 ft, and its lateral extent is approximately 1 mile. On both the northwest and southeast boundaries of this layer is the fourth geoelectric unit, a layer which is characterized by a resistivity of about 30 ohm-m and which is interpreted as a layer of hot water in low-porosity rocks.

At the northwest end of the section, beneath VES 1, there is a thick (about 600 ft) low-resistivity (10-12 ohm-m) layer which represents lacustrine deposits in Hayden Valley. In the southeastern part of the section, however, beneath VES 16 and VES 2, the layer resistivities generally are high (40-800 ohm-m) to depths of at least about 600 ft, thus reducing the probab-

ity for the p comparable

IN
The 16 v using the electrode sp 3000 ft. In made by cu bums of the 1966; Rijkv grams (Zoh method for curves (Zoi geologically tion as wel observed a:

The curv where it is one calcula based on a other calcul obtained by terpretatio cate the pi

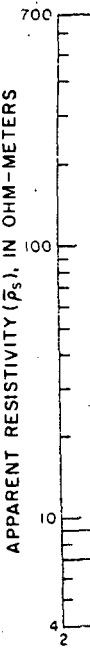


FIG. 3. Si: subsequently terpreted true i

ity for the presence of thermal activity at depths comparable to those at the middle of the section.

INTERPRETATION OF VES CURVES

The 16 vertical electrical soundings were made using the Schlumberger array with maximum electrode spacings (AB/2) ranging from 500 to 3000 ft. Interpretation of the VES curves was made by curve-matching procedures in which albums of theoretical curves (Orellana and Mooney, 1966; Rijkwaterstaat, 1969), auxiliary point diagrams (Zohdy, 1965), Dar Zarrouk curves, and a method for the automatic interpretation of VES curves (Zohdy, 1972) were all used to reach a geologically and geoelectrically acceptable solution as well as to achieve excellent fits between observed and calculated VES curves.

The curve of VES 1 is shown in Figures 3 and 4, where it is matched with two theoretical curves, one calculated for a six-layer model (Figure 3), based on auxiliary point interpretation, and the other calculated for a 19-layer model that was obtained by the computer using the automatic interpretation program. The interpretations indicate the presence of either a sequence of low-

resistivity layers (5-23 ohm-m) that extends from a depth of about 100 ft to a depth of about 1000 ft, or a single low-resistivity layer (11-12 ohm-m) that extends from a depth of about 100 ft to a depth of about 700 ft. This low-resistivity layer is probably composed of clayey and silty lake deposits and is not necessarily related to the geothermal system. It is underlain by one layer of 125 ohm-m or by two layers of 50 and 125 ohm-m, respectively. These layers are underlain by a thick layer of low resistivity (≤ 35 ohm-m). Because of the lack of geologic information and other VES data in the immediate vicinity of this sounding, it is difficult to decide which interpretation is more accurate. The two interpretations are presented here to illustrate the problems of equivalence between multilayer sections in the interpretation of a single VES curve.

Figure 5 shows the curve of VES 7 and its interpretation in terms of a five-layer section. The third, fourth, and fifth layers are not clearly manifested on the VES curve, but correlation with the curves of VES 5 and VES 6, which are shown in Figure 6, clearly indicates that the small maximum and minimum on the curve of VES 7 (be-

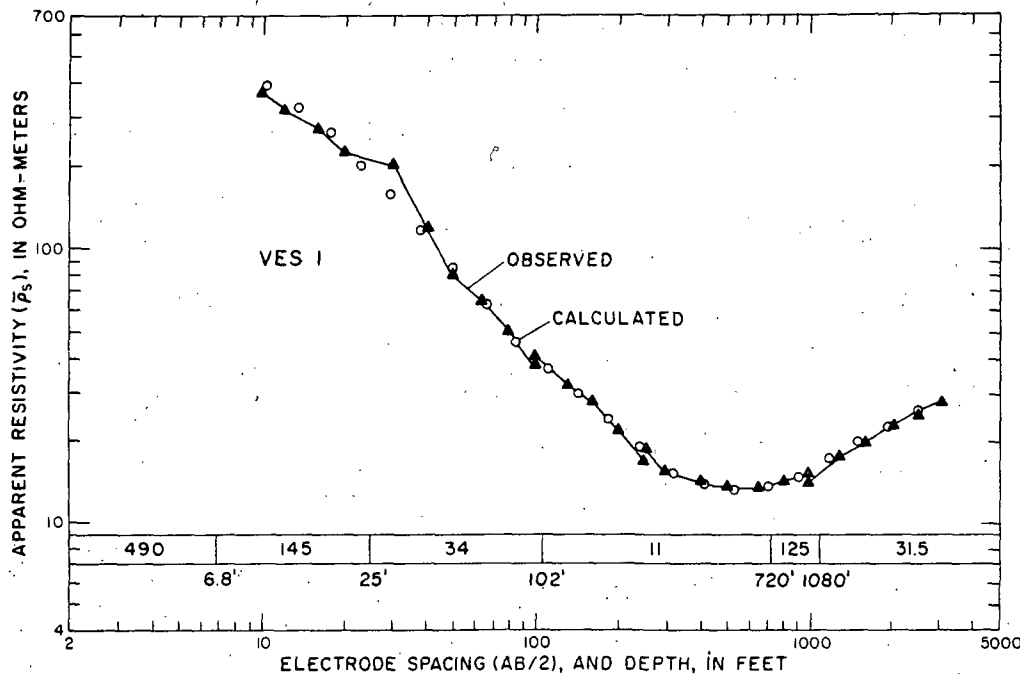


FIG. 3. Six-layer interpretation of VES 1 curve. Interpretation initially made with auxiliary point method and subsequently verified by computer calculation of interpreted model. Numbers in and below bar designate interpreted true resistivities in ohm-meters and interpreted depths in feet, respectively.

out 50
out 250
ed as a
er, and
te. and
ectrical
75-130
5-ohm-
e "dry
tes the
s. The
ayer is
t 1000
1 mile.
adaries
a layer
about
ayer of

eneath
) low-
resents
n the
er, be-
ivities
ths of
abil-

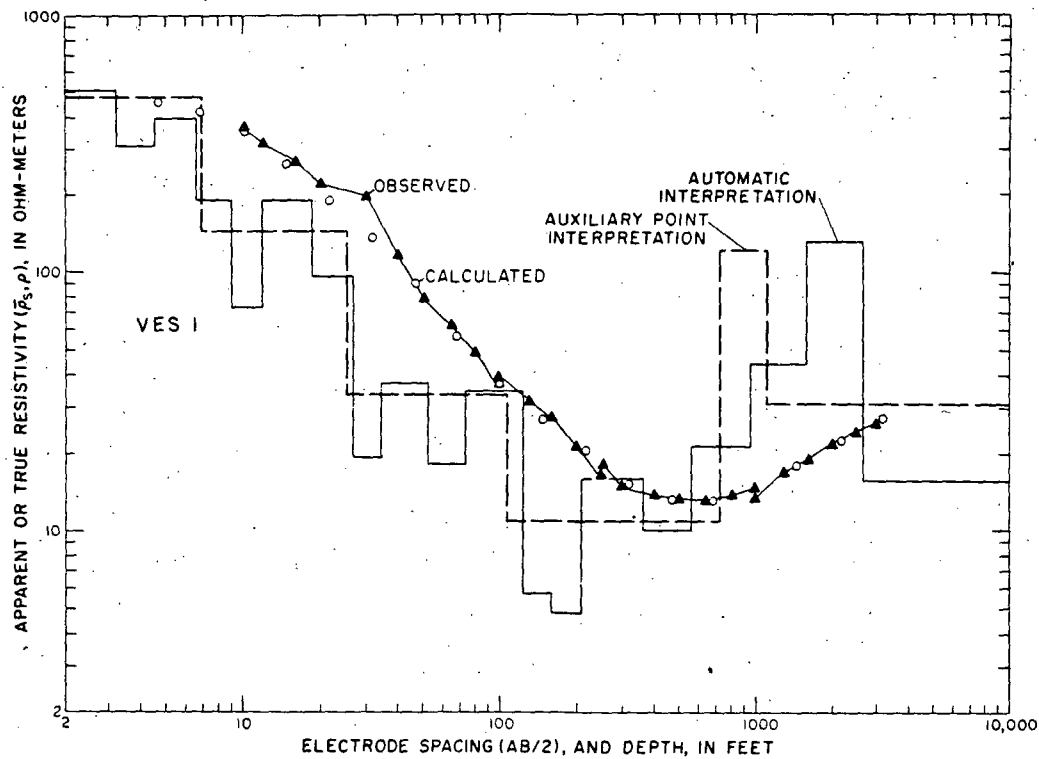


Fig. 4. Equivalence between 19-layer automatic interpretation and six-layer auxiliary point interpretation of VES 1 curve.

tween $AB/2 = 100$ and 1000 ft) are meaningful. They express the presence of the same layers that are represented by the well-developed maxima and minima on the curves of VES 5 and VES 6. The value of the apparent resistivity on the minimum of VES 6 is about 6.2 ohm-m and this is the first concrete evidence obtained on the northwest side of the section of the presence of a layer that must have a true resistivity of less than 6 ohm-m. For VES 6 the true resistivity of that layer is interpreted to be about 2 ohm-m, whereas for VES 5 and VES 7 it is interpreted to be about 4 and 4.5 ohm-m, respectively. The rising terminal branch on VES 7 curve is not well developed, but on the VES 5 curve the well-developed terminal branch indicates that the bottommost layer must have a resistivity of about 30 ohm-m. The curvature of the terminal branch of VES 6 curve is fitted best with a theoretical curve for a section in which a layer of about 75 ohm-m (or more) must exist between the very low (2 ohm-m) resistivity layer and the bottommost layer of about 30 ohm-m.

This 75-ohm-m layer is interpreted to represent the northwest edge of the vapor-dominated layer.

The center of VES 4 was located about 100 ft north of well Y-11. The observed curve and its interpretation are shown in Figure 7 together with the geologic log of Y-11. The curve was interpreted in terms of a five-layer geoelectric section, the first layer of which has a resistivity of about 1700 ohm-m and a thickness of about 7 ft. The first layer corresponds to the layer of dry river gravel which lies within 6 inches above the water table. The second and third layers have resistivities of about 170 and 28 ohm-m, respectively, and extend to a depth of about 60 ft. These two layers correlate well with a layer of conglomerate composed of white pumice and black obsidian underlain by a layer of sandstone of the same composition. The depth to the bottom of the sandstone layer is about 65 ft which is in good agreement with the interpreted depth of about 60 ft. The fourth layer, on the interpreted geoelectric section beneath VES 4, has a low resistivity of

about 6.3
195 ft wt
layer of a
correspon
the well
and it ext
Mineralog
Y-11 (un
L. J. P. M
pyrite arc
to the bo
posits occ
tinue to c
at which t
cellent ag
195 ft to t

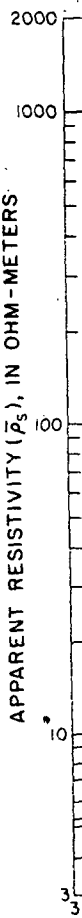


Fig. 5. I

about 6.3 ohm-m and extends to a depth of about 195 ft where it is underlain by a high-resistivity layer of about 120 ohm-m of large thickness. The corresponding geologic formation encountered in the well is composed of rhyolitic ash-flow tuff, and it extends to the bottom of the well at 347 ft. Mineralogical analysis of core samples from well Y-11 (unpublished data of K. E. Bargar and L. J. P. Muffler) indicates that clay minerals and pyrite are present from a depth of about 50 ft to the bottom of the well. Some chalcedony deposits occur at a depth of about 200 ft and continue to exist to the bottom of the well. The depth at which these chalcedony deposits occur is in excellent agreement with the interpreted depth of 195 ft to the high-resistivity layer of 120 ohm-m.

Therefore, it is tempting to conclude that it is the chalcedony deposits that have caused the rise in resistivity. However, because the porosity of the ash-flow tuff (according to drilling data) did not change significantly at the depth of 200 ft, and because the conductive clay minerals and pyrite continue to exist in essentially the same amounts to the bottom of the well, we interpret the decrease in resistivity to about 6.3 ohm-m and its subsequent increase to about 120 ohm-m (on the curve of VES 4, as well as on the curves of VES 8, VES 9, and VES 10) to be governed mostly by the abundance of hot liquid water in the 2-6.5-ohm-m layer and by the dominance of steam in the 75-130-ohm-m layer. The drilling results of well Y-11 indicate that steam dominates

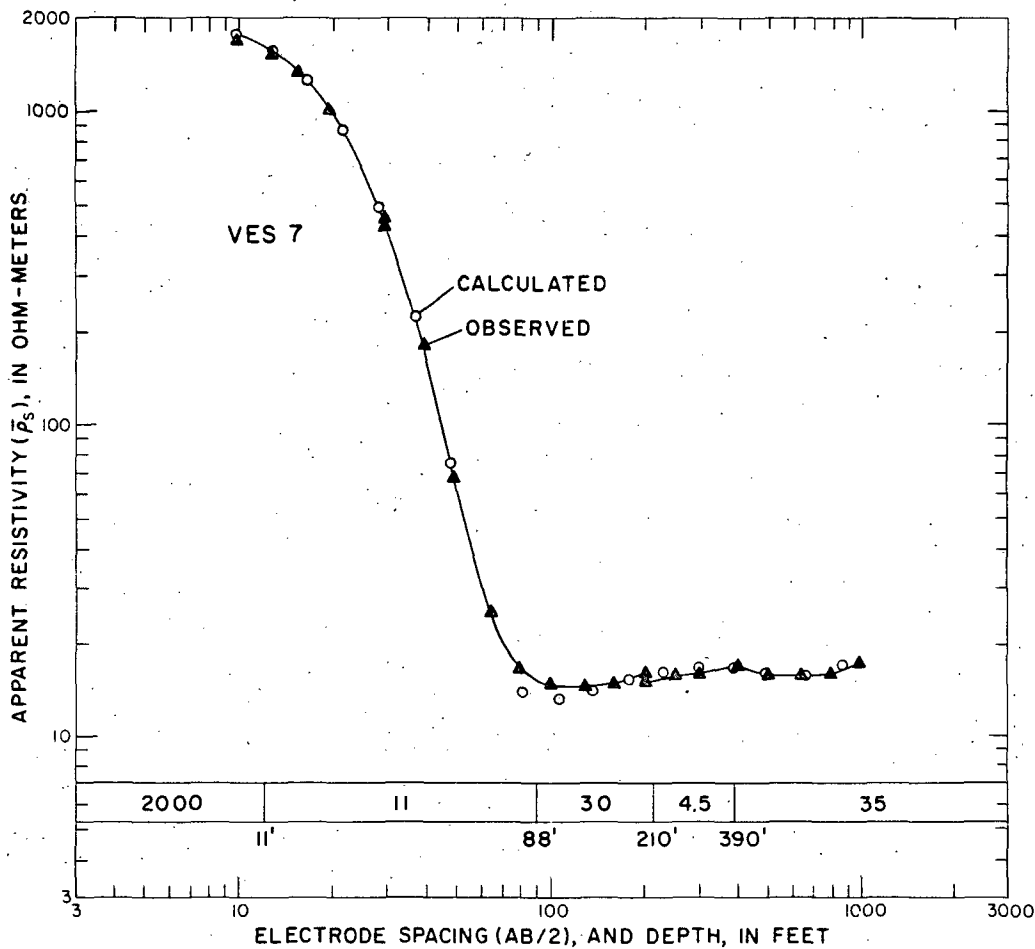


FIG. 5. Interpretation of VES 7 curve in terms of a five-layer model. Numbers in and below bar designate interpreted true resistivities, in ohm-meters, and interpreted depths, in feet, respectively.

resent layer. 100 ft and its r with inter- ction, about . The river water resistivity, e two erate n un- com- sand- gree- 50 ft. electric ty of

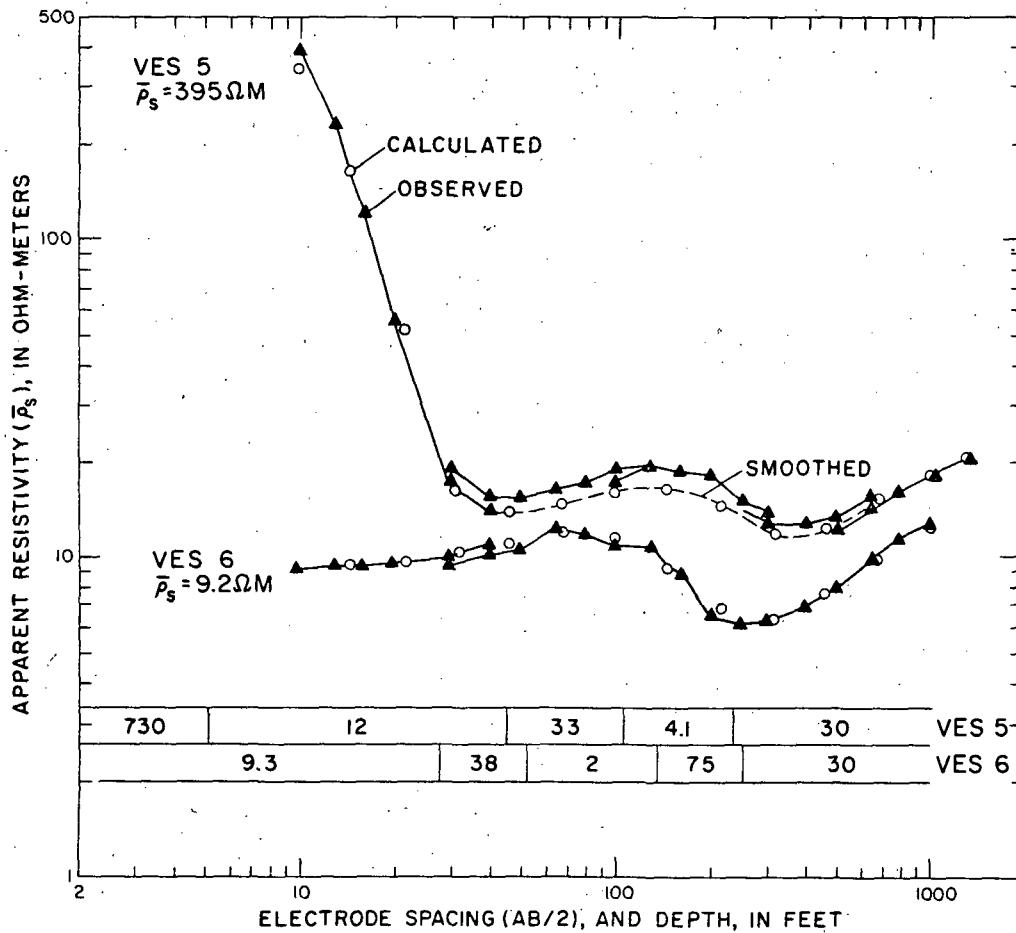


FIG. 6. Interpretation of VES 5 and VES 6 curves. Numbers in bars designate interpreted true resistivities, in ohm-meters.

the system from a depth of at least 307 ft to the bottom of the hole (White et al, 1971), but according to the interpretation of VES 4 the steam may dominate the system to a depth as shallow as 200 ft.

Figure 8 shows the curve of VES 10 which was obtained near the middle of the geothermal field (see Figure 2). The magnitude and the direction of the discontinuities on the observed curve (which were observed upon the expansion of the potential electrodes) are not in agreement with those prescribed for horizontal layering (Deppermann, 1954; Zohdy, 1969). Following a procedure which has been found to be most satisfactory in practice, the various segments on the VES curve were shifted to conform to the position of the last

segment on the curve. The shifted segments then are smoothed, to remove cusps which are caused by the crossing of lateral heterogeneities by the current electrodes, and the smoothed curve is fitted with a theoretical one as shown in Figure 8 for VES 10. Similar smoothing was made for VES 5 and for other curves. This smoothing procedure results in modifying the interpreted true resistivities of the shallower layers in the section, which in general are quite variable, but it does not alter their interpreted thicknesses nor does it create undulations on the smoothed curve (which may be interpreted as layers) that were not actually manifested on the observed curve. These undulations often are created when the smoothing is made by drawing a curve that passes between

significantly interpreted beneath the

The curve their interpretation illustrate the conductive (90-100 ohm curves. The and about 4 respectively, the resistive the geotherm

Figure 10 and VES 13

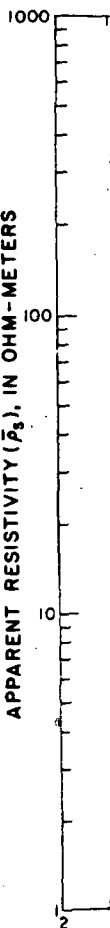


FIG. 7. Curve designate interpreted composed of white

significantly displaced segments. For VES 10 the interpreted depth to the vapor-dominated layer, beneath the low-resistivity layer, is about 300 ft.

The curves of VES 8, VES 9, and VES 3 and their interpretations are shown in Figure 9 to illustrate the continuity of the detection of the conductive (2.4-5.2 ohm-m) and the resistive (90-100 ohm-m) bottom layers on the VES curves. The interpreted depths of about 340 ft and about 400 ft, beneath VES 9 and VES 8, respectively, are the largest interpreted depths to the resistive bottom layer over the middle part of the geothermal section.

Figure 10 shows the curves of VES 15, VES 14, and VES 13 and their interpretations. Using the

automatic interpretation computer program, the curve of VES 15 is the only curve in this group of VES curves that can be interpreted so that a layer with a low resistivity of about 5 ohm-m can be included legitimately in the section. Thus VES 15 reflects the nearness of the southeastern boundary of the geothermal system. On all three VES curves there is a strong indication that the bottommost layer, which lies at an average depth of about 550 ft, has a resistivity of about 30 ohm-m. This layer bounds the geothermal system on the southeast as it did on the northwest.

The curves of VES 12, VES 16, and VES 2 are shown in Figure 11 together with their interpretation as obtained for the reduced model of the

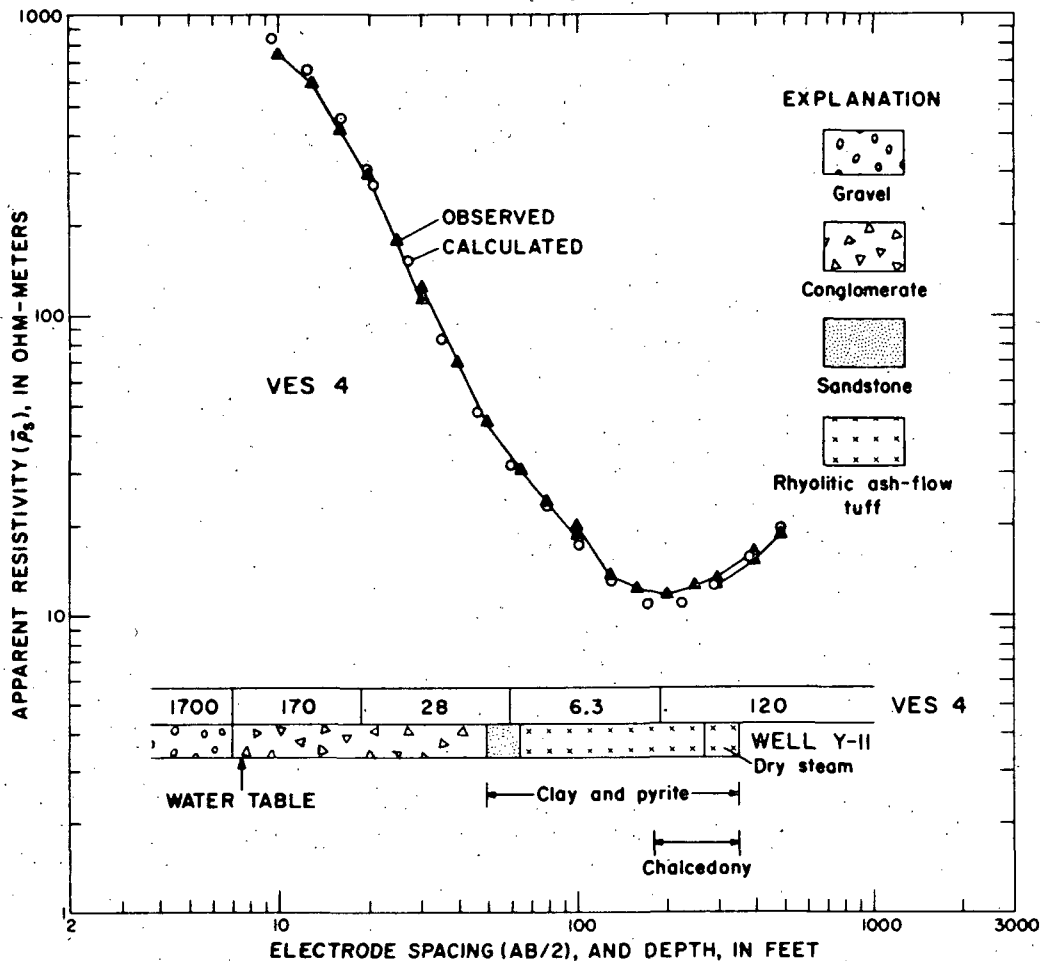


FIG. 7. Comparison between interpretation of VES 4 curve and geologic data of well Y-11. Numbers in bar designate interpreted true resistivities, in ohm-meters. Conglomerate and sandstone layers in well Y-11 are composed of white pumice and black obsidian.

S 5
S 6

nts then
e caused
by the
curve is
Figure 8
for VES
cedure
e resist-
section,
it does
r does it
e (which
not ac-
e. These
oothing
between

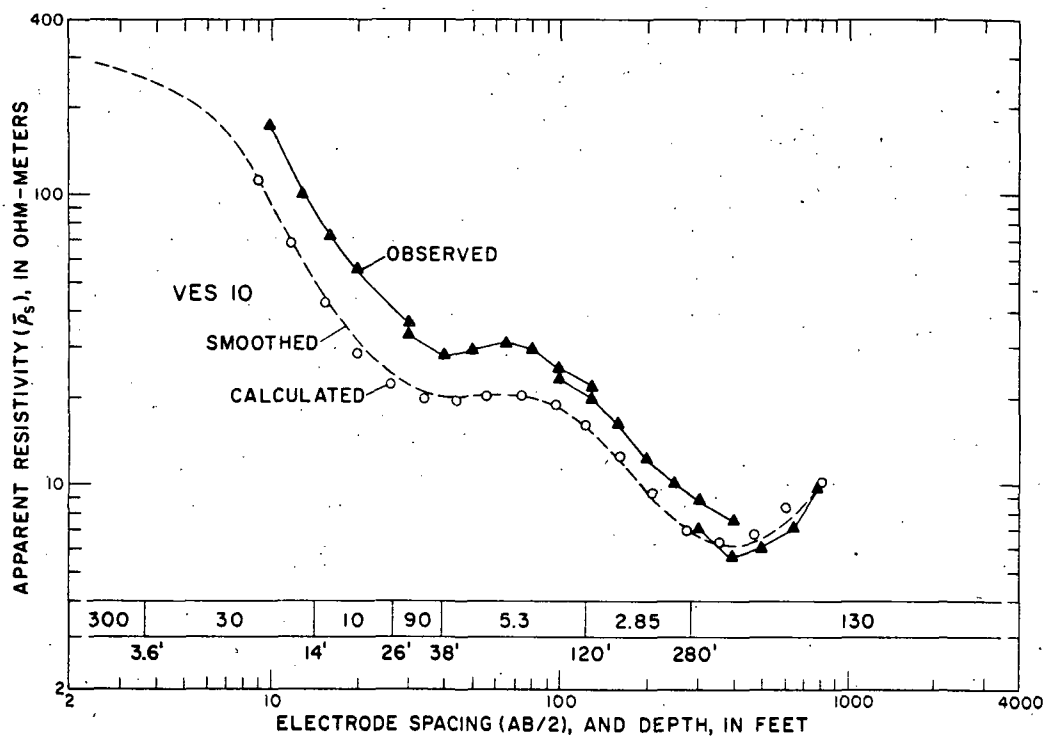
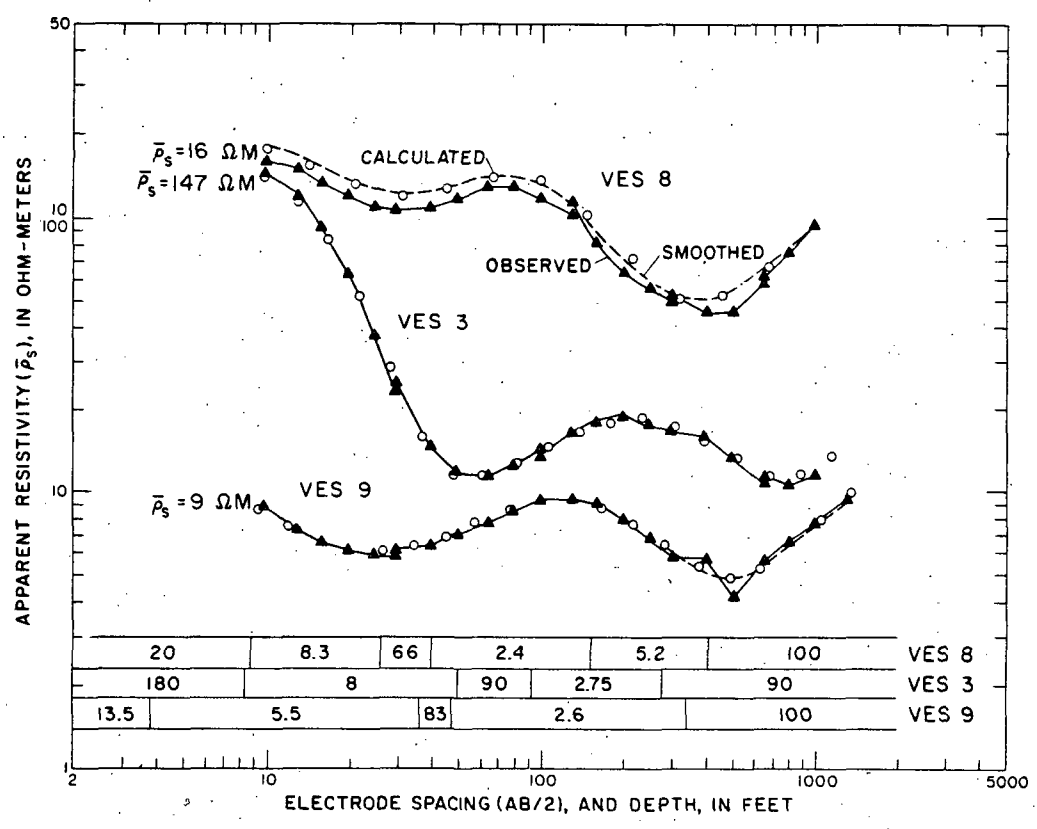


FIG. 8. Interpretation of VES 10 curve in terms of a seven-layer section. Numbers in and below bar designate interpreted true resistivities, in ohm-meters, and interpreted depths, in feet, respectively.



700

100

100

10

2

APPARENT RESISTIVITY ($\bar{\rho}_s$), IN OHM-METERS

FIG.

automati
30-ohm-r
VES 2 cu
greater
resistivit
bottom l
section, y
thermal
rhyolitic



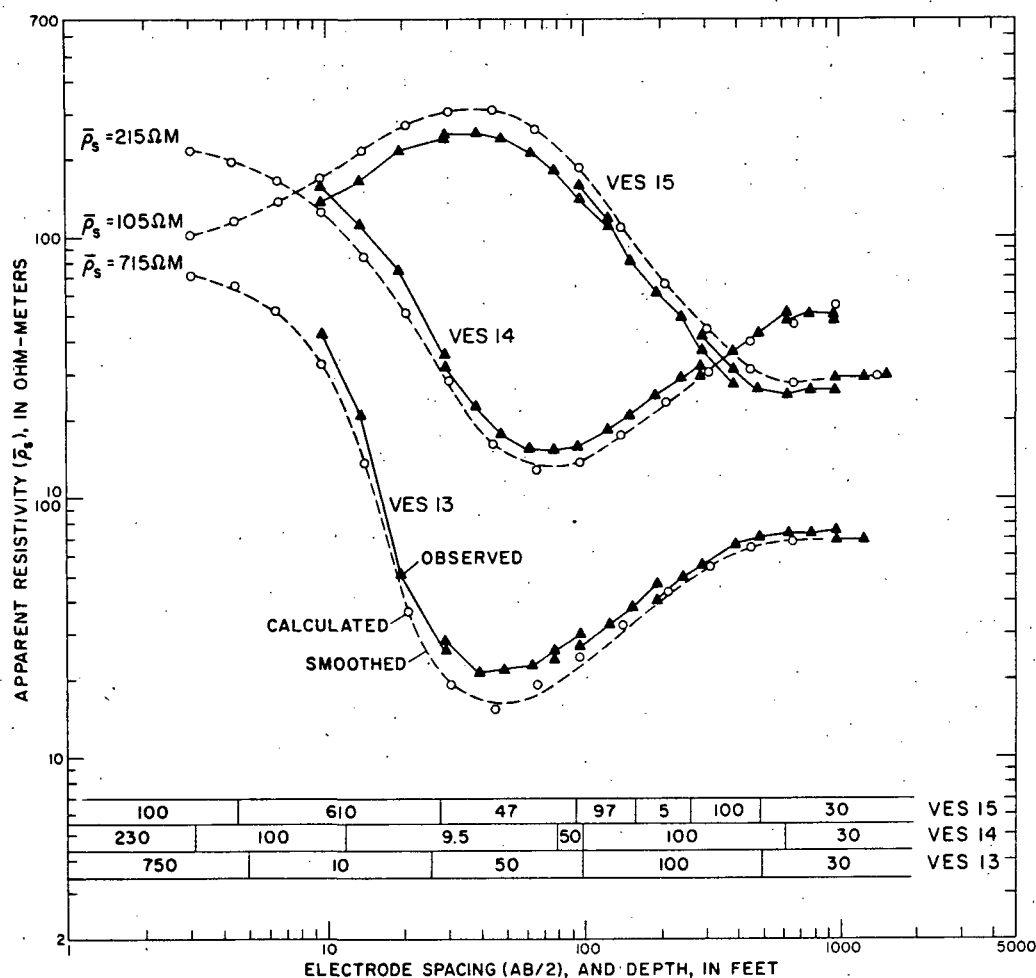


Fig. 10. Curves of VES 13, VES 14, and VES 15 obtained near the southeastern boundary of the geothermal field. Numbers in bars designate interpreted true resistivities, in ohm-meters.

automatic interpretation computer program. The 30-ohm-m bottom layer is not detected on the VES 2 curve, and if it exists it must be at a depth greater than about 1500 ft. Instead, high-resistivity layers of 800 and 300 ohm-m form the bottom layers in the automatically interpreted section, which indicates that there is no shallow thermal activity beneath VES 2 and that the rhyolitic ash flow tuff believed to form the bed-

rock in the area is probably replaced by rhyolite rocks of intermediate to high resistivities.

From the preceding description and documentation of the VES curves, and from the hydrogeologic information obtained from well Y-11, we conclude that the shallow vapor-dominated reservoir in the Mud Volcano area has a high resistivity of about 75-130 ohm-m and that it is characterized by the presence of a low-resistivity layer



Fig. 9. Curves of VES 8, VES 3, and VES 9 obtained over the center of the geothermal field. Numbers in bars designate interpreted true resistivities, in ohm-meters.

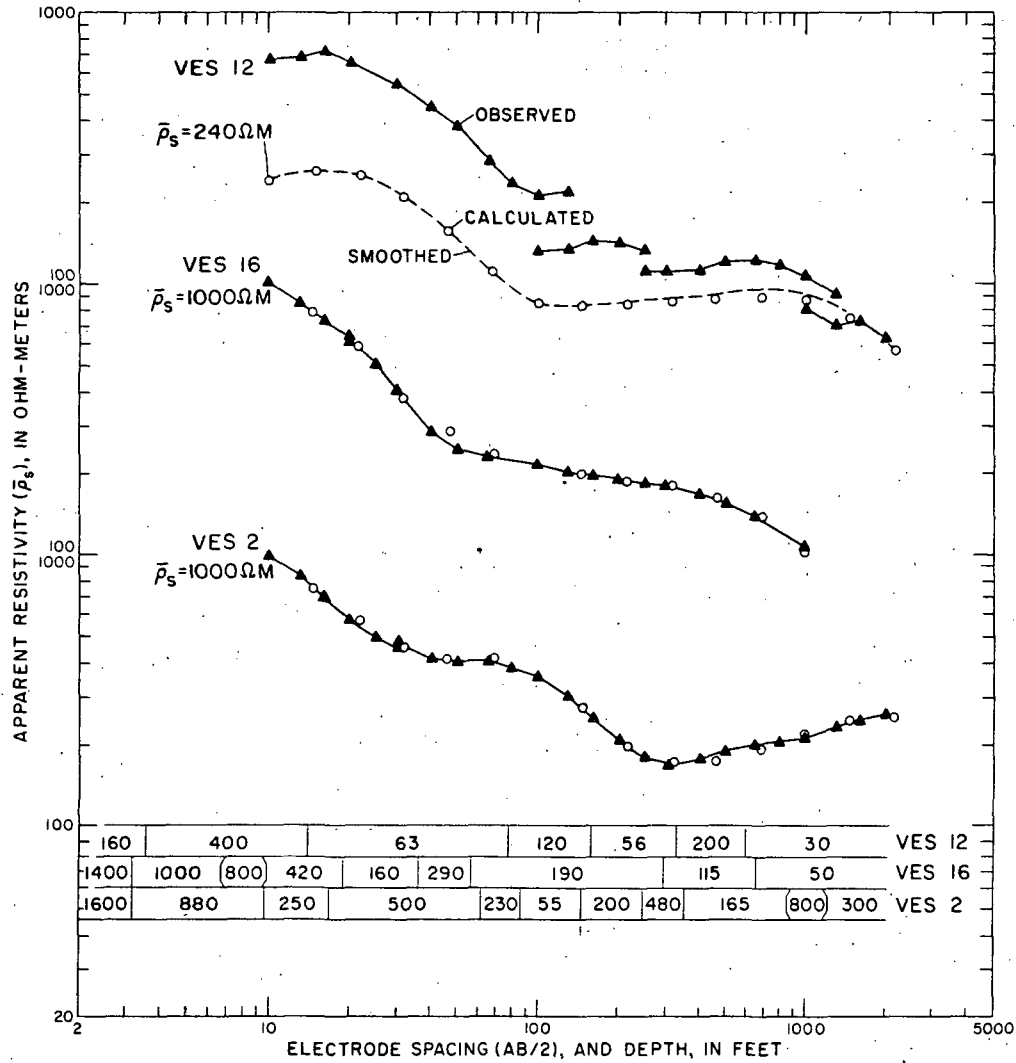


FIG. 11. Curves of VES 2, VES 12, and VES 16 obtained south of the southeastern boundary of the geothermal field. Numbers in bars designate interpreted true resistivities, in ohm-meters. Layering is based on automatically calculated models.

(2-6.5 ohm-m) above it, and a moderately resistive layer (~30 ohm-m) around it. It is interesting to note the similarity between this interpreted geoelectric section and the general model of a vapor-dominated system presented by White et al (1971). A simplified version of White's model is presented in Figure 12.

RESISTIVITY, SP, AND IP HORIZONTAL PROFILES

In 1971, two years after the VES data were obtained, horizontal profiles of resistivity, SP, and

IP were made along the road from point A to A' (see Figure 1). The resistivity and the IP were measured at two electrode spacings of a three-electrode (AMN) array. The electrode spacings (AO) between the current electrode (A) and the center (O) of the potential electrodes (M and N) was 600 ft for one profile and 1000 ft for the other. The distance (MN) between the potential electrodes for both profiles was 400 ft. The SP measurements were made prior to the 600-ft resistivity measurement. The IP measurements were made

in the
the po
calcul

where
measu
The
zontal
ter of i
the 2-
segmen
sistivit
1000 ft
smaller
parent
robora
the pr
(vapor-
resistiv
therma
low be
lacustri
southea

FIG. 1.
rich in s
from con
conducti
section).
heat flow

in the frequency domain at 0.1 and 1.0 hz, and the percent frequency effect (PFE) values were calculated using the formula

$$\text{PFE} = \frac{(\bar{\rho}_{0.1} - \bar{\rho}_{1.0})}{\sqrt{\bar{\rho}_{0.1} \cdot \bar{\rho}_{1.0}}} \cdot 100,$$

where $\bar{\rho}_{0.1}$ and $\bar{\rho}_{1.0}$ are the apparent resistivities measured at 0.1 and 1.0 hz, respectively.

The lowest apparent resistivities of the horizontal profiling data were measured over the center of the geothermal field, where the thickness of the 2- to 6.5-ohm-m layer is largest. Along this segment of the profiling data, the apparent resistivity values measured with the AO spacing of 1000 ft are larger than those measured with the smaller AO spacing of 600 ft. This increase in apparent resistivity at larger electrode spacings corroborates the VES data interpretation in terms of the presence of a deep high-resistivity layer (vapor-dominated layer) beneath a shallower low-resistivity cover. To the northwest of the geothermal field, the apparent resistivity is generally low because of the presence of a thick section of lacustrine deposits in Hayden Valley. To the southeast of the geothermal field, a marked in-

crease in apparent resistivity is observed on the resistivity profiles and a broad resistivity high is formed which extends to the southeastern boundary of the section. Within this broad resistivity high, there are three zones of lower resistivity which can be interpreted as due to alteration zones resulting from the upward movement of thermal waters at a time when near-surface geothermal activity may have existed to the south-east of the presently active zone.

SP measurements, referenced to the first station on the northwest end of the traverse, produced the broad, positive anomaly shown in Figure 13. The amplitude of the anomaly is small and may be attributed to a variety of electric potential producing effects. However, an experiment by Poldini (1938 and 1939) proved that upward-migrating water, confined within a column, produced a positive potential when a measurement was made near the top of the column with respect to an arbitrary distant point. The potential attributed to solutions moving through porous media has been observed by several investigators and is known by various names such as electro-filtration, streaming, flow, and electrokinetic potentials (Sato and Mooney, 1960). This type of

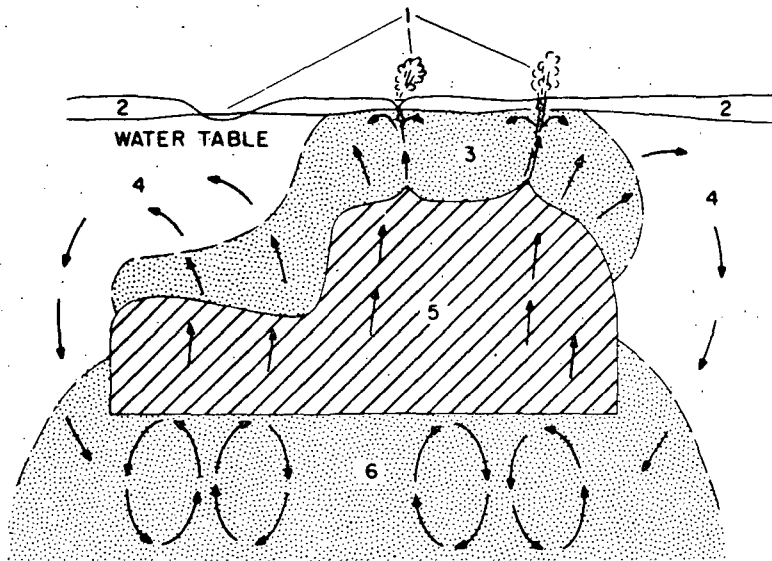


FIG. 12. Model of a vapor-dominated reservoir surrounded by water-saturated ground: (1) Springs and fumaroles rich in sulfates. (2) Zone between ground surface and water table. (3) Zone where liquid water, largely derived from condensing steam, is dominant (2-6.5-ohm-m layer in geoelectric section). (4) Zone where convective and/or conductive heat flow exists, with heat supplied from condensing steam in zone 3 (30-ohm-m layer in geoelectric section). (5) Vapor-dominated reservoir (75-130-ohm-m layer in geoelectric section). (6) Deep zone of convective heat flow above which is a boiling-water table (simplified from White et al, 1971).

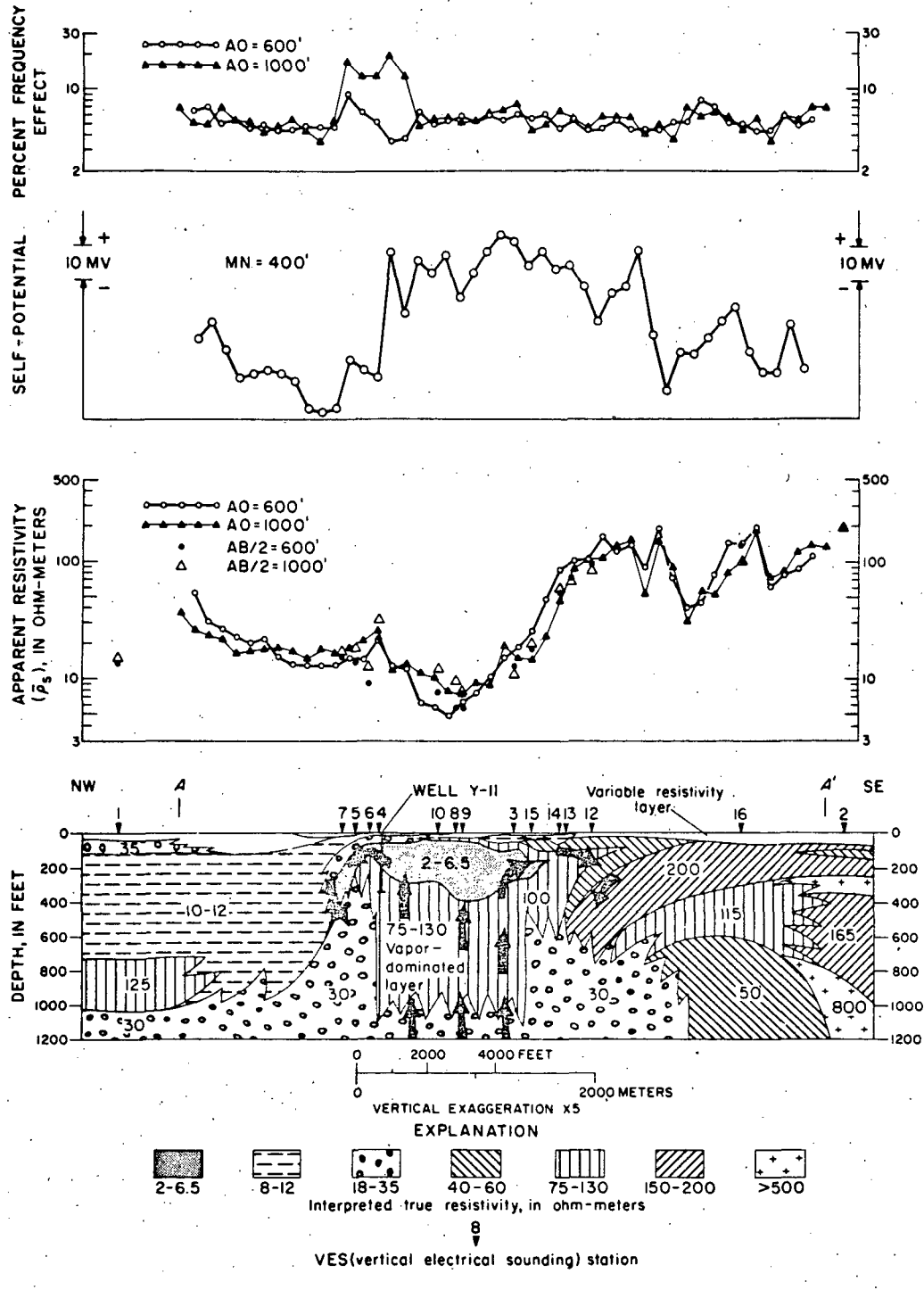


FIG. 13. Horizontal profiling data obtained with resistivity, SP, and IP (percent frequency effect). Arrows designate movement of steam and water. AO, distance from current electrode, A, to center of potential electrodes, O. MN, distance between potential electrodes. AB/2, Schlumberger-electrode spacing of VES curves.

potential is caused by the concentration of anions by the thermal waters. The small IP anomaly in the vicinity of the well is caused by the concentration of anions by the thermal waters.

On the basis of the above, it is assumed that the IP anomaly is due to the upward movement of thermal waters from the geothermal reservoir. The IP anomaly is a result of downward movement of thermal waters from the geothermal reservoir (White et al, 1977).

The reason for the IP anomaly beyond the geothermal field is not understood. It is assumed that the IP anomaly is a result of the downward movement of thermal waters from the geothermal reservoir. The downward movement of thermal waters from the geothermal reservoir is observed in the form of low resistivity zones of low resistivity.

The two IP curves are plotted on an arithmetic scale. The profiles are relatively high IP values which is attributed to the presence of clayey material layers. Differences in the amplitude of the IP curves, particularly in the vicinity of the well, are due to the increase in the polarization of the well by an increased amount of pyrite deposited by the mineralization. The presence of pyrite at the bottom of the well is also seen on the IP curves that the pyrite is at depth at the bottom of the well. It is possibly a similar situation to the small IP anomaly in the vicinity of the well.

potential is caused by cation enrichment of the pore waters owing to the preferential adsorption of anions by the rock. The upward-moving waters concentrate the cations near the surface resulting in a positive anomaly over the zone of migrating water.

On the basis of Poldini's work, it is reasonable to assume that the broad SP anomaly, at least the portion directly over the thermal zone, arises from upward-moving waters set in motion by convection currents emanating from the thermal energy source. The low SP values bordering the northwest edge of the thermal area are possibly a result of downward-moving waters, part of the cycling process involved in the movement of thermal waters (compare Figures 12 and 7 of White et al, 1971).

The reason for the continuation of the SP anomaly beyond the southeast boundary of the geothermal field (as interpreted from VES data) is not understood. Possibly, however, significant amounts of the thermal waters upon approaching the ground surface move laterally, and not until they reach the more permeable altered zones of low apparent resistivity do they begin to descend. The downward-moving water would produce the observed low level of SP coincident with the zones of low resistivity.

The two IP profiles were plotted on semilogarithmic scale in the upper part of Figure 13. The profiles are similar, both indicating a relatively high IP background level of about 5 percent which is attributable to a wide distribution of clayey materials and pyrite in the near-surface layers. Differences between the profiles occur in the amplitude of the observed anomalies, particularly in the vicinity of the northwest boundary of the inferred vapor-dominated zone. The increase in the polarization effect is probably caused by an increased quantity of disseminated pyrite deposited by circulating thermal waters. Indeed, the mineralogical analysis of well Y-11 indicates that pyrite exists from a depth of about 50 ft to the bottom of the well at 347 ft. The fact that the AO=1000 ft anomaly is significantly larger than that seen on the shorter spaced profile suggests that the pyrite and its distribution increases with depth at the boundary of the thermal zone. Possibly a similar pyrite enrichment exists beneath the small IP anomaly shown on both profiles in the vicinity of VES 16.

SUMMARY AND CONCLUSIONS

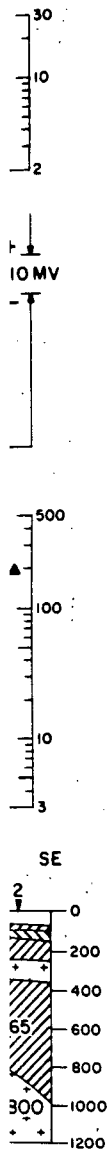
Vertical electrical soundings in the Mud Volcano area of Yellowstone National Park indicate that the vapor-dominated reservoir is characterized by high resistivities and that it occurs under a cover of very low resistivity. Because of this low-resistivity layer, reconnaissance surveys with horizontal profiling will delineate the thermally active zone by a low-resistivity anomaly. The boundaries of the geothermal field as defined by the quantitative interpretation of the VES curve is in excellent agreement with the approximate boundaries inferred from mapping the surface geology. Beneath VES 1 and VES 16, the geothermal conditions may exist at depths slightly greater than about 1000 ft, whereas beneath VES 2 the thermal activity, if it exists, must be at depths greater than 1500 ft.

The SP anomalies seem to be directly related and interpretable in terms of the thermal water circulation system, and although the SP anomaly observed in the Mud Volcano area is relatively small, its existence warrants the further study and measurement of SP in other geothermal areas.

The IP anomalies observed at the northwestern boundary and south of the southeastern boundary were interpreted in terms of pyrite concentrations deposited by sulfur-rich thermal waters at those locations where the thermal waters intermix with meteoric waters and begin a downward movement in the hydrological recycling process surrounding the geothermal cell.

REFERENCES

- Alfano, L., 1961, Geoelectrical explorations for natural steam near "Monte Amiata": *Quad. Geofisica Appl.*, v. 21, p. 3-17.
- Banwell, C. J., and MacDonald, W. J. P., 1965, Resistivity surveying in New Zealand thermal areas: Presented at 8th Commonwealth Mining and Metall. Cong., Australia and New Zealand, Paper 213, p. 1-7.
- Breusse, J. J., and Mathiez, J. P., 1956, Application of electrical prospecting methods to tectonics in the search for natural steam at Larderello, Italy, in *Geophysical case histories: Vol. II*, Paul L. Lyons, Editor, Tulsa, SEG, p. 623-630.
- Cheng, W. T., 1970, Geophysical exploration in the Tatun volcanic region, Taiwan: *Geothermics Spec. Issue 2, v. 2, pt. 1*, p. 262-274.
- Deppermann, K., 1954, Die Abhängigkeit des scheinbaren Widerstandes vom Sondenabstand bei der Vierpunkt-Methode: *Netherlands, Geophys. Prosp.*, v. 2, p. 262-273.
- Duprat, A., 1970, Contribution of geophysics to the study of the geothermal region of Denizli-Saraykoy, Turkey: *Geothermics Spec. Iss. 2, v. 2, pt. 1*, p. 275-286.
- Hatherton, T., MacDonald, W. J. P., and Thompson,



Arrows design electrodes, O.

- G. F. K., 1966, Geophysical methods in geothermal prospecting in New Zealand: *Bull. Volcanol.*, v. 29, p. 485-498.
- McEuen, R. B., 1970, Delineation of geothermal deposits by means of long-spacing resistivity and airborne magnetics: *Geothermics Spec. Iss. 2*, v. 2, pt. 1, p. 295-302.
- Meidav, T., 1970, Application of electrical resistivity and gravimetry in deep geothermal exploration: *Geothermics Spec. Iss. 2*, v. 2, pt. 1, p. 303-310.
- Orellana, Ernesto, and Mooney, H. M., 1966, Master tables and curves for vertical electrical sounding over layered structures: Madrid, Interciencia.
- Poldini, E., 1938, Geophysical exploration by spontaneous polarization methods: *Mining Mag.*, London, v. 59, p. 278-282, 347-352.
- 1939, Geophysical exploration by spontaneous polarization methods: *Mining Mag.* London, v. 60, p. 22-27, 90-94.
- Rijkwaterstaat, 1969, Standard graphs for resistivity prospecting: EAEG, Netherlands.
- Risk, G. F., MacDonald, W. J. P., and Dawson, G. B., 1970, D.C. resistivity surveys of the Broadlands geothermal region, New Zealand: *Geothermics Spec. Iss. 2*, v. 2, pt. 1, p. 287-294.
- Sato, Motoaki, and Mooney, H. M., 1960, The electrochemical mechanism of sulfide self-potentials: *Geophysics*, v. 25, p. 226-249.
- White, D. E., Muffler, L. J. P., and Truesdell, A. H., 1971, Vapor-dominated hydrothermal systems compared with hot-water systems: *Econ. Geol.*, v. 66, p. 75-97.
- Zohdy, A. A. R., 1965, The auxiliary point method of electrical sounding interpretation and its relationship to the Dar Zarrouk parameters: *Geophysics*, v. 30, p. 644-660.
- 1969, The use of Schlumberger and equatorial soundings in groundwater investigations near El Paso, Texas: *Geophysics*, v. 34, p. 713-728.
- 1972, Automatic interpretation of resistivity sounding curves using modified Dar Zarrouk functions [abs.]: *Geophysics*, v. 38, p. 196-197.

QUANTITATIVE

G. J. PALA

Recent improvements in quantitative geophysical methods have made it possible to obtain more quantitative information from geophysical surveys. The necessary improvements have been obtained in two systems and ground truthing. Both approaches are being compared. In the former, the system is compared with the apparent resistivity curves.

INPUT¹ (the system) is a transmitter whose frequency is Barringer in the most widely used surveys were explained in Figure 1.

Brief description

The primary current pulses with a constant polarity. The magnetic field is 0.48, 0.75, 1.0 transmitter spacing over a time interval of 0.22 msec to 0.44 msec.

The present system operates in the same manner as the superimposed current system, but it is as a decaying primary pulse.

¹ Registered trademark.

† Manuscript received.

* Now with Barringer Geophysical Services, Ontario, Canada.

‡ University of Toronto.

© 1973 Society of Professional Geophysicists.

Ward

RESISTIVITY, SELF-POTENTIAL, AND INDUCED-POLARIZATION
SURVEYS OF A VAPOR-DOMINATED GEOTHERMAL SYSTEM†

A. A. R. ZOHDY*, L. A. ANDERSON*, AND L. J. P. MUFFLER‡

The Mud Volcano area in Yellowstone National Park provides an example of a vapor-dominated geothermal system. A test well drilled to a depth of about 347 ft penetrated the vapor-dominated reservoir at a depth of less than 300 ft. Subsequently, 16 vertical electrical soundings (VES) of the Schlumberger type were made along a 3.7-mile traverse to evaluate the electrical resistivity distribution within this geothermal field. Interpretation of the VES curves by computer modeling indicates that the vapor-dominated layer has a resistivity of about 75-130 ohm-m and that its lateral extent is about 1 mile. It is characteristically overlain by a low-resistivity layer of about 2-6.5 ohm-m, and it is laterally confined by a layer of about 30 ohm-m. This 30-ohm-m layer, which probably represents hot water circulating in low-porosity rocks, also underlies most of the

survey area at an average depth of about 1000 ft.

Horizontal resistivity profiles, measured with two electrode spacings of an AMN array, qualitatively corroborate the sounding interpretation. The profiling data delineate the southeast boundary of the geothermal field as a distinct transition from low to high apparent resistivities. The northwest boundary is less distinctly defined because of the presence of thick lake deposits of low resistivities.

A broad positive self-potential anomaly is observed over the geothermal field, and it is interpretable in terms of the circulation of the thermal waters. Induced-polarization anomalies were obtained at the northwest boundary and near the southeast boundary of the vapor-dominated field. These anomalies probably are caused by relatively high concentrations of pyrite.

INTRODUCTION

Geophysical surveys of geothermal areas, particularly with electrical methods, have been made in several parts of the world. In Italy, Schlumberger electrical soundings were made in Larderello (Breusse and Mathiez, 1956) and in the two areas of Monte Labbro and San Filippo near Monte Amiata (Alfano, 1961). These surveys were made in order to map high-resistivity limestone bedrock under a low-resistivity and impermeable cover. Faults thus delineated in the limestone bedrock were interpreted to be zones where natural steam was most likely to be found. In New Zealand the boundaries of geothermal fields in the Taupo volcanic zone were outlined by the use of Wenner soundings, Wenner horizontal pro-

files, and bipole-dipole total field apparent resistivity mapping (Banwell and MacDonald, 1965; Hatherton et al, 1966; Risk et al, 1970). In Turkey (Duprat, 1970) and in Taiwan (Cheng, 1970), Schlumberger soundings were used to map geothermal areas. In the U.S., reconnaissance resistivity measurements were made in the Salton Trough, Imperial Valley, California, by Meidav (1970) and by McEuen (1970).

Geothermal systems, according to White et al (1971), are of two types: hot-water systems and (of less common occurrence) vapor-dominated systems. The Geysers, California, Larderello, Italy, and the Mud Volcano area, Yellowstone National Park, are examples of vapor-dominated systems. Geochemically, water samples from

† Publication authorized by the Director, U.S. Geological Survey. Presented at the Symposium on Electrical Properties of Rocks, Salt Lake City, Utah, March 16, 1972. Manuscript received by the Editor June 6, 1973; revised manuscript received July 24, 1973.

* U.S. Geological Survey, Denver, Colo. 80225.

‡ U.S. Geological Survey, Menlo Park, Calif. 94025.

© 1973 Society of Exploration Geophysicists. All rights reserved.

spring
domain
concentrations
the s
bonat
sulfat
cally
phuri
sedia
have
water
centr
subst
duce
In
Geol
Yell
pulk
lent
crup

springs and drill holes in the vicinity of vapor-dominated systems are characterized by high concentrations of sulfate anions and low concentrations of chlorides (<20 ppm). Less commonly the spring waters may be rich in sodium bicarbonate instead of sulfate. The pH values of the sulfate-rich spring waters are also characteristically low (2 to 3) because of the formation of sulphuric acid from oxidation of rising H_2S gas. The sodium bicarbonate waters discharge feebly and have neutral pH values. In contrast, most hot-water systems are characterized by high concentrations of chlorides, and those systems with subsurface temperatures of $180^\circ C$ or higher produce hot springs that deposit sinter.

In May 1968, hole Y-11 was drilled by the U.S. Geological Survey in the Mud Volcano area, Yellowstone National Park. After the core was pulled from depths of both 307 and 347 ft, a violent eruption of water occurred, followed by an eruption that consisted almost entirely of steam.

White et al (1971) estimated that in these eruptions steam was associated with less than 10 percent liquid water by weight. For a hot water system to yield a comparable ratio of vapor to liquid, the permeability of the rocks must be low; but in Y-11, high rock permeabilities were evidenced by the large losses in circulation at all depths below 122 ft. Therefore, it must be the deficiency in liquid water, rather than the low permeability of rocks, that caused the steam to dominate the eruptions. Furthermore, according to White et al (1971), all the geochemical manifestations of vapor-dominated systems are exhibited in the Mud Volcano area.

Subsequent to the drilling of Y-11, the USGS made VES (vertical electrical sounding), resistivity horizontal profiles, SP (self-potential), and IP (induced-polarization) measurements in the Mud Volcano area to evaluate the geoelectrical properties of a section containing a vapor-dominated geothermal system.

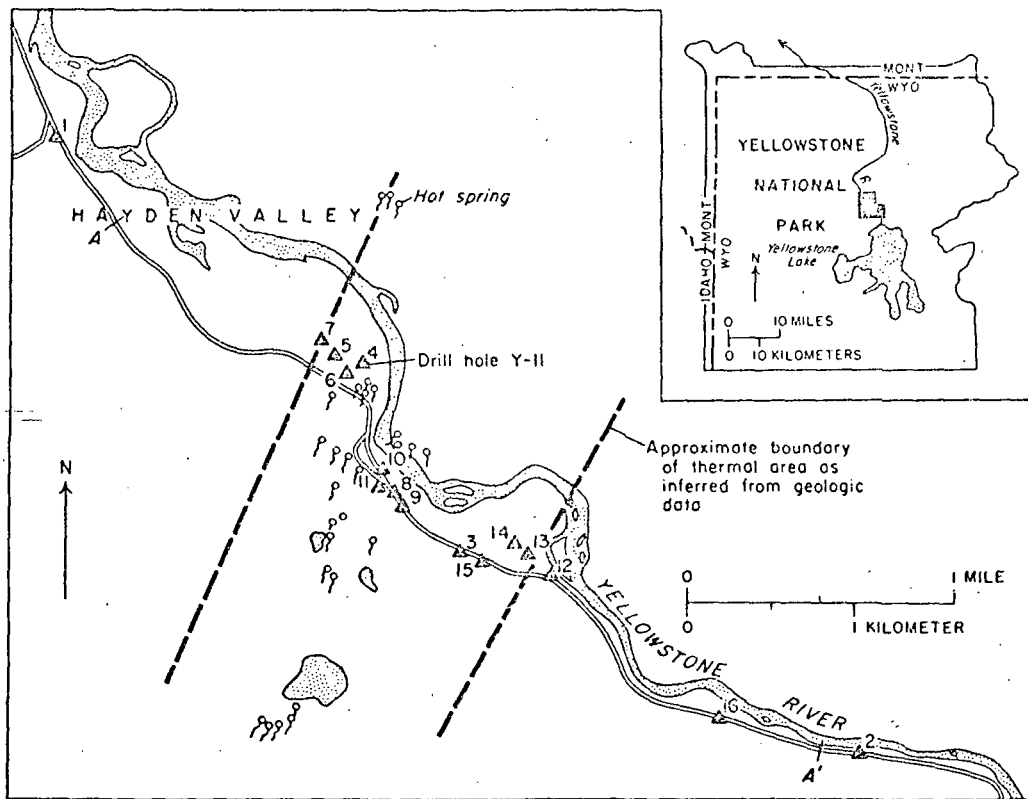


FIG. 1. Index map showing locations of VES stations (numbered triangles) and drill hole Y-11 in the Mud Volcano thermal area. Resistivity, SP, and IP profiles were measured along the road from A to A'.

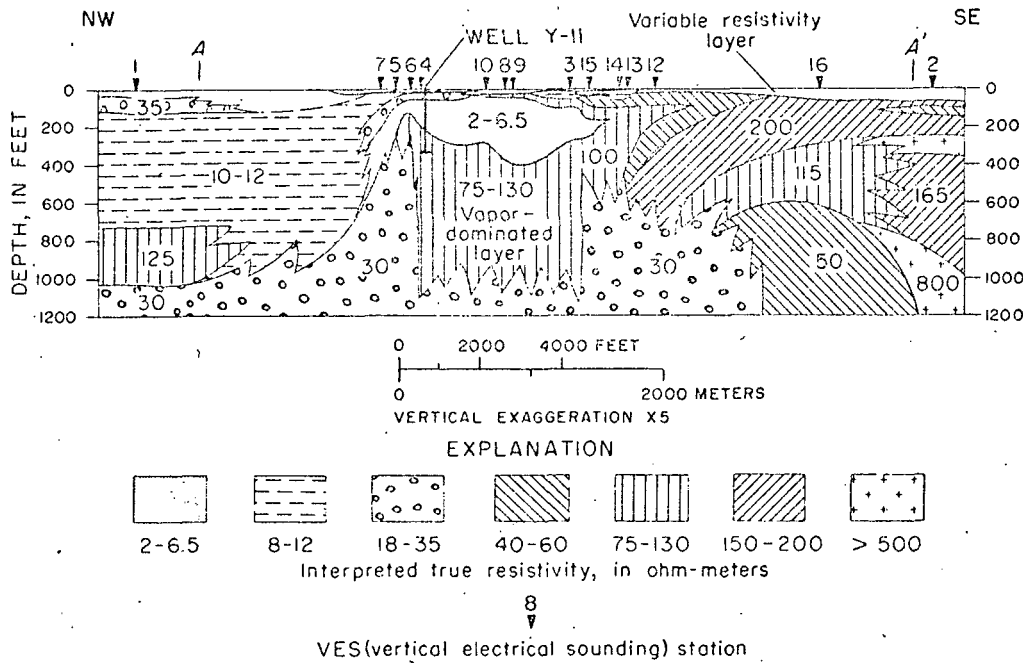


FIG. 2. Geoelectric section of the Mud Volcano area, Yellowstone National Park.

GENERAL SETTING

The Mud Volcano area (Figure 1) lies along the Yellowstone River approximately 5 miles north of Yellowstone Lake. Most of the area is covered by glacial silt, sand, and gravel which are underlain by rhyolitic ash-flow tuff; the area contains numerous mud pots and acid-sulfate springs. Some nearly neutral bicarbonate-sulfate springs occur along the river, but there are no chloride-rich springs in the area.

The location of the 16 VES stations, the test well Y-11, and the resistivity, SP, and IP profiles (which were made along the road from A to A') are shown in Figure 1. The approximate boundaries of the geothermal field, as inferred from geologic data are also shown.

THE GEOELECTRIC SECTION

Figure 2 shows the geoelectric section obtained from the interpretation of the VES curves. In the middle of the section, beneath VES 7 to VES 12, there are basically four electrical units. The first unit is composed of several near-surface layers, some of which are of small lateral extent (about 1,000 ft or less) and of variable resistivities. The second electrical unit is a fairly uniform single layer of remarkably low resistivity of about 2-6.5

ohm-m. It occurs at an average depth of about 50 ft and extends to an average depth of about 250 ft. This low-resistivity layer is interpreted as a layer where steam condenses into hot water, and where pyrite and clay minerals (kaolinite and montmorillonite) are present. The third electrical unit is a high-resistivity layer of about 75-130 ohm-m. Where this layer underlies the 2-6.5-ohm-m layer, it is interpreted as a zone where "dry steam," rather than liquid water, dominates the larger pores and open fractures in the rocks. The maximum depth to the bottom of this layer is unknown, but the minimum depth is about 1000 ft, and its lateral extent is approximately 1 mile. On both the northwest and southeast boundaries of this layer is the fourth geoelectric unit, a layer which is characterized by a resistivity of about 30 ohm-m and which is interpreted as a layer of hot water in low-porosity rocks.

At the northwest end of the section, beneath VES 1, there is a thick (about 600 ft) low-resistivity (10-12 ohm-m) layer which represents lacustrine deposits in Hayden Valley. In the southeastern part of the section, however, beneath VES 16 and VES 2, the layer resistivities generally are high (40-800 ohm-m) to depths of at least about 600 ft, thus reducing the probab-

ity for the p comparable

IN-
The 16 v
using the
electrode
3000 ft. I
made by c
cubms of t
1966; Rijk
grams (Zoh
method for
curves (Zo
geologically
tion as we
observed a

The curv
where it is
one calcul
based on :
other calc
obtained b
interpretati
cate the

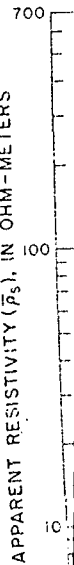


FIG. 3
subsequ
preted t

ity for the presence of thermal activity at depths comparable to those at the middle of the section.

INTERPRETATION OF VES CURVES

The 16 vertical electrical soundings were made using the Schlumberger array with maximum electrode spacings (AB/2) ranging from 500 to 3000 ft. Interpretation of the VES curves was made by curve-matching procedures in which albums of theoretical curves (Orellana and Mooney, 1966; Rijkwaterstaat, 1969), auxiliary point diagrams (Zohdy, 1965), Dar Zarrouk curves, and a method for the automatic interpretation of VES curves (Zohdy, 1972) were all used to reach a geologically and geoelectrically acceptable solution as well as to achieve excellent fits between observed and calculated VES curves.

The curve of VES 1 is shown in Figures 3 and 4, where it is matched with two theoretical curves, one calculated for a six-layer model (Figure 3), based on auxiliary point interpretation, and the other calculated for a 19-layer model that was obtained by the computer using the automatic interpretation program. The interpretations indicate the presence of either a sequence of low-

resistivity layers (5-23 ohm-m) that extends from a depth of about 100 ft to a depth of about 1000 ft, or a single low-resistivity layer (11-12 ohm-m) that extends from a depth of about 100 ft to a depth of about 700 ft. This low-resistivity layer is probably composed of clayey and silty lake deposits and is not necessarily related to the geothermal system. It is underlain by one layer of 125 ohm-m or by two layers of 50 and 125 ohm-m, respectively. These layers are underlain by a thick layer of low resistivity (≤ 35 ohm-m). Because of the lack of geologic information and other VES data in the immediate vicinity of this sounding, it is difficult to decide which interpretation is more accurate. The two interpretations are presented here to illustrate the problems of equivalence between multilayer sections in the interpretation of a single VES curve.

Figure 5 shows the curve of VES 7 and its interpretation in terms of a five-layer section. The third, fourth, and fifth layers are not clearly manifested on the VES curve, but correlation with the curves of VES 5 and VES 6, which are shown in Figure 6, clearly indicates that the small maximum and minimum on the curve of VES 7 (be-

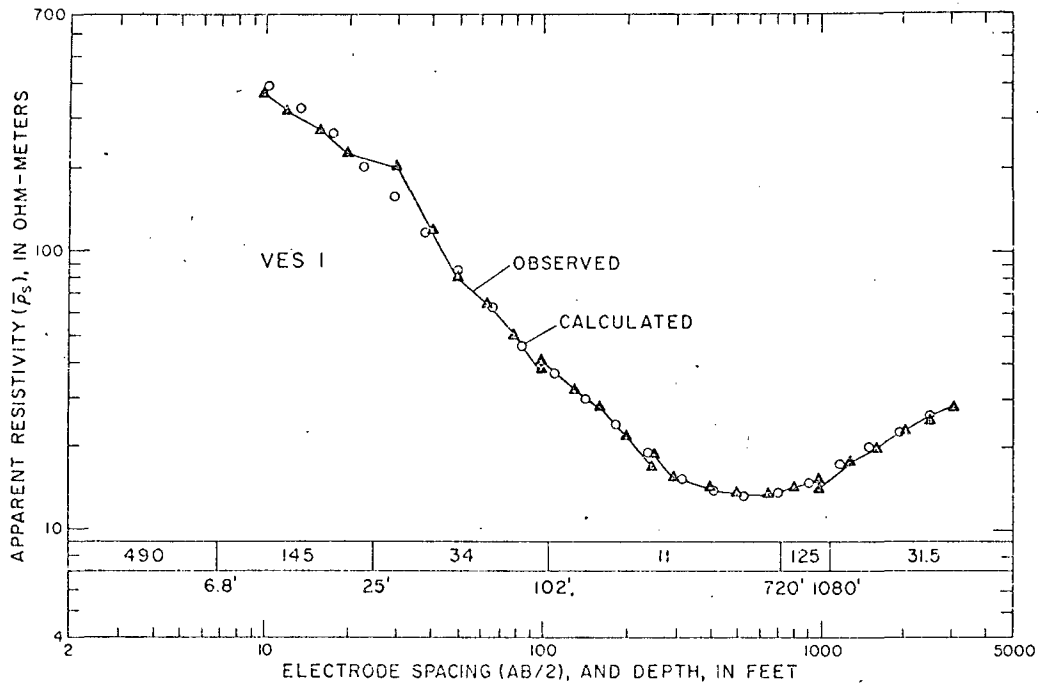


FIG. 3. Six-layer interpretation of VES 1 curve. Interpretation initially made with auxiliary point method and subsequently verified by computer calculation of interpreted model. Numbers in and below bar designate interpreted true resistivities in ohm-meters and interpreted depths in feet, respectively.

SE
12
0
200
400
600
800
1000
1200

of about 50
about 250
reted as a
water, and
finite and
l electrical
ut 75-130
-6.5-ohm-
here "dry
inates the
ocks. The
s layer is
out 1000
ly 1 mile.
oundaries
t, a layer
of about
layer of

beneath
ft) low-
presents
In the
ver, be-
stivities
pths of
robabil-

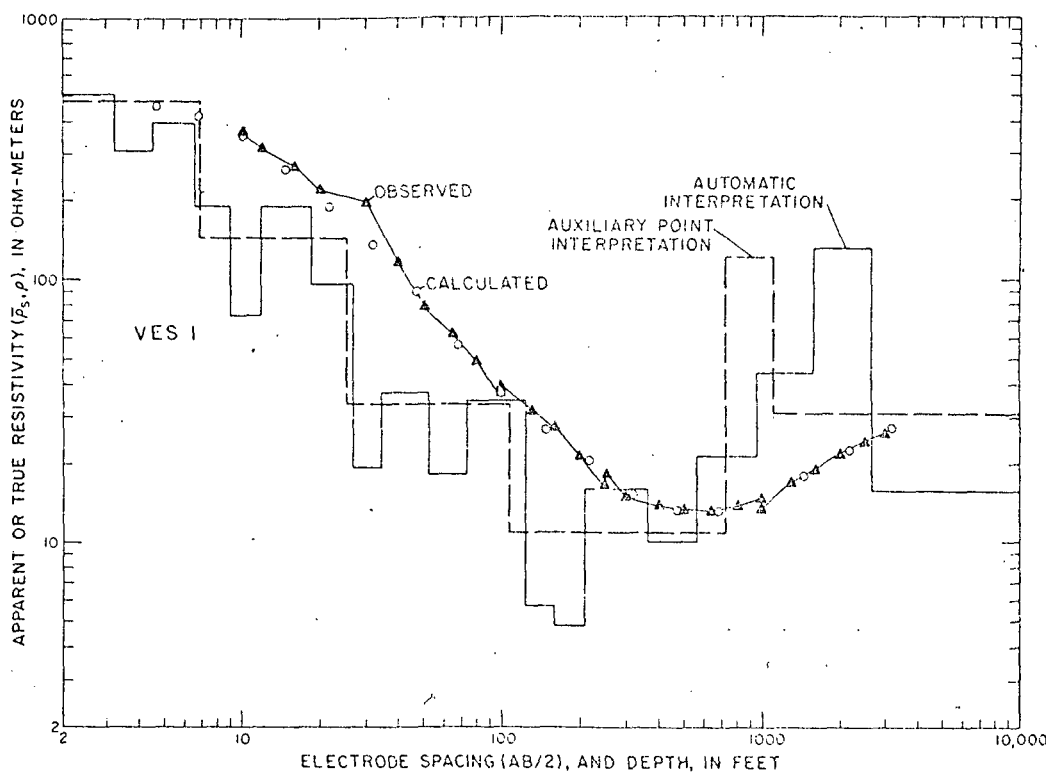


FIG. 4. Equivalence between 19-layer automatic interpretation and six-layer auxiliary point interpretation of VES 1 curve.

tween $AB/2=100$ and 1000 ft) are meaningful. They express the presence of the same layers that are represented by the well-developed maxima and minima on the curves of VES 5 and VES 6. The value of the apparent resistivity on the minimum of VES 6 is about 6.2 ohm-m and this is the first concrete evidence obtained on the northwest side of the section of the presence of a layer that must have a true resistivity of less than 6 ohm-m. For VES 6 the true resistivity of that layer is interpreted to be about 2 ohm-m, whereas for VES 5 and VES 7 it is interpreted to be about 4 and 4.5 ohm-m, respectively. The rising terminal branch on VES 7 curve is not well developed, but on the VES 5 curve the well-developed terminal branch indicates that the bottommost layer must have a resistivity of about 30 ohm-m. The curvature of the terminal branch of VES 6 curve is fitted best with a theoretical curve for a section in which a layer of about 75 ohm-m (or more) must exist between the very low (2 ohm-m) resistivity layer and the bottommost layer of about 30 ohm-m.

This 75-ohm-m layer is interpreted to represent the northwest edge of the vapor-dominated layer. The center of VES 4 was located about 100 ft north of well Y-11. The observed curve and its interpretation are shown in Figure 7 together with the geologic log of Y-11. The curve was interpreted in terms of a five-layer geoelectric section, the first layer of which has a resistivity of about 1700 ohm-m and a thickness of about 7 ft. The first layer corresponds to the layer of dry river gravel which lies within 6 inches above the water table. The second and third layers have resistivities of about 170 and 28 ohm-m, respectively, and extend to a depth of about 60 ft. These two layers correlate well with a layer of conglomerate composed of white pumice and black obsidian underlain by a layer of sandstone of the same composition. The depth to the bottom of the sandstone layer is about 65 ft which is in good agreement with the interpreted depth of about 60 ft. The fourth layer, on the interpreted geoelectric section beneath VES 4, has a low resistivity of

about 6.3 ohm-m at 195 ft where it is a layer of about 120 corresponding geologic well is composed and it extends to the top. Mineralogical analysis of Y-11 (unpublished by L. J. P. Muller) indicates that pyrite and other minerals are present to the bottom of the section. It is assumed that these minerals continue to exist to the top of the section at which these changes occur. The excellent agreement between the observed and interpreted curves from 195 ft to the high

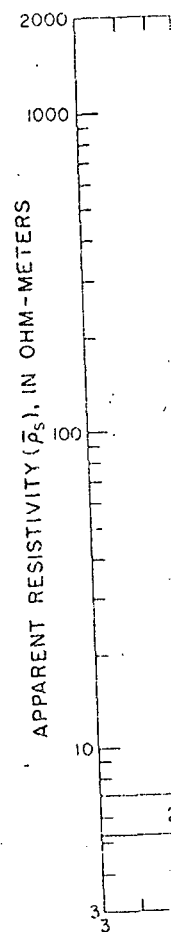


FIG. 5. Interpretation of VES 4 curve.

about 6.3 ohm-m and extends to a depth of about 195 ft where it is underlain by a high-resistivity layer of about 120 ohm-m of large thickness. The corresponding geologic formation encountered in the well is composed of rhyolitic ash-flow tuff, and it extends to the bottom of the well at 347 ft. Mineralogical analysis of core samples from well Y-11 (unpublished data of K. E. Bargar and L. J. P. Muffler) indicates that clay minerals and pyrite are present from a depth of about 50 ft to the bottom of the well. Some chalcedony deposits occur at a depth of about 200 ft and continue to exist to the bottom of the well. The depth at which these chalcedony deposits occur is in excellent agreement with the interpreted depth of 195 ft to the high-resistivity layer of 120 ohm-m.

Therefore, it is tempting to conclude that it is the chalcedony deposits that have caused the rise in resistivity. However, because the porosity of the ash-flow tuff (according to drilling data) did not change significantly at the depth of 200 ft, and because the conductive clay minerals and pyrite continue to exist in essentially the same amounts to the bottom of the well, we interpret the decrease in resistivity to about 6.3 ohm-m and its subsequent increase to about 120 ohm-m (on the curve of VES 4, as well as on the curves of VES 8, VES 9, and VES 10) to be governed mostly by the abundance of hot liquid water in the 2-6.5-ohm-m layer and by the dominance of steam in the 75-130-ohm-m layer. The drilling results of well Y-11 indicate that steam dominates

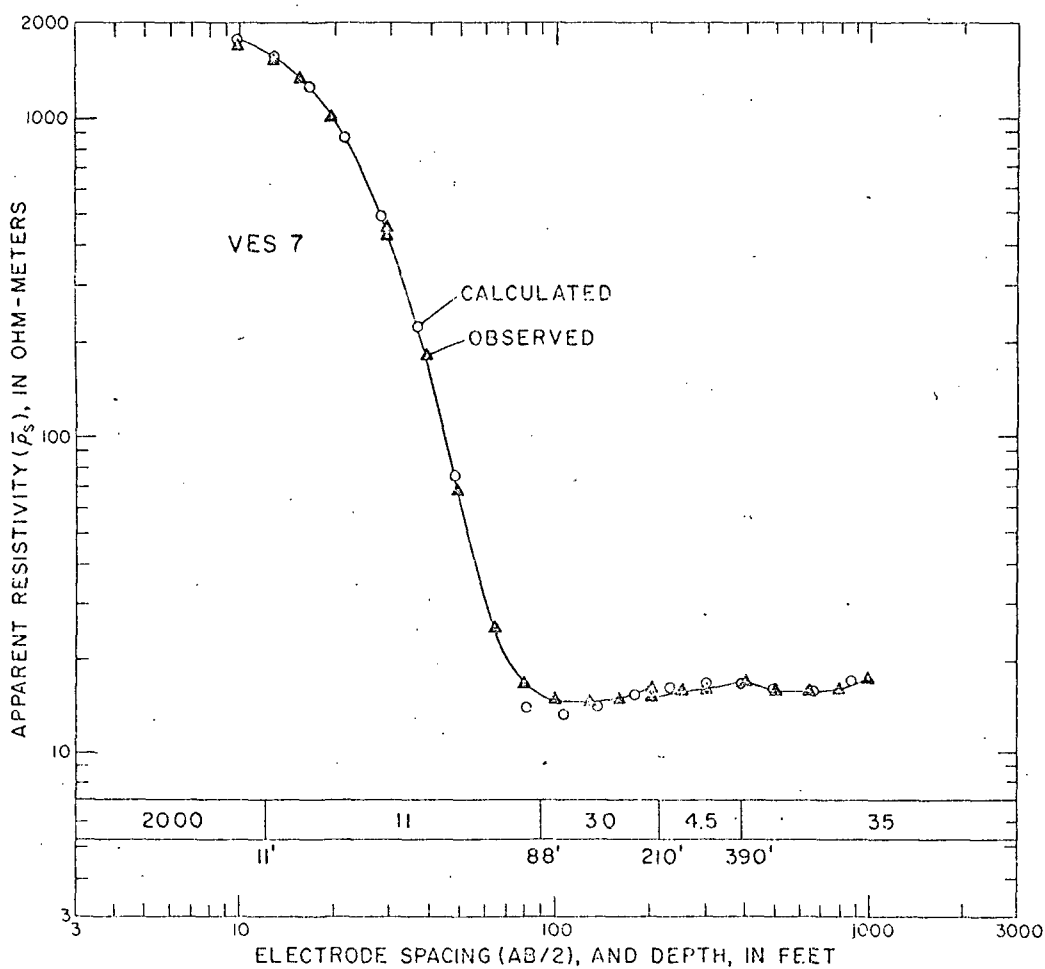


Fig. 5. Interpretation of VES 7 curve in terms of a five-layer model. Numbers in and below bar designate interpreted true resistivities, in ohm-meters, and interpreted depths, in feet, respectively.

o represent
nated layer.
bout 100 ft
rve and its
rve and its
together with
was inter-
tric section,
ty of about
t 7 ft. The
of dry river
e the water
ve resistiv-
spectively,
These two
nglomerate
bsidian un-
same com-
the sand-
ood agree-
out 60 ft.
geoelectric
istivity of

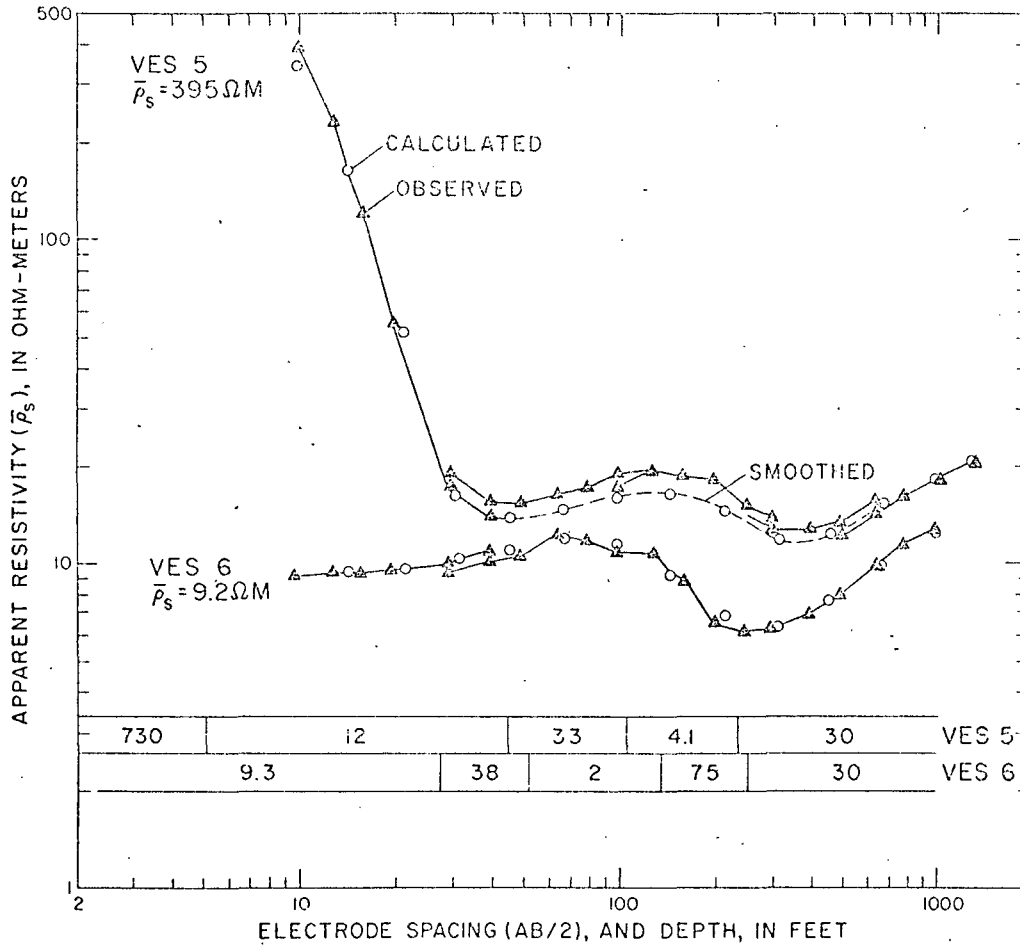


FIG. 6. Interpretation of VES 5 and VES 6 curves. Numbers in bars designate interpreted true resistivities, in ohm-meters.

the system from a depth of at least 307 ft to the bottom of the hole (White et al, 1971), but according to the interpretation of VES 4 the steam may dominate the system to a depth as shallow as 200 ft.

Figure 8 shows the curve of VES 10 which was obtained near the middle of the geothermal field (see Figure 2). The magnitude and the direction of the discontinuities on the observed curve (which were observed upon the expansion of the potential electrodes) are not in agreement with those prescribed for horizontal layering (Deppermann, 1954; Zohdy, 1969). Following a procedure which has been found to be most satisfactory in practice, the various segments on the VES curve were shifted to conform to the position of the last

segment on the curve. The shifted segments then are smoothed, to remove cusps which are caused by the crossing of lateral heterogeneities by the current electrodes, and the smoothed curve is fitted with a theoretical one as shown in Figure 8 for VES 10. Similar smoothing was made for VES 5 and for other curves. This smoothing procedure results in modifying the interpreted true resistivities of the shallower layers in the section, which in general are quite variable, but it does not alter their interpreted thicknesses nor does it create undulations on the smoothed curve (which may be interpreted as layers) that were not actually manifested on the observed curve. These undulations often are created when the smoothing is made by drawing a curve that passes between

significant
interpret
beneath t
The cu
their inte
illustrate
conductiv
(90-100
curves. T
and abo
respective
the resist
the geoth
Figure
and VES

1000
100
10
APPARENT RESISTIVITY ($\bar{\rho}_s$), IN OHM-METERS

FIG.
designa
posed o

significantly displaced segments. For VES 10 the interpreted depth to the vapor-dominated layer, beneath the low-resistivity layer, is about 300 ft.

The curves of VES 8, VES 9, and VES 3 and their interpretations are shown in Figure 9 to illustrate the continuity of the detection of the conductive (2.4-5.2 ohm-m) and the resistive (90-100 ohm-m) bottom layers on the VES curves. The interpreted depths of about 340 ft and about 400 ft, beneath VES 9 and VES 8, respectively, are the largest interpreted depths to the resistive bottom layer over the middle part of the geothermal section.

Figure 10 shows the curves of VES 15, VES 14, and VES 13 and their interpretations. Using the

automatic interpretation computer program, the curve of VES 15 is the only curve in this group of VES curves that can be interpreted so that a layer with a low resistivity of about 5 ohm-m can be included legitimately in the section. Thus VES 15 reflects the nearness of the southeastern boundary of the geothermal system. On all three VES curves there is a strong indication that the bottommost layer, which lies at an average depth of about 550 ft, has a resistivity of about 30 ohm-m. This layer bounds the geothermal system on the southeast as it did on the northwest.

The curves of VES 12, VES 16, and VES 2 are shown in Figure 11 together with their interpretation as obtained for the reduced model of the

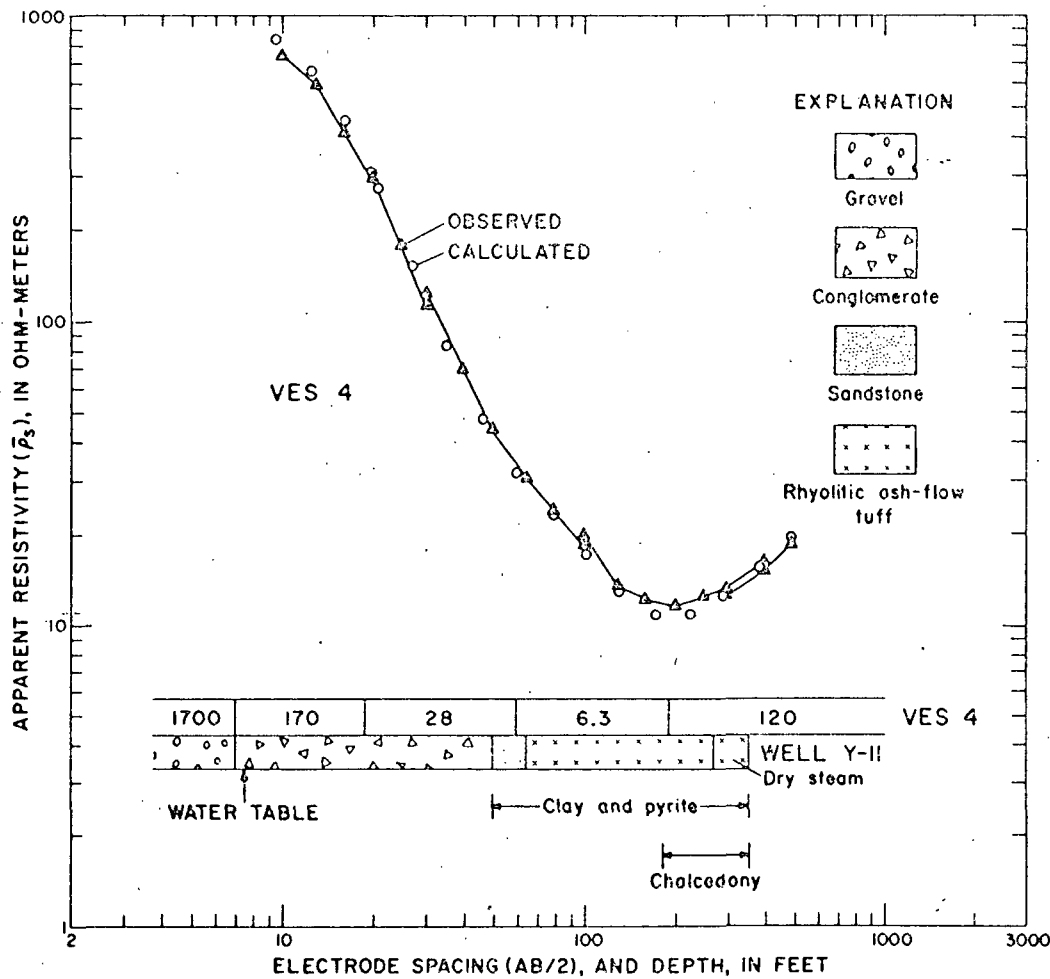


FIG. 7. Comparison between interpretation of VES 4 curve and geologic data of well Y-11. Numbers in bar designate interpreted true resistivities, in ohm-meters. Conglomerate and sandstone layers in well Y-11 are composed of white pumice and black obsidian.

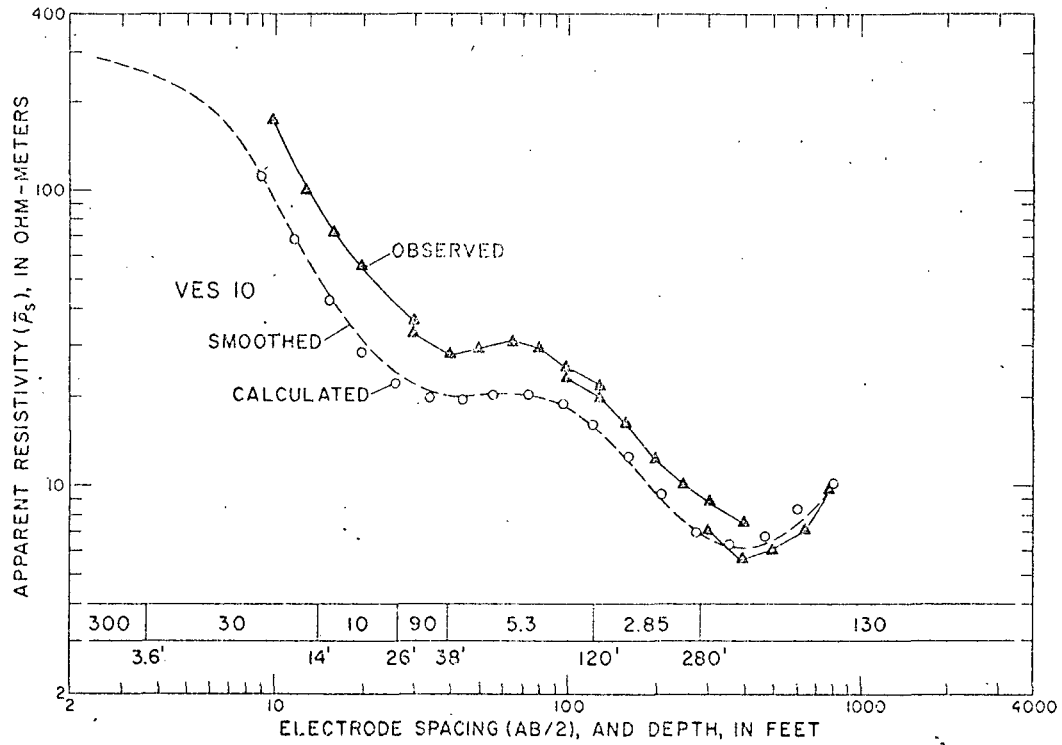


Fig. 8. Interpretation of VES 10 curve in terms of a seven-layer section. Numbers in and below bar designate interpreted true resistivities, in ohm-meters, and interpreted depths, in feet, respectively.

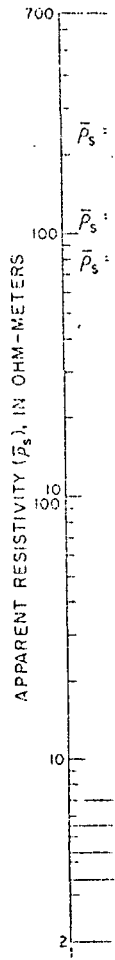
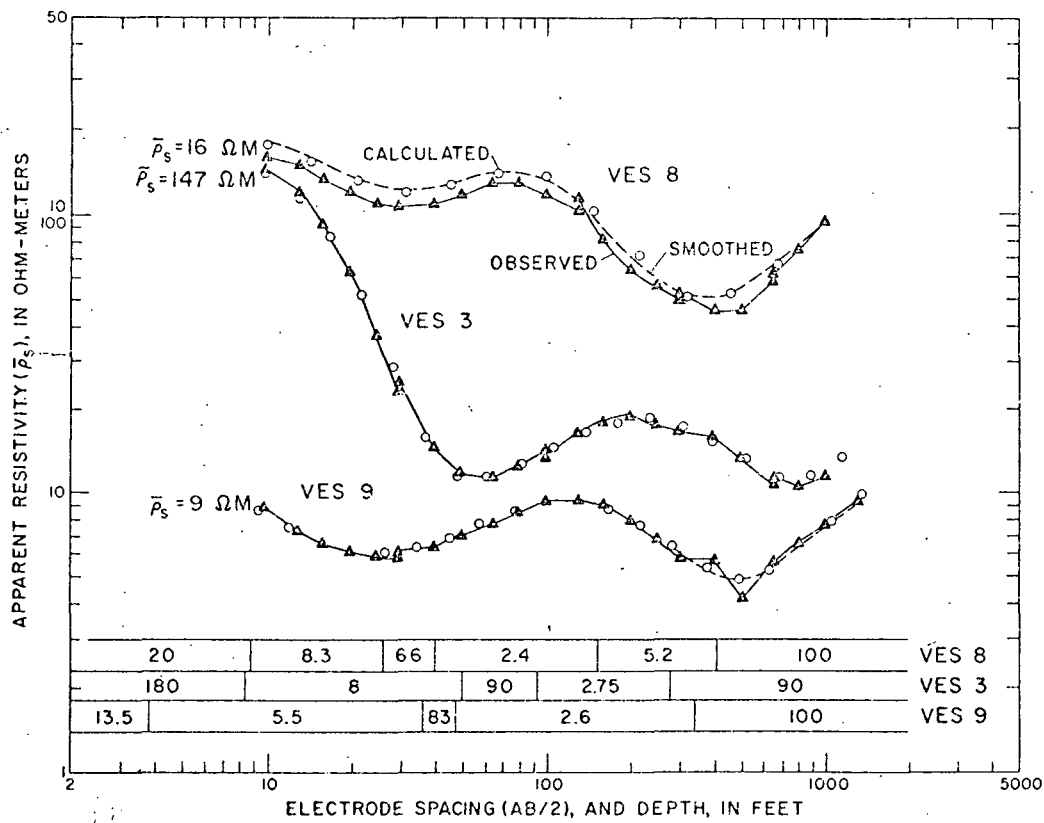


Fig. 10

automatic
30-ohm-m
VES 2 curv
greater th
resistivity
bottom lay
section, wi
thermal ac
rhyolitic a



Fi

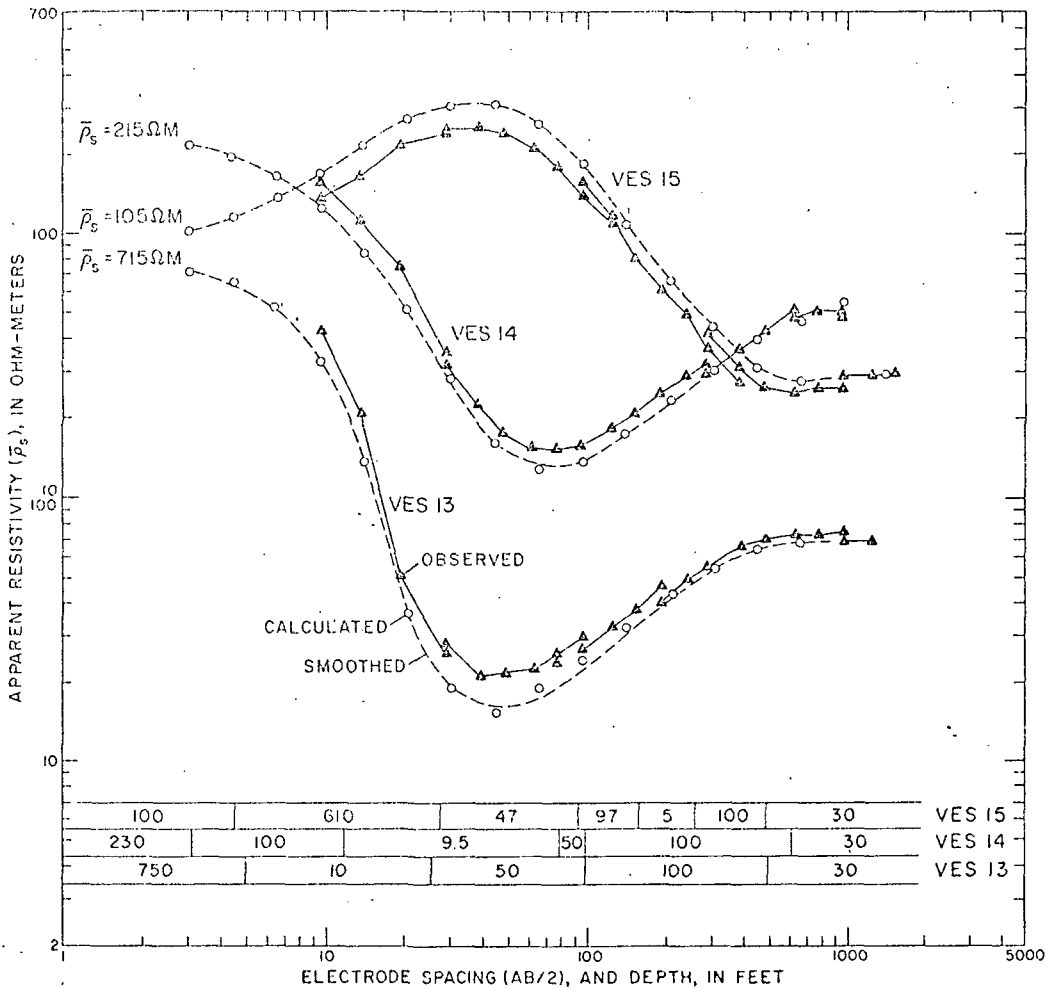


FIG. 10. Curves of VES 13, VES 14, and VES 15 obtained near the southeastern boundary of the geothermal field. Numbers in bars designate interpreted true resistivities, in ohm-meters.

automatic interpretation computer program. The 30-ohm-m bottom layer is not detected on the VES 2 curve, and if it exists it must be at a depth greater than about 1500 ft. Instead, high-resistivity layers of 800 and 300 ohm-m form the bottom layers in the automatically interpreted section, which indicates that there is no shallow thermal activity beneath VES 2 and that the rhyolitic ash flow tuff believed to form the bed-

rock in the area is probably replaced by rhyolite rocks of intermediate to high resistivities.

From the preceding description and documentation of the VES curves, and from the hydrogeologic information obtained from well Y-11, we conclude that the shallow vapor-dominated reservoir in the Mud Volcano area has a high resistivity of about 75-130 ohm-m and that it is characterized by the presence of a low-resistivity layer



FIG. 9. Curves of VES 8, VES 3, and VES 9 obtained over the center of the geothermal field. Numbers in bars designate interpreted true resistivities, in ohm-meters.

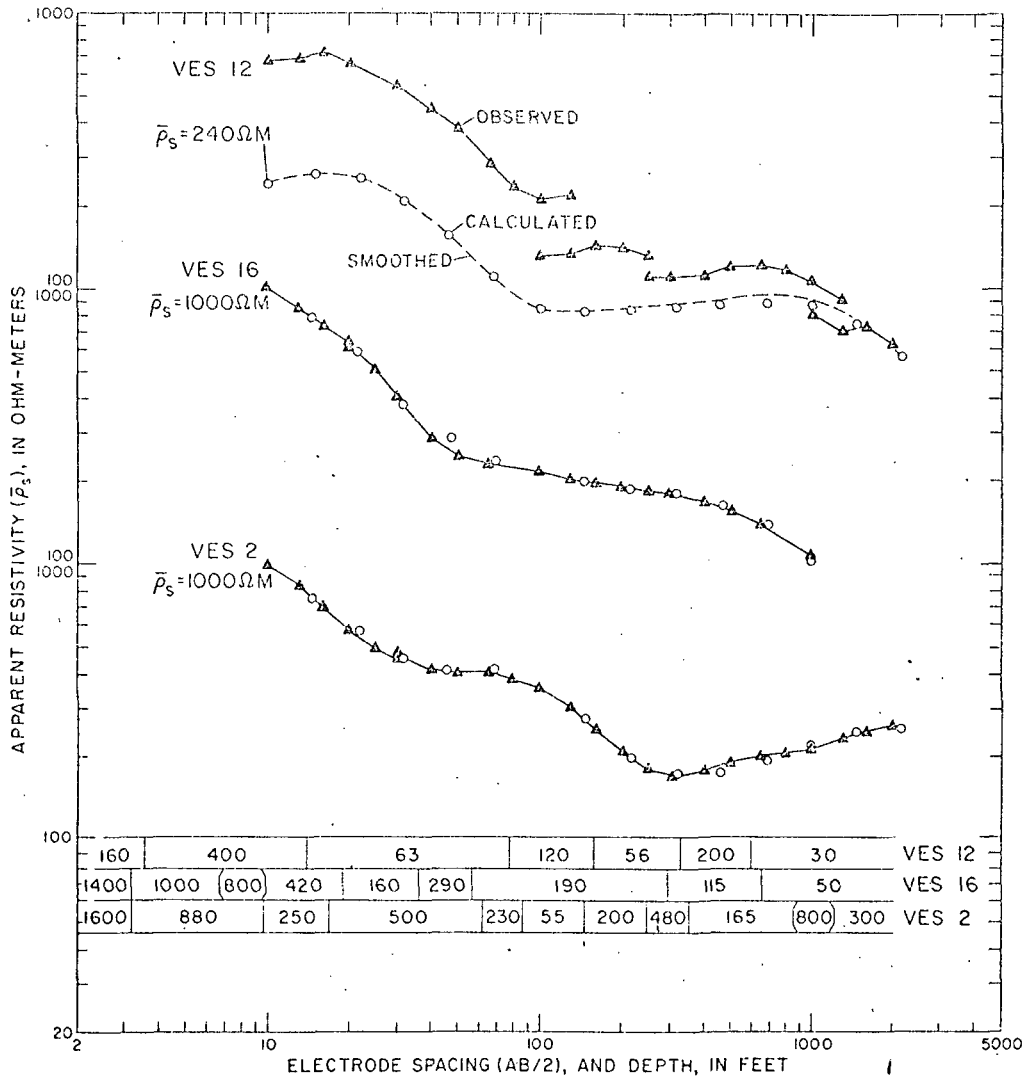


Fig. 11. Curves of VES 2, VES 12, and VES 16 obtained south of the southeastern boundary of the geothermal field. Numbers in bars designate interpreted true resistivities, in ohm-meters. Layering is based on automatically calculated models.

(2–6.5 ohm-m) above it, and a moderately resistive layer (~30 ohm-m) around it. It is interesting to note the similarity between this interpreted geoelectric section and the general model of a vapor-dominated system presented by White et al (1971). A simplified version of White's model is presented in Figure 12.

RESISTIVITY, SP, AND IP HORIZONTAL PROFILES

In 1971, two years after the VES data were obtained, horizontal profiles of resistivity, SP, and

IP were made along the road from point A to A' (see Figure 1). The resistivity and the IP were measured at two electrode spacings of a three-electrode (AMN) array. The electrode spacings (AO) between the current electrode (A) and the center (O) of the potential electrodes (M and N) was 600 ft for one profile and 1000 ft for the other. The distance (MN) between the potential electrodes for both profiles was 400 ft. The SP measurements were made prior to the 600-ft resistivity measurement. The IP measurements were made

in the fro
the perce
calculated

where $\bar{\rho}_{0.1}$
measured
The lo
zontal pro
fer of the
the 2- to
segment
sistivity v
1000 ft a
smaller At
parent res
roborates
the prese
(vapor-do
resistivity
thermal fi
low becau
lacustrine
southeast

FIG. 12. A
rich in sulfu
from conden
conductive
section). (5)
heat flow al-

in the frequency domain at 0.1 and 1.0 hz, and the percent frequency effect (PFE) values were calculated using the formula

$$\text{PFE} = \frac{(\bar{\rho}_{0.1} - \bar{\rho}_{1.0})}{\sqrt{\bar{\rho}_{0.1} \cdot \bar{\rho}_{1.0}}} \cdot 100,$$

where $\bar{\rho}_{0.1}$ and $\bar{\rho}_{1.0}$ are the apparent resistivities measured at 0.1 and 1.0 hz, respectively.

The lowest apparent resistivities of the horizontal profiling data were measured over the center of the geothermal field, where the thickness of the 2- to 6.5-ohm-m layer is largest. Along this segment of the profiling data, the apparent resistivity values measured with the AO spacing of 1000 ft are larger than those measured with the smaller AO spacing of 600 ft. This increase in apparent resistivity at larger electrode spacings corroborates the VES data interpretation in terms of the presence of a deep high-resistivity layer (vapor-dominated layer) beneath a shallower low-resistivity cover. To the northwest of the geothermal field, the apparent resistivity is generally low because of the presence of a thick section of lacustrine deposits in Hayden Valley. To the southeast of the geothermal field, a marked in-

crease in apparent resistivity is observed on the resistivity profiles and a broad resistivity high is formed which extends to the southeastern boundary of the section. Within this broad resistivity high, there are three zones of lower resistivity which can be interpreted as due to alteration zones resulting from the upward movement of thermal waters at a time when near-surface geothermal activity may have existed to the southeast of the presently active zone.

SP measurements, referenced to the first station on the northwest end of the traverse, produced the broad, positive anomaly shown in Figure 13. The amplitude of the anomaly is small and may be attributed to a variety of electric potential producing effects. However, an experiment by Poldini (1938 and 1939) proved that upward-migrating water, confined within a column, produced a positive potential when a measurement was made near the top of the column with respect to an arbitrary distant point. The potential attributed to solutions moving through porous media has been observed by several investigators and is known by various names such as electro-filtration, streaming, flow, and electrokinetic potentials (Sato and Mooney, 1960). This type of

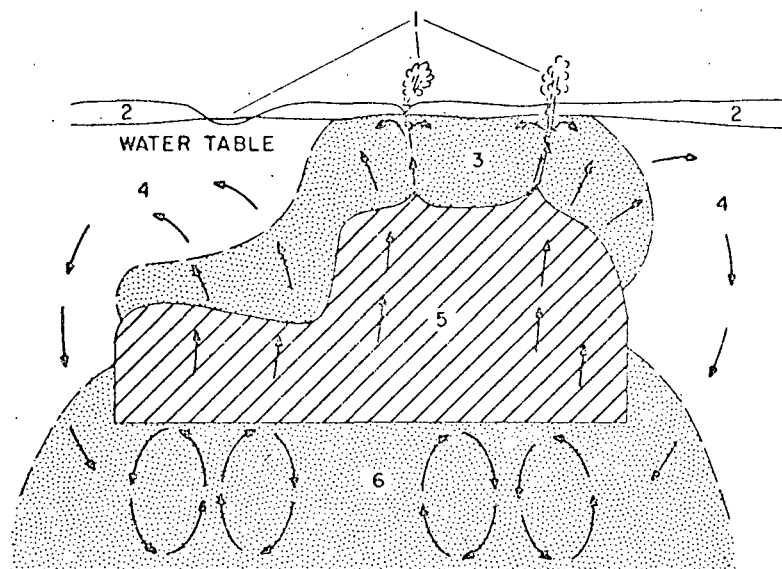


FIG. 12. Model of a vapor-dominated reservoir surrounded by water-saturated ground: (1) Springs and fumaroles rich in sulfates. (2) Zone between ground surface and water table. (3) Zone where liquid water, largely derived from condensing steam, is dominant (2-6.5-ohm-m layer in geoelectric section). (4) Zone where convective and/or conductive heat flow exists, with heat supplied from condensing steam in zone 3 (30-ohm-m layer in geoelectric section). (5) Vapor-dominated reservoir (75-130-ohm-m layer in geoelectric section). (6) Deep zone of convective heat flow above which is a boiling-water table (simplified from White et al, 1971).

geothermal
electrically

A to A'
IP were
a three-
spacings
and the
(and N)
re other.
ial elec-
SP mea-
sistivity
re made

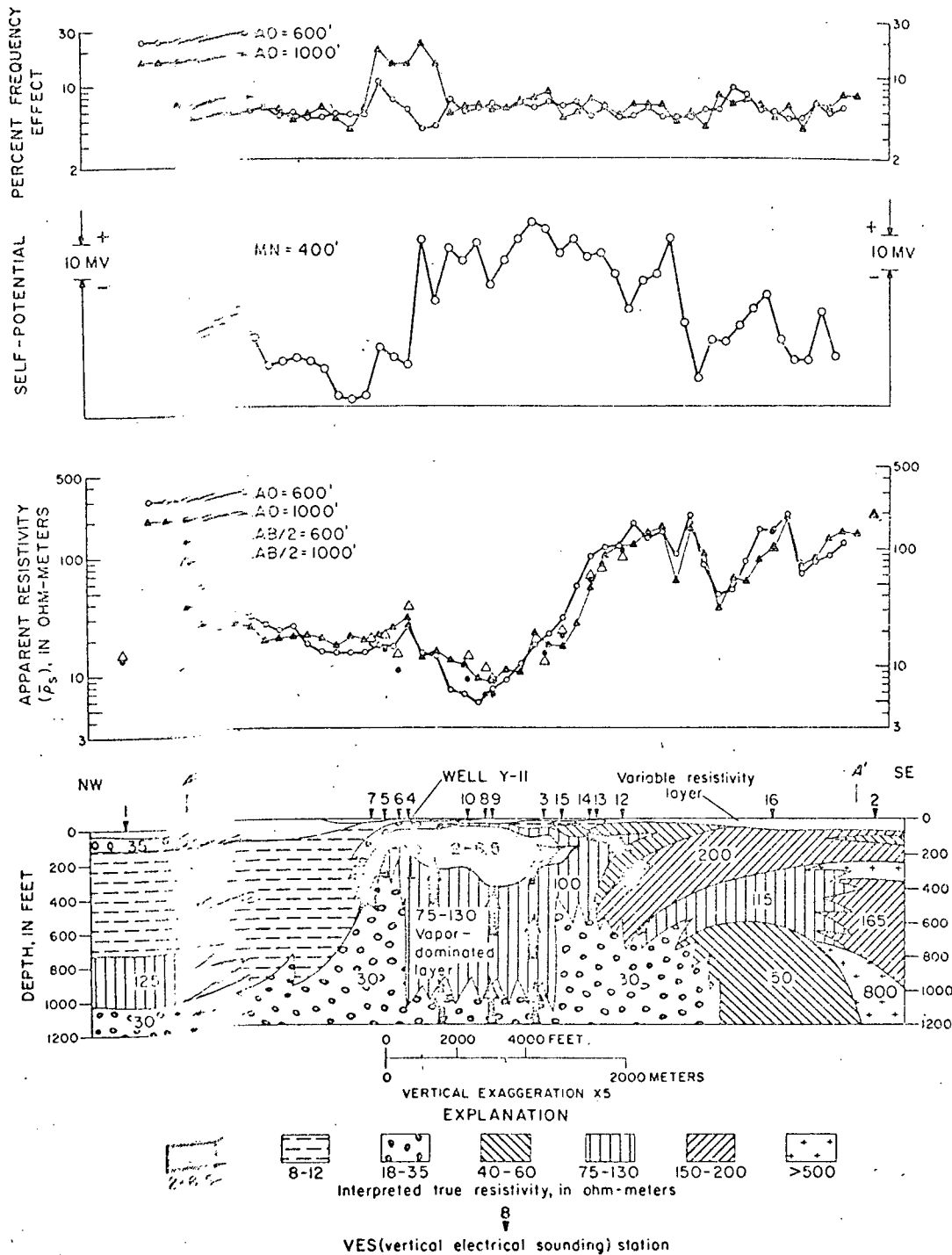


Fig. 13. Horizontal geophysical data obtained with resistivity, SP, and IP (percent frequency effect). Arrows designate movement of steam and water. AO, distance from current electrode, A, to center of potential electrodes, O. MN, distance between potential electrodes. AB/2, Schlumberger-electrode spacing of VES curves.

potential is cap pore waters ow of anions by the concentrate the in a positive at water.

On the basis to assume that portion direct from upward-n. vvection current energy source. The northwest edge result of down cycling proces thermal water. White et al, 19

The reason anomaly beyor geothermal field is not underst amounts of the the ground sur they reach the low apparent r. The downward observed low zones of low r

The two H arithmetic scale. The profiles a tively high H cent which is of clayey mat layers. Differ the amplitud ticularly in th of the inferre crease in the by an increas deposited by the minerals that pyrite e the bottom of AO = 1000 ft that seen on that the pyr depth at the sibly a simil the small H the vicinity

potential is caused by cation enrichment of the pore waters owing to the preferential adsorption of anions by the rock. The upward-moving waters concentrate the cations near the surface resulting in a positive anomaly over the zone of migrating water.

On the basis of Poldini's work, it is reasonable to assume that the broad SP anomaly, at least the portion directly over the thermal zone, arises from upward-moving waters set in motion by convection currents emanating from the thermal energy source. The low SP values bordering the northwest edge of the thermal area are possibly a result of downward-moving waters, part of the cycling process involved in the movement of thermal waters (compare Figures 12 and 7 of White et al, 1971).

The reason for the continuation of the SP anomaly beyond the southeast boundary of the geothermal field (as interpreted from VES data) is not understood. Possibly, however, significant amounts of the thermal waters upon approaching the ground surface move laterally, and not until they reach the more permeable altered zones of low apparent resistivity do they begin to descend. The downward-moving water would produce the observed low level of SP coincident with the zones of low resistivity.

The two IP profiles were plotted on semilogarithmic scale in the upper part of Figure 13. The profiles are similar, both indicating a relatively high IP background level of about 5 percent which is attributable to a wide distribution of clayey materials and pyrite in the near-surface layers. Differences between the profiles occur in the amplitude of the observed anomalies, particularly in the vicinity of the northwest boundary of the inferred vapor-dominated zone. The increase in the polarization effect is probably caused by an increased quantity of disseminated pyrite deposited by circulating thermal waters. Indeed, the mineralogical analysis of well Y-11 indicates that pyrite exists from a depth of about 50 ft to the bottom of the well at 347 ft. The fact that the AO = 1000 ft anomaly is significantly larger than that seen on the shorter spaced profile suggests that the pyrite and its distribution increases with depth at the boundary of the thermal zone. Possibly a similar pyrite enrichment exists beneath the small IP anomaly shown on both profiles in the vicinity of VES 16.

SUMMARY AND CONCLUSIONS

Vertical electrical soundings in the Mud Volcano area of Yellowstone National Park indicate that the vapor-dominated reservoir is characterized by high resistivities and that it occurs under a cover of very low resistivity. Because of this low-resistivity layer, reconnaissance surveys with horizontal profiling will delineate the thermally active zone by a low-resistivity anomaly. The boundaries of the geothermal field as defined by the quantitative interpretation of the VES curve is in excellent agreement with the approximate boundaries inferred from mapping the surface geology. Beneath VES 1 and VES 16, the geothermal conditions may exist at depths slightly greater than about 1000 ft, whereas beneath VES 2 the thermal activity, if it exists, must be at depths greater than 1500 ft.

The SP anomalies seem to be directly related and interpretable in terms of the thermal water circulation system, and although the SP anomaly observed in the Mud Volcano area is relatively small, its existence warrants the further study and measurement of SP in other geothermal areas.

The IP anomalies observed at the northwestern boundary and south of the southeastern boundary were interpreted in terms of pyrite concentrations deposited by sulfur-rich thermal waters at those locations where the thermal waters intermix with meteoric waters and begin a downward movement in the hydrological recycling process surrounding the geothermal cell.

REFERENCES

- Alfano, L., 1961. Geoelectrical explorations for natural steam near "Monte Amiata": *Quad. Geofisica Appl.*, v. 21, p. 3-17.
- Banwell, C. J., and MacDonald, W. J. P., 1965. Resistivity surveying in New Zealand thermal areas: Presented at 8th Commonwealth Mining and Metall. Cong., Australia and New Zealand, Paper 213, p. 1-7.
- Brusse, J. J., and Mathiez, J. P., 1956. Application of electrical prospecting methods to tectonics in the search for natural steam at Larderello, Italy, in *Geophysical case histories: Vol. II*, Paul L. Lyons, Editor, Tulsa, SEG, p. 623-630.
- Cheng, W. T., 1970. Geophysical exploration in the Tatun volcanic region, Taiwan: *Geothermics Spec. Issue 2*, v. 2, pt. 1, p. 262-274.
- Deppermann, K., 1954. Die Abhängigkeit des scheinbaren Widerstandes vom Sondenabstand bei der Vierpunkt-Methode: *Netherlands, Geophys. Prosp.*, v. 2, p. 262-273.
- Duprat, A., 1970. Contribution of geophysics to the study of the geothermal region of Denizli-Saraykoy, Turkey: *Geothermics Spec. Iss. 2*, v. 2, pt. 1, p. 275-286.
- Hatherton, T., MacDonald, W. J. P., and Thompson,

- G. F. K., 1966, Geophysical methods in geothermal prospecting in New Zealand: *Bull. Volcanol.*, v. 29, p. 485-498.
- McEuen, R. B., 1970, Delineation of geothermal deposits by means of long-spacing resistivity and airborne magnetics: *Geothermics Spec. Iss. 2*, v. 2, pt. 1, p. 295-302.
- Meidav, T., 1970, Application of electrical resistivity and gravimetry in deep geothermal exploration: *Geothermics Spec. Iss. 2*, v. 2, pt. 1, p. 303-310.
- Orellana, Ernesto, and Mooney, H. M., 1966, Master tables and curves for vertical electrical sounding over layered structures: Madrid, Interciencia.
- Poldini, E., 1938, Geophysical exploration by spontaneous polarization methods: *Mining Mag.*, London, v. 59, p. 278-282, 347-352.
- 1939, Geophysical exploration by spontaneous polarization methods: *Mining Mag.* London, v. 60, p. 22-27, 90-94.
- Rijkwaterstaat, 1969, Standard graphs for resistivity prospecting: EAEG, Netherlands.
- Risk, G. F., MacDonald, W. J. P., and Dawson, G. B., 1970, D.C. resistivity surveys of the Broadlands geothermal region, New Zealand: *Geothermics Spec. Iss. 2*, v. 2, pt. 1, p. 287-294.
- Sato, Motoaki, and Mooney, H. M., 1960, The electrochemical mechanism of sulfide self-potentials: *Geophysics*, v. 25, p. 226-249.
- White, D. E., Muffler, L. J. P., and Truesdell, A. H., 1971, Vapor-dominated hydrothermal systems compared with hot-water systems: *Econ. Geol.*, v. 66, p. 75-97.
- Zohdy, A. A. R., 1965, The auxiliary point method of electrical sounding interpretation and its relationship to the Dar Zarrouk parameters: *Geophysics*, v. 30, p. 644-660.
- 1969, The use of Schlumberger and equatorial soundings in groundwater investigations near El Paso, Texas: *Geophysics*, v. 34, p. 713-728.
- 1972, Automatic interpretation of resistivity sounding curves using modified Dar Zarrouk functions [abs.]: *Geophysics*, v. 38, p. 196-197.

QUANT

G. J. P.

Recent
electrom
more qu
The nec
tained in
tem and
ing comp
Both ap
former, t
with the

INPU
system) i
tem who
Barringer
most wid
surveys v
plained in

Brief desc

The pr
rent puls
in polarit
netic fiel
0.48, 0.7
transmitt
over a t
0.22 msec

The pr
erates in
superimp
torts it, b
as a deca
primary |

† Regista

† Manusc

* Now wit
Ontario, C

† Universi

© 1973 S

The charge-out number (Accession No.)
for this book is 34699;

Announced on
NTI- 16124

AREA
Wy
Park
Yellowstone
IR anon 5



NATIONAL AERONAUTICS AND SPACE ADMINISTRATION

REFERENCE COPY

EARTH RESOURCES AIRCRAFT PROGRAM

STATUS REVIEW

VOLUME I

GEOLOGY, GEOGRAPHY, AND SENSOR STUDIES

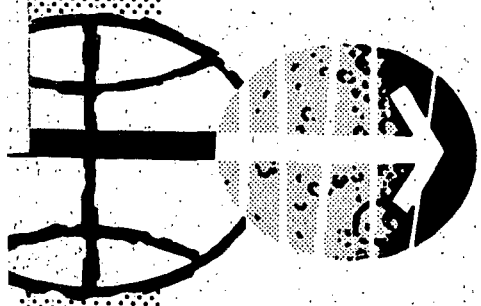
Presented at the

NASA Manned Spacecraft Center
Houston, Texas

September 16 to 18, 1968

UNIVERSITY OF UTAH
RESEARCH INSTITUTE
EARTH SCIENCE LAB.

MANNED SPACECRAFT CENTER
HOUSTON, TEXAS



NASA MSC TECHNICAL LIBRARY

GEOHERMAL INFRARED ANOMALIES OF LOW INTENSITY,
YELLOWSTONE NATIONAL PARK

By Donald E. White and Lee D. Miller
U.S. Geological Survey, Menlo Park, California,
and Department of Recreation and Watershed Resources,
Colorado State University, Fort Collins, Colorado

INTRODUCTION

Infrared remote sensing of hot springs and other high-temperature geothermal phenomena has been feasible for many years; its usefulness in searching for inconspicuous anomalies of low intensity has not been demonstrated in the past. Future search for sources of geothermal energy must aim at deep reservoirs of hot water and steam at temperatures generally above 200° C. Hot springs are associated with some of these reservoirs, but most hot springs are unreliable evidence for commercial reservoirs. The most significant evidence for a concealed geothermal reservoir would be temperature gradients and heat flows three to 10 times higher than the worldwide averages. "Normal" gradients average about 1° C/50 meters in depth, and "normal" conductive heat flow averages 1.5 $\mu\text{cal}/\text{cm}^2\text{sec}$. Solar energy is roughly 1000 times this value; therefore, the "noise" problem is severe.

OLD FAITHFUL TEST SITE

Infrared (IR) anomalies are actually differences in apparent surface temperature, which shows wide daily, seasonal, and microclimatic differences. Can IR anomalies also be calibrated in terms of heat flow, which is of more fundamental geothermal interest than temperature alone? A small area around Old Faithful was being used last year to test a new rapid method for mapping differences in heat flow, utilizing individual heavy snowfalls as calorimeters. These heat-flow data are also useful in attempting to calibrate IR data recently acquired and computer processed by the University of Michigan Infrared and Optical Sensor Laboratory for the U.S.G.S. Heat-flow contours of 1000 and 450 $\mu\text{cal}/\text{cm}^2\text{sec}$ were mapped in this test area.

The oral presentation included the following:

1. A vertical color photograph of the test area, showing locations of Old Faithful and other thermal anomalies to be discussed and the different surface materials of the area
2. A heat-flow map of the test area
3. Analog thermal IR, 8μ to 14μ , conventional unprocessed scanner imagery, taken at 2:00 a.m. and showing the anomalies; of these, Old Faithful being the only visible conspicuous one.
4. Analog computer processing of the original magnetic tape data, quantized between 0° and 20° C into eight levels, each with an interval of $2-1/2^{\circ}$ C
5. Apparent surface temperatures, contoured by intervals of 5° C; not as effective in black and white as some other types of processing
6. Separate images, each of a different temperature interval, with 0° to 20° C divided into 16 different levels, each with $1-1/4^{\circ}$ C temperature span

The first interval (16-1) includes all temperatures above $18-3/4^{\circ}$ C. Several visually inconspicuous anomalies are more pronounced on IR than Old Faithful, but other anomalies are not yet evident. Representative levels or slices, with decreasing temperature, first show the appearance and then the enlargement of other anomalies. Separate images of temperature intervals below 10° C are especially useful. Interval 16-14 ($2-1/2^{\circ}$ to $3-3/4^{\circ}$ C) shows anomalies that are similar in shape to the 1000- μ cal contour, and interval 16-15 ($1-1/4^{\circ}$ to $2-1/2^{\circ}$ C) is most nearly similar to the 450- μ cal contour. The eastern anomalies have apparent surface temperatures 3° to 4° C lower than equivalent heat flows in the western part, because of differences either in real temperatures or in emissivities of ground materials.

BLACK SAND TEST SITE

Extensive physical studies have been made of a geothermal anomaly northwest of Old Faithful. Winter mapping of snow lines and snow depths adjacent to this warm ground provides qualitative differences in heat flow. Temperature-depth profiles permit calculation of heat flow by assuming reasonable thermal conductivities. A map of the radiation temperature of the warm area was made on the ground with a radiometer during one of the series of IR overflights. This radiation temperature map approximates a real surface temperature map for the surface material of

the area which is black sand with emissivity near 1 and little vegetative cover. Analog computer processing of the thermal IR imagery taken at this time produced multiple images, each representing the ground area with a different preselected $1\text{-}1/4^\circ\text{C}$ radiation temperature range. Temperature separates were prepared for the temperature interval of -5° to 20°C . A system was developed for presenting these individual temperature separates in a single reconstituted color image by color coding the separates and rephotographing them. This color-coded image differs from a continuous-tone, black and white thermal IR image in that the boundaries between the colors represent isotherms of known value. The isothermal map obtained in this fashion correlated closely with the ground radiometer map. Heat flows between 5500 and $300\ \mu\text{cal}/\text{cm}^2\text{sec}$ have been measured in this test area.

The oral presentation included the following:

1. A map presenting isolines of equal snow depth around the test site
2. Winter soil temperature profiles for various positions on the test site
3. A soil heat-flow map of the test area
4. An isoline map of radiation temperatures recorded on the site with a radiometer during the mission overflight
5. A color-coded thermal image of the site

Separate images representing each $1\text{-}1/4^\circ\text{C}$ temperature span in the original 0° to 20°C , interval 8-14 image obtained at 2:00 a.m. were prepared. Each of these separate images was transformed into a colored image. A sandwich was made by registering these colored separates. A color photograph of the sandwich is a colored thermal image on which each color represents a different radiation temperature interval. The colors are selected so that the "hotter" colors such as red represent the warmer ground areas and so forth.

In summary, IR easily "sees" the obvious geothermal anomalies and also sees, by means of computer processing, inconspicuous anomalies not readily visible by ground inspection at intensity levels near and even below the average "noise" level. Low-intensity anomalies can be calibrated, at least roughly, in terms of heat flow at rates that range down to about $400\ \mu\text{cal}/\text{cm}^2\text{sec}$ or somewhat less. Equal radiation ground temperatures at any instant, even in early morning, cannot be equated strictly with heat flow. We are still considerably above our hoped-for

objective of detecting heat flows only three to 10 times "normal," but major progress has been made in calibrating low-intensity anomalies and in computer processing of the data. The limits of both calibration and processing have not yet been fully tested; future investigations will explore these limits further.

AREA
1/2
2/26
Yellowstone
tag + Seis

UNIVERSITY OF UTAH
RESEARCH INSTITUTE
EARTH-SCIENCE LAB.

Yellowstone Hot Spot New Magnetic and Seismic Evidence

R. B. Smith, R. T. Shuey, R. O. Freidline, R. M. Otis, L. B. Alley
Department of Geology and Geophysics, University of Utah, Salt Lake City, Utah 84112.

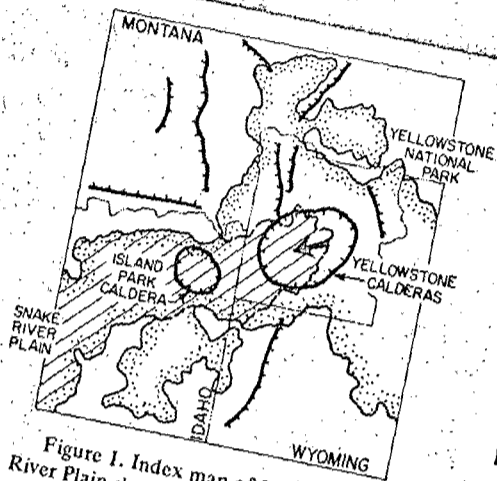


Figure 1. Index map of Yellowstone-Snake River Plain showing extent of Quaternary volcanic rocks (dash-dot line), Cenozoic volcanic rocks (dots), and late Cenozoic faults (ticked lines). Arrow indicates direction of relative motion of North American plate over Yellowstone hot spot (Smith and Sbar, 1974).

at a junction of major tectonic trends but does not directly bear on the hypothesis of a mantle plume. Key words: caldera, pseudogravity, heat flow, fault-plane solutions.

INTRODUCTION

Yellowstone National Park provides a major display of geyser and hot spring phenomena. To the southwest, the Snake River Plain, a basalt-filled depression, has been interpreted as a tension rift (Hamilton and Myers, 1966), consistent with an upper mantle hot spot tracking northeastward beneath the plain to its present position beneath Yellowstone (Morgan, 1972; Smith and Sbar, 1974; Fig. 1). Late Cenozoic and Quaternary volcanism of the Snake River Plain and Yellowstone lies on a northeast-trending volcano-tectonic system (Christiansen and Blank, 1969) that evolved progressively northeastward at a rate of about 4.0 cm/yr (Armstrong and others, 1974). The central Yellowstone plateau overlying the proposed hot spot is centered on two large resurgent calderas related to eruption of rhyolitic ash flows, some as young as 60,000 yr (Keefer, 1972). North-trending normal faulting of Cenozoic age extends north from the Basin Range province to the Yellowstone calderas but does not deform or crosscut the caldera structures. Normal faulting begins again at the north edge of the calderas along northwest trends that continue into Montana.

The Intermountain Seismic Belt (ISB) is a major zone of seismicity that extends from southern Utah to the Yellowstone caldera, then northwestward through Montana generally coincident with the Cenozoic fault zones. A secondary seismic zone begins in Yellowstone and extends west through central Idaho, including the Hebgen fault zone immediately west of the park (Smith and Sbar, 1974). The intersection of the ISB with the Idaho seismic zone

includes the general area of Yellowstone as well as the epicenter of the August 18, 1959, Hebgen Lake earthquake of magnitude 7.1. Fault-plane solutions for the Intermountain region show east-west extension north and south of Yellowstone and north-south extension along the Hebgen fault zone (Smith and Sbar, 1974; Trimble and Smith, 1973). The intersection at Yellowstone of these seismic zones may represent a continental triple junction that forms a vertex of intraplate deformation of the western United States.

Thus, a broad range of geologic and seismic evidence suggests an anomalous crust and upper-mantle beneath Yellowstone. This paper presents new seismic and magnetic data interpreted as evidence for a hot upper crust beneath the Yellowstone calderas.

GEOPHYSICAL DATA

Residual Magnetic Map. An aeromagnetic map of Yellowstone and vicinity is on open file with the U.S. Geological Survey. We digitized this map at a 2.08-km grid spacing for computer analysis. The initial processing removed the Earth's main geomagnetic field and reduced the data to the north pole, an operation that removes asymmetry due to nonvertical magnetic inclination. The principal features of the Yellowstone residual map (Fig. 2) are a series of magnetic highs, up to +250 γ , which encircle the western caldera. The center of the calderas is marked by a series of broad magnetic lows, as large as -230 γ . These anomalies are interpreted to represent a deep-seated ring intrusion surrounding hot upper crustal material. East of the park and in its northeast corner are numerous magnetic highs over the early Cenozoic Absaroka volcanics and some Precambrian exposures.

Pseudogravity Map. In order to enhance the regional features, we performed a pseudogravity transformation (Baranov,

ABSTRACT

We present new magnetic and seismic evidence relevant to the hypothesis of a hot spot beneath Yellowstone National Park. A pseudogravity transformation enhances the regional magnetic anomalies, and the resultant map can also be interpreted to show regional variation in geothermal gradient. We propose that a pseudogravity lineament along the eastern margin of the park marks a heat-flow province boundary, whereas closure within Yellowstone marks a crustal boundary roughly coincident with a double caldera mapped geologically. Magnetic highs at the caldera boundary may represent ring intrusions. Seismically, Yellowstone is at the most active part of the Intermountain Seismic Belt, where it changes strike from north to northwest and is intersected by a west-trending secondary seismic belt. Within the caldera, the earthquakes decrease in frequency of occurrence and abruptly decrease in focal depth. At the caldera boundary, four composite fault-plane solutions indicate radial compression, possibly due to resurgent magmatism. These geophysical data support the concept of a roughly circular region of anomalously hot crust

GEOLOGY

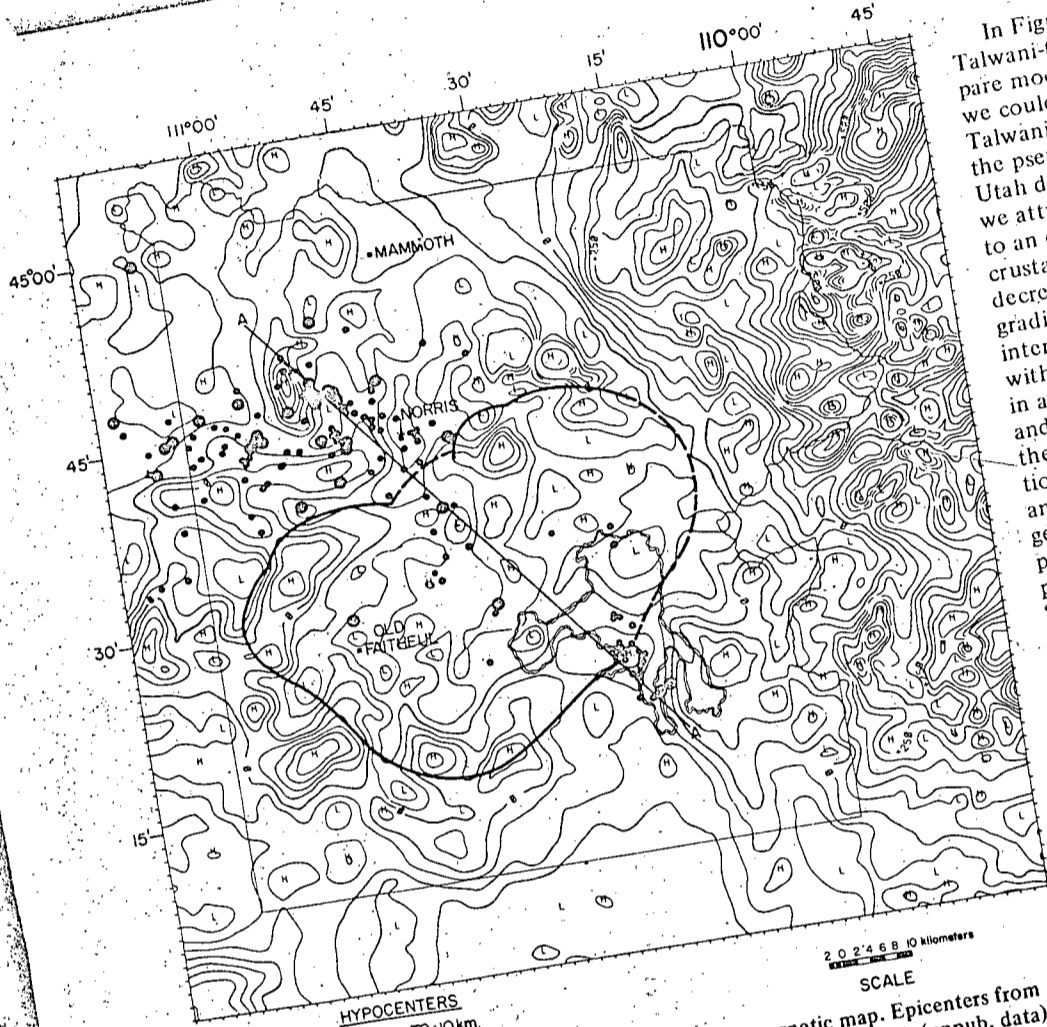


Figure 2. Seismicity map of Yellowstone plotted on residual magnetic map. Epicenters from 1972 survey of Trimble and Smith (1973) and 1973 survey by University of Utah (unpub. data). Focal depth range: 0 to 10 km, small circles; greater than 10 km, large circles. Residual magnetic map was produced from open-file map of U.S. Geological Survey by removal of main geomagnetic field. Contour interval 50 γ . Caldera boundaries from Geologic Map of Yellowstone National Park (U.S. Geological Survey, 1972). Yellowstone Lake outlined by double lines.

1957) on the residual magnetic map. This operation is mathematically equivalent to integration of the residual field from an arbitrarily high altitude down to the plane of observation. In the Fourier frequency domain, it is division by $2\pi f$, where f is the spatial frequency (cycles per kilometer). This gives the "equivalent stratum," which is the magnetization-thickness product of a fictitious non-thickness product of a fictitious non-uniformly magnetized thin sheet that, if located immediately below the plane of observation, would produce the observed residual field. Note that it is much smoother than the residual magnetic field. Pseudogravity (Fig. 3) is the equivalent stratum multiplied by a constant factor $\gamma\rho/kF$, where γ is the gravitational constant, F is the geomagnetic field strength, and ρ/k is an assumed density/susceptibility ratio. This gives the gravity field that would be

452

observed if density and susceptibility varied proportionately.

The outstanding feature of the pseudogravity map is the strong gradient along the eastern Yellowstone boundary. At the northeast corner of the park, this gradient appears to abruptly change to a northwesterly strike. The satellite map of Zietz and others (1970) suggests that this gradient may continue along the Montana disturbed belt, although this is not obvious on the lower level strip survey of Zietz and others (1971). It is tempting to speculate that southward this gradient may connect with the one traced through Utah by Shuey and others (1973). A seismic refraction profile in Utah and Wyoming shows a continuation of Basin Range crustal structure 100 km east of the province boundary (Braile and others, 1974) and lends support to this hypothesis.

In Figure 4 we used a magnetic Talwani-type computer program to compare models with the magnetic map, but we could just as well have used a gravity Talwani-type program to compare with the pseudogravity map. As with the Utah data (Shuey and others, 1973), we attribute the broad magnetic anomaly to an eastward increase in magnetic crustal thickness, corresponding to a decrease in the vertical geothermal gradient. This suggests an alternative interpretation of the pseudogravity map: with the assumption of no lateral change in average crustal magnetic susceptibility, and with the Bouguer slab approximation, the pseudogravity field varies proportionately with the depth to Curie isotherm and therefore inversely as the crustal geothermal gradient. From this viewpoint, the closure in Figure 3 is of particular interest because it defines a "hot spot." However, lateral susceptibility changes might also contribute; for example, the closure could be attributed to extensive hydrothermal alteration.

Spectral Analysis. The Fourier power spectrum of the Yellowstone aeromagnetic map (Fig. 5) is a classic "double-ensemble" case as described by Spector and Grant (1970). The high-frequency ensemble represents the surficial volcanics. Because the mean terrain clearance is only about 1 km, the average logarithmic slope of 3 km is more indicative of horizontal dimensions than vertical dimensions of the typical magnetic material within the volcanic complex.

Notable in the low-frequency part of the spectrum is a peak centered at about 0.01 c/km. The presence of such a peak shows the magnetic map is large enough to resolve the depth to the Curie isotherm. Schellinger (1972) and Shuey and others (1974) have described mathematical techniques to extract Curie depth estimates in such cases. For Yellowstone these computations indicate a depth of 10 ± 3 km below sea level. This implies an average crustal geothermal gradient of about $45^\circ\text{C}/\text{km}$. Assuming an average crustal thermal conductivity of $0.006 \text{ cal}/\text{cm}\cdot\text{sec}\cdot^\circ\text{C}$ (Schatz and Simmons, 1972) the reduced conductive heat flow would be $2.7 \mu\text{cal}/\text{cm}^2\cdot\text{sec}$, anomalously high for continental areas.

The Curie depth estimate is an average for the entire area west of the pseudogravity gradient described earlier, which apparently includes a "hot" central area surrounded by "cooler" crust. However, the estimate is mostly based on the broad highs peripheral to the central magnetic low (Figs. 3, 7). Thus, within the caldera the Curie isotherm might well be shallower than 10 km below sea level.

SEPTEMBER 1974

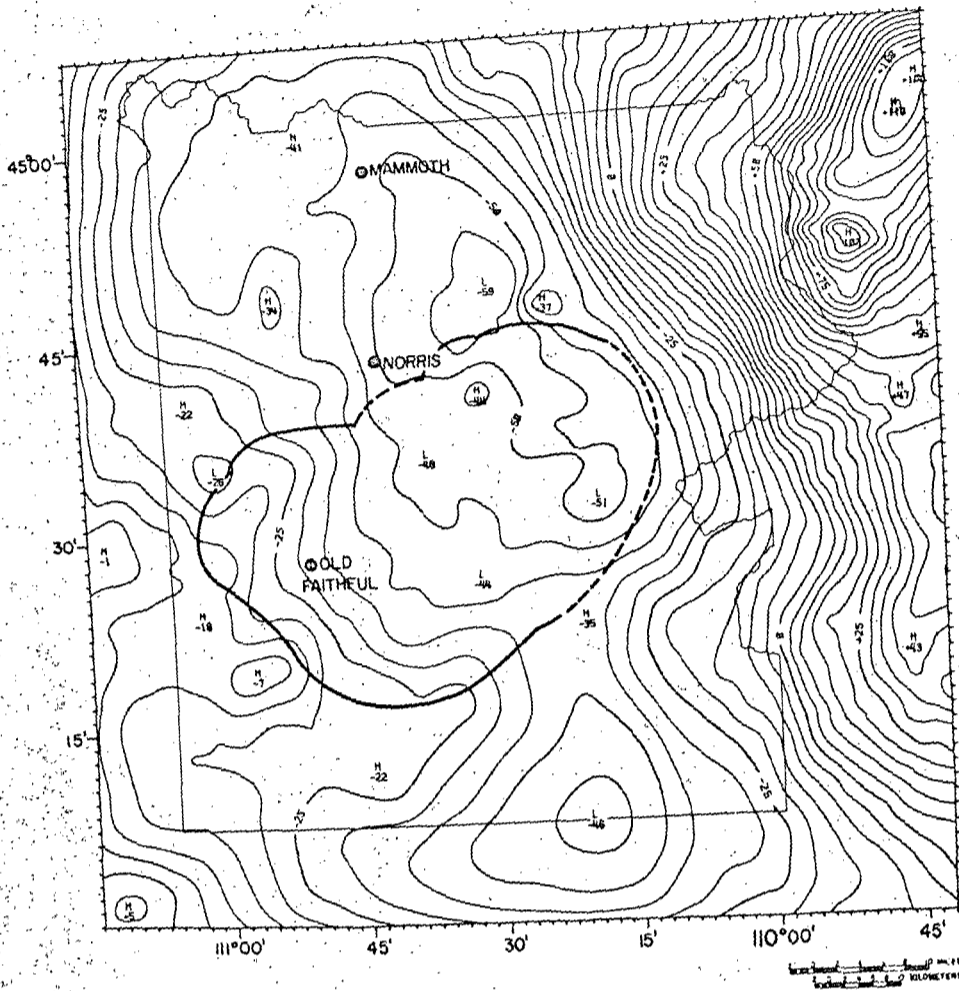


Figure 3. Pseudogravity map of Yellowstone. Contour interval = 5 mgal. Computation assumed density/susceptibility ratio of 100 CGS units, for example, density contrast of 0.1 gm/cc and susceptibility contrast of 0.001 emu/cc. For lower assumed density/susceptibility ratio, pseudogravity effect in milligals would be proportionally less. Residual magnetic field data were simply bordered with zeros prior to computation, therefore contours shown are unreliable near map edges.

Seismicity. Western Yellowstone and the Hebgen Lake fault zone to the west correspond to the most seismically active area of the Intermountain Seismic Belt. Activity is characterized by shallow focal depths and pronounced earthquake swarms, particularly in association with some geothermal features and dominant along a zone from Norris geyser basin to the western boundary of the park.

To investigate the seismicity of Yellowstone, the University of Utah has conducted detailed earthquake surveys using portable high-gain seismographs. The 1972 survey (Trimble and Smith, 1973) was conducted throughout the Hebgen Lake-West Yellowstone area, and the 1973 survey was conducted in southeastern Yellowstone. Epicenters from these surveys are plotted in Figure 2.

The zone of most pronounced seismic

activity extends 80 km west from Norris geyser basin along a N. 80° W. trend. Earthquakes in western Yellowstone are not located on mapped faults but appear along a diffuse trend indicative of a broad zone of deformation, perhaps along a pre-existing zone of weakness. Activity immediately northwest of Norris geyser basin appears to correlate with northwest-trending normal faults, but the activity abruptly decreases at the caldera boundary. Extensive swarms occur throughout western Yellowstone with pronounced activity in Norris geyser basin. Episodic earthquakes occurring at constant intervals of several seconds are closely confined to Norris geyser basin and may reflect pore-pressure variations, not tectonic strain release (Trimble and Smith, 1973).

Focal depths range from near surface

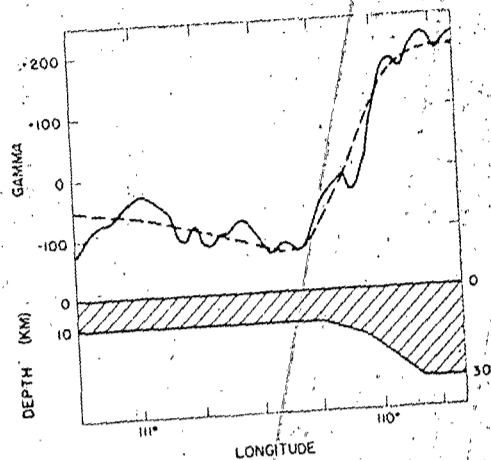


Figure 4. Interpretation of magnetic gradient along eastern margin of Yellowstone. Solid line = residual magnetic field averaged over latitude from 44°08' to 44°45'. Dashed line = theoretical anomaly for indicated eastward thickening of magnetic crust, assuming susceptibility of 0.004 cgs.

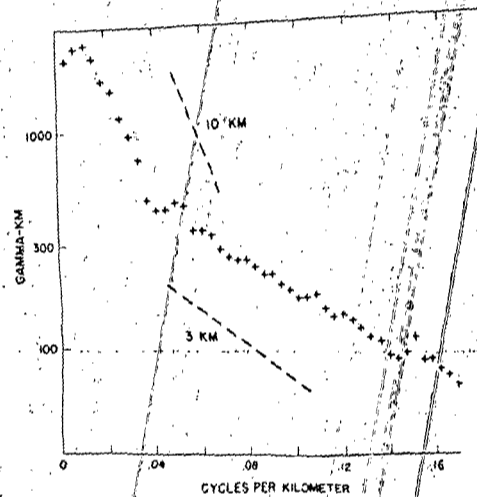


Figure 5. Fourier amplitude spectrum (logarithmic scale) for area of Yellowstone caldera. Dashed lines have logarithmic slope of $-2\pi D$, where D is indicated depth

to 17 km in western Yellowstone (Figure 2). In the northwestern caldera area, the maximum focal depth is only 5 km, this changes abruptly near the caldera boundary. Scattered earthquakes with shallow focal depths occurred throughout the central caldera area, although appear to follow a northwest trend extends to an active seismic zone beneath Yellowstone Lake. Diffuse northwest-trending activity with central Yellowstone plateau may be a more brittle zone separating the calderas. At Yellowstone Lake earthquake swarm was outlined by two north-trending zones of activity. depths ranged from near surface to 12 km.

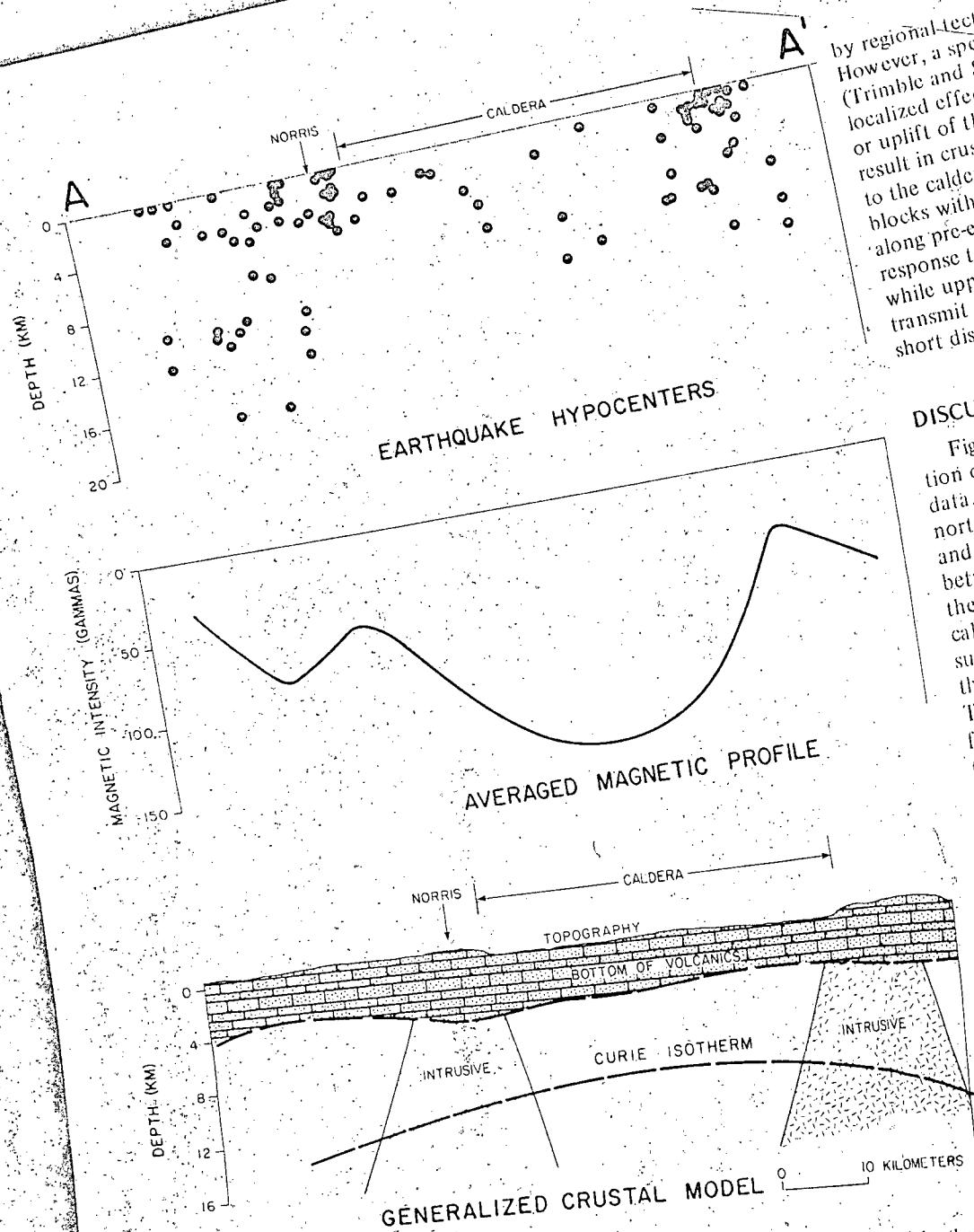


Figure 6. Northwest profile, A-A', across Yellowstone calderas. Top: projected focal depths; middle: smoothed aeromagnetics; bottom: generalized interpretation of magnetics based on filtered maps and spectral analysis.

The decrease in frequency of occurrence and the abrupt decrease in focal depths within the calderas may reflect increased temperatures (Brace and Byerlee, 1970), but increased pore pressures expected in this thermal environment may also be sufficient to inhibit brittle fracture. Therefore the general seismicity outside the calderas probably reflects tectonic activity, whereas seismic activity overlying the thermal zones of the calderas may be partly related to pore-pressure and temperature effects.

Fault-Plane Solutions. Two single and nine composite fault-plane solutions

for the Yellowstone region are plotted in Figure 7. Seven solutions along the Hebgen-West Yellowstone trend, including the 1959 Hebgen Lake earthquake, show normal faulting, with the down-thrown blocks to the south. The T-axes trend north-south, indicating north-south regional extension that continues westward along the Idaho seismic zone. However, four composite fault-plane solutions around the caldera boundary with P-axes radial to the caldera indicate thrust faulting and imply crustal shortening in the radial direction. It is difficult to explain this abrupt change in stress

by regional tectonic strain variations. However, a speculative interpretation (Trimble and Smith, 1973) suggests localized effects produced by resurgence or uplift of the inner caldera that could result in crustal shortening perpendicular to the caldera boundary. Downfaulted blocks within the caldera may be rising along pre-existing boundary faults in response to magma chamber inflation, while upper crustal layers passively transmit the resultant stresses only a short distance.

DISCUSSION

Figure 6 summarizes our interpretation of the hypocenter and magnetic data. This figure represents a generalized northwest profile across the calderas and shows the excellent correlation between the shallow focal depths and the broad magnetic low within the calderas. Included in the model are the surficial volcanic flows responsible for the high-frequency part of the spectrum. The surrounding intrusives are inferred from the broad magnetic highs bordering the calderas principally to the southwest. Thrust faulting indicated by the fault-plane solutions along these intrusive contacts could represent resurgence or uplift of the inner calderas.

Seismic and magnetic evidence presented here indicate that anomalously "hot" rock in the upper crust underlies the Yellowstone calderas, possibly reflecting a shallow granitic batholith. Presence of a magma chamber cannot be discerned by our data, but a 10-km Curie depth would allow a water-saturated granitic partial melt at about 13 km (Wylie, 1971).

That the geothermal and volcanic patterns of Yellowstone are related mantle hot spots or plumes cannot be proven by our data. However, those models by Morgan (1972) and Smith and Sbar (1974) for a Yellowstone plume suggest southwest migration of the North American plate over the plume at a rate of about 4 cm/yr are consistent with our data. Radial extension fractures produced in the lithosphere over the plume could be the regional fracturing of the lithosphere now seismically active along the Snake River Plain which has been interpreted as a pre-existing lithospheric zone of weakness that has migrated northeastward as a wedge-shaped feature in response to intraplate deformation. This model would place the tip of the lithospheric fracture at Yellowstone. Resultant stresses could produce



Figure 7. Fault-plane solutions. Data from Trimble and Smith (1973), Dewey and others (1973), and University of Utah (unpub. data). Upper hemisphere, equal-area stereographic nets. Dark quadrants = compression, light quadrants = dilatation. Inward arrow = P-axis, outward arrows = T-axis.

active seismicity, and crustal fractures would facilitate the widespread volcanism of Yellowstone.

REFERENCES CITED

- Armstrong, R. L., Leman, W. P., and Malde, H. E., 1974, K-Ar dating, Neogene volcanic rocks of the Snake River Plain, Idaho: *Am. Jour. Sci.* (in press).
- Baranov, V., 1957, A new method for interpretation of aeromagnetic maps: Pseudo-gravimetric anomalies: *Geophysics*, v. 22, p. 827-829.
- Brace, W. F., and Byerlee, J. D., 1970, California earthquakes: why only shallow focus?: *Science*, v. 168, p. 1573-1576.
- Braile, L., Smith, R. B., Keller, G. R., Welch, R. M., and Meyer, R. P., 1974, Crustal structure along the Wasatch Front from detailed seismic refraction profiles: *Jour. Geophys. Research* (in press).
- Christiansen, R. L., and Blank, H. R., Jr., 1969, Volcanic evolution of the Yellowstone Rhyolite Plateau and eastern Snake River Plain, in *Symposium on volcanoes and their roots* [abs. vol.]: Oxford, Internat. Assoc. Volcanology and Chemistry of the Earth's Interior, p. 220-221.
- Dewey, J. W., Dillinger, W. H., Taggart, J., and Algermissen, S. T., 1973, A technique for seismic zoning: Analysis of earthquake locations and mechanisms in northern Utah, Wyoming, Idaho and Montana:

- U.S. Dept. Commerce, NOAA Tech. Rept. ERL 267-ESL 30, p. 29-48.
- Hamilton, W., and Meyers, W. B., 1966, Cenozoic tectonics of the western United States: *Rev. Geophysics*, v. 4, p. 509-549.
- Keefer, W. R., 1972, The geologic story of Yellowstone National Park: U.S. Geol. Survey Bull. 1347, 92 p.
- Morgan, W. J., 1972, Deep mantle convection plumes and plate motions: *Am. Assoc. Petroleum Geologists Bull.*, v. 56, p. 203-213.
- Schatz, J. F., and Simmons, G., 1972, Thermal conductivity of earth materials at high temperatures: *Jour. Geophys. Research*, v. 77, p. 6966-6983.
- Schellinger, D. K., 1972, Curie depth determinations in the High Plateaus, Utah [M.S. thesis]: Salt Lake City, Univ. Utah, 76 p.
- Shuey, R. T., Schellinger, D. K., Johnson, E. H., and Alley, L. B., 1973, Aeromagnetism and the transition between the Colorado Plateau and Basin Range provinces: *Geology*, v. 1, p. 107-110.
- Shuey, R. T., Schellinger, D. K., and Alley, L. B., 1974, Curie depth determinations along the eastern margin of the Basin Range: *Geol. Soc. America Abs. with Programs* (Cordilleran Sec.), v. 6, no. 3, p. 252.
- Smith, R. B., and Sbar, M. L., 1974, Contemporary tectonics and seismicity of the western United States with emphasis on the Intermountain Seismic Belt: *Geol. Soc. America Bull.*, v. 85, p. 1205-1218.

PRINTED IN U.S.A.

- Spector, A., and Grant, F. S., 1970, Statistical models for interpreting aeromagnetic data: *Geophysics*, v. 35, p. 293-302.
- Trimble, A., and Smith, R. B., 1973, Seismicity and contemporary tectonics of the Yellowstone Park-Hebgen Lake region [abs.]: *Seismol. Soc. America 68th Natl. Mtg. Program*, p. 27.
- U.S. Geological Survey, 1972, Geologic map of Yellowstone National Park: U.S. Geol. Survey Misc. Geol. Inv. Map 4-711.
- Wylie, P. J., 1971, The dynamic earth: New York, John Wiley & Sons, Inc., p. 183.
- Zietz, L., Andreasen, G. E., and Cain, J. G., 1970, Magnetic anomalies from satellite magnetometer: *Jour. Geophys. Research*, v. 75, p. 4007-4015.
- Zietz, L., Hearn, B. C., Jr., Higgins, M. W., Robinson, G. D., and Swanson, D. A., 1971, Interpretation of an aeromagnetic strip across the northwestern United States: *Geol. Soc. America Bull.*, v. 82, p. 3347-3372.

ACKNOWLEDGMENTS

Reviewed by W. E. Bonini and D. Mabey.

Supported by National Science Foundation Grants GA-31300 and GA-12870 and Oceanic and Atmospheric Administration Grant 04-3-022-13.

We thank the U.S. Geological Survey for their cooperative support and the Park Service, Yellowstone National Park for their permission and help during

MANUSCRIPT RECEIVED
MANUSCRIPT ACCEPTED